

**School of Civil and Mechanical Engineering  
Department of Civil Engineering**

**Analysis of Edgelift Anchor Failures in  
Experimental Precast Panels**

**Andrew Barraclough**

**This thesis is presented for the Degree of  
Doctor of Philosophy  
of  
Curtin University**

**July 2016**

## **Declaration**

To the best of my knowledge and belief this thesis contains no material previously published by any other person except where due acknowledgement has been made.

This thesis contains no material which has been accepted for the award of any other degree or diploma in any university.

Signature:

Date:

29/06/16



## Original work declaration

During this research the author was on the committee responsible for the revision of the Australian Standard, AS3850 – Prefabricated Concrete Elements, where the committee was formed in 2009 and the revised standard was published in 2015. As a consequence, AS3850 (SAI 2015) has adopted some cast-in Edgelift anchor performance in early age concrete aspects which are highlighted by the findings of this research. References in AS3850 (SAI 2015) are: Part 1 clause 2.2 (c), and detailed in A7, Appendix A and Appendix B.

Even though this thesis is not a thesis by publication, during this research various peer reviewed papers were published as conference proceedings, where the findings of these published papers are findings described in this thesis, specifically in relation to the following papers;

Barracough, A S. "A Plate Type Edge-Lift Anchor: Panel reinforcement influence on failure loads." *Australasian Structural & Engineering Conference*. Perth: Structural Engineering Institute of Australia, 2012.

Barracough, A S. "Tensile and compressive behaviour of early age concrete." *Conference proceedings*. Nashville, USA: Precast Concrete Institute, 2012.

Barracough, A S.. "Tensile and compressive behaviour of early age concrete." *Precast Concrete Institute Convention*. Melbourne: Concrete Institute of Australia, 2012.

Barracough, A S, and N Lloyd. "A Plate Type Edge-Lift Anchor: Influence of reinforcing configurations on failure modes." *Concrete 2011*. Melbourne: Concrete Institute of Australia, 2011.

Barracough, A S, and N Lloyd. "A Plate Type Edge-Lift anchor: Shear reinforcement influence on failure loads." *Australasian Structural & Engineering Conference: Sustainability for the future*. Perth, Australia: ASEC, 2012.

Barracough, A S, and N Lloyd. "Early age tensile and compressive strength of concrete - Impact on predictions for anchor pull-out capacity." *Concrete 2013*. Brisbane: Concrete Institute of Australia, 2013.





# Contents










<b>CONTENTS.....</b>	<b>II</b>
<b>NOTATION.....</b>	<b>V</b>
<b>LIST OF TABLES.....</b>	<b>VII</b>
<b>LIST OF FIGURES .....</b>	<b>VIII</b>
<b>ABSTRACT .....</b>	<b>1</b>
<b>1. INTRODUCTION.....</b>	<b>3</b>
1.1. PROBLEM STATEMENT.....	4
1.2. AIM.....	4
1.3. SCOPE .....	5
1.4. OVERVIEW OF THIS RESEARCH .....	6
1.5. STRUCTURE OF THIS THESIS .....	7
<b>2 LITERATURE REVIEW – CAST-IN PLACE ANCHORS .....</b>	<b>11</b>
2.1. DESIGN CONSIDERATIONS FOR CAST-IN PLACE EDGELIFT ANCHORS .....	11
2.1.1 <i>Background</i> .....	13
2.1.2 <i>Concrete resistance</i> .....	17
2.2. CAST-IN HEADED ANCHOR DESIGN AND THEIR HISTORICAL DEVELOPMENT .....	18
2.3. NON-HEADED CAST-IN ANCHOR DESIGN GUIDELINES .....	20
2.3.1 <i>Concrete Capacity Design</i> .....	22
2.3.2 <i>Models defined by the Standards</i> .....	24
2.3.3 <i>Summary of design models used for cast-in Edgelif</i> 2.3.3.1 <i>Concrete cone capacity</i> .....	28 29
233.1.1 <i>Insert edge distance</i> .....	30
233.1.2 <i>Effect of a thin wall</i> .....	31
2.4. PREFABRICATED WALL PANEL LIFTING DESIGN.....	32
2.4.1 <i>Edgelif</i> 2.4.1.1 <i>Insert – testing to derive capacity</i> .....	32 32
2.5. CAST-IN EDGELIFT ANCHOR INDIVIDUAL LOAD RESISTANCE COMPONENTS .....	34
2.5.1 <i>Edgelif anchor - Cracked or un-cracked concrete</i> .....	35
2.6. CURRENT PERFORMANCE MODELS – ASSUMED CONCRETE BEHAVIOUR.....	35
<b>3 LITERATURE REVIEW - EARLY AGE CONCRETE STRENGTH PARAMETERS.....</b>	<b>40</b>
3.1. EARLY AGE CONCRETE - MATERIAL CONSIDERATIONS.....	40
3.2. TEMPERATURE RELATED STRENGTH MODELS .....	45
3.3. EARLY AGE CONCRETE - MECHANICAL PROPERTIES .....	47
3.3.1 <i>Compressive Strength</i> .....	47
3.3.2 <i>Tensile Strength</i> .....	48
3.3.3 <i>Tensile vs compressive strength</i> .....	52

3.3.4	<i>The derivation of tensile strength .....</i>	53
3.3.5	<i>Factors affecting tensile strain capacity.....</i>	54
3.3.6	<i>Predictions for anchor pull-out capacity.....</i>	54
3.3.7	<i>Concrete tensile behaviour .....</i>	56
<b>4</b>	<b>EXPERIMENTAL RESEARCH – CONCRETE STRENGTH AND CAST-IN HEADED INSERT CAPACITIES .....</b>	<b>58</b>
4.1.	CONCRETE TENSILE STRENGTH AND CAST-IN INSERTS .....	59
4.1.1	<i>Experimental Program .....</i>	59
4.1.2	<i>Test Results and Analysis.....</i>	63
4.1.3	<i>Concluding remarks.....</i>	67
4.2.	CAST-IN HEADED INSERT CAPACITIES .....	69
4.2.1	<i>Experimental Program .....</i>	69
4.2.2	<i>Test Results and Analysis.....</i>	75
4.2.2.1	Concrete failure test results .....	77
4.2.2.2	Concrete strength results .....	78
4.2.3	<i>Concluding remarks.....</i>	79
<b>5</b>	<b>EXPERIMENTAL RESEARCH - EDGELIFT ANCHOR CAPACITIES IN EARLY AGE CONCRETE .....</b>	<b>81</b>
5.1.	EDGELIFT TEST 1 – ANCHOR SHAPE AND CONFIGURATION EXPERIMENTAL PROGRAM. 83	
5.1.1	Experimental Program.....	83
5.1.2	Test Results and Analysis .....	88
5.1.3	Concluding remarks .....	91
5.2.	EDGELIFT TEST 2 - PANEL REINFORCEMENT INFLUENCE ON FAILURE LOADS .....	94
5.2.1	Experimental Program.....	96
5.2.2	Test Results and Analysis .....	102
5.2.3	Concluding remarks .....	111
5.3.	EDGELIFT TEST 3 - INFLUENCE OF ANCHOR REINFORCING ON FAILURE LOADS.....	115
5.3.1	Experimental Program.....	116
5.3.2	Test Results and Analysis .....	121
5.3.3	Concluding remarks .....	133
5.4.	EDGELIFT TEST 4 – ANCHOR REINFORCEMENT INFLUENCE ON SHEAR FAILURE LOADS 135	
5.4.1	Predictive Strength Equations.....	137
5.4.2	Experimental Program.....	140
5.4.3	Test Results and Analysis .....	145
5.4.4	Concluding remarks .....	148
5.5.	EDGELIFT TEST 5 - STRESS DISTRIBUTION ALONG AN EDGELIFT ANCHORS LENGTH ..	152
5.5.1	Experimental Program.....	152
5.5.2	Test Results and Analysis .....	156
5.5.3	Concluding remarks .....	161

<b>6</b>	<b>DISCUSSION AND ANALYSIS.....</b>	<b>162</b>
<b>7</b>	<b>CONCLUSIONS.....</b>	<b>167</b>
<b>8</b>	<b>RECOMMENDATIONS .....</b>	<b>169</b>
<b>9</b>	<b>REFERENCES.....</b>	<b>171</b>
	<b>APPENDIX A – LIFTING DESIGN .....</b>	<b>175</b>
	<i>Wall panel lifting .....</i>	<i>175</i>
	<i>Basic Principles of wall panel lifting using cast-in inserts .....</i>	<i>176</i>
	<b>APPENDIX B - TEST DATA .....</b>	<b>180</b>

## Notation

$A_{\text{eff}}$	- Actual projected area for concrete cone failure
$A_{\text{eff}}^0$	- Projected concrete failure area of an insert with edge distance equal to or greater than $1.5h_{\text{ef}}$
$A_{\text{eff}}$	- unrestricted project concrete failure area,
$A_{\text{ec}}$	- edge distance reduced projected concrete failure area,
$A_h$	- Load bearing area of the head of the insert
$C_{\text{eff}}$	- Minimum value for edge distance to achieve characteristic resistance to tension load
$C_{\text{eff}}'$	- Modified minimum value for edge distance to achieve characteristic resistance to tension load
$e_{\text{max}}$	- Maximum distance from centre of an insert to the edge of element $< 4e_{\text{max}}$
$d_h$	- Diameter of the head of the insert
$f_{\text{cm}}$	- Characteristic compressive strength of concrete at 28 day
$f_{\text{cm,t}}$	- Mean concrete tensile strength at time of test
$f_{\text{cm,t}}'$	- Characteristic compressive strength of the concrete at time of loading
$f_{\text{cm,t}}'$	- Characteristic compressive strength of concrete derived from cubes
$f_{\text{ct}}$	- Uniaxial tensile strength of concrete
$f_{\text{ct}}'$	- Characteristic uniaxial tensile strength of concrete
$f_{\text{ct}}'$	- Modulus of rupture
$f_{\text{ct}}'$	- Splitting tensile strength
$f_{\text{ct}}'$	- Concrete tensile strength
$f_{\text{ct}}'$	- Characteristic tensile strength of concrete
$f_{\text{ct}}'$	- Modulus of rupture
$f_{\text{ct}}'$	- Characteristic tensile strength, derived from a Splitting test
$f_{\text{ct}}^{5\%}$	- 5% fractile or characteristic capacity
$f_{\text{yk}}$	- Nominal yield strength of splitting reinforcement steel
$k_1$	- Coefficient for modulus of rupture conversion
$k_2$	- Direct tensile strength conversion
$h_{\text{ef}}$	- Effective embedment depth of a cast-in anchor
$h_{\text{ef,mod}}$	- Modified effective depth of embedment for narrow elements
$k_{\text{cr}}$	- Factor relating to the condition of concrete (cracked or un-cracked)
$k_s$	- Sampling factor
$R_{\text{d}}$	- Design resistance of insert or group of anchors to tension
$N_b$	- Basic concrete breakout shear capacity of a single anchor,
$N_{\text{t,Rd}}$	- Predicted tensile breakout strength
$N_{\text{t,Rd}}^0$	- Characteristic resistance of a tested single anchor placed in un-cracked concrete
$N_{\text{t,Rd}}^0$	- Characteristic tensile pull-out strength of a cast-in headed anchor
$N_{\text{t,Rd}}^0$	- Predicted characteristic resistance of single anchors placed in un-cracked concrete
$N_{\text{t,Rd}}^0, \beta$	- Characteristic resistance in the case of blow-out failure for a single insert with shape factor
$N_{\text{t,Rd}}^0$	- Characteristic resistance in the case of splitting failure
$F_{\text{d}}$	- Design tension load
$P_{\text{d}}$	- Maximum force recorded on load cell during a test

	- Design resistance
	- Design actions
	- Critical spacing so adjacent inserts do not influence characteristic tensile insert resistance
	- Critical spacing so adjacent inserts do not influence characteristic tensile insert resistance
	- Critical spacing so adjacent inserts do not influence characteristic splitting insert resistance
	- Modified critical spacing so characteristic tensile resistance of insert in a narrow member
	- Design shear resistance of insert or insert group
	- Design shear load
$v$	- Coefficient of variation
$\beta$	- Shape modification factor
$\beta_{\text{ed}}$	- Tension shape modification factor for concrete cone failure
$\emptyset$	- Capacity factor
$\emptyset_t$	- Tensile Capacity factor
$\psi_{\text{ucr},N}$	- Factor relating to the state of the concrete (cracked/non-cracked) for concrete cone failure
$\Psi_{\text{ed},N}$	- Tensile edge modification factor
$\Psi_{\text{ep},N}$	- Modification factor for post-installed anchor edge reduction
$\Psi_{\text{C},N}$	- Modification factor for post-installed anchor for un-cracked concrete
	- Unit weight of concrete (kg/m <sup>3</sup> )
$\lambda_{\text{d}}$	- Light-weight concrete modification factor
$\phi_{\text{ed}}$	- Concrete crack modification factor (1.4 for non-cracked) for pull-out strength
$\phi_{\text{br}}$	- Concrete crack modification factor (1.25 for non-cracked) for break-out strength

## List of Tables

TABLE 1 - DIFFERENT PUBLISHED CCD MODELS USED AS COMPARABLE MODELS THROUGHOUT THIS RESEARCH .....	20
TABLE 2 - VARIOUS PUBLISHED CONCRETE TENSILE STRENGTH MODELS, WINTERS ET AL (2013)..	48
TABLE 3 - E MODULUS OF CONCRETE VALUES .....	53
TABLE 4 - CONCRETE STRENGTH GAIN SERIES OF TESTS IN EARLY AGE CONCRETE .....	59
TABLE 5 - TEST PROGRAM SERIES FOR HEADED INSERT TENSILE TESTS .....	69
TABLE 6 - CONCRETE SPECIFICATIONS USED IN ALL TESTS THROUGHOUT RESEARCH .....	71
TABLE 7 - ULTIMATE LOAD VS PREDICTED LOAD RATIOS FOR HEADED INSERTS (LOAD APPLIED RATE 20kN/MIN) .....	76
TABLE 8 - EXPERIMENT TEST SERIES .....	85
TABLE 9 - REINFORCEMENT CONFIGURATIONS FOR TEST SERIES TA1 – TA7 .....	86
TABLE 10 - REINFORCEMENT CONFIGURATIONS FOR TEST SERIES .....	99
TABLE 11 - CONCRETE COMPRESSIVE DATA, TESTED AT 3 PROGRESSIVE STRENGTHS FOR EACH TEST PANEL .....	100
TABLE 12 - TENSILE CAPACITY RESULTS FOR TEST SERIES EP1 - EP6.....	103
TABLE 13 - SHEAR CAPACITY RESULTS FOR TEST SERIES EP7 AND EP8.....	107
TABLE 14 - ANOVA ANALYSIS FOR EP3, EP4 AND EP6 .....	113
TABLE 15 - EP3 TO EP6 F-TEST AND T-TEST STATISTICAL DIFFERENCES IN DATA.....	114
TABLE 16 - COMBINATIONS OF ANOVA DATA DISTRIBUTION, ACCEPTED OR REJECTED NULL HYPOTHESIS.....	114
TABLE 17 - EDGELIFT ANCHOR EXPERIMENTAL PROGRAM - VARIOUS REINFORCEMENT .....	116
TABLE 18 – DIFFERENT CONCRETE COMPRESSIVE DATA FOR THE BATCHES USED DURING THIS EXPERIMENT .....	118
TABLE 19 - ASSESSMENT OF TENSILE STRENGTH DUE TO CONCRETE FORMULA OF ACI318 (2008) FOR PANEL TESTS CONDUCTED WITH EDGE-LIFT ANCHORS.....	122
TABLE 20 - ANOVA STATISTICAL ANALYSIS FOR TEST AND REINFORCEMENT SIGNIFICANCE.....	133
TABLE 21 - CONCRETE COMPRESSIVE STRENGTH DATA FOR TEST SERIES .....	142
TABLE 22 - REINFORCEMENT CONFIGURATIONS FOR TEST SERIES .....	144
TABLE 23 - TENSILE BREAKOUT STRENGTH, $P_u$ , COMPARED WITH THE REDUCED CONCRETE BREAKOUT CAPACITIES, $N_{CB}^0$ , PRESENTED BY ACI318 (2008) D5.2 .....	148
TABLE 24 - TEST SERIES FOR EDGELIFT ANCHOR STRESS DISTRIBUTION.....	153
TABLE 25 - TENSION TEST DATA .....	158
TABLE 26 - CASTING BED SUCTION COEFFICIENTS, AS3850 (SAI 2003).....	178
TABLE 27 - LIFTING EQUIPMENT DYNAMIC COEFFICIENTS, AS3850 (SAI 2003).....	178
TABLE 28 - RIGGING EQUIPMENT SLING ANGLE COEFFICIENTS, AS3850 (SAI 2003) .....	178

## List of Figures

FIGURE 1 - ADAPTED DESIGN FLOWCHART FOR POST-INSTALLED AND CAST-IN-PLACE HEADED ANCHORS, CEB (TTL 1997), 233, REVISED EDITION OF BULLETIN 226, PART 1 .....	14
FIGURE 2 - LOAD RESISTANCE MODEL OF AN EDGELIFT ANCHOR SYSTEM IN A WALL PANEL .....	15
FIGURE 3 - ADAPTION OF A FLOWCHART FOR CALCULATING CHARACTERISTIC RESISTANCES OF INSERTS WITH HEADED ANCHORS WITH SPECIAL REINFORCEMENT: ELASTIC DESIGN APPROACH, CEB (TTL 1997) .....	16
FIGURE 4 - CONCRETE BLOW-OUT FAILURE, .....	17
FIGURE 5 - PULL-OUT FAILURE, .....	17
FIGURE 6 - EDGELIFT PLATE STYLE ANCHOR INTERACTION WITH LIFTING CLUTCH .....	18
FIGURE 7 - CONICAL FAILURE SURFACE OF PCI HANDBOOK, (PCI (2004)).....	19
FIGURE 8 - ACI318 (2008) APPENDIX D (FIG RD.1) CAST-IN ANCHOR TYPES .....	22
FIGURE 9 - CONICAL CRACKS PREDICTED BY NON-LINEAR FRACTURE MECHANICS ANALYSIS OF PULL-OUT TESTS, DAO, ET AL (2009) .....	23
FIGURE 10 - ACI349.2R (2007) D.4.2.2 BREAKOUT CONE FOR TENSION .....	25
FIGURE 11 - ACI349.2R (2007) D.4.2.2 BREAKOUT CONE FOR SHEAR .....	25
FIGURE 12 - TENSILE FAILURE TYPE I) STEEL FAILURE, II) PULL-OUT .....	27
FIGURE 13 - TENSILE FAILURE TYPE III) CONCRETE CONE .....	27
FIGURE 14 - TENSILE FAILURE TYPE IV) SIDE-FACE BLOWOUT, V) CONCRETE SPLITTING .....	27
FIGURE 15 - SHEAR FAILURE TYPE I) STEEL FAILURE PRECEDED BY CONCRETE SPALL, II) CONCRETE PRY-OUT WITH NO ANCHOR EDGE REDUCTION .....	27
FIGURE 16 - SHEAR FAILURE TYPE III) CONCRETE BREAKOUT .....	28
FIGURE 17 - TYPICAL PLATE STYLE EDGELIFT ANCHOR USED IN THIN CONCRETE WALL PANELS.....	29
FIGURE 18 - CONCRETE WALL PANEL BEING LIFTED, AND PLACED VERTICALLY INTO THE BUILDING STRUCTURE .....	29
FIGURE 19- IDEALISED SINGLE EDGE TRUNCATED FAILURE CONE, ETAG 001 (EOTA 2013).....	30
FIGURE 20 - ACTUAL PROJECTED AREA OF THE IDEALIZED CONCRETE CONE AT THE EDGE OF A CONCRETE ELEMENT, ETAG 001 (EOTA 2013) .....	31
FIGURE 21 - EDGE REDUCTION EFFECT IN THIN WALLED PANELS .....	31
FIGURE 22 - TYPICAL SHEAR BAR DESIGN.....	33
FIGURE 23 - TYPICAL TEST PANEL ARRANGEMENT TO MEASURED LATERAL TENSION CAPACITIES OF EDGELIFT ANCHORS.....	33
FIGURE 24 - THE SHEAR BAR, AS SHOWN, IS SUBJECTED TO BENDING WITH AN APPLIED SHEAR LOAD .....	34
FIGURE 25 - LOAD RESISTANCE MODEL OF AN EDGELIFT ANCHOR SYSTEM .....	34
FIGURE 26 - ADVANCED CONCRETE TECHNOLOGY: COMPLETE STRESS-STRAIN CURVE OF NSC, ISO-AHOLA, ET AL (2012) .....	37
FIGURE 27 - COMPLETE STRESS-STRAIN CURVE OF HSC, ISO-AHOLA, ET AL (2012) .....	37
FIGURE 28 - HYDRATION OF THE CLINKER MINERALS IN CEMENT PAST, MINDESS, ET AL (2002) .....	41



FIGURE 29 - PRINCIPLE OF THE CRACKING FRAME, (A) FREE SPECIMEN, AND (B) LOADED SPECIMEN .....	42
FIGURE 30 –RECORDED SELF-STRESSES OF A FULLY RESTRAINED SPECIMEN DELA (2000) .....	43
FIGURE 31 - HYDROSTATIC PRESSURE EXERTED ON STRESS SENSOR WITH TIME FOR TWO DIFFERENT CEMENT PASTES (P00 IS WITHOUT SF AND P20 IS WITH 20% SF.), DELA (2000) .....	44
FIGURE 32 - RELATIONSHIP BETWEEN TENSILE AND COMPRESSIVE STRENGTH GAIN, ELIGEHAUSEN (2014).....	51
FIGURE 33 - UNIAXIAL TENSILE STRENGTH GAIN FOR VARYING CEMENT TYPES AND W/C RATIOS. KASAI (1971).....	51
FIGURE 34 - CRACK PROPAGATION INTERACTIONS OF CONCRETE IN TENSION .....	54
FIGURE 35 - A TYPICAL STRESS-DISPLACEMENT CURVE OF CONCRETE, (W = LENGTH OF CRACK ZONE) .....	57
FIGURE 36 - CYLINDER MOULDS, AND A DEMOULDED CYLINDER PRIOR TO THE REDUCED SECTION BEING STRIPPED .....	60
FIGURE 37 - COMPRESSION TEST SETUP, AND A TYPICAL FAILURE AT EARLY AGE (1 DAY) .....	60
FIGURE 38 - DIRECT TENSION TEST SPECIMEN, OVERALL DIMENSIONS OF 100MM DIAMETER, 200MM LONG.....	61
FIGURE 39 - TENSILE TEST SETUP, AND TYPICAL FAILURES OF TENSILE CYLINDER .....	62
FIGURE 40 - SPLITTING TENSILE CYLINDER TEST SETUP .....	63
FIGURE 41 - SPLIT TEST SETUP, AND TYPICAL FRACTURE .....	63
FIGURE 42 - STRESS-STRAIN CURVES OF CONCRETE IN DIRECT UNIAXIAL TENSION .....	64
FIGURE 43 - CONCRETE STRENGTHS OBSERVED IN THE 1ST BATCH OF CONCRETE ( $F'_c$ 20MPa) ...	64
FIGURE 44 - CONCRETE STRENGTHS OBSERVED IN THE 2ND BATCH OF CONCRETE ( $F'_c$ 40MPa) ...	65
FIGURE 45 - CONCRETE COMPRESSIVE STRENGTHS MEASURED FOR BOTH TESTS .....	65
FIGURE 46 - COMPARISON OF MEASURED INDIRECT AND DIRECT TENSILE STRENGTHS.....	66
FIGURE 47 - COMPARISON OF MEASURED DIRECT TENSILE STRENGTHS FOR BOTH BATCHES .....	66
FIGURE 48 - COMPARISON OF TENSILE/COMPRESSIVE RATIOS BETWEEN BOTH BATCHES .....	67
FIGURE 49 - PANEL INSERT EDGE AND SPACING MINIMA. B1-B5 8 ANCHORS PER BLOCK, B6-B8 3 ANCHORS PER BLOCK .....	70
FIGURE 50 – EXPERIMENTAL HEADED INSERT DIMENSIONS .....	70
FIGURE 51 - EXAMPLE OF THE REACTION FRAME TENSION RIG SETUP, ETAG 001 (EOTA 2013) APPENDIX A .....	73
FIGURE 52 - LOADING FRAME FOR THE SERIES OF TENSILE TESTS .....	74
FIGURE 53 - PULL-OUT TEST BLOCK AT 16 HOURS (SERIES B2) .....	75
FIGURE 54 - COMPARISON OF PREDICTED BREAKOUT STRENGTH VS. TESTED DATA .....	76
FIGURE 55 - TESTED VERSUS PREDICTED TO EQUATION 4 RESULTS .....	77
FIGURE 56 - PREDICATED AND TESTED CONCRETE TENSILE VS COMPRESSIVE STRENGTH .....	78
FIGURE 57 – TESTED VERSUS PREDICTED CHARACTERISTIC RESISTANCE, $N^0_{CB}$ , NORMALISED CONCRETE STRENGTH, CONCRETE CONE FAILURE ONLY (1 TO 14 DAYS, TEST SERIES B1-B6) .....	79

FIGURE 58 - PREDICTIVE MODELS FOR CAST-IN INSERT CONCRETE CONE CAPACITY AGAINST TESTED CHARACTERISTIC VALUES, $N_{u,c}^0$ .....	80
FIGURE 59 - ANCHOR WITH INTERNAL INTERLOCK AND THE BOTTOM ANCHOR WITH INTERNAL AND EXTERNAL INTERLOCK .....	83
FIGURE 60 - REINFORCEMENT LAYOUT .....	85
FIGURE 61 - TYPICAL TEST PANELS PRIOR TO CASTING .....	86
FIGURE 62 - PANEL PLAN INDICATING OPEN SPAN OF THE REACTION FRAME (EDGELIFT PLATE ANCHOR TESTS) .....	87
FIGURE 63 – VARIOUS $H_{EF}$ TESTED LOADS VS ACI318 (2008) AND AS3850 (SAI 2015) (TEST SERIES TA1 – TA4).....	88
FIGURE 64 – VARIOUS $H_{EF}$ TESTED LOADS VS EDGE MODIFIED CONE CAPACITY IN ACI318 (2008) AND AS3850 (SAI 2015) (TEST SERIES TA5-TA8) .....	88
FIGURE 65 - LOAD VS DISPLACEMENT CURVES FOR TEST SERIES TA1 - TA4 .....	89
FIGURE 66 - PANEL OF SERIES TA11 WITH FAILED HEADED ANCHOR.....	90
FIGURE 67 - TESTED TENSILE RESISTANCE VERSUS PREDICTED CHARACTERISTIC RESISTANCE OF CAST-IN EDGELIFT ANCHORS .....	92
FIGURE 68 - DISTANCE TO FOUR EDGES FOR EDGE REDUCTION MODIFICATION, FOR $C_{i,1}$ , $C_{i,2}$ , $C_{i,3}$ AND $C_{i,4}$ .....	93
FIGURE 69 - PANEL REINFORCEMENT LAYOUT IN RELATION TO THE LIFTING INSERT .....	95
FIGURE 70 - ANCHOR SPACING, $S_{i,N}$ AND EDGE DISTANCES, $C_{i,CR,N}$ .....	96
FIGURE 71 - ANCHOR TYPES .....	96
FIGURE 72 - SIDE VIEW OF MESH AND PERIMETER BAR PLACED CENTRAL .....	97
FIGURE 73 - SIDE VIEW OF DOUBLE LAYER MESH AND PERIMETER BARS.....	97
FIGURE 74 - SIDE VIEW OF TENSION BAR, MESH AND PERIMETER BAR PLACED CENTRAL.....	98
FIGURE 75 - TENSILE APPLIED LOAD RATE 20kN/MIN, 150MM THICK PANEL, AND OPEN SPAN 1.8M	98
FIGURE 76 - VIEW OF EP2 PANEL SETUP – TENSILE TEST .....	100
FIGURE 77 - VIEW OF EP6 PANEL SETUP – TENSILE TEST .....	100
FIGURE 78 - VIEW OF EP8 PANEL SETUP – SHEAR TEST .....	101
FIGURE 79 - TENSION PANEL REINFORCEMENT PLACEMENT, WHERE APPLICABLE.....	101
FIGURE 80 - PREDICTED CONCRETE FRACTURE CONE FROM A CAST-IN ANCHOR IN A THIN PANEL, TENSILE LOAD DIRECTION .....	102
FIGURE 81 - SERIES EP1 TYPICAL FAILURE, NO PANEL REINFORCEMENT .....	103
FIGURE 82 - SERIES EP2 TYPICAL FAILURE, N16 CENTRAL PERIMETER BAR .....	104
FIGURE 83 - SERIES EP3 TYPICAL FAILURE, N16 CENTRAL PERIMETER BAR, N16 X 90MM SHEAR BAR .....	105
FIGURE 84 - SERIES EP4 TYPICAL FAILURE, SL82 CENTRAL MESH, N16 CENTRAL PERIMETER BAR .....	105
FIGURE 85 - SERIES EP5 TYPICAL FAILURE, N12 DOUBLE PERIMETER BARS.....	106
FIGURE 86 - SERIES EP6 TYPICAL FAILURE, N12 DOUBLE PERIMETER BARS, SL82 DOUBLE LAYER MESH .....	106

FIGURE 87 - SERIES EP7 TYPICAL SURFACE CRACKS .....	107
FIGURE 88 - PANEL NEAR FACE FAILURE SURFACE OBSERVED FOR SERIES EP7 AND EP8 .....	108
FIGURE 89 - SERIES EP8 TYPICAL SURFACE CRACKS .....	108
FIGURE 90- CHARACTERISTIC TENSILE FAILURE LOADS AT VARIOUS CONCRETE STRENGTHS, $F_{C,AGE}$ , MPA .....	109
FIGURE 91 - CHARACTERISTIC SHEAR FAILURE LOADS AT CONCRETE COMPRESSIVE STRENGTHS, $F_{C,AGE}$ , MPA.....	111
FIGURE 92 - EDGELIFT ANCHOR REINFORCEMENT LAYOUT .....	117
FIGURE 93 - PLACEMENT OF EDGELIFT ANCHOR AND ANCHOR REINFORCEMENT IN A THIN WALLED CONCRETE PANEL .....	117
FIGURE 94 - EL1 - ANCHOR WITH NO REINFORCEMENT .....	119
FIGURE 95 – EL2 PRIOR TO INSTALLATION OF SHEAR BAR .....	119
FIGURE 96 – EL3 PANEL PRIOR TO INSTALLATION OF PERIMETER BAR WITH SL82 MESH .....	120
FIGURE 97 – EL4 & EL5 PANEL INSTALLED WITH EDGELIFT ANCHOR, SHEAR BAR, PANEL MESH AND PERIMETER BAR .....	120
FIGURE 98 - PANEL PLAN INDICATING OPEN SPAN TO THE REACTION FRAME (FOR EDGELIFT PLATE ANCHOR TESTS) .....	121
FIGURE 99 - EDGELIFT ANCHOR TEST REACTION FRAME SETUP .....	121
FIGURE 100 - TYPICAL LOAD VS DISPLACEMENT CURVES FOR EL1 .....	123
FIGURE 101 - EL1 NO REINFORCEMENT ANCHOR CAPACITY VS ACI318 (2008) AND AS3850 (SAI 2015) MODELS .....	123
FIGURE 102 - TYPICAL LOAD VS DISPLACEMENT CURVES FOR EL2 AND EL3 .....	124
FIGURE 103 - TYPICAL FRACTURE SURFACE OF EL2 AND EL3 POST ULTIMATE LOAD .....	125
FIGURE 104 - EL2 ANCHOR CAPACITY VS ACI318 (2008) AND AS3850 (SAI 2015) MODELS.....	125
FIGURE 105 - EL3 ANCHOR CAPACITY VS ACI318 (2008) AND AS3850 (SAI 2015) MODELS.....	126
FIGURE 106 - TYPICAL LOAD VS DISPLACEMENT CURVES FOR EL4 AND EL5 .....	126
FIGURE 107 - EL4 ANCHOR CAPACITY VS ACI318 (2008) AND AS3850 (SAI 2015) MODELS.....	127
FIGURE 108 - EL5 ANCHOR CAPACITY VS ACI318 (2008) AND AS3850 (SAI 2015) MODELS.....	127
FIGURE 109 - EL6 $H_{EF}$ 39MM HEADED ANCHOR CAPACITY VS ACI318 (2008) AND AS3850 (SAI 2015) MODELS .....	128
FIGURE 110 - EL6 $H_{EF}$ 50MM HEADED ANCHOR CAPACITY VS ACI318 (2008) AND AS3850 (SAI 2015) MODELS, (ACI318 AND AS3850 DATA ARE SIMILAR) .....	128
FIGURE 111 - EL6 $H_{EF}$ 55MM HEADED ANCHOR CAPACITY VS ACI318 (2008) AND AS3850 (SAI 2015) MODELS .....	129
FIGURE 112 - EL6 $H_{EF}$ 90MM HEADED ANCHOR CAPACITY VS ACI318 (2008) AND AS3850 (SAI 2015) MODELS (ACI318 AND AS3850 DATA ARE SIMILAR) .....	129
FIGURE 113 - PHOTO OF EL7 HEADED ANCHOR, $H_{EF}$ 70MM, FAILURE SURFACE .....	130
FIGURE 114 - CONCRETE BLOCK LAYOUT FOR HEADED INSERTS (2M X 2M X 150MM) FOR EL7 ...	130
FIGURE 115 - EL7 90MM HEADED ANCHOR CAPACITY VS ACI318 (2008) AND AS3850 (SAI 2015) MODELS (ACI318 AND AS3850 DATA ARE SIMILAR) .....	131

FIGURE 116 - TYPICAL CONCRETE FAILURE SURFACE .....	132
FIGURE 117 - RATIO OF TEST FAILURE LOAD TO PREDICTED CHARACTERISTIC RESISTANCE FOR EACH TEST SERIES .....	132
FIGURE 118 - PLAN VIEW OF A TYPICAL PANEL SETUP FOR EDGELIFTING .....	135
FIGURE 119 - SIDE VIEW OF A TYPICAL PANEL SETUP FOR EDGELIFTING .....	136
FIGURE 120 - VIEW OF A TYPICAL ANCHOR SETUP FOR THIN PANEL EDGELIFTING .....	136
FIGURE 121 - TYPICAL SHEAR PANEL SETUP PRIOR TO CONCRETE POUR .....	137
FIGURE 122 - PREDICTED CONCRETE FRACTURE CONE FROM A CAST-IN ANCHOR TO PANEL EDGE, SHEAR LOAD DIRECTION .....	138
FIGURE 123 - TYPICAL SHEAR BAR DESIGN.....	139
FIGURE 124 - THE SHEAR BAR BRIDGE IS SUBJECTED TO BENDING WHEN A SHEAR LOAD IS APPLIED .....	140
FIGURE 125 - SHEAR LOADS APPLIED IN A LATERAL TENSILE DIRECTION .....	141
FIGURE 126 - SERIES ES3 TYPICAL PANEL SETUPS.....	142
FIGURE 127 - SERIES ES7 TYPICAL PANEL SETUPS.....	143
FIGURE 128 - SERIES ES6 TYPICAL PANEL SETUPS.....	143
FIGURE 129 - SERIES ES2 TYPICAL PANEL SETUPS.....	144
FIGURE 130 - SHEAR LOADS APPLIED WITH 2.0M OPEN SPAN REACTION FRAME .....	145
FIGURE 131 - TYPICAL FAILURE SURFACE PROPAGATING TO THE PANEL THIN EDGE.....	146
FIGURE 132 - IDEALISED FRACTURE PATH AS STATED IN ACI318 (2008) FOR A SINGLE CAST-IN ANCHOR .....	146
FIGURE 133 - ESTIMATE FRACTURE PATH FROM TEST RESULTS .....	146
FIGURE 134 - ACTUAL FRACTURE SURFACE .....	147
FIGURE 135 – AVERAGE CAPACITY VS CHARACTERISTIC RESISTANCE OF TESTED REINFORCED CAST- IN EDGELIFT 75X16MM ANCHORS, 150MM PANEL .....	149
FIGURE 136 - SAMPLING FACTOR, $K_s$ , USED FOR SAMPLE SIZE OF THE TEST .....	150
FIGURE 137 - AVERAGE CAPACITY VS CHARACTERISTIC RESISTANCE OF TESTED UNREINFORCED CAST-IN EDGELIFT 75X16MM ANCHOR, 150MM PANEL .....	150
FIGURE 138 - LIFTING INSERT WITH STRAIN GAUGE POSITIONS.....	152
FIGURE 139 - STRAIN GAUGE LOCATIONS.....	153
FIGURE 140 - TYPICAL PANEL LAYOUT FOR TEST PANELS A & B.....	154
FIGURE 141 - TYPICAL PANEL SETUP FOR TEST PANELS C, D AND E.....	154
FIGURE 142 - REACTION FRAME BEING GREATER THAN 4 $X_{HEF}$ OPEN SPAN .....	155
FIGURE 143 - LOAD VS TIME FOR TESTED EDGELIFT ANCHORS 1 TO 6 (7 <sup>TH</sup> ANCHOR WAS REJECTED), REFER TABLE 25 .....	156
FIGURE 144 - POST TEST CONCRETE FAILURE.....	157
FIGURE 145 - POST-TEST EDGELIFT ANCHOR EXHIBITING NO PLASTIC DEFORMATION, ANCHOR 2 TEST PANEL D .....	157
FIGURE 146 - STRAIN V LOAD RELATIONSHIP FOR ANCHOR 2 TEST PANEL D .....	158
FIGURE 147 - STRAIN V LOAD RELATIONSHIP FOR ANCHOR 3 TEST PANEL C.....	159

FIGURE 148 - STRAIN V LOAD RELATIONSHIP FOR ANCHOR 4 TEST PANEL A .....	160
FIGURE 149 - STRAIN V LOAD RELATIONSHIP FOR ANCHOR 6 TEST PANEL B .....	160
FIGURE 150 - EDGELIFT ANCHOR LOAD SHARING %.....	161
FIGURE 151 – 20MPa TENSILE CAPACITY MODELS FOR VARIOUS EMBEDMENT DEPTHS.....	162
FIGURE 152 - CALCULATED BY VARIOUS MODELS VERSUS $N_{uc}$ TESTED IN ACCORDANCE WITH AS3850 (SAI 2015) APPENDIX B, HEF 257MM IN A 150MM PANEL (DOUBLE EDGE REDUCED) .....	163
FIGURE 153 - AVERAGE CAPACITY VS CHARACTERISTIC RESISTANCE OF TESTED, HEF 257MM CAST-IN EDGELIFT ANCHOR, N16x500MM TENSION BAR, 150MM PANEL .....	164
FIGURE 154 - INTERNAL SERRATIONS AND WAVY LEGGED EDGELIFT ANCHORS .....	164
FIGURE 155 - AVERAGE CAPACITY VS CHARACTERISTIC RESISTANCE OF TESTED, HEF 257MM, 150MM PANEL, NO SHEAR BAR, SL82 AND N16 PANEL MESH .....	165
FIGURE 156 - TESTED VS PREDICTED IN ACCORDANCE WITH AS3850 (SAI 2015) APPENDIX B, SERRATIONS TO INSIDE OF ANCHOR TEETH, HEF 257MM, 150MM PANEL, NO SHEAR BAR, SL82 AND N16 PANEL MESH .....	165
FIGURE 157 - AVERAGE CAPACITY VS CHARACTERISTIC RESISTANCE OF TESTED, HEF 370MM, 150MM PANEL, NO SHEAR BAR, SL82 AND N16 PANEL MESH .....	166
FIGURE 158 - TESTED VS PREDICTED IN ACCORDANCE WITH AS3850 (SAI 2015) APPENDIX B, SERRATIONS TO BOTH SIDES OF ANCHOR LEGS, HEF 370MM, 150MM PANEL, NO SHEAR BAR, SL82 AND N16 PANEL MESH .....	166
FIGURE 159 - LOAD RESISTANCE ELEMENTS OF AN ANCHOR SYSTEM IN A WALL PANEL,.....	175
FIGURE 160 - LIFTING SYSTEM MODEL FOR A THIN SECTION WALL PANEL.....	175
FIGURE 161 - RIGGING CONFIGURATIONS DETERMINING LOAD SHARING PER ANCHOR.....	176
FIGURE 162 - 2 ANCHORS HAVING THE SAME OVERALL LENGTH, BUT DIFFERENT EFFECTIVE EMBEDMENT DEPTHS, HEF .....	177
FIGURE 163 - 2 ANCHORS HAVING DIFFERENT CONCRETE LOAD INTERACTIONS, WHERE THE FOOTED ANCHOR IS MORE SUSCEPTIBLE TO SIDE BLOW-OUT IN THIN WALL SECTIONS .....	178
FIGURE 164 - TYPICAL TILT-UP FACELIFT SYSTEMS – THIN WALL PANELS OR THIN SECTION ELEMENTS REQUIRED TO BE FACE LIFTED .....	179
FIGURE 165 - TYPICAL GENERAL ELEMENT SYSTEMS – FACELIFT ANCHORS NORMALLY PLACED IN GENERAL PRECAST ELEMENTS .....	179
FIGURE 166 - TYPICAL EDGELIFT SYSTEMS – USED FOR THE MAJORITY OF WALL PANEL EDGELIFTING .....	179

## Thanks and acknowledgements

Firstly, I would like to thank my supervisor, Dr Natalie Lloyd, for her relentless commitment to my doctoral work. I thank her for the hours of advising me about the ways of testing regimes, civil engineering knowledge and research thinking. I also thank her for her ability to actively listen to my ideas about this research, and keeping me focussed, the revisions to my thesis, and her willingness to engage with me along my doctoral journey.

My work as Research and Development Manager at Reid Construction Systems involved me with many aspects relevant to this research; I am indebted to Robert 'Bob' Connell for his support of this research and his relentless desire to explore new boundaries. His support allowed me to start on this research journey, and begin my involvement in the revision of the AS3850 (SAI 2015) standard. This standard has been a major point in my career, and influential in my thinking within this research, whilst providing giving some industry relevance to this research.

I owe my thanks to Reid Construction Systems, now Ramsetreid, an Illinois Tool Works (ITW) company, for their financial support. Without this company's desire to examine new technologies, create innovative systems, and engagement in being a trusted advisor to industry, this research would not have been possible. I thank Tom Southall, Vice President of Innovation at ITW, for taking the time to acknowledge the significance of this research. Without innovative thinking within ITW, the potential of doing this kind of research would never have been possible.

Thanks to Professor Rolf Eligehausen and Dr Vladimir Cervenka for their time to listen to my crazy ideas, and genuinely contribute on my knowledge journey. I am in awe of all their work and hope this research puts a bit of knowledge into their already vast vault.

I owe my thanks to the Precast Concrete Institute for their support and willingness to hear an unknown Australian Engineer talk and present some of this research at their Tennessee conference. Having been through some of their precast training modules, I have found them to be an informative and supportive industry body, engaged to maintaining the concrete prefabricated concrete industry a leading construction method of choice.

I cannot thank my wife enough for her relentless patience over the last six years, where she has on many occasions been the sole parent to our lovely kids whilst I was away from home studying in Perth. Thanks to my kids for their support and understanding that this research has been another passion of mine that I've enjoyed immensely.

This page intentionally left blank



## Abstract

An extensive literature review of early age concrete material behaviour and concrete strength models highlights that research relating to early age concrete cast-in place anchors is very sparse. From the literature review it is evident that the early age concrete tensile strength is the predominant concrete material strength criterion influencing the performance of cast-in-place anchors, or more specifically the mechanical interaction of Edgelift anchors in a prefabricated concrete early age application. Additionally, design criteria for anchors are predominately grounded in research of headed anchors in mature concrete. The experimental research in this thesis addressed the research deficiency; performance in early age<sup>1</sup> concrete of Edgelift anchors.

The models presented in ACI318 (2008), Building code requirements for structural concrete, and AS3850 (SAI 2015), Prefabricated concrete elements, applicable to cast-in anchors include physical anchor and material parameters, anchor effective embedment depth,  $h_{ef}$ , and concrete compressive strength, either  $f'_c$  or  $f_{c,age}$ . Anchor bearing area and tensile strength of concrete are not included in the capacity models presented in these standards. This research highlights the significance of these currently excluded parameters that determine the load bearing capacity of a cast-in edgelift anchor. This research provides analysis and experimental evaluation of the concrete capacity models of ACI318 (2008) and AS3850 (SAI 2015) for the capacity design of cast-in Edgelift anchors performance.

A literature reviews of the typical concrete strength test methods and their application for early age concrete highlights the significance of concrete tensile strength for cast-in edgelift anchors. An experimental program examining uniaxial direct tension and splitting tensile test methods was conducted. These concrete strength test methods were compared for suitability in early age concrete lifting applications. Concrete compressive and tensile strength gain with age was experimentally assessed. This showed a variable strength gain relationship especially in concrete aged less than 3 days for various concrete mixtures types. The significance between the compressive

---

<sup>1</sup> 'Early age' is a term used throughout this thesis, and refers to concrete during its early stages of hydration, less than 3 days from water being added.

strength and tensile strength relationships for the concrete mixtures and testing load rates used in the experimental program showed that measuring concrete compressive strength was an adequate measure to estimate the failure of an edgelift anchor.

The experimental program tests cast-in headed anchors and compares the results against the published models in ACI318 (2008) and AS3850 (SAI 2015). The cast-in place headed anchor capacities in early age experimentation program includes headed anchors, at various embedment depths tested at early ages. Two concrete mix types and two applied load strain rates were also used in the test program and the test confirms changes in load carrying capacity of the anchors when different concrete mix designs are used. The strain rate, between 1 and 5  $\mu\epsilon/\text{min}$ , made no significant difference to the tested anchor capacities.

The cast-in Edgelift testing experimental testing of this research highlights the significance between the differences of tested and models included in current published models, mainly ACI318 (2008) and AS3850 (SAI 2105), and their suitability for early age concrete as used with cast-in-place Edgelift anchors. Furthermore, the test program explores the interaction and capacity contribution of various steel reinforcement configurations on cast-in-place Edgelift anchors in thin wall concrete panels.

Edgelift anchor capacities in early age experimentation program includes tensile and shear tests, with different steel reinforcement configurations, concrete mixtures and concrete ages. This series of tests involved the largest data set collected during this research (over 800 pull-out tests conducted) and details the load contribution various steel reinforcements has on edgelift anchors, for both tensile and shear load directions.

Edgelift anchor stress distribution experiments assess the load sharing capacity of an Edgelift anchor at early concrete age. The conclusion of this test series showed that at different positions along the length of the anchor, the bearing area of the anchor influences the stress distribution from the applied load. This load bearing area geometry of the edgelift anchor in turn influences the load carrying capacity of the anchor and the mechanical interlock with the concrete.

## 1. Introduction

This thesis provides details of research conducted into lifting anchor failures of concrete wall panels using cast-in-place Edgelift anchors. In addition to the eight hundred and four, 804, cast-in anchor tests and one hundred and fifty, 150, concrete strength experimental tests of this research, an extensive literature review has been included to highlight the relevant current literature which highlights the research gap that is the subject of this research. The results of this research will ultimately assist the design engineer when assessing the efficiencies of concrete wall panel cast-in-place Edgelift anchors in early age concrete and contribute to the body of knowledge of prefabricated concrete lifting.

Cast-in anchors are widespread in prefabricated concrete construction. One type of cast-in anchor is the Edgelift anchor used to lift prefabricated wall panels. Concrete elements, termed 'tilt-up panels' are defined as a flat concrete panels frequently cast in the horizontal position. Lifted by rotation about one edge until in a vertical position, they may then be lifted into position and incorporated into the main structure. The typical lifting of these panels is by means of placing a cast-in steel insert at the edge of the centre of the thin section, thus termed Edgelifting.

Research into the performance of cast-in headed anchors has been on-going since the 1970's to establish the load-bearing behaviour of cast-in place anchors, as a general performance model for cast-in anchors, as used in prefabricated concrete elements, Eligehausen (2014); Dao, et al (2009). The outcomes of the research into the general performance of cast-in headed anchors have been included in industry construction guidelines, such as ACI318 (2008) - Building code requirements for structural concrete, CEN/TR 15728 (ECS 2008) - Design and use of inserts for lifting and handling of precast concrete elements, and AS3850 (SAI 2015) – Prefabricated concrete elements. The Edgelift anchor concept was first introduced in the 1990's. Cast-in anchors can be loaded in various directions, such as shear, tension or combined loads, during a wall panel lift, and at various concrete strengths or phases of maturation due to different concrete ages during lifting, transportation and installation. However, experimental investigation of the failure mode due to different load combinations and the modelling of the early age concrete, especially after the initial crack has occurred, are scarce. The way the material responds at the onset of a crack, the concrete material strength properties in early age, how they are

determined from tests, and how they relate to cast-in place Edgelift anchors are not previously researched in detail despite existing design guidelines based upon earlier research on headed anchors. Engineering judgement is adopted when different anchor configurations are not covered within industry guidelines, which is the default design position in relation to Edgelift cast-in place anchors in early age concrete.

### **1.1. Problem statement**

Cast-in anchors are used extensively in civil engineering mainly in lifting structural and non-structural concrete elements. Such inserts allow for a wide application and are flexible in dimensions such as embedment depth, edge distances and the use of supplementary reinforcement. Typical applications are lifting inserts for concrete wall panels. In general, the actions placed on the lifting inserts are axial tension or shear. Applying the action with a lever arm, or with an eccentricity to the centre of the insert, results in a bending or torsional moment.

Mature age concrete testing data is transferred to design of inserts at early concrete ages without experimental verification of the veracity of models to be applied at early age or the veracity of safety factors used in design. In addition to this, previous research extensively conducted on inserts in tension (e.g. pull out tests) have been transferred to shear loaded inserts without significant experimental verification.

Some recent in-depth studies on inserts have been performed Fuchs, et al (1995) and Anderson, et al (2007). However, many questions related to inserts loaded in shear at early concrete age remain open. For instance, questions regarding the behaviour of edge lift anchors in tension, shear and combined loading conditions, the impact of reinforcing configurations on anchor capacity, and the influence of concrete maturation on the failure mechanism.

### **1.2. Aim**

This research aims to establish the behaviour of Edgelift inserts loaded in tension and shear with different combinations of reinforcing steel configurations in the panel, with differing torsional moments, and thus propose design guidelines for industry application. A number of objectives were articulated which were met via experimental

investigations and numerical studies. The outcomes of these objectives were the generation of design recommendations.

The objectives of the research were:

1. Establish the concrete tensile capacities at early concrete age using statistical analysis of results from tests of headed anchors as described in the American Concrete Institute code ACI318 (2008), reference section D5.2. The significance of early age concrete tensile strength versus compressive strength are to be defined.
2. Evaluate the correlation between capacities of Edgelift anchors tested in early concrete age and the predicated capacity using the Concrete Capacity Design model AS3850 (SAI 2015), Appendix B. This evaluation involved different reinforcing configurations and applied load rates, concrete mixture designs and at early age concrete strengths.
3. Determine the stress distribution along the length of the cast-in edgelift anchors and consider how this relates to mechanical interlock, concrete crushing and stresses.

### 1.3. Scope

This thesis presents experimental research conducted on the load-bearing behaviour of cast-in place Edgelift inserts in prefabricated wall panels in early age concrete. All panels were tested at early ages, mostly less than three days old, and anchors were subjected to a range of loading in panels with varying reinforcing configurations. This research addresses the current deficiencies in research on this specific type of anchor capacity and the influence of concrete maturation on the failure mechanism.

Design provisions are available to calculate the resistance for most of the standard applications of anchors including shear loaded anchors. However, these calculation methods included within some industry guidelines may not be conservative for anchors loaded in immature concrete, as they are derived from the application of data published for headed anchors in mature concrete ACI318 (2008) Appendix C. The most common design method in current literature is termed the Concrete Capacity

Design, CCD, model published in Europe and America since the 1980's. A limitation of the CCD methodology, in addition to its derivation from tests in mature concrete, is that it has been developed from tests in Europe where the concrete large aggregate is mostly smooth rounded river pebbles. In Australia the large aggregate is mostly rough cut quartzite, which differentiates itself as mechanical interlock is a significant failure mode when compared to river pebbles and adhesion at similar stress levels, and especially when the concrete paste has lower fracture energy than the shear capacity of quartz aggregate. Limited experimental data is available for anchors tested in concrete with coarse aggregates such as experienced in Australia and this research addresses this current limited Australian context data.

Modern high performance concretes have low water cement ratios and often include silica fume, SF (Mindess, et al 2002). Early age high strength cements are commonly used within the prefabricated concrete industry. These factors result in dramatically increased cracking sensitivity in comparison with ordinary Portland cement and normal strength concrete. The reasons are the increased autogenous deformation, the high rate of heat development and a higher brittleness of these high performing concretes. Therefore, the mixes used throughout this research are high early strength silica fume concrete mixes typical in the prefabrication industry, and detailed in Table 6.

### **1.4. Overview of this Research**

An extensive testing program was conducted and is detailed in this thesis. Test data is provided for cast-in lifting applications which are not covered in current design standards since it is known that these anchor configurations are used in practice and this specific design guidance is not included in industry guidelines. This is worthwhile to extend the applicability of current design methods for cast-in inserts currently used in practice but outside the scope of existing design literature.

Experimental test data including failure load and crack development patterns and finite element numerical analysis are compared in the discussion chapters of this thesis. The experimental and numerical studies were used to compare the load-bearing behaviour of the anchors and to analyse the accuracy to predict cast-in place Edgelifit anchors capacities in early age concrete.

As concrete hydrates its strength progressively increases, this strength may be indicated by the compressive or tensile strengths, fracture energy, modulus of elasticity, and/or stress strain relationship. To establish the concrete strength of the mixtures, tests using established methods, like Brazilian, three-point bending, direct or indirect tests were used. The fracture mechanism, cohesion, adhesion, mechanical interlock or shear, are influenced by the time since hydration started and the ingredients included in the concrete mixture. Establishing the fracture mechanisms of a particular concrete mix is explored in this research by comparing a direct tensile test and an in-direct tensile test. This test data was used to define the significance of the tensile strength test method, but to also further the knowledge of the significance between the compressive and tensile strength relationships in early age concrete.

At concrete early age, the failure mode, or crack pattern, relies heavily on the cohesion and adhesion properties of concrete paste, and further still the mechanical interlock of the large aggregate. As the concrete matures, these failure modes become less dominant, as the shear strength of the concrete mix is the predominant mode of failure.

### **1.5. Structure of this thesis**

The literature review, Chapter 2, examines the relevant issues within the prefabricated concrete wall element industry that provided the motivation to research failure mechanisms of concrete wall panel cast-in place edgelifit anchors. The issues include the applications, what performance expectations are needed of the anchors in the design of wall panels, some of the assumptions made from the model codes that the designs are based, and an extensive review of the material properties of early age concrete. Chapter 3 is a literature review of concrete test methods, where the results were used to define the significance of the tensile to compressive relationship at early age concrete strengths.

The test program of this research was designed to evaluate the significance of the assumptions made when selecting early age concrete material properties and cast-in anchors' performance at early ages. The experimental program consists of a series of 7 series of experiments, which are detailed in chapters 4 and 5.

## 1 Introduction

The 2 experiments in chapter 4 explores the significance between the compressive and tensile strength gains in early age concrete and the comparison of performance of headed anchor when compare to the models published in ACI318 (2008) and AS3850 (SAI 2015). The series of test programs involved the following:

- Concrete tensile strength relevance to cast-in headed inserts, (section 4.4, test series A1 – A3)
- Cast-in headed anchor experimental research, (section 4.2, test series B1 – B10)

Section 4.1, details the experimental concrete tensile strength gains during early age concrete, as well as experimental tests which compare the compressive strength gain and tensile strength gain at various concrete ages. There are 150 concrete tests (mainly tensile strength) conducted in this section. These series of tests are referred to as A1 – A3.

Section 4.2 includes a sample size of 140 tests to challenge the early age concrete assumptions made by adopting the commonly used Concrete Capacity Design model, where an unrestrained pull-out of headed anchors is conducted. Embedment depth and concrete compressive strength are the two parameters included in the CCD calculation of anchor pull-out capacity (effective anchor embedment depth and characteristic concrete compressive strength), and it is these two parameters that are extensively tested to evaluate the early concrete strength significance using the CCD model. These series of tests are referred to as B1 – B10.

Chapter 5 details the 5 series of experiments, including 664 individual tests, conducted to establish the tensile capacity effect different steel reinforcing configurations around various cast-in edgelift anchor has at various concrete compressive strengths and concrete mixes.

Each experiment in this series of tests explores the fracture characteristics of different failure mechanisms. Cast-in place Edgelift insert performance in early age experimental research, Chapter 5, including:



## 1 Introduction

- Edgelift test 1 – Anchor shape and configuration experimental program (section 5.1, test series TA1 – TA11)
- Edgelift test 2 – Panel Reinforcement influence of failure loads (section 5.2, test series EP1 – EP8)
- Edgelift test 3 - Influence of anchor reinforcing on failure loads (section 5.3, test series EL1 – EL7)
- Edgelift test 4 – Anchor reinforcement influence on shear failure loads (section 5.4, test series EL1 – EL7)
- Edgelift test 5 - Stress distribution along an edgelift anchors length (section 5.5, test series A - G)

Section 5.1 includes a series of tests on Edgelift inserts to research the prediction of capacity in early age concrete. These tests include the results of 150 tests conducted on 3 anchor types at various concrete compressive strengths and concrete maturity ages. Of the 3 types of anchor there is (a) 3 anchor embedment's depths,  $h_{ef}$ , with internally serrated teeth, (b) 1 anchor with wavy legs, (c) 7 anchor embedment's depths,  $h_{ef}$ , as headed anchors. This series of tests are referred to as TA1 – TA11.

Section 5.2 experimental program was conducted with one anchor type (internally serrated teeth) and one embedment depth, and with various steel reinforcement, both steel complimentary (attached to the anchor and part of the cast-in anchor configuration), and steel supplementary reinforcement (not attached to the anchor, but traversing across the anticipated concrete fracture surface) at various concrete compressive strengths and one concrete mixture. 110 tests are included in this section. This series of tests are referred to as EP1-EP8.

Section 5.3 includes 269 tests, where the tests include 154 Edgelift anchor tests and 115 headed anchor tests. This is research assessed the effect of various panel steel reinforcement compared against a series of cast-in headed anchor tensile tests, to relate the cast-in Edgelift anchor performance against the published headed anchor CCD model in ACI318 (ACI 2008) and AS3850 (SAI 2015). This test series included various cast-in headed anchors effective embedment, and one type of cast-in Edgelift

anchor, all at various embedment depths, concrete compressive strengths and reinforcement configurations. This series of tests are referred to as EL1 – EL7,

Section 5.4 assesses one type of cast-in Edgelift anchors performance subject to a load applied in a shear direction, which is the first loading a concrete wall panel experiences as it is lifted from the casting bed. This experiment was conducted using variable panel thicknesses, various steel complimentary reinforcements and various concrete compressive strengths. 126 tests are included in this section. This series of tests are referred to as ES1 – ES7.

Section 5.5 is an experiment on a single cast-in Edgelift anchor using strain gauges along the legs of the anchor, while loading the cast-in anchor in tension. There are 9 tests in this series. The assessment of the tests shows the stress distribution along the length of the cast-in edgelift anchor that will be typically experienced and how this related to mechanical interlock, concrete crushing and stresses that may be induced on the surrounding concrete to the anchor. This series of tests are referred to as A – G.

The discussion and analysis section of this thesis combines the issues highlighted in the literature review and discusses the significance between published models and the physical tested results. Performance models are discussed within this section. Specific design consideration in relation to prefabricated concrete panel lifting and transportation, specific to edgelift anchors, is included in Appendix A. All the test data conducted in this research has been tabulated and included in Appendix B.

## **2 LITERATURE REVIEW – Cast-in place Anchors**

The design of inserts for multiple anchor configurations loaded in shear is guided by current standards for post installed mechanical anchors, which is not the case for cast-in edgelift anchors in early age concrete, as typically used in the prefabricated concrete industry. Depending on the location of the cast-in insert (bulk concrete or close to a concrete element edge) as well as the geometry and material properties of the anchor, the failure strength is governed by either steel, concrete cone capacity or pry-out failure. Recommendations are available to calculate the resistance for all three failure modes. Basic equations to calculate the strength of single anchors failing due to concrete cone in concrete, differs depending on the design standard used for the verification especially for non-direct tensile load directions. The simplified models as presented in the current codes are readily accessible and practical for everyday use in comparison to fracture mechanics principles. In fracture mechanics, design is based on multiple regression analysis and a best curve model fitting with test data and may be impractical for everyday design situations. In addition, the material parameters that govern the capacity of concrete are Modulus of Elasticity and Fracture Energy whereas the design engineer has access to the physical attributes of the inserts, such as embedment depth, and readily measurable concrete properties, such as concrete compressive cylinder strength.

The literature review summarizes and critically examines the current design methods and their limitations when applied to Edgelift anchors, highlights the use and limitations of fracture mechanics for the capacity determination of Edgelift anchors and reviews early age concrete properties that have an impact on the capacity and design of Edgelift anchors.

### **2.1. Design considerations for cast-in place edgelift anchors**

This section outlines design considerations in the definition of a load resistance model for cast-in-place edgelift lifting anchors. “Design of products is normally based on resistance models giving the product properties as a function of the geometry and the properties of the material used in the product. The resistance model normally expresses the mean value of the property when the mean values of the parameter

## 2 LITERATURE REVIEW – Cast-in place Anchors

are inserted into the model. It is assumed that the same model expresses the characteristic value or the design value of the property if characteristic values or design values of the parameters are inserted in the model.” CEN/TR 14862 (ECS 2004). Currently cast-in-place edgelifit anchors do not have a resistance model that defines the product properties as a function of its geometry.

Since lifting inserts are not permanently loaded and are used for transportation and erection, and up to the time the concrete element is fixed into the permanent structure, the international structural codes do not consider them. In Europe, Australia and North America, to date, there does not seem to be a mandate to work on bridging this gap.

The European guidelines for design and use of inserts for lifting and handling of precast concrete elements, CEN/TR 15728 (ECS 2008), includes guidance on the design and identification of lifting inserts, the selection with their intended application, assembly and installation conditions, quantitative data used to determine the actions on lifting inserts, methods for determining applied load resistance through the insert and from reproducible test results, and finally analysis of test data methods. In this standard the load resistance model is calculated using formulae and generalized graphs, which have been derived by regression analysis on the basis of parameters selected by a few manufacturers of inserts. Hence the data set has a bias towards the design geometry from these manufacturers lifting inserts. Further to this additional supplementary reinforcement was not considered in any of the models, therefore the failure modes types would not have been considered in order to derive the formulae, or assessed in the interpretation of the graphs. In other words, actual test results and all contribution factors would not have been evaluated in the derivation of the insert load resistance model. This would have the effect of manufacturers publishing conservative load capacities when they use the models proposed in this European standard.

Lifting insert load capacity considering factors such as: element weight, suction during initial lift, dynamic loads during lifting and element placing and the applied load from the sling angle, are considered in National Code of Practice for Precast, Tilt-up and concrete elements in building construction Safe Work Australia (2016). In the latest revision of the Australian Prefabricated Concrete Element Standard, AS3850 (SAI 2015), now considers these aspects. National Code of Practice for Precast, Tilt-up and concrete elements in building construction BS8110 (BCI 2010) does not state the

## 2 LITERATURE REVIEW – Cast-in place Anchors

data to be collated by the manufacturer to define the rated anchor capacity or the safety factors that should be applied, whereas the equivalent Australian Standard AS3850 (SAI 2015), takes these considerations into account. Again the similarities cross paths when considering the load resistance, which can be determined by calculation or by test, where the inserts are loaded to failure and global safety factors applied.

In all standards, when considering the evaluation of ultimate load data, it is not articulated why test data can be considered from a mean value or 5% fractile, as opposed to failure mode and its associated reliability/repeatability index. It is not articulated as to why the minimum samples sizes of test data vary between codes, and a sample size of 1 may be used, as was published in the Australian Standard for Tilt-up concrete construction AS3850 (SAI 2003).

Testing conditions such as the geometry of the test rig or loading rate were not considered in Safe Work Australia (2016) and AS3850 (SAI 2003). Both these factors can be altered and it is hypothesized that it may significantly influence test outcomes.

This ambiguity leads to the added confusion where manufacturers of similar lifting inserts may publish technical specifications for use in identical applications can vary. All of these considerations are present, not through bad engineering, but through the lack of extensive research and evaluation of failure mechanisms induced by lifting inserts in concrete. Cast-in place lifting inserts require a rated capacity whilst embedded in early age concrete. There are many unanswered questions as to the evaluation of the compressive and tensile strengths in early age concrete (less than 3 days old) and the reliability of the concrete behaviour at these strengths.

### **2.1.1 Background**

Before failure mechanisms can be established, a standard test method should be established. Here the available knowledge that defines tests methods for Edgelifting is used in Europe and America, and was not included within the Australian suite of Standards until AS3850 (SAI 2015) was published. The definition of a test method that is practical for anchor manufacturers, relevant to industry practice, and is adequately similar to actual practice by prefabricated concrete manufacturers, increases the relevance of anchor test results and published rated capacities.

## 2 LITERATURE REVIEW – Cast-in place Anchors

A design guide for post-installed and cast-in-place headed anchors was published for Fastenings to concrete and masonry structures, State of the art CEB (TTL 1997) and has become the suitable reference text for a design model for cast-in-place headed anchors. As such these models should only be applied whilst considering design performance of post-installed and cast-in-place headed anchors.

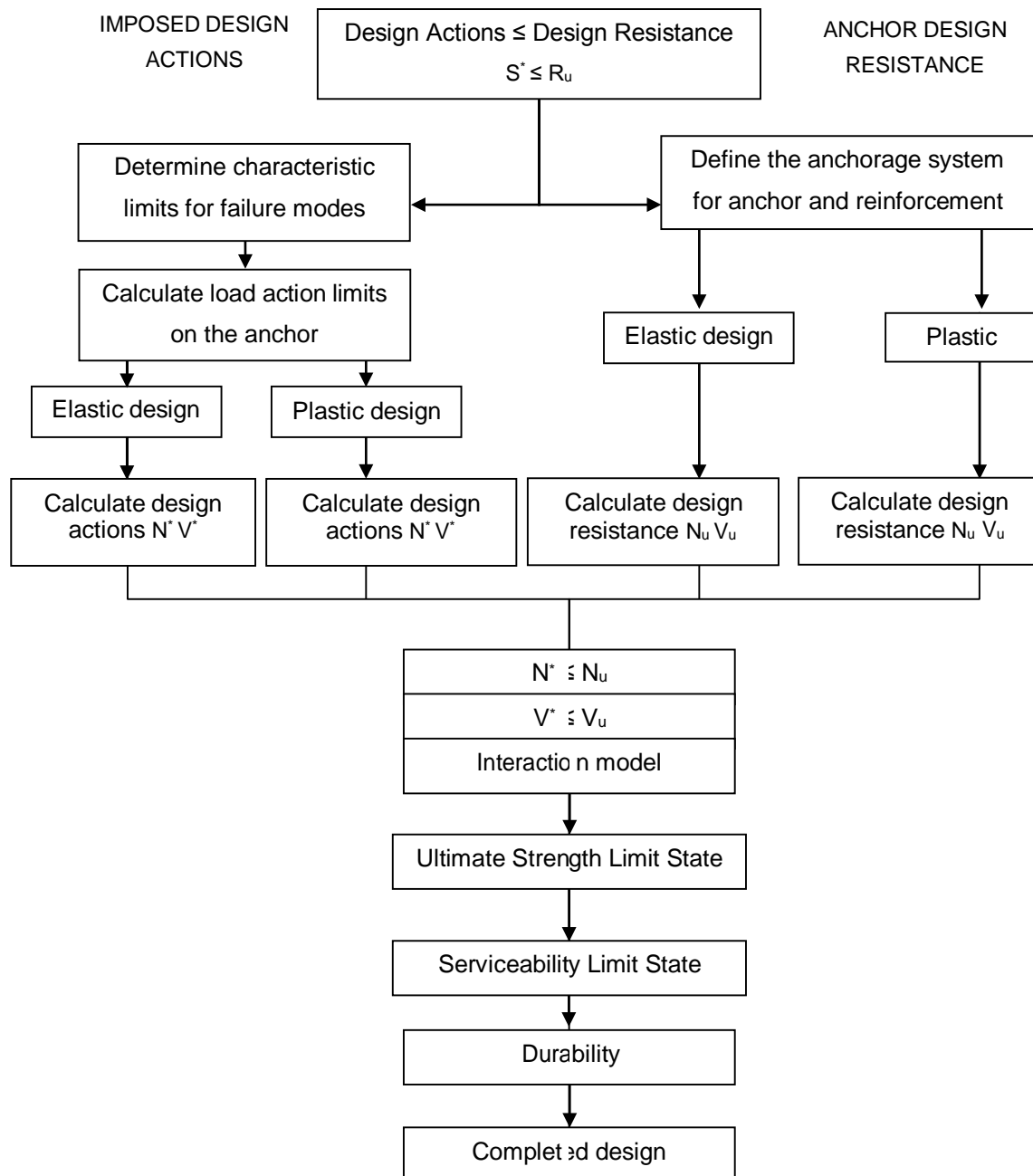


**Figure 1 - Adapted Design flowchart for post-installed and cast-in-place headed anchors, CEB (TTL 1997), 233, revised edition of Bulletin 226, part 1**

Assuming that actions imposed on the element are defined by the lifting design engineer, the resistance to these loads is defined by the anchor manufacturer. Plastic

## 2 LITERATURE REVIEW – Cast-in place Anchors

resistance to load should only be applied when failure is governed by ductile steel failure of the anchor. Whereas the action effects on an anchor at the concrete surface should be calculated according to an elastic analysis from the action effects on the insert. Static elastic analysis should be considered when brittle concrete failure is expected, which is in the majority of failure modes, refer to Figure 2 which shows the various steel components of a cast-in Edgelift anchor system that contribute to the overall capacity.

Optimal ductility of an anchor can be determined by the degree of load redistribution, which is tested in Chapter 5.5. In plastic analysis the ductility must be adequate to accommodate yielding in the tension direction. When ductile behaviour of anchors is experienced, the elastic design approach is a conservative one.

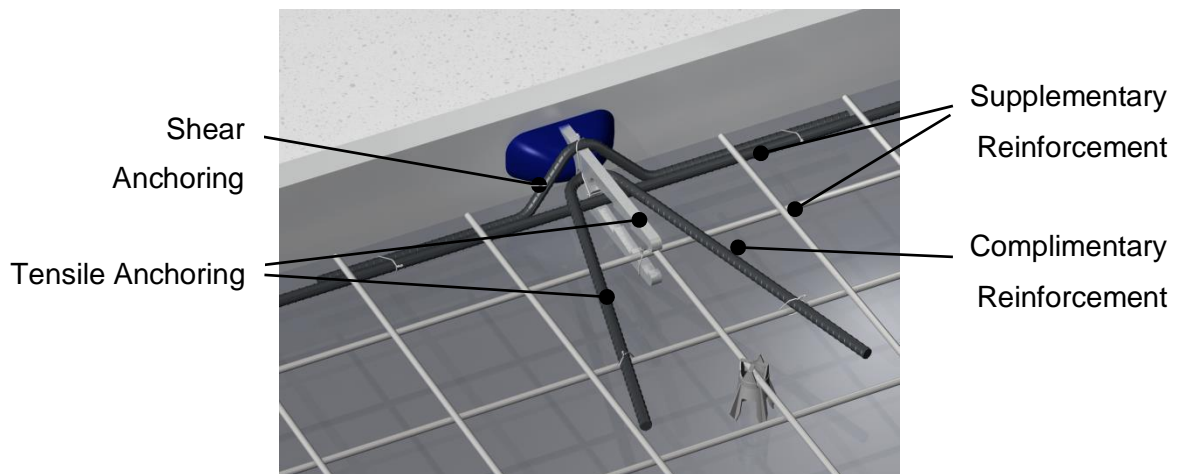


**Figure 2 - Load resistance model of an Edgelift anchor system in a wall panel**

According to the safety concept of partial safety factors, as applied in Australian Standards, where Design Actions  $\leq$  Design Resistance, ( $S^* \leq R_d$ ), should be used for all load directions on the anchor (tension, shear, combined shear and tension) as well as for all failure modes (steel failure, pull-out failure and concrete failure). As Edgelift anchors are connected when the load is applied via anchor clutches, 100% shear loads are not normally achieved. Different anchor designs will determine the absolute ultimate shear/tensile limits that would be experienced during the load cycle. This interface will establish an interaction model defined by the manufacturer.

## 2 LITERATURE REVIEW – Cast-in place Anchors

The intent of this section is to define the design considerations of load resistance models for cast-in-place edgelifth anchors, as per the flowchart depicted Figure 3. Further load cases that should be considered by the lifting design engineer are serviceability limit state, durability and fatigue, which are not included in the CEB (TTL 1997) guidelines, but should be assessed in accordance to the relevance of the application.

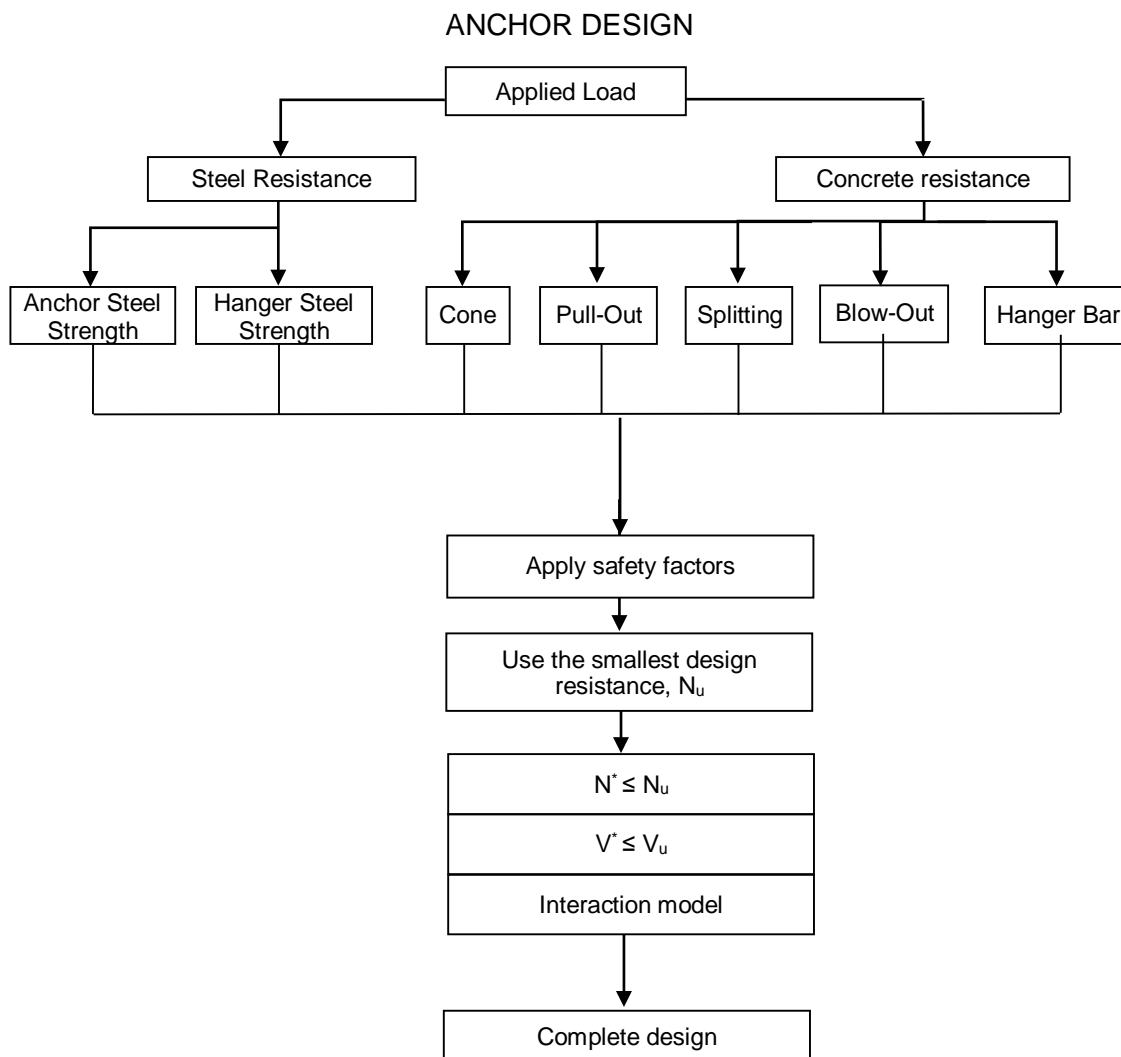


**Figure 3 - Adaption of a flowchart for calculating characteristic resistances of inserts with headed anchors with special reinforcement: elastic design approach, CEB (TTL 1997)**



### 2.1.2 Concrete resistance

Every anchor will have a load reduction factor applied in certain circumstances, like anchor spacing and edge distances, leading to various capacities that change with certain parameter variables. For example, headed foot anchors have a tendency to overload concrete cover when close to an edge, hence is more susceptible to side blow-out, Figure 4, or pull-out failure, Figure 5, than a hairpin style anchor.

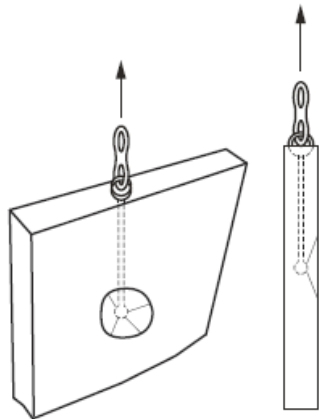
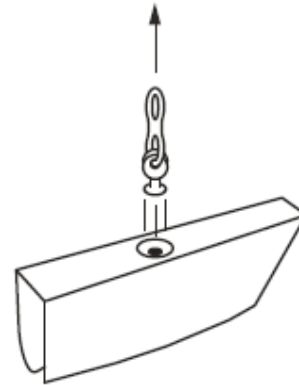


**Figure 4 - Concrete blow-out failure,  
AS3850 (SAI 2015)**

**Figure 5 - Pull-out failure,**



**AS3850 (SAI 2015)**

The edgelifit anchor may not be loaded in shear, where the anchor clutch loads the anchor in a moment couple, Figure 6. The load sharing, between full tensile to full shear, will be different proportions for each anchor style, and the geometry of the attached anchor clutch. The interaction models detailed in the current codes allow for the fact that a steel plate (a connection) can load the anchor in shear, hence a total capacity at the two extremes is shown a 100% tensile + 20% shear through to 20% tensile + 100% shear. Whereas for an 'embedded' cast-in-place edgelifit style anchor the shape of the anchor/clutch connection means that the anchor will never get to 100% tensile, or 100% shear, when the panel is lifted from the horizontal to vertical positions. At present the interaction for these anchor types have not been researched extensively, and therefore generalised models have been included in the published design models.

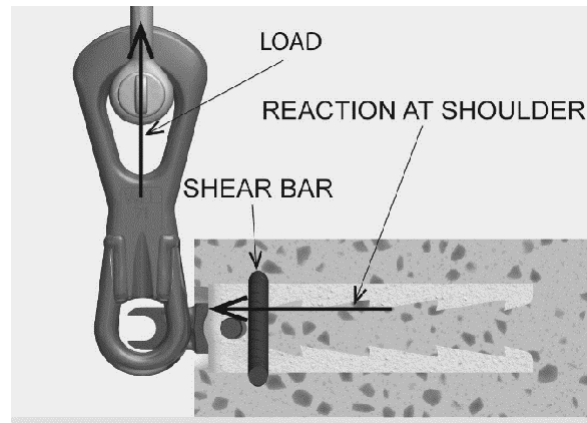


Figure 6 - Edgelifit plate style anchor interaction with lifting clutch

### 2.2. Cast-in headed anchor design and their historical development

Two similar methodologies have been published to predict brittle tension failure of a cast-in headed anchor, being the 45° conical failure surface method PCI (P/PCI (2004) and a square-pyramidal failure surface method with a 35° inclination ACI318 (2008). For the 45° cone method the concrete strength of an anchor is calculated assuming a conical surface (Figure 7) taking the slope between the failure surface and the concrete surface as 45°. As the depth of embedment of the lifting insert increases, the area of the conical section increases proportionately up to the point of full embedment. Following this capacity guideline and test data, it has been stated that an embedment depth of 8 to 10 times the anchor shank diameter, for headed anchors, was required for the concrete breakout strength to be larger than the tensile strength of the steel in headed anchors CEN/TR 15728 (ECS 2008). In relation to Edgelifit hairpin anchors the minimum stress area that interlocks with the concrete can be matched by total area to follow the design recommendation minimum area. Eligehausen at al (1990) proposed to calculate the capacity of anchors subjected to tension, shear and combined loads. The resulting recommendations included using a conical failure surface to calculate the tensile strength and were adopted in ACI 355 (2007). The design strength of concrete for insert was based on a uniform tensile stress of  $\phi_t$  ( $0.4 \sqrt{f_c}$ ). The resistance factor,  $\phi_t$  was 0.65. The Precast/Prestressed Concrete Institute, PCI, adopted the conical failure surface to predict a brittle failure of the concrete and this method was retained in the revised PCI (2004). However, PCI later adopted the provisions in ACI318 (2008) which are based on Concrete Capacity

## 2 LITERATURE REVIEW – Cast-in place Anchors

Design (CCD), to calculate the tensile strength of anchors assuming un-cracked concrete. In the CCD method the concrete strength of a single anchor is calculated assuming a four-sided pyramid failure surface, with a slope between the failure surface and the surface of the concrete member of  $35^\circ$ . The more recent versions of ACI318 (2008) use this approach.

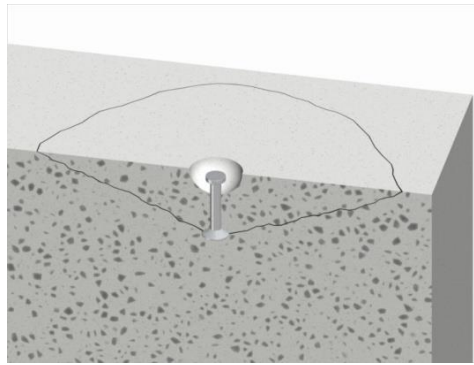


**Figure 7 - Conical failure surface of PCI Handbook, (PCI (2004))**

A comprehensive state-of-the-art of cast-in-place and post installed anchors are included in ACI 355 (2007), and examples using ACI318 (2008) & CEB (TTL 1994). These reports summarize the basis for current, general insert provisions of embedded anchors subjected to tension and tension plus shear interaction.

In the PCI editions, there have been several formulations to compute the tensile strength of an anchor. A conical failure surface for an anchor in tension was adopted up to PCI (2004), as presented in Table 1 with a resistance factor of 0.85. As discussed earlier, PCI (2004) changed the approach to a four sided pyramid cone, adopting a similar formulation to ACI318 (2008), though working with coefficients related to un-cracked concrete. The results given by PCI (2004) then correspond with results given by the ACI318 (2008). The expressions used to calculate the pull-out and breakout strengths are presented in Table 1, presenting the 5% fractile formula (which is used as the nominal strength formula) for PCI 5th and distinguishing between the 5% fractile (nominal strength) formula and the average formula for the ACI318 (2008) (CCD method), since the average formulae of CCD may be found elsewhere. PCI (2004) adopted the ACI318 (2008) formulas in the particular case of un-cracked concrete. The nominal strength (5% fractile) formula used in ACI318 (2008) Appendix D for anchoring, such as Wollmershauser (2004) reported, presents a 90% confidence that 95% of the anchor ultimate loads exceed the 5% fractile value. The formulas are

## 2 LITERATURE REVIEW – Cast-in place Anchors

summarized in the Table 1 for the various editions of codes and handbooks. These formulae will be used throughout this thesis to compare against the tested anchor capacities.

**Table 1 - Different published CCD models used as comparable models throughout this research**

	Concrete Capacity Design Models
Eligehausen, et al (1990)	$0.217 \left( \frac{f_c}{f_{ct}} \right)^{2/3} (h_{ef})^2$ <p style="text-align: right;"><b>Equation 1</b></p>
ACI318 (2008) (5% fractile)	$24 \lambda \sqrt{f_c} (h_{ef})^3 \phi$ <p style="text-align: right;"><b>Equation 2</b></p>
AS3850 (SAI 2015)	$13 \beta \sqrt{f_{ct}} (h_{ef})^{3/2}$ <p style="text-align: right;"><b>Equation 3</b></p>

$f'_c$ - 28 day characteristic concrete compressive strength

$\phi_{crack}$ - concrete crack modification factor (1.25 for non-cracked) for break-out strength

$h_{ef}$ - effective embedment of the cast-in anchor

$\lambda$ - light-weight concrete modification factor

$\beta$  - Anchor shape modification factor

$f_{ct}$  - Characteristic concrete compressive strength at time of test

### 2.3. Non-headed cast-in anchor design guidelines

Design methods provide guidance on the design of a cast-in anchor system (normally headed foot anchors) and essentially details simplified models of typical failure modes. ACI318 (2008), Appendix D contains provisions for cast-in headed bolts, L-bolts, and J-bolts, as well as the common “welded-stud” anchors. There are also inclusions for post-installed (drilled-in) mechanical anchors, specifically undercut anchors, torque-controlled expansion anchors, and displacement-controlled expansion anchors (drop-in). ACI Committees 318 and 355 has both adhesive anchors (and grouted anchors) and some of the newer post-installed anchor systems not previously addressed in ACI318 (2008) Appendix D. Edgelift style anchors have not been included by these committees and demonstrate the level of research, and publically available information, relating to the failure modes of these anchors and their respective mechanical interlock behaviour’s in concrete.

## 2 LITERATURE REVIEW – Cast-in place Anchors

The long standing acceptance of the 'cone' type failure for a Headed anchor is well regarded and predictive models are available as detailed in preceding section. When the insert system deviates from a typical headed anchor the concrete cone becomes a different shape and the mechanical interlock between concrete and steel changes. While relationships of insert capacity to concrete strength and effective embedment are well researched and might not appear complex, it is unreliable to apply an empirical model that was derived for simple concrete insert mechanisms, like headed anchors. But this maybe the case with some anchor manufacturers where they have insufficient test data to use for their particular anchor and reinforcing configurations. If an anchor manufacturer does not employ an extensive testing regime that verifies the anchor capacity, the capacity derivation method they ordinarily employ is based on standards such as ACI318 (2008).

The mechanism of interactions between steel and concrete is complex for concentrated loads being transferred between steel and concrete. Add to this the complexity of compression and tension stresses in three dimensions, and different anchor applications, it becomes uneconomic to conduct physical testing for all applications.

A load capacity derivation approach is not to rely on complex theory to predict all possible interactions when determining anchor capacities, but to reliably analyse and interpret a set of controlled experimental data to statistically establish a lower bound of test data repeatable test. This data set should also be defined from predetermined boundary conditions, for example  $f_{c,age}$ , embedment, age of concrete, anchor bearing area, shear anchoring, anchor clutch geometry, et al.

Regarding Edgelifting thin wall panels, a reliable predictive model is not currently standardised, and the designer/manufacturer is required to rely solely on in-house and individual manufacturer testing to derive lifting insert capacities. It is this full scale testing that has not been detailed sufficiently in research literature or encapsulated in the Australian standards to provide a consistent and repeatable test method between manufacturers. European and American standards provide for more information to assist the definition of testing methodologies for particular anchor designs.

## 2 LITERATURE REVIEW – Cast-in place Anchors

It is the intent of this section to highlight the issues around the design differences between Edgelift anchors and those models defined in current standards. The technology of Edgelifting is complex and largely manufacturer controlled and commercially driven to the point that there is limited published research.

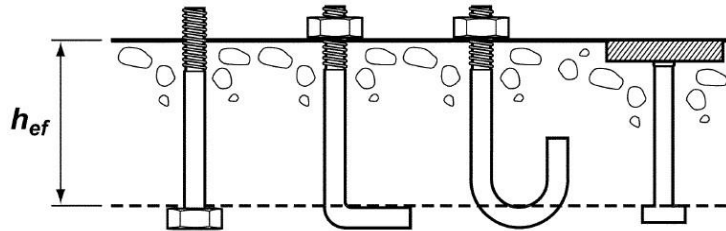


Figure 8 - ACI318 (2008) Appendix D (Fig RD.1) Cast-in anchor types

### 2.3.1 Concrete Capacity Design

In 2002 the American Concrete Institute, ACI318 (2002) Appendix D introduced a new design method into the world of anchoring to structural concrete. Commonly referred to as the Concrete Capacity Design (CCD) method, it is actually much more; the concrete capacity being just one aspect of this method. Australian, European and American codes reference ACI318 (2008), and whichever code is adopted; the same anchor design methodology applies.

The predictive model of the CCD method is derived from a series of experimental studies, which were conducted to determine the failure mechanism of a headed anchor loaded in tension, as is depicted in the below Figure 9. Whilst conclusions from these studies vary slightly, it is generally agreed that the concrete failure cone begins in a highly stressed area next to the cast-in insert foot at a load. There is no conclusion on the nature of the final failure mechanism, which determines the ultimate failure load. The discussion remains un-resolved about crack formation, propagation and toughening mechanisms in the fracture process zone.

When assessing the test data for headed anchors, as detailed in ACI228.1R (2003), detailed that the failure process zone is formed due to 'crushing' of concrete in a narrow band between the insert foot and the surface of the concrete element. Meaning the ultimate load may be directly related to the compressive strength of the concrete. Dao, et al (2009) concluded that the ultimate load is a factor of the fracture toughness of the concrete mix. In another study Khan, et al (2002) found that before ultimate load, circumferential (conical) cracking extends from the foot of the insert to the

## 2 LITERATURE REVIEW – Cast-in place Anchors

concrete surface, and that the applied load is resisted by aggregate interlock across the failure surface, otherwise termed post failure mechanical interlock. This failure mode was measured when sufficient aggregate particles had been dislodged from the mortar mix, and the ultimate load was concluded to be not directly related to compressive strength or tensile capacity of the concrete. Alternatively, there is good correlation between ultimate load and compressive and/or tensile strength, as both variables are a function of the mortar mix, where Figure 9 depicts a non-linear finite element model that was confirmed by observation by the researchers Dao, et al (2009). The primary crack stopped propagating when it reached a non-tensile zone. A secondary crack then begins to form and propagates within the tensile zone, closer to the surface. This research concludes that the ultimate load is not directly associated by the compressive strength of the mix, but the failure crack path is directly related to the stress zones in the concrete.

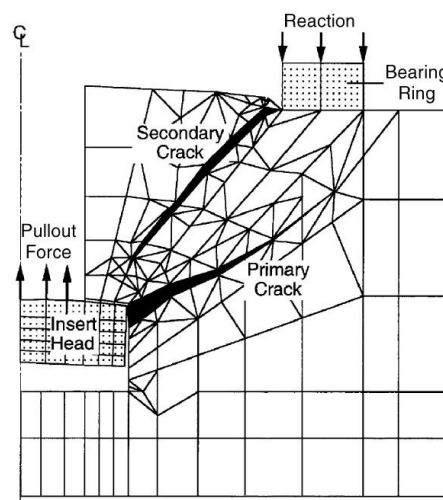


**Figure 9 - Conical cracks predicted by non-linear fracture mechanics analysis of pull-out tests, Dao, et al (2009)**

To add to the discussion, the question arises as to if headed inserts develop the majority of their capacity from the tensile properties of concrete. Since the precast industry conducts a concrete elements initial lift while the concrete is less than 3 days old, knowledge around the failure mechanisms that occur in green concrete become particularly relevant during this early concrete age. Direct uniaxial tensile properties are independent of compressive strength within the first 3 days from the onset of hydration Dao, et al (2009).

## 2 LITERATURE REVIEW – Cast-in place Anchors

However, concrete capacity design models used to predict failure are largely based on generalized simple concrete failure models that are correlated directly to compressive strength and insert embedment depth. The research in this thesis examines how the capacity of cast-in inserts in early age concrete is impacted by the fracture properties of the concrete at early age, where the tensile and compressive strength are parameters that only partially represent the fracture properties of early age concrete.

### **2.3.2 Models defined by the Standards**

The ACI318 (2008) cast-in insert capacity design approach is based on strength design as opposed to the guidelines of AS3850 (SAI 2003) providing allowable load information based on mean values divided by a safety factor. Both the older ACI load factors and the factored load combinations found in Chapter 16 of the International Building Code have two sets of strength reduction factors corresponding to a variety of failure modes (steel failure, concrete cone failure, etc.). Design strengths predicted by this method are generally based on the lower normally distributed 5% of calculated test results. The design resistance of anchors must equal or exceed design loads calculated from the given applied load combinations, including in-service loads for cast-in anchors and post-installed anchors. ACI318 (2008) further allows the design resistance provided by anchors to be determined from the characteristic of the derived loads in tension and shear (determined separately) for performance.



## 2 LITERATURE REVIEW – Cast-in place Anchors

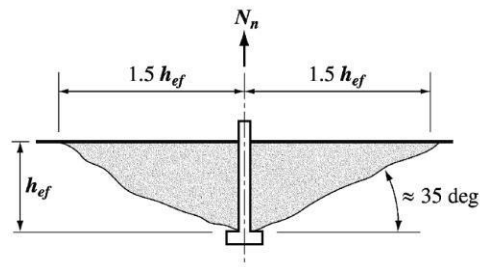


Figure 10 - ACI349.2R (2007) D.4.2.2 Breakout cone for tension

Tension considerations;

- Steel strength of the anchor and anchorage stiffness
- Concrete capacity in tension load direction
- Pull-out strength of the anchor
- Concrete blow-out capacity (cast-in anchors only)

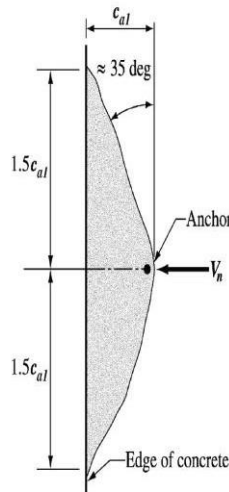


Figure 11 - ACI349.2R (2007) D.4.2.2 Breakout cone for Shear

Shear considerations;

- Steel strength of the anchor
- Concrete capacity in shear load direction
- Pull-out strength of the anchor

Anchor performance modification factors, cracked or reinforced concrete and use of statistical test data are three anchor model considerations published by the American Concrete Institute ACI318 (2008). This ACI standard allows anchor load resistances to be modified, including proximity to an edge, eccentric loading, and spacing to other anchors or lightweight concrete. The load resistance can be increased by use of a  $\Psi$ -factor if the anchor is to be placed in a location that is not expected to crack under service loading. Strength reduction factors ( $\phi$ ) are given to account for seismic loading (ACI reduction factor of  $\phi = 0.75$ ), whether the anchor is governed by a ductile (higher

## 2 LITERATURE REVIEW – Cast-in place Anchors

$\phi$ ) or brittle (lower  $\phi$ ) failure, or whether there is additional supplementary reinforcement (panel reinforcement/mesh, or shrinkage reinforcement) present that will reinforce the concrete cone back into the concrete.

Secondly the American Concrete Institute ACI318 (2008) expands on this further, where the cast-in anchors are designed for specific locations in a concrete element, being where cracking may be expected to occur (tension zones), or zones that are not expected to crack (compression zones) during the service life of the anchor. The basic underlying assumption of ACI318 (2008) Appendix D is that the anchors maybe located in a tension zone (cracked concrete). If the concrete will not crack under service loading, then anchors for non-cracked concrete can be used and a higher capacity is allowed. This design method allows a design for single and multiple anchors, where both maybe subject to combined tension and shear loading.

Thirdly, the calculated or reported capacities according to the methods of ACI318 (2008) Appendix D, are not mean ultimate capacities, but are characteristic capacities (5% fractile) that have a 90% probability of being exceeded by 95% of the population. For systems exhibiting normal scatter (Co-efficient of Variation between 5 & 10%), the characteristic capacity is approximately 75% of the mean anchor capacity. If the test results are tightly grouped (yielding a low coefficient of variation), the characteristic capacity is close to the calculated mean capacity. Conversely, if the test results indicate a wider scatter in the data, then the characteristic capacity is further from the calculated mean capacity. Thus, an anchor system which is consistent in its performance is rewarded with a higher capacity, while a less-consistent anchor system receives a lower capacity. This scatter uses a Coefficient of Variation (standard Deviation  $\div$  Mean Ultimate Load) as the factor that must be considered when establishing the anchor performance.

Failure types denoted in ACI318 (2008) Appendix D, Fig RD.4.1, refer below figures,

## 2 LITERATURE REVIEW – Cast-in place Anchors

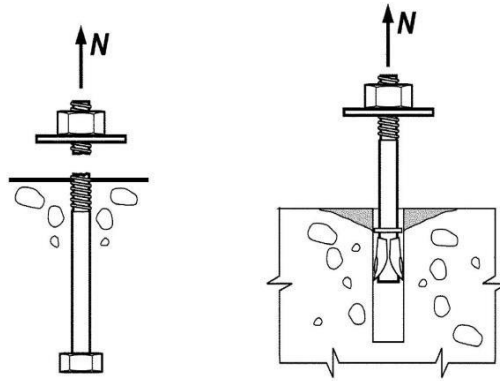


Figure 12 - Tensile Failure Type i) Steel Failure, ii) Pull-out

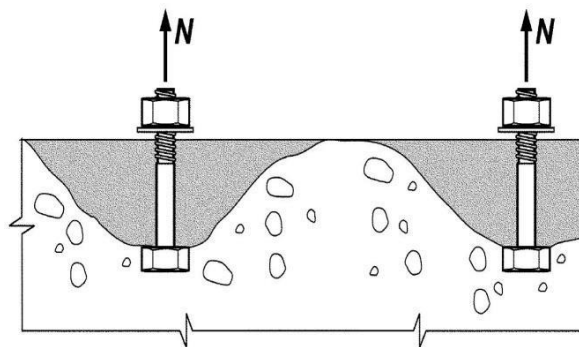


Figure 13 - Tensile Failure Type iii) Concrete Cone

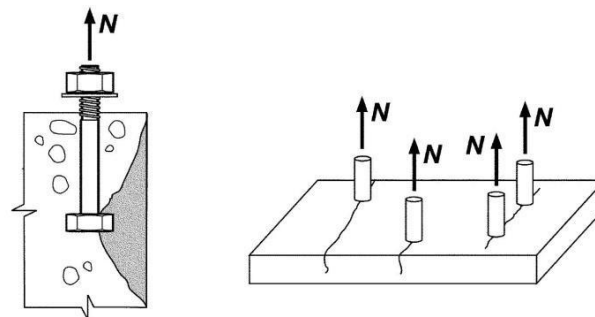


Figure 14 - Tensile Failure Type iv) Side-face blowout, v) Concrete Splitting

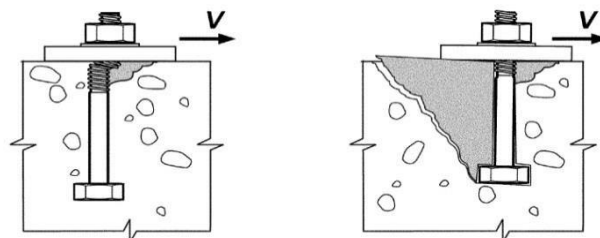
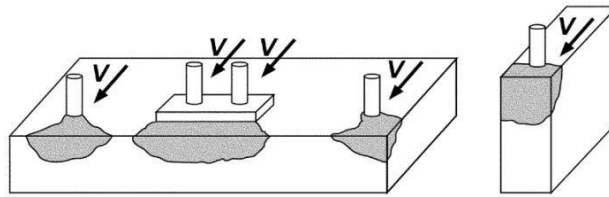


Figure 15 - Shear Failure Type i) Steel failure preceded by concrete spall, ii) Concrete pry-out with no anchor edge reduction



**Figure 16 - Shear Failure Type iii) Concrete breakout**

### 2.3.3 Summary of design models used for cast-in Edgelift anchors

The main body of accepted anchor performance data originates from CCD and the published work from Elgehausen, et al (1990). The CCD research has been published from the 1970's to date, where cast-in headed anchor designs were used to establish this published data.

The American Concrete Institute, ACI349.2 (2008), and European Standards, BSI8110 (BCI 2002), CEN/TR15728 (ECS 2008), and E-TAG001 (EOTA 2006) have all adopted the principles of the CCD research as the basis for cast-in headed anchor calculations. These standards, including Standard Australia AS3850 (SAI 2003), does not adequately cover cast-in-place Edgelift anchors.

Cast-in headed and post-installed mechanical anchors have established worldwide use and application, as well as being able to utilise significant test data and academic research, which makes it appropriate to use predictive models. Load resistance data derived from characteristic values, mean values and minima should be sufficient to develop a reliable predictive model. Since cast-in-place non-footed type anchors vary widely in design, an example being shown in Figure 17, the concrete steel interaction relating to mechanical interlock with concrete can vary widely between anchor designs. For each anchor design, sufficient test data is needed to determine the load capacities and to develop a generalized (non-product specific) design capacity model.

The models adopted in this research for the evaluation of test data against published model are those highlighted below and their suitability for use with Edgelift anchors similar to that in Figure 17.

## 2 LITERATURE REVIEW – Cast-in place Anchors

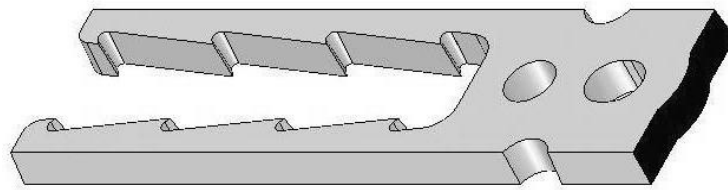


Figure 17 - Typical plate style Edgelift anchor used in thin concrete wall panels

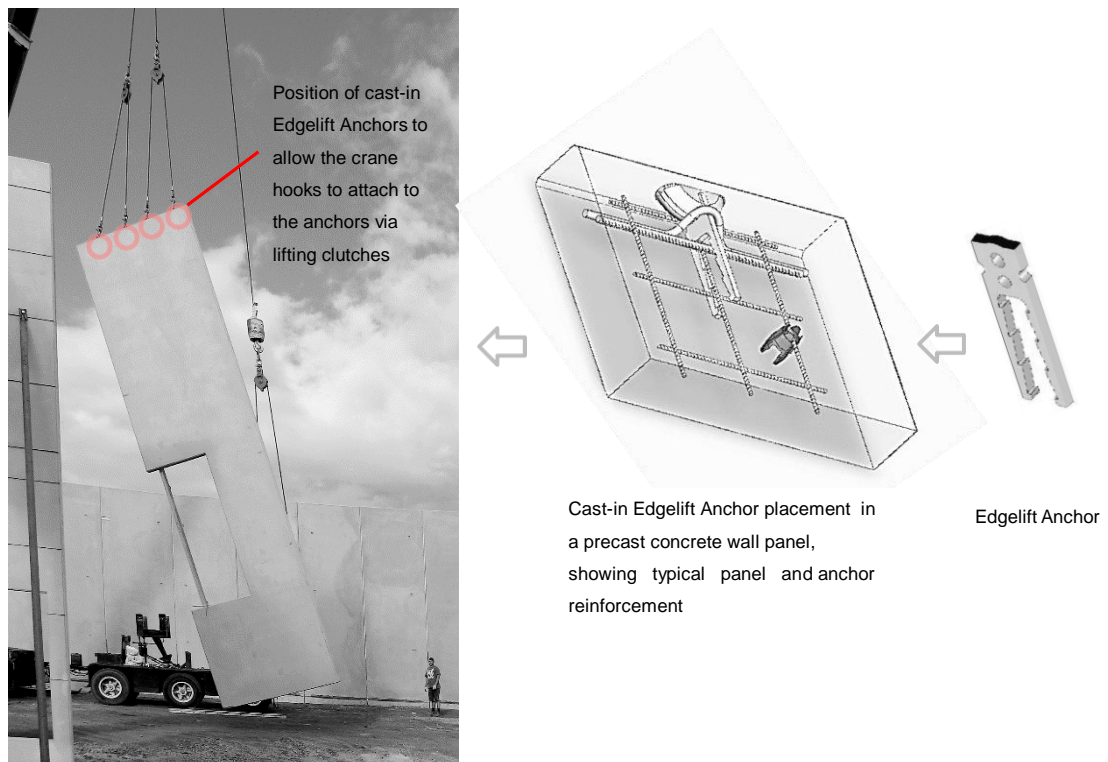


Figure 18 - Concrete wall panel being lifted, and placed vertically into the building structure

The capacity models presented in AS3850 (SAI 2015) are listed below as the comparison against these will be made in the test section of this thesis.

### 2.3.3.1 Concrete cone capacity

$$P_{t0} = \beta_{t0} \cdot P_{c0}$$

Equation 4

$\beta_{t0}$  = tension shape modification factor for concrete cone failure  
 = 1.0 for a reference headed cast-in insert  
 = value determined from testing for other cast-in inserts

## 2 LITERATURE REVIEW – Cast-in place Anchors

$$F_{t,Rk} = \chi \cdot \sqrt{f_{ctd}} \cdot (h_{ef})^{3/2}$$

Equation 5

Where

- $\chi$  = factor relating to the condition of concrete (cracked or un-cracked)
- = 10 for headed cast-in inserts in cracked concrete
- = 13 for headed cast-in inserts in non-cracked concrete

### 2.3.3.1.1 Insert edge distance

$$A_{c,N}^0 / A_{c,N}$$

Equation 6

Where

$A_{c,N}^0$  = projected concrete failure area of a single insert of height  $h_{ef}$  and base length  $l_{cr,N} = 3h_{ef}$  where the distance to an edge is equal or greater than  $1.5h_{ef}$

$$= l_{cr,N} \cdot h_{ef}$$

$l_{cr,N}$  = critical spacing to ensure adjacent inserts do not influence characteristic tensile resistance of the insert

$c_{i,cr,N}$  = minimum edge distance required to achieve the characteristic tension load resistance

=  $1.5 h_{ef}$  for headed cast-in inserts according to current experience

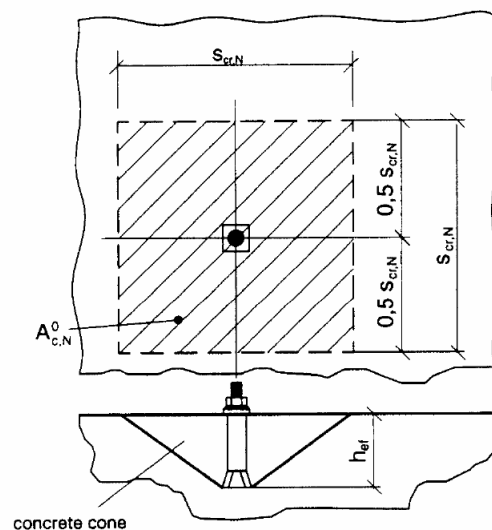


Figure 19- Idealised single edge truncated failure cone, ETAG 001 (EOTA 2013)

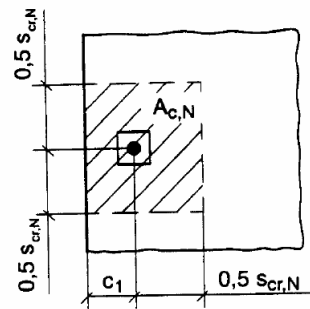


Figure 20 - Actual projected area of the idealized concrete cone at the edge of a concrete element, ETAG 001 (EOTA 2013)

As distance to the edge,  $c_1$ , is less than  $1.5 h_{eff}$ , then the edge distance reduced projected concrete failure area,  $A_{c,N}$ , (see figure 10) is:

$$A_{c,N} = (c_1 + 1.5 h_{eff}) \cdot (2 c_1 + 1.5 h_{eff})$$

Equation 7

### 2.3.3.1.2 Effect of a thin wall

$$h_{eff} = \frac{h_{eff}}{h_{eff}} \cdot h_{eff}$$

Equation 8

Where

- $h_{eff}$  = modified effective depth of embedment for narrow elements
- $c_1$  = maximum distance from centre of an insert to the edge of element
- $c_1 < 1.5 h_{eff}$
- $c_{min}$  = minimum value for edge distance to achieve characteristic tensile resistance

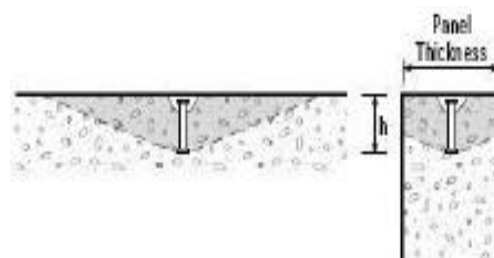


Figure 21 - Edge reduction effect in thin walled panels

### **2.4. Prefabricated wall panel lifting design**

When it comes to dimensioning and tolerance of precast elements, the guidelines are detailed in various industry guidelines PCI (2004) and AS3850 (SAI 2003). These documents ensure that in-service, serviceability, manufacturability and durability of the concrete element are suitably designed and manufactured in a safe way. It is the considerations of lifting, transportation and placement where the guidelines and design regulations are not specific to allow a consistent approach by designers and specifying engineers. This is further exaggerated by the fact that regulations may contain statements like, “refer to the manufacturers specification for the design of lifting anchors...”, where the design methods and compliance testing of these products are not controlled by a prescriptive approach. State of the art information has not been sufficiently researched and documented for public review for there to be an industry accepted approach. Therefore, there are various conflicting interpretations that can be taken from the existing applicable standards for Load Case and Load Resistance calculations.

#### **2.4.1 Edgelift Insert – testing to derive capacity**

Lifting design if done correctly will consider many aspects which should be considered through the transportation load cycle of the concrete element. The considerations should cover the lifting system components and the load resistance components, refer to Appendix A – Lifting Design. Using suitably qualified and experienced engineers is certainly recommended as the consequences of getting the lifting design incorrect can be fatal. Efficiencies can be gained from getting the lifting design correct, by optimizing the number of anchors, correct reinforcement detail of the element, the correct selection of the anchor type and the minimizing the complexities of the load resistance components.



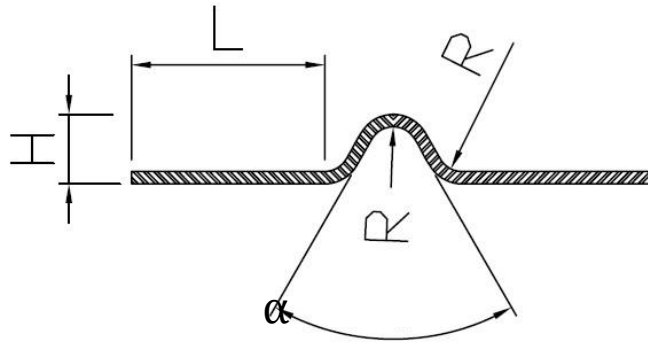


**Figure 22 - Typical shear bar design**

Shear bars, typical to the above, Figure 22, are used to increase the shear capacity of Edgelift anchors. A typical shear bar is defined with variables such as height,  $H$ , (which is a function of embedment depth of the Edgelift anchor in the shear direction) leg length,  $L$ , (which is related to the stress development length) and the bend angle,  $\alpha$ , (which is required to clear the anchor void and allow the shear bar to sit in a position minimising the bending stresses of the bar). The mandrel diameter used to bend the shear bar, if cold bent, is limited to at least  $4 \times$  the diameter of the bar, in accordance with AS4671 (SAI 2001).

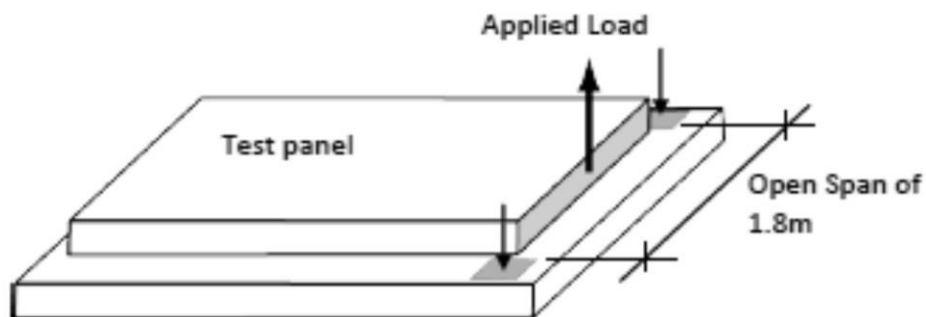


**Figure 23 - Typical test panel arrangement to measure lateral tension capacities of Edgelift anchors**

When a load is applied to the anchor, as shown in the above Figure 23, the shear bar is initially subject to bending, especially at the centre of the bridge which is in contact with the anchor.

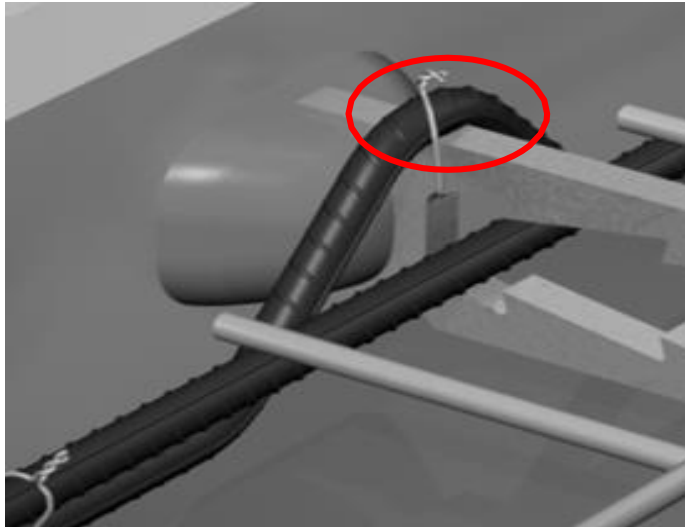


**Figure 24 - The shear bar, as shown, is subjected to bending with an applied shear load**

When the shear bar is being installed into the panel formwork it is important for the installer to ensure that the bend radius sits in contact with the anchor, as highlighted in Figure 24, and is adequately tied in. In the case where there is a gap between the anchor and shear bar at this point, and a shear load is applied, the anchor can move until it engages the shear bar, and the concrete will crack around the head of the anchor. Special care should be taken during the test setup to ensure the shear bar is suitably tied in. This is done by first tying in the shear bar bridge prior to tying in the shear bar legs.

### **2.5. Cast-in Edgelif anchor individual load resistance components**

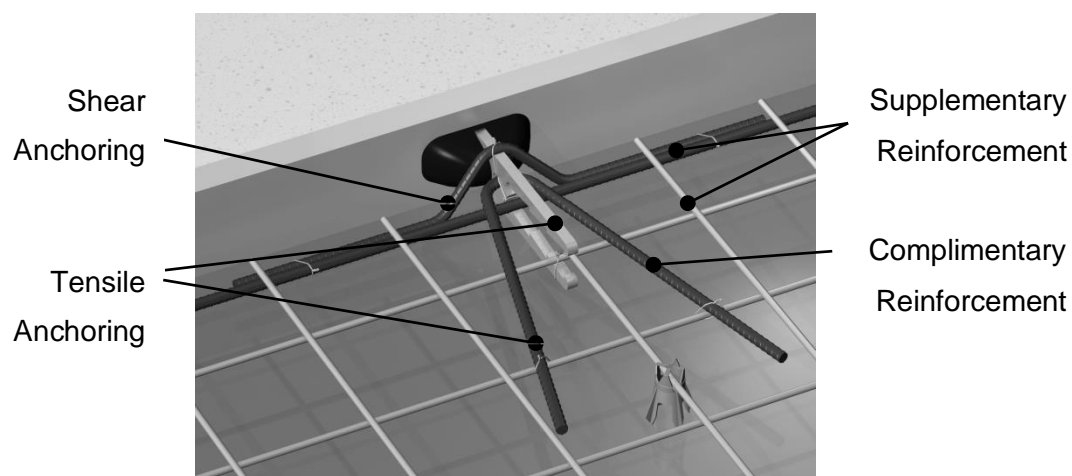


**Figure 25 - Load resistance model of an edgelif anchor system**

### 2.5.1 Edgelift anchor - Cracked or un-cracked concrete

In the design of reinforced concrete flexural or tension components, a cracked tension zone is assumed because concrete possesses relatively low tensile strength, which may be fully or partly used by internal or restraint tensile stresses not taken into account in the design. There is sufficient documented evidence which demonstrates that crack widths resulting from quasi-permanent loads (a dead load plus a factored live load) do not exceed ~0.3mm to 0.4mm. These crack widths are acknowledged as permissible. Wider cracks are to be expected under maximum permissible service loads, which according to Elgehausen, et al (1990), reach ~0.5mm to 0.6mm. Even wider individual cracks can occur under conditions of restraint if no additional reinforcement has been included to limit crack widths.

As a practical position from an anchor design perspective, the precast concrete element designer should calculate the flexure in a concrete element and include additional reinforcement to not induce a crack  $> 0.4\text{mm}$  prior to placement of the panel. There should be an additional Limit State Factors (LSF) applied to the Ultimate Load Capacity Elgehausen (2014) and ACI318 (2008) suggest a 25% reduction in ultimate capacity, if flexure induces a crack  $> 0.4\text{mm}$ . On the other hand, if there is sufficient reinforcement in the element to keep the flexural cracks  $< 0.4\text{mm}$  then anchor un-cracked Working Load Limits, WLL, are sufficient.

AS3850 (SAI 2015), Appendix B defines a practical capacity derivation, including provision of other failure modes that should be assessed with cast-in anchors. Where the characteristic ultimate tensile strength is determined from the 5%-fractile of the ultimate loads and assuming a normal distribution with unknown standard deviation and a confidence level equal to 90% in the assessment of the described modes of failure.

## 2.6. Current performance models – assumed concrete behaviour

The compressive, splitting and bond strength for concrete at early ages has been the subject of limited research. The relationships between compressive strength and

## 2 LITERATURE REVIEW – Cast-in place Anchors

splitting strength are influenced by different temperature profiles, and the degree of hydration of the cement paste Dao, et al (2009).

Gardner (1990) studied the tensile strength capacity material property development of young concrete with the incorporation of fly ash and proposed some empirical formulas.

Testing has previously researched the tensile strength measurements of early age concrete, and determined the differences in mechanical properties for normal and high-strength concretes Iso-Ahola, et al (2012).

A complete stress-strain curve, published by Iso-Ahola,et al (2012), is used as an example to show the mechanical property differences between early age and mature concrete, shown in Figure 26. This curve demonstrates the behaviour of concrete under an external force. Curves at ages 18hours, 1, 2, 3, 7 and 28 days are represented in Figure 26. There are significant differences in the shape of the compressive stress-strain response at various ages. The slope of the ascending part of the stress-strain curve becomes steeper for the concrete after 7 days for Normal Strength Concrete (NSC), and after 2 days for High Strength Concrete (HSC), and so does the slope of the descending part. As the compressive strength increases, both the ascending and descending portions of the compressive stress-strain curve become steeper and more linear, which implies that the concrete becomes more brittle as the age increases. Noise in the curve can be observed, which is as a consequence of micro-crack propagation. It was seen that the modulus of elasticity increases with age.

## 2 LITERATURE REVIEW – Cast-in place Anchors

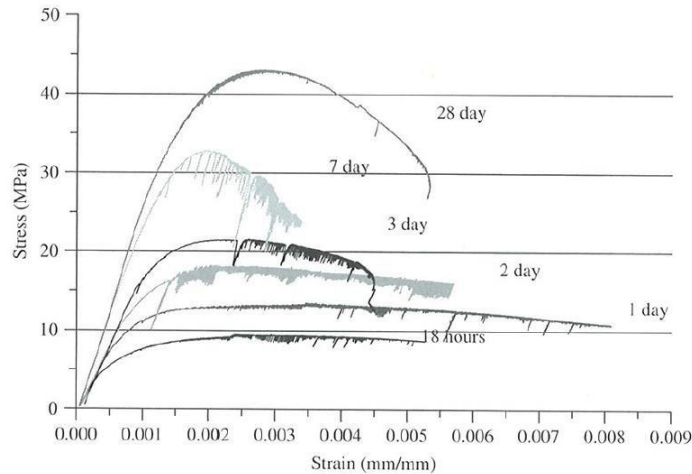


**Figure 26 - Advanced Concrete Technology: Complete stress-strain curve of NSC, Iso-Ahola, et al (2012)**

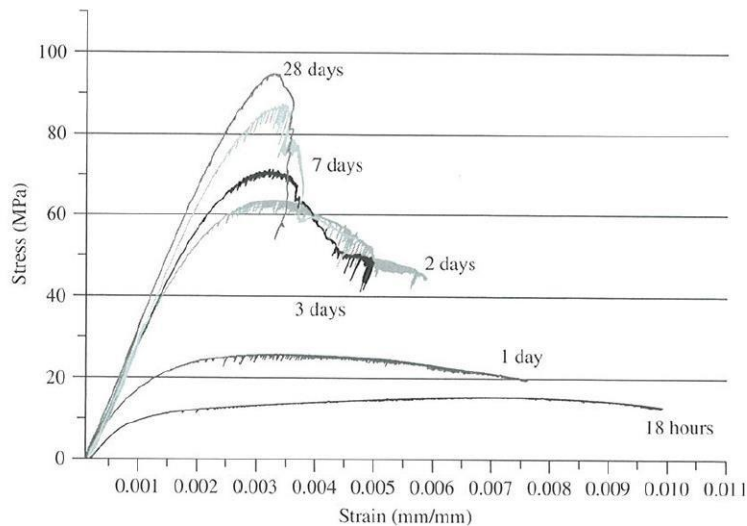


**Figure 27 - Complete stress-strain curve of HSC, Iso-Ahola, et al (2012)**

Other considerations when deriving the capacity of an embedded cast-in Edgelift anchor is the presence of cracks, which can be influenced by shrinkage or creep. There is sufficient research, Bischoff (2001), Browning, et al. (2011) & Scanlon, et al (2011), available reporting that shrinkage causes cracks, meaning that the concrete cracking moment can be reduced by shrinkage caused during cracking. Also, the creep and shrinkage effect can be increased if the loading starts at early age. Long term loss of tension stiffening also needs to be considered when considering time-dependent effects.

The ratio between tensile and compressive strength development in relation to hydration age is critical to this research because of the emphasis on early age

## 2 LITERATURE REVIEW – Cast-in place Anchors

concrete performance on cast-in inserts used for lifting of prefabricated concrete elements. While the concrete tensile strength affects breakout capacity of the anchor, compressive strength is most commonly measured and reported. In the literature review, concrete compressive strength is the most commonly applied strength characteristic used to predict anchor capacity and the concrete tensile strength.

Although sometimes it is unclear in the published research whether it is the mature compressive strength,  $f'_c$ , or the strength at the age of the concrete testing,  $f_{c,age}$ , that has been used to determine a concrete's tensile strength or cast-in anchors capacity, the relationship between the two appears to be that as the compressive strength increases so, too, does the tensile strength, but at a decreasing rate, and also has a direct relationship to the concrete mix design, and other strength parameters, as will be discussed in the testing sections of this thesis. These tensile and compressive strength ratios are presented and used for comparison with the tested values obtained later in this thesis.

Parameters affecting the ratio of concrete compressive strength to tensile strength have been researched Mindess, et al (2002). In addition, their research explores the difference between tensile test methods and how they produce different ratios. The ratio of splitting tension to compressive strength is usually in the range of  $f_{sp}/f'_c$  equal to 0.08 to 0.14 (where  $f_{sp}$  is the splitting tensile strength, and  $f'_c$  is the characteristic concrete compressive strength at 28 days). However, the ratio of direct tensile strength to compressive strength is about 0.07 to 0.11, and the ratio of modulus of rupture to compressive strength is about 0.11 to 0.23.

Some comparisons to  $f'_{t,sp}$  are noted below:

$$f'_{t,sp} = 0.48\sqrt{f'_c} \text{ MPa}$$

Equation 9

*The following equation is proposed by ACI Committee 363.5 (2008)*

$$f'_{t,sp} = 0.59\sqrt{f'_c} \text{ MPa}$$

Equation 10

The following best fit of the data is proposed by Mindess, et al (2002).

## 2 LITERATURE REVIEW – Cast-in place Anchors

$$f'_{t,sp} = 0.305 f'_c{}^{0.55} \text{ MPa}$$

**Equation 11**

This best fit equation is in general agreement except when the best fit exponent is larger than the  $\frac{1}{2}$  proposed by the American Concrete Institute, ACI318 (2008). This exponent models the non-linear relationship of the cast-in anchor capacity and the concrete compressive strength.

Oluokun (1991) state that the ACI318 (2011) exponent of  $\frac{1}{2}$  is not valid for early-age concrete. They tested three laboratory-prepared test mixtures and one sample from a precast, pre-stressed concrete producer. The 28-day compressive strengths ranged from 28 to 62 MPa for the four mixtures. Standard 150 × 300 mm cylinders were cast from a single batch for each series of testing. The coarse aggregate size for all mixtures was 90% to 100%, as retained on a 19mm sieve, with 100% of the large aggregate being less than 25mm. The fine aggregate was a manufactured crushed limestone aggregate. Oluokun (1991) concluded that crushed aggregate produced a tensile strength about 25% higher than smooth aggregate. Equation 12 is the recommended formulation proposed for tensile strength.

$$f'_t = 0.584 f'_c{}^{0.79} \text{ MPa}$$

**Equation 12**

Khan, et al (2002) selected the modulus of rupture as a measure of the tensile strength. Three different curing conditions were investigated, including temperature-matched curing, sealed curing, and air-dried curing. The three concretes design strength included a nominal 30, 70, and 100MPa compressive strength at 28 days. Khan, et al (2002) concluded that ACI318 (2008) overestimates the modulus of rupture for concrete compressive strengths less than 15MPa and underestimates it for strengths above 15MPa.

### **3 LITERATURE REVIEW - Early Age Concrete Strength Parameters**

This literature reviews of the different material properties that develop whilst the concrete is curing will be compared against tested experimental values and used as approximations for properties which have not been determined via physical tests in this research.

An important reference is the work carried out by Hengjing, et al (2008), in which the development of almost all properties of concrete was reviewed in literature and where they conducted independent experiments of these properties to cross-reference against the literature.

#### **3.1. Early age concrete - Material considerations**

Concrete at early ages is characterized by the rapid development of its properties due to the chemical and physical processes that take place between Portland cement and water. The properties change, after an apparent initial in-active period, very fast in the first days, thereafter the changes slow down and reach a steady state after three to seven days. The hydration continues in this final stage, if sufficient water is present, for years at an ever-slower rate until eventually the degree of hydration of the clinker minerals has approached 100%. Note that total hydration may only be approached asymptotically due to the diffusion control of the reactions, Mindess, et al (2002). In this period, the hydration of the clinker minerals, except for the Belite ( $C_2S$ ), takes place and thus the majority of the properties are developed. This is illustrated in Figure 28 where the degree of hydration of the different clinker minerals is plotted as a function of time. At an age of only 3 days around 70% of the  $C_3A$  and 50% of the Alite ( $C_3S$ ) phases have hydrated, while 45% of the ferrite phase and 20% of the Belite phase has hydrated. The diffusion controlled slow rate of hydration is seen to finally dominate the rate of hydration at around two to four weeks.



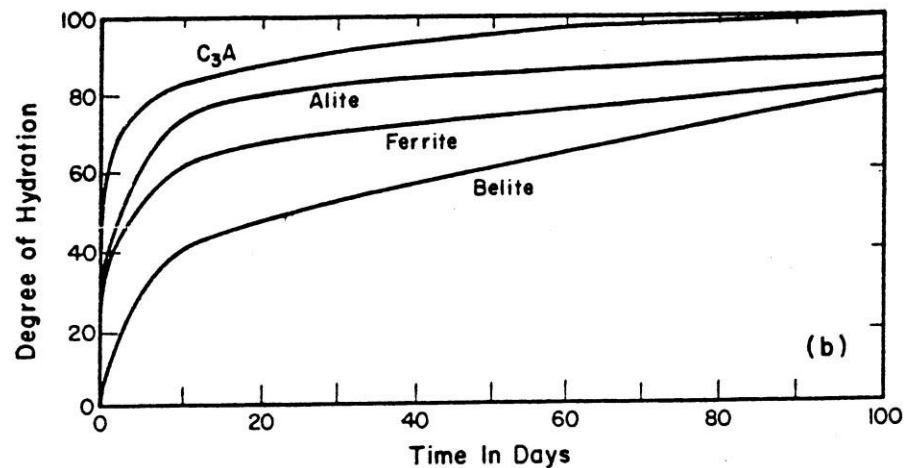


Figure 28 - Hydration of the clinker minerals in cement past, Mindess, et al (2002)

The hydration of the cement is highly exothermic and large amounts of heat are released during the process. This heat release is called the heat of hydration. The heat of hydration is dependent on the type of clinker mineral. Alite and C<sub>3</sub>A releases high amounts of heat while hydrating as opposite to Belite and C<sub>4</sub>AF, which only release moderate to low amounts of heat, Mindess, et al (2002). One-way temperature raises in concrete may be controlled by lowering the content of Alite and C<sub>3</sub>A since these compounds have the highest hydration heats, and also the highest rate of heat development. On contrary, early age high strength, or rapid, cements usually have high amounts of Alite compared with Belite in combination with a finer grinding. The latter increases the surface area of the cement and gives therefore the water easier access to the cement, Gambhir (2004). These two measures increase the rate of hydration and thus the rate of development of properties.

The heat of hydration will lead to an increase of the concrete temperature and is not the case for thin wall concrete panels.

Sealed curing concrete exhibits dilation due to heat of hydration and autogenous shrinkage. It is clear that these volumetric expansions and contractions by themselves will not result in cracks forming in the concrete mix. In order to build up stresses in the volume, some sort of restraint should be present. In practice this will occur to some extent, either externally or internally.

External restraints include structural restraints, for example when the volume is not free to dilate due to contact with a sub-base or a previously cast structure or when the

### 3 LITERATURE REVIEW - Early Age Concrete

concrete is cast around rigid corners or around rigid inserts, as is the case with this research.

Internal restraints are caused by gradients in the dilation of the material or by rigid parts of the material itself, e.g. shrinkage cracking around aggregates. The latter mechanism was explored in Dela (2000), where a device suited for measuring the shrinkage stress around aggregates was developed.

External restraints are often simulated using a cracking frame in which either the length of the specimen or the stress in the specimen is kept constant, refer to RILEM Report 25 (SARL 2002); Dao, et al (2009); Altoubat (2000) and a number of examples in ACI Committee 446 (2004). A variation is a cracking frame where the temperature is controlled where either isothermal conditions or certain temperature histories may be simulated; ACI Committee 446 (2004). An example of a cracking frame is shown in Figure 29. In this setup two specimens are tested. The left one in Figure 29 (a) is free and may expand or shrink as a function of the thermal and autogenous dilations plus any extra dilation caused by exchange of energy with the surrounding environment. This specimen is a reference on which the free length change is measured. The right specimen is loaded with either a constant load that suppresses the length change of this specimen. The latter situation simulates a fully restrained situation and makes it possible to measure the self-stresses, which are building up under such conditions - including the early age creep effects, which work as significant shrinkage mechanisms.

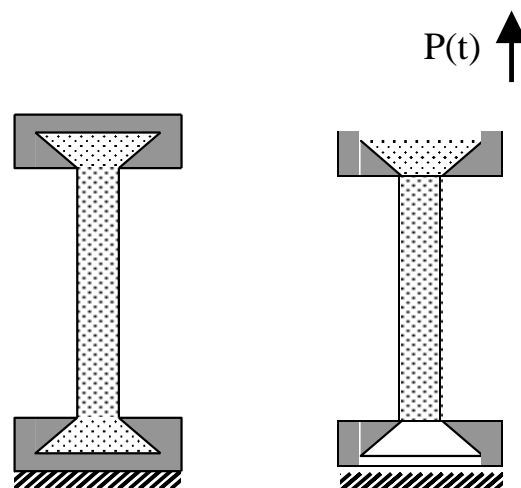


Figure 29 - Principle of the cracking frame, (a) free specimen, and (b) loaded specimen

### 3 LITERATURE REVIEW - Early Age Concrete

A setup similar to the one shown in Figure 29 was used by RILEM Report 25 (SARL 2002) and a sample result is shown in Figure 30. In this experiment, the temperature and the force were measured restraining the specimen. Due to the hydration a temperature rise was reported in the first 15 hours. Then, as the rate of heat development decreased, the specimen starts to cool off and the specimen approaches ambient temperature, 20°C, at 100 hours. As the lower part of figure 30 shows, this temperature rises results in compressive stresses in the specimen, peaking at 10 hours. Then, due to the early age shrinkage of the stress and the decrease in rate of heat development, the compressive stress decreases at 12 hours, the specimen experiences tensile stress. Now, the specimen contracts due to cooling and autogenous shrinkage, and these effects results in tensile stress being recorded. Also the tensile strength development is displayed on the lower part of the figure 30 and, at approximately 70 hours, the tensile stress surpasses the tensile strength and cracking occurs.

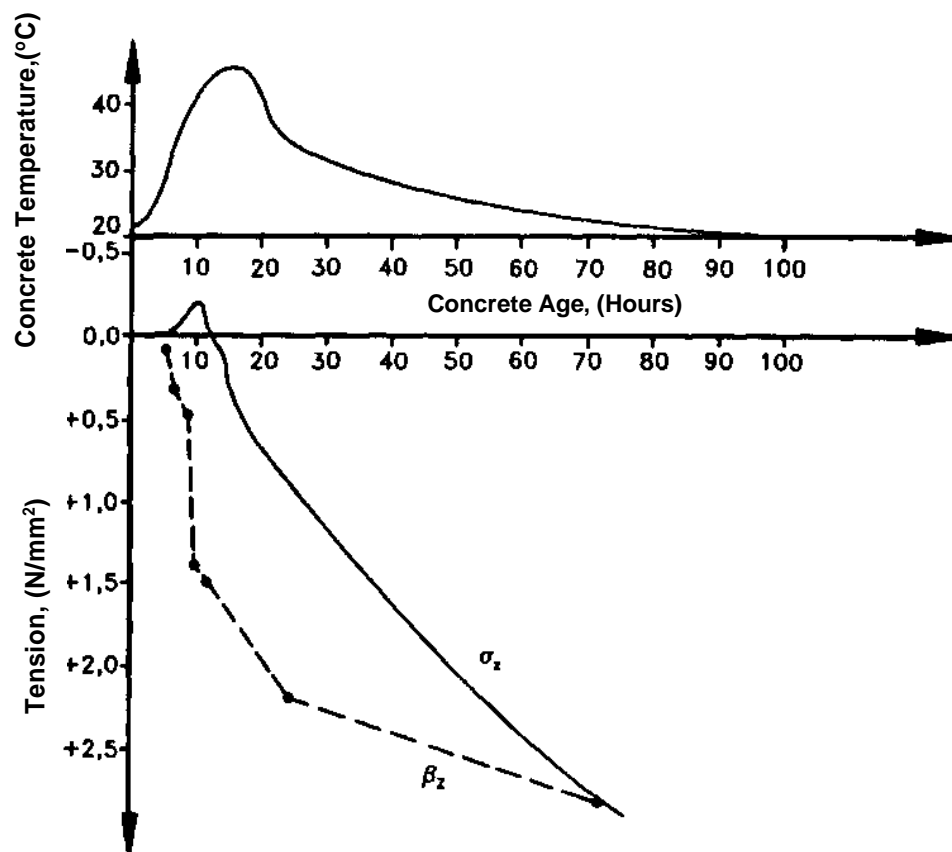
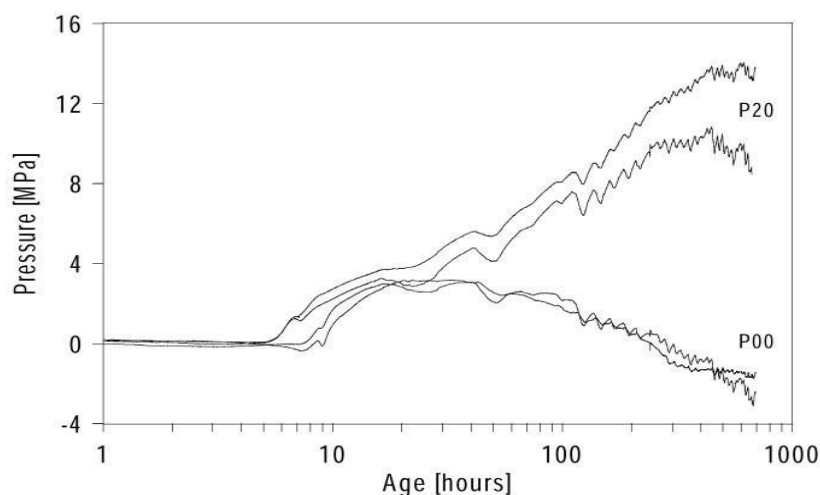


Figure 30 – Recorded self-stresses of a fully restrained specimen Dela (2000)

### 3 LITERATURE REVIEW - Early Age Concrete

The problem illustrated with this example is experienced during testing of Edgelifit anchors. Full or partial restraining of the early age dilations occurs in numerous situations and they do result in cracking.

As with an edgelifit anchor, the restraint could also be internal which is caused by gradients in the concrete temperature (Prasanna, et al 2010; Gambhir 2004). Temperature gradients will occur when heat is dissipated from the surface of the concrete volume. In the initial heating phase internal tensile stress may occur at the surface and result in thermal cracks. Later, in the cooling phase, where the surface regions of the concrete have reached ambient temperature, these regions will restrain the thermal contraction of the central parts and result in tensile stress here and possibly tensile cracking.



**Figure 31 - Hydrostatic pressure exerted on stress sensor with time for two different cement pastes (P00 is without SF and P20 is with 20% SF.), Dela (2000)**

As mentioned, self-stresses in the concrete will occur due to the shrinkage of the cement paste. This was investigated by Dao, et al (2009) where the shrinkage-induced clamping pressure on an inhomogeneity (in this case a thermometer) was measured experimentally. It is clear from these experiments that the clamping pressure is significant and strongly dependent of the amount of micro-silica added to the paste. Shrinkage cracking around aggregates was investigated in Dela (2000) employing a stress sensor, which was developed for the particular test. Figure 31 shows the measured stresses, which are built up around the aggregate with respect to time for the two different cement pastes tested. It is seen that the hydrostatic pressure in the case of 20% SF reaches high values and it was demonstrated that

shrinkage-induced cracking around cylindrical aggregates did occur in the case of 20% SF.

#### **3.2. Temperature related strength models**

Volumetric dilations occur in early age concrete and cracking may occur if these deformations are restrained - which is likely in practice. It is therefore not always possible or preferable to avoid early age cracking. Ultimately if the cracked situation is well understood and can be modelled then cracking can be allowed. This is acceptable if the crack widths are kept below acceptable serviceable values.

To model early age cracking a detailed knowledge of the development of all the important material properties, and preferably their interactions, must be obtained. Important properties to monitor are tensile strength, modulus of elasticity, thermal dilation coefficient, Poisson's ratio, creep and shrinkage properties, and the development of these properties with time. However, measured fracture mechanics properties to understand the crack initiation stresses, and the crack propagation paths related to the material properties help establish a failure mode assessment.

Once these properties are established, they can form the material parameters used in a numerical simulation or performance model to shown position of cracks, crack paths and size. Based on these models, the choice of material and structural design may be selected depending on the calculated outcomes. Alternatively, your models can assist the selection of particular material properties, where they are selected from the most desirable model outcomes, in order to select the best concrete mix appropriate to the application being considered.

In the past, the risk of cracking in early age concrete was based on a temperature criterion (Jensen and Hansen 2001). In its most simple form, a temperature profile may be applied by limiting the maximum temperature in the concrete volume and the difference between parts of the concrete structure. This is done by controlling a maximum difference in temperature within the cast concrete, and by controlling a maximum temperature gap between any existing structure or sub-base and the concrete, which is being poured. This simple temperature profile can be based on experience where it has been found that concrete can withstand the thermal dilations caused by a temperature difference of 15°C- 20°C, (Jensen and Hansen 2001). However, this temperature related method has clear limitations and may not be a safe

### 3 LITERATURE REVIEW - Early Age Concrete

assumption if applied to unique elements, ACI Committee 446 (2004). The method does not take into account the development of strength properties or the temperature history. Neither is the influence of any external restraint regarded, which may cause thermal cracking, or build-up or stresses around aggregate. Depending on the temperature history, a temperature difference may or may not be detrimental. This was discussed in RILEM Report 25 (SARL 2002) which demonstrated that the internal restraint stresses depend on the temperature history and that they are not necessarily zero when the temperature stabilizes. Only a certain temperature gradient, dependent on the temperature history, will produce zero stresses in the structure. In Institute of Civil Engineers (2014) it was found that if no external restraint is present, the simple temperature-differential method is adequate, but also that any external restraint may cause thermal cracking for temperature differentials lower than 15°C. For large structures, the method may yield unreliable results (Browning, et al 2011).

More importantly with respect to this research and application with edgelif anchors, the differential temperature based criterion will not suffice for modern prefabricated concrete mix designs, which show significant autogenous shrinkage.

The only way to cope with cracking occurring due to autogenous shrinkage is technologically to reduce the magnitude of these dilations. This was the subject of the work by Seigneur, et al (2000) and RILEM Report 25 (SARL 2002) who found that the use of Shrinkage Reducing Admixtures (SRA) is a very efficient method to reduce autogenous shrinkage as well as drying shrinkage. This was also concluded by Holt and Leivo (2000) and noting similar conclusions. Another technique has been explored by Jensen and Hansen (2001). Here, water filled Super-Absorbent Polymers (SAP) are entrained in the cement paste and represent a water-supply, which suppresses the self-desiccation of the paste, thereby preventing the self-desiccation shrinkage and thus reducing the autogenous shrinkage. Also water filled lightweight aggregates have been employed for the same purpose Browning, et al (2011).

### 3.3. Early age concrete - Mechanical Properties

Besides detailed published knowledge of early age volumetric dilations, the mechanical properties must be determined in order to be able to model the mechanical behaviour of early age concrete. The compressive and tensile strengths determine whether failure will occur, while modulus of elasticity gives an estimate of the stresses, which are building up as a result of the volumetric dilations and the degree of restraint. Poisson's ratio must be known in order to make 2D and 3D generalizations suitable for finite element modelling. (Poisson's ratio is the –ve ratio of transverse to axial strain). Each of these are discussed in this section showing the relevance to early age concrete property strength capacity.

#### 3.3.1 Compressive Strength

The development of the compressive strength is probably one of the most intensively studied parameters of concrete. This is due to the fact that this parameter, along with the modulus of elasticity, is the most important one in structural analysis. Literature surveys of the development of the compressive strength may be found in Hengjing, et al. (2008) and Hoyer, et al (2000), as well as in text books like Mindess, et al (2002).

The development of concrete compressive strength is mainly dependent on the water-cement ratio, type of cement, additives, pozzolans and curing conditions (temperature and moisture). A common framework for describing compressive failure of concrete is the theory of plasticity (Nielsen 1999). The plastic yield surface used is the modified Mohr-Coulomb yield surface. This surface is determined by three parameters, namely the cohesion, the friction angle and the tensile strength. While the development of the tensile strength is investigated in more detail later in this thesis, information of the development of the cohesion and the friction angle is lacking in current research. Bazant, Concrete fracture models: Testing & Practice 2002 report the friction angle for concrete before maturity is reached. The measuring technique adopted was the tri-axial test. The experiments were conducted on concrete with a water-cement ratio range of 0.44 to 0.66 and a maximum aggregate size of 20mm, similar mix designs used in this research, and it was assumed that the cohesion was zero, refer to mixture designs in Table 6.

### 3.3.2 Tensile Strength

The development of the tensile strength of concrete is important to assist the prediction of the crack initiation, and especially within the context of this research. The uniaxial tension test, which is believed to give the best estimate of the tensile strength, is not widely used due to the difficulties conducting the test. Instead several indirect methods have been developed, e.g. the Splitting test (also known as the Brazilian test) and the three-point bending test (which gives the modulus of rupture), refer Section 4.1 - Concrete tensile strength and cast-in inserts. However, the interpretation of these indirect test methods often relies on linear elastic formulas combined with correction factors determined empirically. The use of the models for indirect tension are unreliable if the tensile strength in unusual situations, for example concrete in early age or fibre reinforced concrete, are to be determined. This is due to the fact that the correction factors are compensating for the actual behaviour of the concrete, which is not linear elastic and ideal-brittle, but quasi- brittle. The brittleness of the concrete is significantly changed in early age and for fibre reinforced concrete compared with matured, normal strength and fibre-free concrete.

Oluokun (1991) predicted a lower initial tensile strength than the ACI318 (2008) model, which is consistent with Khan's findings, Khan, et al (2002). In both cases, the initial tensile capacity gain is higher than the compressive capacity. Thus, experimental validation should result in tensile strength gains on the order of 30% to 50% more than compressive strength gains based on Oluokun (1991) hypothesis. Theoretically, the inserts should perform well at early age. Table 2 summarizes the model equations evaluated for tensile capacity.

**Table 2 - Various published concrete tensile strength models, Winters et al (2013)**

CEB	$f_{ct} = 0.79 \sqrt{f'_c}$
Oluokun	$f_{ct} = 0.2 \cdot f'_c^{0.7}$
ACI318	$f_{ct} = 0.48 \sqrt{f'_c}$
ACI363	$f_{ct} = 0.59 \sqrt{f'_c}$
Mindess, Young & Darwin	$f_{ct} = 0.305 \cdot f'_c^{0.56}$
Oluokun, > 6hours & >5MPa	$f_{ct} = 0.584 \cdot f'_c^{0.79}$
Oluokun, <5MPa	$f_{ct} = 0.928 \cdot f'_c^{0.6}$
Khan (open)	$f_{ct} = 0.085 \sqrt{f'_c}^{2/3}$
Khan (sealed)	$f_{ct} = 0.4 [f'_c]^{2/3}$
( $\phi$ )	,
Khan (dry cured)	$f_{ct}(\phi) = 0.38 [f'_c(\phi)]$



### 3 LITERATURE REVIEW - Early Age Concrete

Courtois (1989) described problems with testing using small blocks that resulted in flexural splitting failure of the block before the ultimate capacity of the insert was reached. In addition, tests conducted in this research showed both concrete compressive strength and embedment depth to be important parameters for determining pull-out capacity. A shear cone breakout failure occurs where a concrete cone defined by the depth of embedment of the insert fails in tension. This is the type of breakout failure that was presented as a simple model and was used in early editions of the PCI Design Handbook. This approach is also similar to punching shear calculations for a slab around a column. Courtois (1989) identifies split cylinder tests as more informative than compression cylinder tests. He suggested that the breakout strengths might be more closely predicted when the concrete tensile strength is known versus when just concrete compressive strength is known.

Sattler (2012) reports the pure tension strength of headed inserts based on a conical failure surface model. Sattler proposes a global safety factor equivalent to a load factor divided by a corresponding strength reduction factor of 2.0 to derive an allowable lifting load. Sattler's work did not address spacing capacity reduction factors for multiple anchors, edge-distance reductions, or anchoring in cracked concrete.

Bode and Roik (1987) recommend design formulas for single inserts loaded in tension based on cube strengths and the square root of the embedment length. They also note that for shorter inserts, 50mm in total length after welding, the standard deviation is greater than for longer inserts because of the non-homogeneous composition of the surrounding concrete and the distance between the anchor head and the concrete surface. Bode and Roik (1987) recommend reducing the strength by 20% for shorter inserts. No further recommendations on other lengths are discussed.

Hawkins (1984) conducted 12 tests on 25mm diameter anchor bolt breakout specimens in 20MPa concrete. Embedment depth varied among 75mm, 125mm, and 175mm. The washer diameter below the bolt varied among 50mm, 100mm, 150 mm. The thickness of this washer also varied as either 16mm or 22mm. Nine specimens were 450 × 450 × 225mm and reinforced near the edges. The other three specimens were 1150 × 1150 × 175mm and also reinforced near the edges.

### 3 LITERATURE REVIEW - Early Age Concrete

Hawkins (1984) used a loading frame which reacted against the concrete with 450mm × 50mm steel beams with 400mm centre-to-centre spacing for the smaller blocks and 760mm × 125mm steel beams with 1,025 mm centre-to-centre spacing for the larger block. Load was applied through a 996kN centre-hole ram positioned over a loading rod attached to the bolt. Only three specimens showed conical breakout failures: one from the smaller block tests and two from the larger block tests. The explanation concluded, is that the moment generated by the testing frame induces flexural cracking in the concrete, causing radial cracking failure before conical breakout failure can be reached. This is similar to the problems listed by Courtois (1989), where the majority of the failures reported were splitting of the concrete.

From Hawkins (1984) conclusions, an embedment depth of 8 to 10 times the bolt diameter is required for ductile behaviour. Splitting failure is likely to occur when the embedment depth-to-bolt diameter ratio exceeds 4. Also, anchor bolts are likely to have ultimate capacities 20% to 30% less than comparable sized headed anchors.

Experimental results using a uniaxial tension test method is not widely researched. This may be a consequence of the perceived difficulties to conduct the test, and due to the problems with self-weight and frictional forces, which become significant in early age concrete. Specimens, which are tested in an upright position, are influenced by self-weight while specimens that lay down are influenced by friction against the sub-base. The latter may, however, be reduced by the use of Teflon sheets. The results for tensile strength are often reported as a function of the compressive strength or the splitting tensile strength. Although this seems relevant from a practical viewpoint it clouds the development of the uniaxial tensile strength since the behaviour of the other test methods change with brittleness and age.

### 3 LITERATURE REVIEW - Early Age Concrete

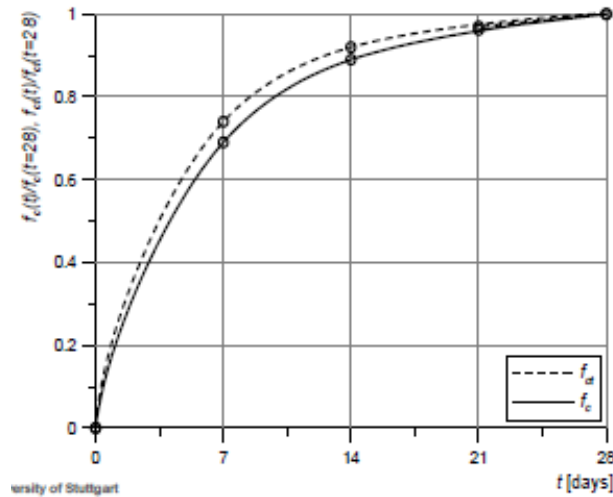


Figure 32 - Relationship between Tensile and compressive strength gain, Eligehausen (2014)

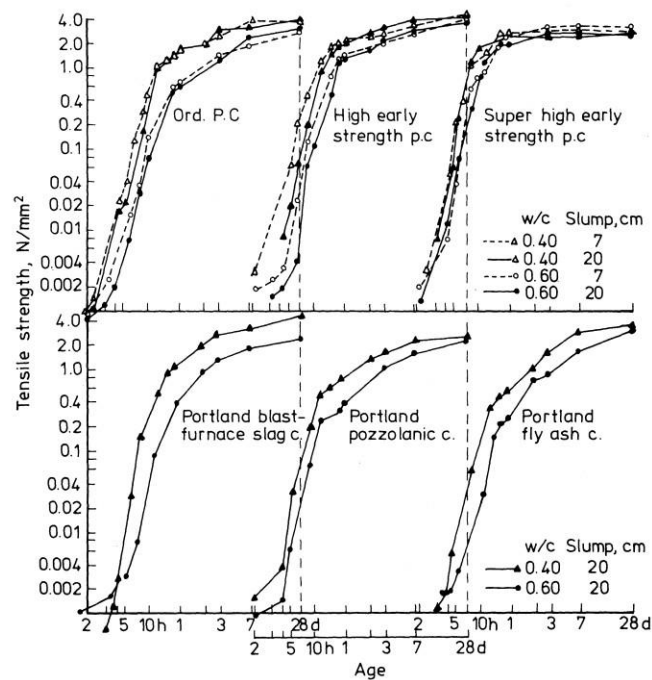


Figure 33 - Uniaxial tensile strength gain for varying cement types and w/c ratios. Kasai (1971)

A uniaxial tension test was conducted by Dao, et al (2009). Figure 33 shows the development of the uniaxial tensile strength at early ages starting at 2 hours. Tensile strength is very low in the beginning (2 hours). It is interesting to note that the tensile strength increases at a higher rate than the compressive strength at very early age, see Dao, et al (2009), and also reported by the author, Barraclough (2012), where the experiment is detailed in Section 4.1.

### 3 LITERATURE REVIEW - Early Age Concrete

In the work by Hengjing, et al. (2008) a large number of uniaxial tension tests were conducted on concrete with different water-cement ratios, cement type and curing conditions. The experiments started at 8 hours and progressed for one month. The results were similar to the ones obtained by Dao, et al (2009) and noted in Section 4.1.

Besides the direct and indirect methods, fracture mechanics test methods are increasingly applied to determine concrete tensile strength. These methods include Crack Mouth Opening Displacement (CMOD) controlled uniaxial tension tests, three-point bending tests and wedge splitting tests. A fracture mechanics interpretation of the three-point bending test in combination with a method for extraction of the tensile strength (inverse analysis) was applied in the report by ACI Committee 446 (2004). Here the experiments were started at an age of 2 days and continued through 28 days.

#### **3.3.3 Tensile vs compressive strength**

Correlations have previously been obtained between flexural tensile strain capacity and flexural strength for various concrete ages Dao, et al (2009), and Prasad, et al (2010). Approximate short term strain capacity in flexure can be estimated if the modulus of elasticity and strength are known. It has been shown Iso-Ahola, et al (2012) that the thermal strain capacity of concretes of similar strength and workability is related to the type of coarse aggregate used, and there is a good correlation between strain capacity and modulus of elasticity for these results. As far as tensile strength is concerned, the splitting tensile test and the three (or four) point bending test have been widely applied. There are some consistent results obtained between flexural tensile strain capacities. But all these tensile tests have the disadvantage of a non-uniform state of stress, which is superimposed over the local stress fluctuations that are present in concrete. With the splitting test a very steep stress gradient develops, and just below where the load is applied compressive stresses develop perpendicular to the axis of the load. This combination of local stress gradients interacting may result in a variance of crack development dependent on aggregate position, size and volume. Thus it may be suggested that various configurations of calibration of the splitting test machine may be necessary versus concrete mix and type being tested.

### 3 LITERATURE REVIEW - Early Age Concrete

Whereas the bending test has its own set of issues to consider, like self-weight of the specimen which may alter the post failure (softening) effect of the test result. Again the damage around the applied load may alter the stress gradients, and crack propagation, for different material types. This results in a degree of confinement within the Fracture Process Zone. Factors affecting the relationship between tensile stress and strain show that this is not a constant value Dao, et al (2009) and is relative to the test method, the type and size of aggregate, the gauge length, the water/cement ratio, curing conditions, age of concrete and test loading rate.

#### 3.3.4 The derivation of tensile strength

The tensile strength and tensile strain capacity of concrete are used widely in the assessment of crack occurrence in concrete members. Based on the tensile strain capacity rather than the tensile strength, it is more convenient and simpler to evaluate cracking where the forces can be expressed in terms of linear changes. The tensile strain capacity can be evaluated from the Modulus of Rupture test, where ACI224.2R (2001) suggests the following expressions to estimate tensile strength as a function of compressive strength

$$\text{Modulus of rupture: } f_{cr} = f_c \sqrt{\frac{\rho_c}{\rho_{c'}}} \quad \text{Equation 13}$$

$$\text{Direct tensile strength: } f_{ct} = f_c \sqrt{\frac{\rho_c}{\rho_{c'}}} \quad \text{Equation 14}$$

where:

- $\rho_c$  = unit weight of concrete (kg/m<sup>3</sup>)
- $\rho_{c'}$  = compressive strength of concrete at time of test (MPa)
- $\rho_c$  = 0.012 to 0.021 (0.013 – 0.014 is recommended)
- $\rho_{c'} = 0.0069$

It can be seen that the elastic modulus of concrete increases with age, as noted by ASTM C469 (2002).

**Table 3 - E Modulus of concrete values**

Age	18hrs	1day	2days	3days	7days	28days
NSC	12.95	14.92	16.12	15.96	24.04	25.47
HSC	10.53	18.88	22.39	28.24	30.02	33.05

Dao, et al (2009) in contrast presented the variation of tensile properties of concrete under various degrees of stress. In BS8110 (BCI 2010) the tensile strain capacity of concrete using granite as a large aggregate was used.

#### 3.3.5 Factors affecting tensile strain capacity

Although it is convenient to assume a constant tensile strain capacity; concrete mixture composition, curing conditions, specimen size, gauge length, loading rate and the presence of a notch, affect the capacity in different proportions. The tensile stress-strain curve, Figure 35, of concrete typically show the curve, up to 75%, as almost linear, thereafter the pre-peak nonlinearity due to micro-cracking occurs. The softening response corresponds approximately in two parts, the first a descending one in which strain localization occurs and the second the later descending part with a long tail Vesely, et al (2010).

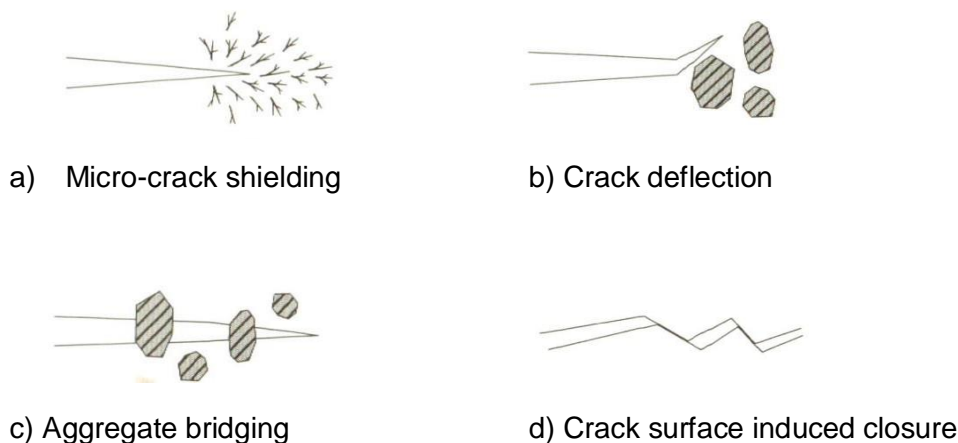


**Figure 34 - Crack propagation interactions of concrete in tension**

#### 3.3.6 Predictions for anchor pull-out capacity

Concrete passes through different states from the initial wet mixing to a stable state several months later. During the early stages of concrete strength development, inserts cast into precast panels depend on being able to predict the inserts strength development, and therefore allowing the element to be lifted from the manufacturing facility to on-site placement. Fracture Energy and Modulus of Elasticity are the controlling material parameters that affect the tensile strength gain Bazant (2002). Concrete up to 3 days old, and loaded near the concrete tensile capacity, will cause

### 3 LITERATURE REVIEW - Early Age Concrete

a fracture surface to propagate through the mortar mix. At early concrete age, and near the lifting inserts ultimate concrete capacity, the induced stresses transmitted through the lifting insert during the precast panel lifting process, are unlikely to have sufficient energy to shear the large aggregate.

Understanding the complete behaviour of concrete subjected to tensile loads is inevitable in precast lifting design, and especially during the lifting process of precast elements. The relationship between compressive and tensile concrete behaviour is specified in Australian Standard - Concrete Structures, AS3600 (SAI 2009), this standard defines the characteristic uniaxial tensile strength, as:

$$f_{ct}' = 0.36 \sqrt{f_{cd}}$$

Equation 15

Alternatively, the uniaxial tensile strength is also defined in AS3600 (SAI 2009), and can be determined from the measured splitting tensile strength, if tested in accordance with AS1012.10 (SAI 2000):

$$f_{ct}' = 0.9 f_{ct}$$

Equation 16

Where:

$$\begin{aligned} f_{cd} &= \text{Characteristic Compressive Concrete Strength (MPa)} \\ f_{ct} &= \text{Characteristic Tensile Concrete Strength (MPa)} \\ f_{ct}' &= \text{Mean Tensile Concrete Strength (MPa)} \\ f_{ct} &= \text{Splitting Tensile Strength (MPa) as per AS1012.10} \end{aligned}$$

A relationship of direct tensile concrete strength to characteristic compressive strength of mature concrete, AS1012.10 (SAI 2000):

$$f_{ct} = g_t \cdot \sqrt{w_c \times f_{cd}}$$

Equation 17

Where:

$$\begin{aligned} f_{ct} &= \text{Direct Tensile Strength of concrete} \\ g_t &= 0.0069 \\ w_c &= \text{Unit Weight of Concrete (kg/m}^3\text{)} \\ f_{cd} &= \text{Characteristic Compressive Concrete Strength (MPa)} \end{aligned}$$

### 3 LITERATURE REVIEW - Early Age Concrete

The tests covered by this research include the comparison of various tensile strength tests, including: Cored cylinder compressive tests, in-direct splitting tensile test, uniaxial direct tensile tests, and cast-in lifting insert tensile tests. Various concrete mixes were tested and appropriate tests were compared against a moulded cylinder compression test.

#### **3.3.7 Concrete tensile behaviour**

The behaviour of concrete subjected to tensile loading has been represented by several researchers, where Holt and Leivo (2000) obtained a stable and complete stress-strain diagram of concrete in direct tension. The tensile stress-displacement curve of concrete, Figure 35, shows the curve, up to 75%, as almost linear, thereafter the pre-peak nonlinearity due to micro-cracking occurs. The softening response corresponds approximately in two parts, the first a descending one in which strain localization occurs and the second the later descending part with a long tail Vesely, et al (2010).

It has been confirmed that substantial non-linearity before peak load is attained ACI Committee 446 (2004). Point A corresponds to about 30% of the peak load up to which propagation of micro-cracks of internal voids is negligible. Point B corresponds to about 75-80% of the peak load, where the cracks propagate between A and B and are isolates and randomly distributed over the specimen volume. According to ACI Committee 446 (2004) the tensile stress is uniformly distributed in the direction of loading over the specimen length. Between B and C the micro-cracks start to localize and the distribution of tensile strain in the loading direction is no longer uniform over the specimen. Beyond the peak load the tensile strain within the fracture zone continually increases, whereas the material outside the fracture zone starts unloading.



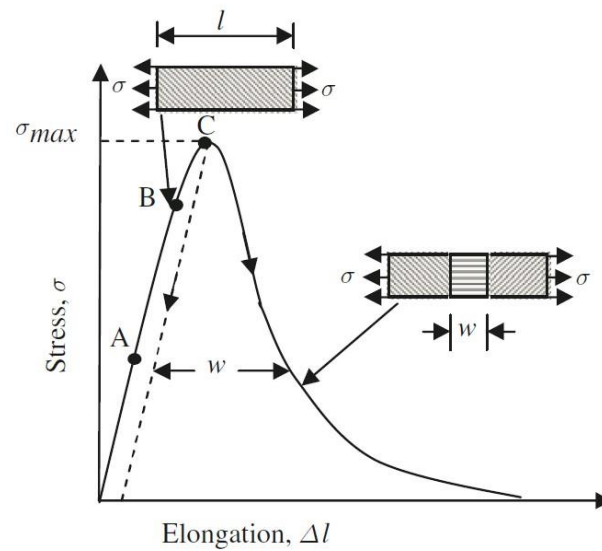


**Figure 35 - A typical stress-displacement curve of concrete, ( $w$  = Length of crack zone)**

The tests discussed in this experiment recorded the maximum load post the elastic phase and in the plastic phase of a typical concrete stress-strain curve.

## **4 EXPERIMENTAL RESEARCH – Concrete Strength and Cast-in headed insert capacities**

The literature reviews highlight available published models and the influence certain parameters and environmental conditions have on concrete strength. This chapter details the tests conducted to measure the significance of the concrete strength parameters discussed in chapter 3.

A series of tests conducted in section 4.1 details the differences between compression cylinder, direct uniaxial tension and indirect tension showing the relationship of concrete strength gain in relation to the test method used. The forty-two, 42, tests in this series are referred to as A1 – A3.

Results of a further series of tests are reported in section 4.2 using headed inserts and loaded in tension to establish their capacity in different concrete ages and mixtures. These test results are compared against compression cylinders and comparisons are made to the models published in the standards of ACI318 (2008) and AS3850 (SAI 2015). The one hundred and forty, 140, tests in this series are referred to as Test Series B1 – B10.

## 4.1 Concrete tensile strength and cast-in inserts

### 4.1. Concrete tensile strength and cast-in inserts

Time, maturity and degree of hydration are described from current published data. Depending on the circumstances, each of these approaches may be appropriate, and they may all be precise, but the reason for this series of tests in this research is to examine the tensile properties of concrete in early age and how it affects the performance of a cast-in edgelift anchor.

**Table 4 - Concrete strength gain series of tests in early age concrete**

Test Series	Test Type	Concrete Age, days	Specimen size, mm	Stress rate, MPa/min	Sample size @ each concrete age, n
A1	Compression	1, 2, 3, 7, 21 and 28	100 x 200 cylinder	20	3
A2	Uniaxial Direct tension		100x 200 cylinder 30mm reduced section	20	3
A3	Indirect splitting		150 x 300	20	1

#### 4.1.1 Experimental Program

This experimental program was conducted as per the tests and specimens denoted in Table 4.

**Compression Cylinder specimens (A1):** Cylinders used for testing were standard 100mm diameter by 200mm long, Figure 36, a cylinder throat was inserted into the mould to create the reduced section. Concrete was prepared in plastic cylinder moulds in accordance with AS1012.8.1 (SAI 2000), with dimensions of 100mm diameter x 200mm long capped cylinders. The cylinder throats reduced the cylinder diameter by 40mm, with a 30mm long reduced section, where the plastic throat was stripped after demoulding. The cylinders were de-moulded at time of test and all cured in a stable shaded atmosphere with a temperature range of 10 to 25°C. 30 cylinders were prepared from a single concrete batch, and tested at 1, 2, 3, 7, 21 and 28 days. At each of the 5 time intervals there were 3 cylinders tested in compression, 3 cylinders tested in direct tension and 1 cylinder in indirect tension. The total time to test the 7 cylinders was within 4 hours. After de-moulding, the ends of the cylinder were prepared in accordance with AS1012.8.1 (SAI 2000).

#### 4.1 Concrete tensile strength and cast-in inserts

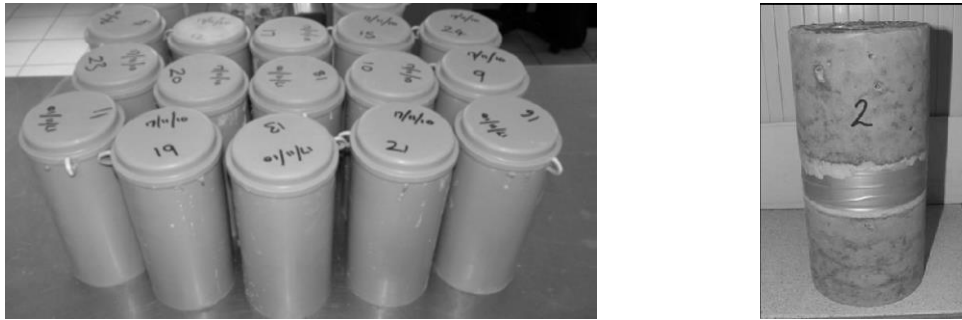


**Figure 36 - Cylinder moulds, and a demoulded cylinder prior to the reduced section being stripped**

The compression cylinders were tested in the methodology as stated in AS1012.8.1 (SAI 2000). Compression testing were conducted by fitting the cylinders with rubber caps at each end. Compressive stress was applied at 20MPa/min until the peak load was achieved and compressive rupture of the cylinders occurred.



**Figure 37 - Compression test setup, and a typical failure at early age (1 day)**

**Uniaxial tensile specimens (A2):** The uniaxial direct tensile cylinders were made up of 100mm diameter x 200mm length cylinders with a reduced diameter in the centre by 30mm as illustrated in figure 37. This was to initiate a fracture surface across the reduced section. Uniaxial direct tensile tests were carried out at 1, 2, 3 and 7 days. Published data by Barraclough (2012), Tensile and compressive behaviour of early age concrete, assessed the direct tensile cylinders which were also tested at early concrete curing ages to further test the relationship between tensile and compressive strength and the compare these results against the indirect splitting tensile results. For each concrete age a compression cylinder test was completed, to compare the results.

#### 4.1 Concrete tensile strength and cast-in inserts

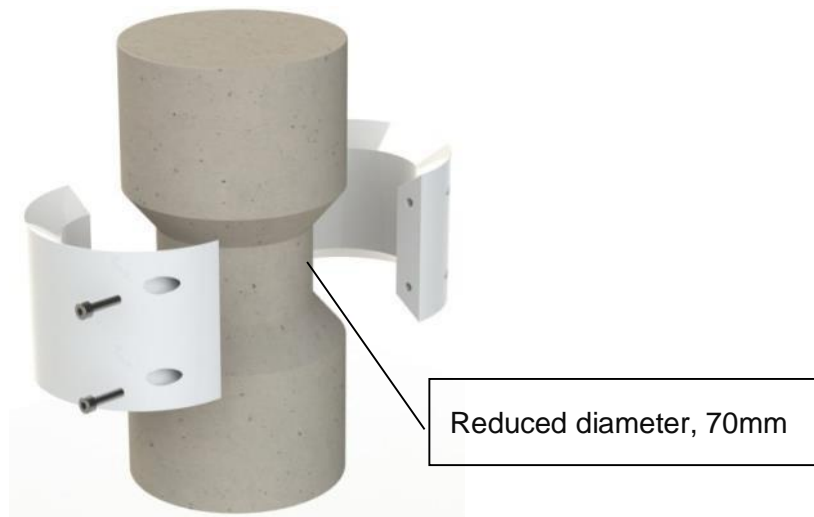


**Figure 38 - Direct tension test specimen, overall dimensions of 100mm Diameter, 200mm long.**

The cylinder throats reduced the cylinder diameter by 40mm, with a 30mm long reduced section, where the plastic throat was stripped after demoulding. After demoulding, the ends of the cylinder were prepared in accordance with AS1012.8.1 (SAI 2000).

To attach the specimens to the tensile test machine, steel plates were glued to each end of the concrete cylinder. Gluing, as prescribed in the RILEM (SARL 2001) uniaxial tension test standard is not as difficult on very early concrete samples as the RILEM (SARL 2001) defined specimen, due to the cylinder not needing a notch to be machined. Using the cylinder reduced sections keeps the notch inside the mould and is sufficiently large so that the crack propagation is more likely to start and finish in the reduced section. This research uses this uniaxial tension method from 24 hours onwards. The dog-bone UTT specimen is well suited to establish early age concrete tensile properties.

It is assumed that this test method minimizes compressive stresses in the test specimen whilst the load is being applied. Two concrete strengths were used, which represent typical mixes used in the precast industry. These were selected to study the relationship between compressive strength and direct tensile strength.

The test specimen was developed to ensure a fracture would occur in the narrowest section of the cylinder throughout all concrete tensile strengths.

#### 4.1 Concrete tensile strength and cast-in inserts

The cementitious materials used was GP Portland cement, as per AS3972 (SAI 2010), and aggregate and sand as per AS2758.0 (SAI 2009). The concrete batch was specified with a typical w/c ratio of 0.4, and detailed specifically in Table 6.

Tensile testing was conducted by capping each end of the cylinders with precision steel caps bonded with epoxy adhesive. The cylinders were then fitted between the universal joints of a tensile testing machine, refer below picture, and loaded at 1.0mm/min until tensile rupture of concrete occurred. Test load and tensile displacement data was recorded for each test.



Figure 39 - Tensile test setup, and typical failures of tensile cylinder

**In-direct Splitting Cylinder specimens (A3):** The cylinders were tested in the methodology as stated in AS1012.10 (SAI 2000) for indirect tension measurement. Indirect tension, or Brazilian testing was conducted by fitting the cylinders horizontally inside 2 plates lined with hard board, Figure 40. Compressive stress was applied at 20MPa/min until the peak load was achieved and rupture of the cylinders occurred.

#### 4.1 Concrete tensile strength and cast-in inserts

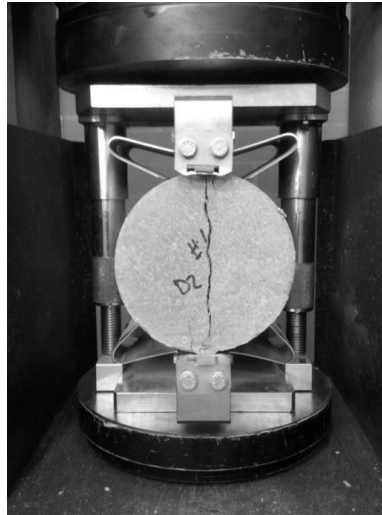


Figure 40 - Splitting tensile cylinder test setup

The splitting tensile strength test was conducted on concrete specimens of 150mm diameter and 300mm in length. The testing was conducted in accordance with AS1012.10 (2000).

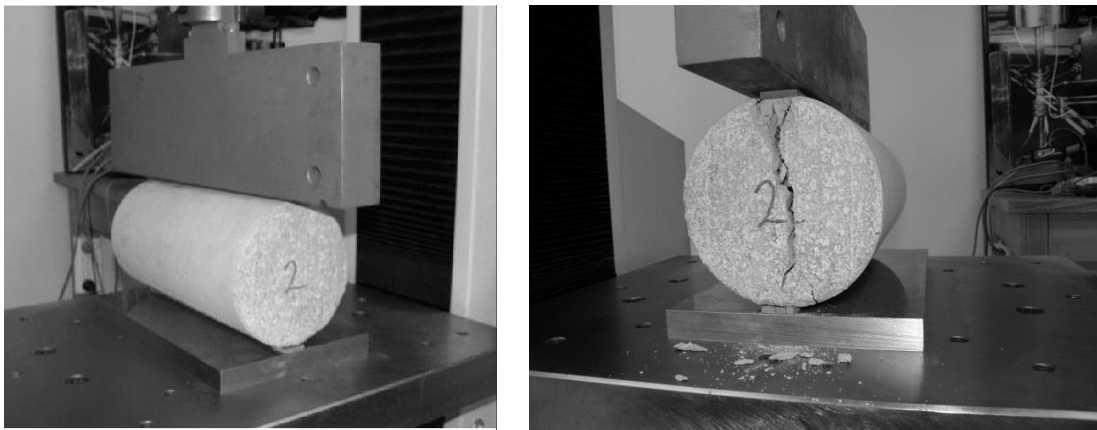


Figure 41 - Split test setup, and typical fracture.

##### 4.1.2 Test Results and Analysis

Typical stress-strain curves recorded from the direct tension tests adopted are shown in Figure 42. As noted by Dao, et al (2009) since concrete is a non-homogeneous material; the curves should deviate at higher stress levels. This deviation is dependent on the stress concentrations at the tips of the micro-cracks, or crack pattern, existing in the test specimen. The load was applied at 1mm/min for each tensile specimen.

#### 4.1 Concrete tensile strength and cast-in inserts

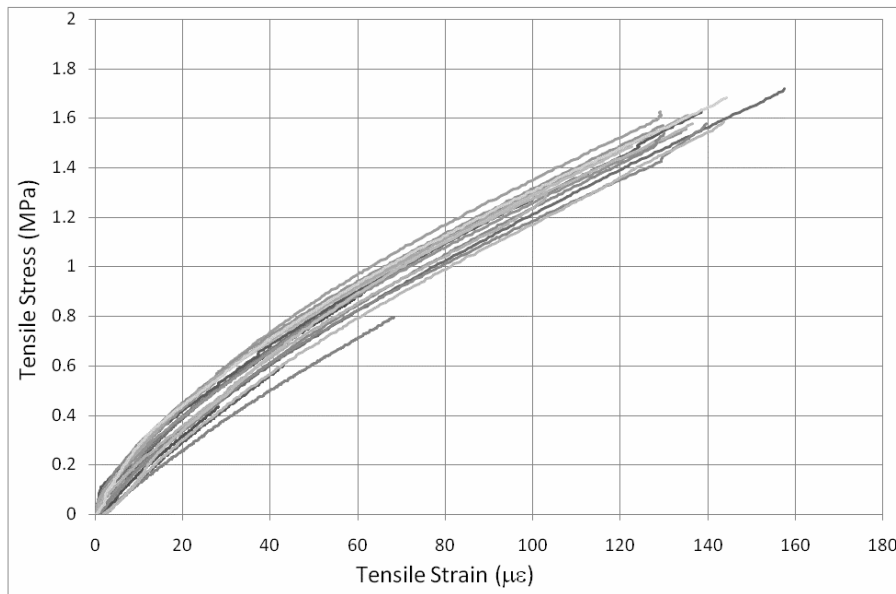


Figure 42 - Stress-strain curves of concrete in direct uniaxial tension

As expected, concrete with lower w/c ratios gain strength faster, Figure 43 and Figure 44. Additionally, Mindess, et al (2002), recorded for the same w/c ratios, the use of larger aggregate reduces the specific area of the aggregate and hence a lower bond strength, resulting in a reduction of concrete tensile strength.

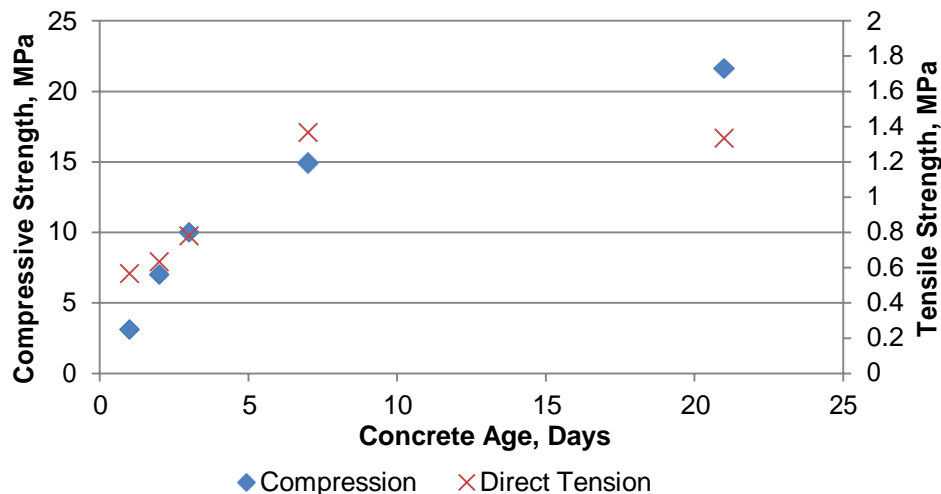
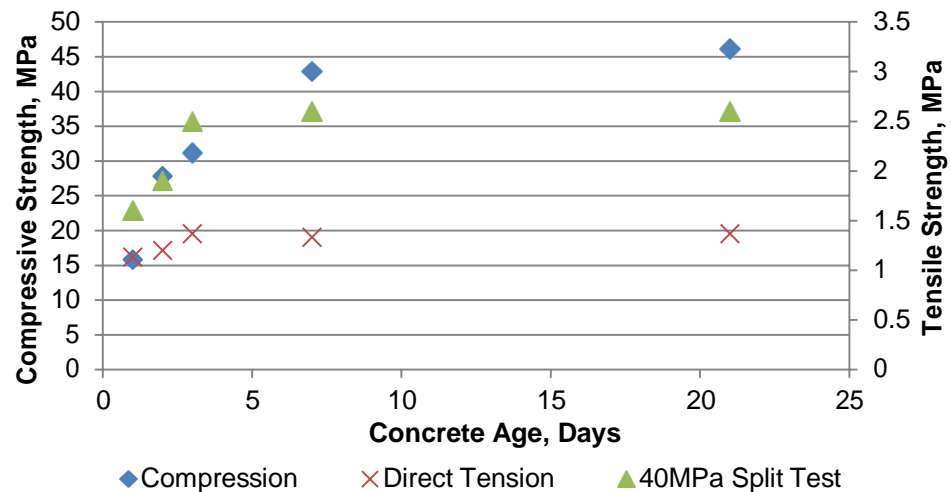


Figure 43 - Concrete strengths observed in the 1st batch of concrete ( $f'_c$  20MPa)

Figure 43 shows the compressive and tensile strength observed, and also showing that the tensile strength stabilized after day 7 whilst showing a typical compressive strength gain curve. Both compression and tensile cylinders were made from the same concrete batch and cured under the same conditions.



#### 4.1 Concrete tensile strength and cast-in inserts



**Figure 44 - Concrete strengths observed in the 2nd batch of concrete ( $f_c$  40Mpa)**

Figure 44 show the compressive and tensile strength observed, and also showing that the tensile strength stabilized after day 7 whilst showing a typical compressive strength gain curve. Both compression and tensile cylinders were made from the same concrete batch and under the same conditions.

Less than 3-day old concrete developed tensile strengths at different rates than the when measured by direct or indirect methods. A maximum tensile strength of just over 2.5MPa was measured by In-direct Splitting Test, whereas a maximum tensile strength of 1.4MPa was measured by the direct Uniaxial Tensile Test.

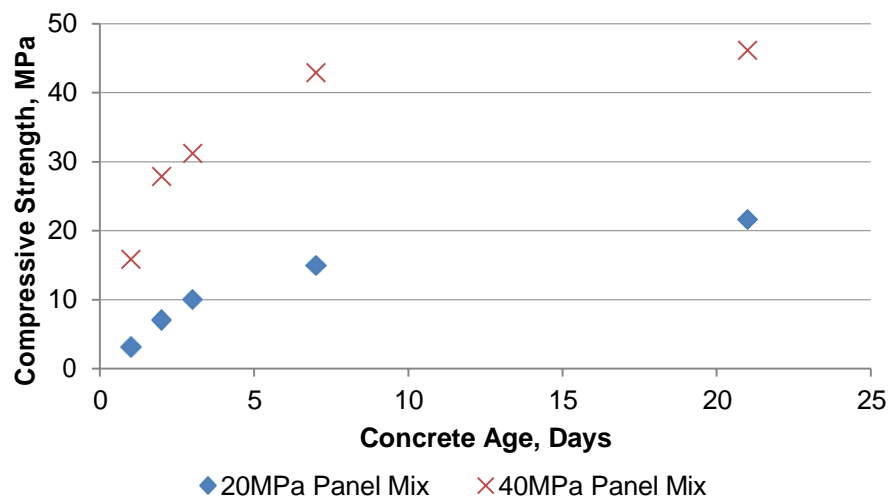


**Figure 45 - Concrete compressive strengths measured for both tests**

#### 4.1 Concrete tensile strength and cast-in inserts

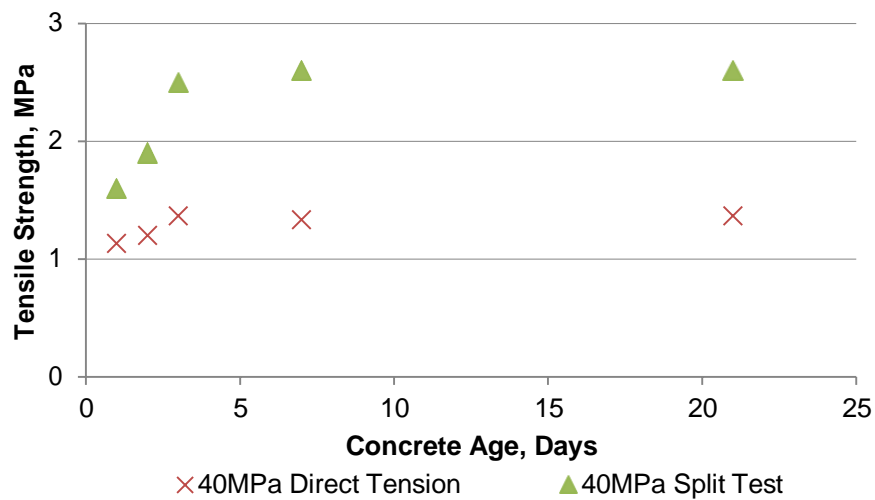


Figure 46 - Comparison of measured indirect and direct tensile strengths

Comparing the indirect and direct tensile strengths shows a gain of 1MPa over 3 days (indirect) and a gain of 0.3MPa (direct)

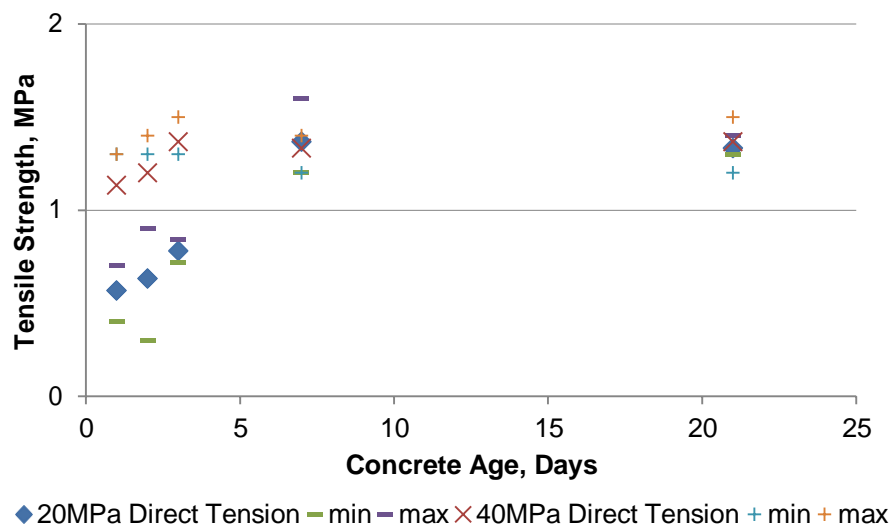


Figure 47 - Comparison of measured direct tensile strengths for both batches

When comparing the measured direct tensile strengths, including minimum and maximum values, it is noted a difference of over 0.6MPa during the first 3 days.

#### 4.1 Concrete tensile strength and cast-in inserts

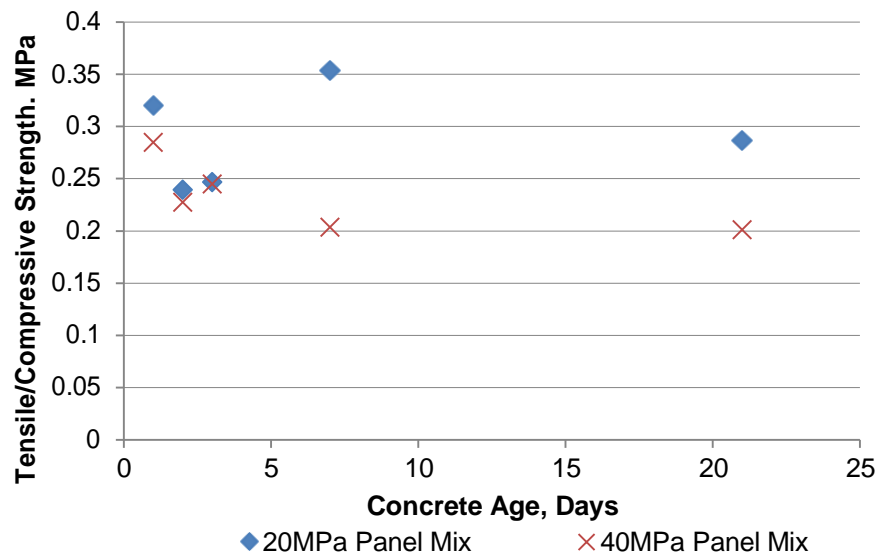


Figure 48 - Comparison of tensile/compressive ratios between both batches

Figure 47 display the relationship between tensile to compressive strength ratio and age of concrete for both concrete batches. The tensile to compressive strength ratio, Figure 48, decreases as concrete matures to day 2 and then increases to day 7. This shows the rate of strength rate in tensile strength is smaller than the increase in compressive strength.

The relationship between tensile to compressive strength ratio and compressive strength of the 2 types of concrete compressive design strength are depicted in Figure 48.

The tensile to compressive strength ratio decreases as compressive strength increases, or concrete ages. By association the tensile strength gain is smaller than the increase in compressive strength. For these tests the tensile to compressive strength ratio varies from 0.2 and 0.35, whereas the data from Mindess, et al (2002), ranged from 0.1 to 0.06 using the indirect test method.

##### 4.1.3 Concluding remarks

Based on the mix proportions, cementitious materials used and the experimental method adopted in this test analysis, the following conclusions can be made:

- 1 The uniaxial tension test, which is designed for ease of use, and is required to have

#### 4.1 Concrete tensile strength and cast-in inserts

a low coefficient of variation and accuracy of concrete tensile reading to be meaningful, produces a larger distribution of results than other direct methods of testing

- 2 For different design strength concrete mixes, the tensile strength gain rate varies, and the uniaxial test records lower tensile values than the Brazilian test.
- 3 Tensile strength of concrete increases with curing age at a lower rate than compressive strength. The direct tensile to compressive strength ratio varies between  $0.2\sqrt{f'_c}$  and  $0.3\sqrt{f'_c}$  for early age concrete less than 7 days old.

## 4.2. Cast-in headed insert capacities

One hundred and forty headed anchors were cast using various concrete compressive strengths and concrete mixtures. Test blocks, 2,000mm x 1,000mm x 300mm, were made. Blocks were tested at concrete ages of 1, 3, 7, 14, and 28 days at a applied load rate of 20kN/min. The remaining three test series were tested at 28-day concrete age and at different strain rates. These three test series were tested at different applied load rates of 20kN/min and two at 60kN/ min. The compressive strength was measured using the mean of three cylinders at each age.

**Table 5 - Test program series for headed insert tensile tests**

Test Date	Test Series	Concrete Age	Minimum insert spacing, $c_i$ , mm	Minimum edge spacing, $S_{i,N}$ , mm	Sample size, n	Load rate, kN/min
04/03/2011	B1	12 hours	330	180	20	20
	B2	16 hours	330	180	20	20
	B3	20 hours	330	180	20	20
	B4	2 days	330	180	20	20
	B5	7 days	330	180	20	20
13/05/2011	B6	14 days	420	210	8	20
	B7	28 days	420	210	8	20
	B8	28 days	420	210	8	20
08/02/2011	B9	28 days	420	210	8	60
	B10	28 days	420	210	8	60

### 4.2.1 Experimental Program

Headed anchors, in accordance with Figure 50, with a nominal length of 75mm and a shank diameter of 13mm were used throughout testing. These specimens had a  $h_{ef}/d$  ratio of approximately 6, where a concrete cone failure is anticipated.

4.2 Cast-in headed insert capacities

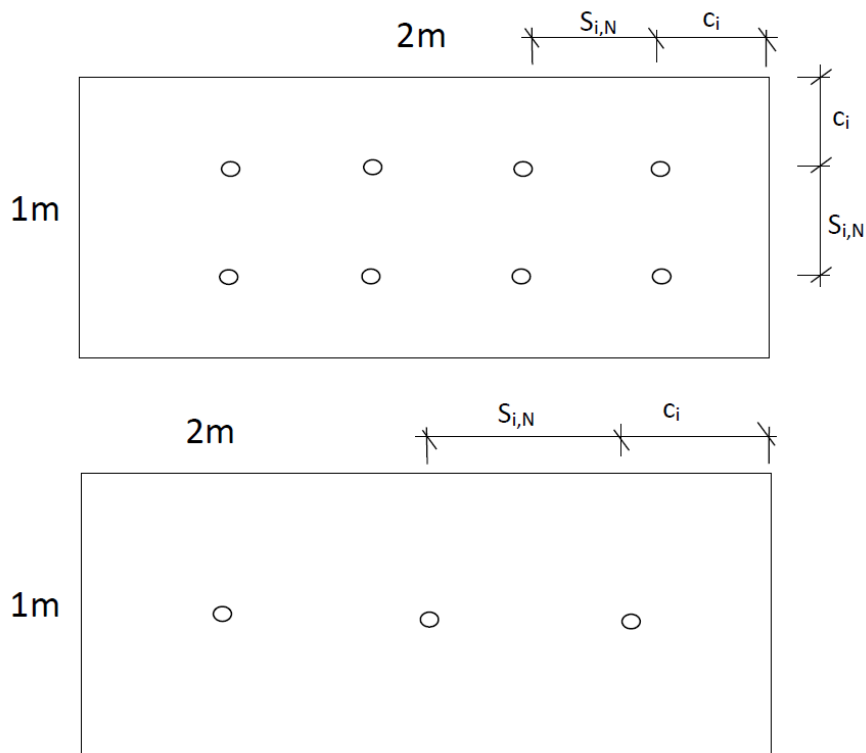


Figure 49 - Panel insert edge and spacing minima. B1-B5 8 anchors per block, B6-B8 3 anchors per block

Each panel used a cast-in headed insert, as shown in Figure 50, which was placed at an embedment depth of 75mm.

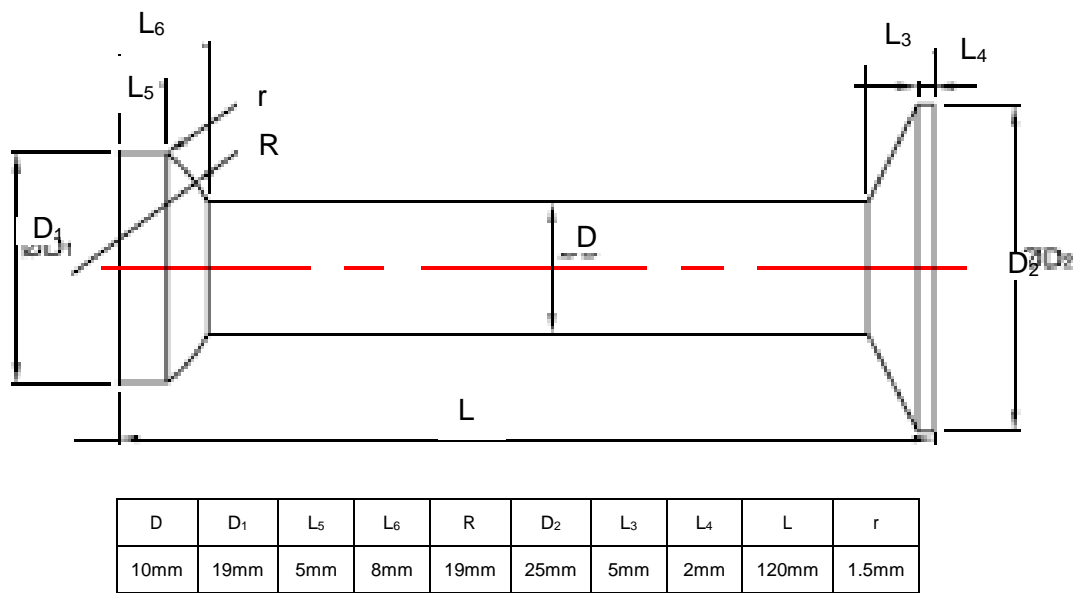


Figure 50 – Experimental headed insert dimensions

## 4.2 Cast-in headed insert capacities

Three uniaxial direct tension tests were conducted on representative headed anchors to establish the average steel strength. The assemblies were loaded to steel failure using a universal tensile testing machine, and tested to have a nominal tensile strength of 530MPa.

All the test blocks were cast, being 2,000mm × 1,000mm x 300mm thick. The concrete was a typical mixture used in prefabricated wall panels, as per Table 6, and designed to have a 28-day characteristic compressive strength of 32MPa. The concrete mixture used a maximum 20mm crushed large aggregate. The inserts were puddled into the near face of the test block after pouring and finishing the concrete pour.

**Table 6 - Concrete specifications used in all tests throughout research**

Strength Grade (f'c) (MPa @ 28 days)		40	32	20
Early Age Strength (MPa @ 3 days)		32	n/a	n/a
Maximum Aggregate Size (mm)		20	20	20
Nominal Slump (mm)		80 ± 15	80 ± 15	80 ± 15
GP Cement <sup>7</sup>	AS3972	293	259	202
20mm Aggregate	AS2758.1	597	577	558
14mm Aggregate	AS2758.1	527	422	496
Manufactured Sand	AS2758.1	158	228	331
Natural Sand	AS2758.1	574	583	574
WR Admix	AS1478	100-500	100-500	100-500
Design Total Free Water (L/m <sup>3</sup> )		177	168	165
Typical Total Cementitious (kg/m <sup>3</sup> )		385	324	251
Cementitious Type to AS3972		GP	GP	GP
Typical W/C ratio		0.44	0.52	0.66

The inserts were spaced more than  $2h_{ef}$  from the edge,  $c_i$ , of the concrete specimen. For spacing,  $s_{i,N}$ , between inserts, this minimum is doubled to  $4h_{ef}$ . The inserts were spaced at no less than 180mm from edges and at a no less than 340mm, from each other.

Each insert was spaced no less than 340mm from each end to minimize the moment created during stripping and to reduce the possibility of cracking the block while moving it into position for testing. The blocks were reinforced with a single N20 reinforcing bar in the centre of each block, and reinforcing mesh (8mm diameter bars

## 4.2 Cast-in headed insert capacities

at 200mm centres, termed SL82<sup>2</sup> panel mesh) to provide tensile strength in the block to help rotating the block after it had been cast. While casting the blocks, thirty- four 100 × 200 mm and twenty-six 150 × 300mm compression cylinders were also cast in PVC moulds to determine the concrete strength during testing. After casting, the specimens and cylinders were then covered with plastic to cure at ambient conditions.

In a second pour, a further 5 blocks were cast, the number of inserts per block was reduced to three to increase the insert spacing and edge distance. The minimum edge distance was increased to 210mm and the insert spacing increased to 420mm, respectively. Twenty 150 × 300mm and twenty 100 × 200mm cylinders were cast to determine the strength of the blocks at the time of testing as well as the 28-day strength. The concrete mixture was the same as used for the first tests. The blocks and cylinder were again covered with plastic to cure.

A difference between the first five series of tests and the second is the use of a different loading frame. ACI318 (2008) recommends that the minimum distance from the centre of the insert to the nearest point of contact on the loading frame be no less than twice the effective embedment depth  $h_{ef}$  of the anchor. Using this criteria, a reaction frame was used with a distance from the axis of the applied load to the nearest point of contact of 150mm, or  $2h_{ef}$ , Figure 51. The frame contacted the concrete with two beams supported by 2 each 50mm × 50mm × 5mm steel plates. This frame was used throughout the test for series B1 to B5. Many of the breakout segments flared out and extended to the frame contact points, which could have affected the insert concrete capacity.

For the subsequent 5 series of test (B6 to B10) of testing, a frame with an open span of 600mm was used. In both series of tests, the load was applied using a 200kN centre-hole hydraulic cylinder, actuated at approximately 20kN/min. The hydraulic cylinder was attached to a 400kN load cell and was then placed on top of the loading frame. The load cell was connected to the inserts by a lifting clutch. This arrangement helped align the rod and anchor so there was minimal bending in the loading frame. Displacement of the stud relative to the concrete was measured by

---

<sup>2</sup> SL82 panel mesh is a Class L reinforcing mesh made from 500 MPa welded ribbed wires and complies with AS/NZS 4671:2001. 8mm wire welded at 200mm centres.



## 4.2 Cast-in headed insert capacities

two linear potentiometers placed on either side of the insert threaded rod. The potentiometers were placed on a bridge so that they would not be affected by the breakout surface or the deflections of the loading frame, as recommended in European Guidelines for technical approval of metal Anchors Used in Concrete, ETAG 001 (EOTA 2013), Appendix A, and depicted below in Figure 51.

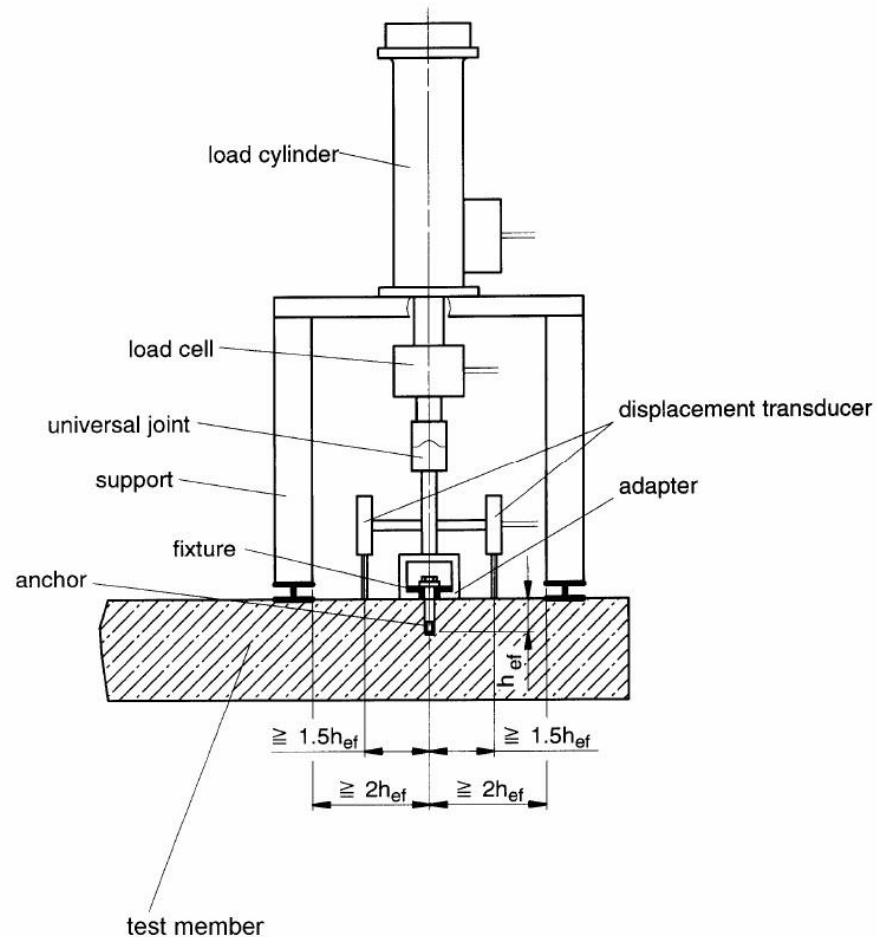


Figure 51 - Example of the reaction frame tension rig setup, ETAG 001 (EOTA 2013) Appendix A

## 4.2 Cast-in headed insert capacities



**Figure 52 - Loading frame for the series of tensile tests**

The reaction frame setup for testing is as per figure 52.

Circles were drawn marking the theoretical breakout diameter as presented in, Figure 53. The predicted breakout load was calculated using Equation 5,  $P_u^0$ , and compared against tested results,  $P_u$ .

During the first five series of tests, each block was removed from the mould, moved into position for testing, and rotated so that the inserts were on the top side of the block two hours prior to the breakout test. One hour prior to testing, three cylinders were tested in compression and two cylinders were tested in a Split Cylinder Test. On the second compression cylinder, a load was applied equal to 40% of the failure load of the first cylinder. The compressive load and stress, and tensile strength was recorded.

An initial load of approximately 900N was applied, and the headed anchor was then pulled to failure using load rate control of the hydraulic pump. The tension tests were performed at concrete ages of 12, 16, and 20 hours and 3, 7, 14, and 28 days.

The second set of 5 series of blocks tested was conducted using the same test method. Because there were fewer inserts per block, two blocks were tested at each of the concrete ages 12, 16, and 20 hours. To be able to test two blocks at once, all blocks were removed from the moulds at a concrete age of 9 hours and placed into

## 4.2 Cast-in headed insert capacities

position to be tested. Supplementing the cylinder tests at the time of the testing, five 150 × 300mm and five 100 × 200mm cylinders were tested in compression and splitting, at 28 days to establish the 28-day strength. Figure 53 shows a typical series of breakout failures.



Figure 53 - Pull-out test block at 16 hours (Series B2)

### 4.2.2 Test Results and Analysis

The data collected from each headed anchor test included the loading, mode of failure, block concrete compressive strength and displacement history, with the loads tabulated in Appendix B - Test Data. The failures were all expected to be concrete cone, but in the first round of testing, steel failure began to occur at a concrete age of 3 days and older.

Applying Equation 5,  $\phi_{p,4}^0 = \phi_{p,4} \sqrt{\phi_{p,4}} \cdot (h_{p,4})^{3/2}$ ,

where:

$$\phi_{p,4} = 13$$

$\phi_{p,4}^0$  is calculated as per Table 7

## 4.2 Cast-in headed insert capacities

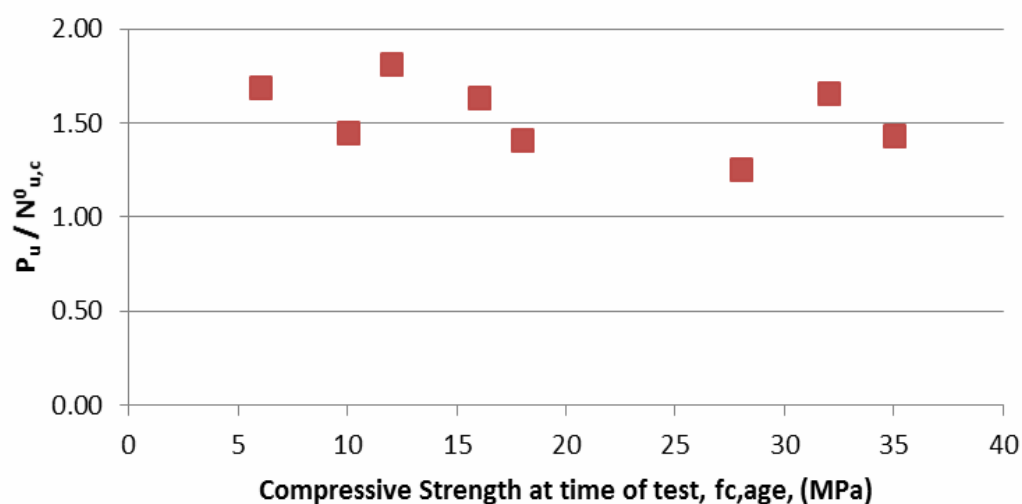


Figure 54 - Comparison of predicted breakout strength vs. tested data

Table 7 - Ultimate load vs predicted load ratios for headed inserts (Load applied rate 20kN/min)

Test Series	B1	B2	B3	B4	B5		B6	B7
Concrete age, hr	12	16	20	24	72	168	336	672
$f_{c,age}$ , MPa	6	10	12	16	18	28	32	35
Tested Data, $P_u / N_{u,cr}^0$	1.43	1.42	1.84	1.64	1.19	0.77	1.34	1.21
	1.55	1.69	1.82	1.62	1.18	1.59	1.45	1.69
	1.46	1.34	2.08	1.75	1.44	1.73	1.48	1.48
	1.31	1.51	1.82	1.52	1.21	1.19	1.29	1.46
	1.72	1.36	1.73	1.65	1.61	1.08	1.74	1.09
	1.98	1.31	1.66	1.52	1.45	1.2	1.96	1.64
	2.1	1.47	1.95	1.82	1.77	1.16	2.15	1.47
	1.95	1.49	1.63	1.56	1.43	1.3	1.88	1.45
$N_{u,cr}^0$ , kN	20.7	26.7	29.3	33.8	35.8	44.7	47.8	50.0
std dev	5.69	3.04	4.07	3.38	7.10	12.46	3.04	9.36
CofV	3.37	2.10	2.24	2.07	5.03	9.95	1.83	6.52
Sample size, n	20	20	20	20	20	20	8	8
Average, $P_u/N_{u,c}^0$	1.69	1.45	1.82	1.64	1.41	1.25	1.66	1.44

$N_{u,c}^0$  - predicted tensile strength, refer Equation 5

$P_u$  - maximum load recorded

## 4.2 Cast-in headed insert capacities

### 4.2.2.1 Concrete failure test results

During the first stage of testing, all failures occurred as concrete breakout until the concrete age was 3 days and older. For the 28-day strength test block, B7, all failures were tensile steel failure of the anchor. The average test-to-predicted (Equation 4) ratios for the concrete breakout failures ranged from 1.4 to 1.8. These concrete capacity equations under predicted the strength in all cases.

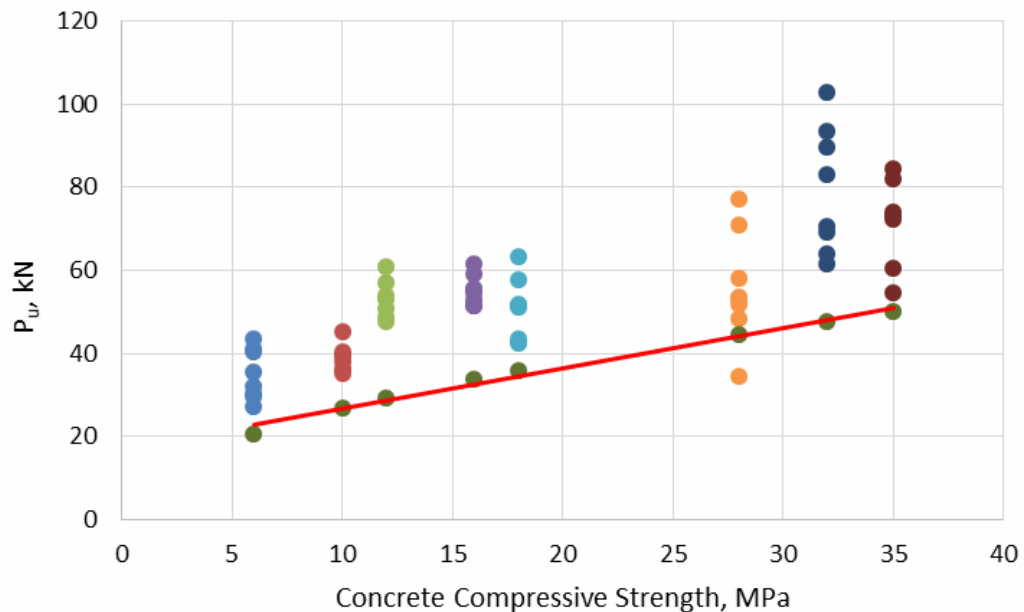


**Figure 55 - Tested versus predicted to EQUATION 4 results**

For the 7 and 28 day tests, the failure mode changes from concrete breakout to steel yield. Thus, only the data for specimens less than 7 days old is appropriate for analysis of concrete breakout capacity. Second, the material specifications for this experiment provides only the minimum yield and ultimate tensile stress. Loads exceeding these minimums are possible. Over strength conditions occurred in tests over 28 days, where both breakout loads and steel yield loads exceed the lower 5% fractile calculated bound of 47.5kN yield and 56.5kN ultimate. All tests were stopped at 90kN to protect the test equipment if brittle failure were to occur.

The second series (14-28 days, B6-B8) of tests was conducted to determine whether the compressive stresses caused by the loading frame may have caused the test-to-predicted ratio to be higher than 1.0. In the tests that had a steel yield failure mode, the average test-to-predicted ratios were all greater than

## 4.2 Cast-in headed insert capacities

1.1. At 14 days, three of the inserts didn't fail at 90kN as the test was stopped to avoid damaging the load cell and transducers. These test results are not included in the test-to-predicted calculations.

### 4.2.2.2 Concrete strength results

The compressive cylinders show a 28-day average compressive strength of 37MPa (+1.2 – 0.8MPa) for the tests. The cylinder's compressive strength increased with age as was to be expected. The strengths were then compared with the equation presented by ACI318 (2008), et al. (Figure 56).

Average tensile strengths were consistently lower than the expected tensile strengths based on the equations presented in the literature review comparing the concrete compressive strength with the splitting tensile strength. The split tensile strength prediction is increased on average by 25% when crushed coarse aggregate is used as suggested in the literature review. Applying this increase to the tested results would have resulted in a better match to predicted strengths.

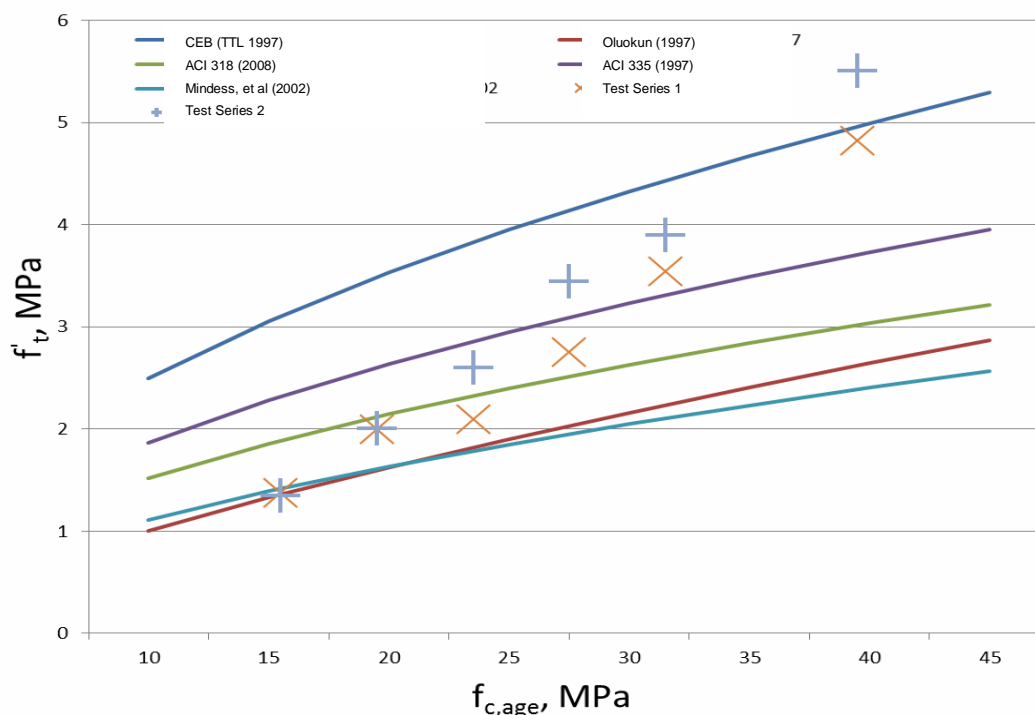


Figure 56 - Predicated and tested concrete tensile vs compressive strength

## 4.2 Cast-in headed insert capacities

### 4.2.3 Concluding remarks

The average tested anchor capacities exceed the predicted concrete failure values compared against experimental data and the model published in ACI318 (2008). Based on this test program and the theoretical tensile strength gain, the capacity predictions in ACI318 (2008) are sufficient for the design of inserts or lifting inserts for concrete compressive strengths as low as 7MPa in un-cracked concrete. This is consistent with the findings in the literature review that tensile strength increases faster than compressive strength at early age.

Although the age of the concrete does not need to be corrected for compressive strength, the strength at release or stripping a concrete element in a prefabrication factory remains an important factor. Low-strength concrete is more sensitive to breakout, as the higher the concrete strength steel failure is the likely failure mode. As can be seen below, Figure 57, the coefficient of variation for the applied loads is less at lower concrete compressive strengths.

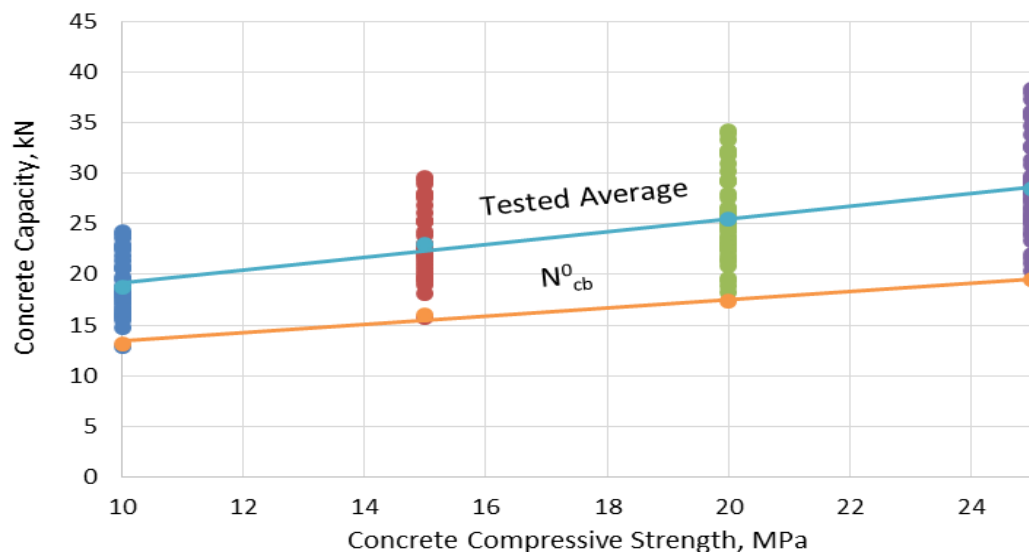


**Figure 57 – Tested versus predicted characteristic resistance,  $N_{cb}^0$  Normalised concrete strength, Concrete Cone Failure only (1 to 14 days, Test series B1-B6)**

Headed anchors have been used as a default geometry for a lifting insert within ACI318 (2008) and AS3850 (SAI 2015). Inserts that vary in geometry from a headed anchor are typically estimated to behave similarly to these inserts, AS3850 (SAI 2015), Appendix B, where a Shape Modification Factor,  $\beta$ , (Equation 3) is used to model the difference in performance. Also the models presented in ACI318 (2008)



## 4.2 Cast-in headed insert capacities

and AS3850 (SAI 2015), assume that the headed anchors behaves as calculated in normal-strength concrete and early age concrete, where  $f_{c,age}$  is used.

It is concluded that the tensile strength increases faster than compressive strength at early age when compared with the corresponding strength gains of mature concrete. This is determined from the higher slope of the tensile-to-compressive strength graph at early ages, figure 58. A prediction method used by ACI318 (2008) underestimates the modulus of rupture at compressive strengths greater than 15MPa.

When comparing the different CCD models, the author proposes the following:  
For  $h_{ef}$  less than 75mm and an unrestrained cone the AS3850 (SAI 2015) adopted model is shown to be suitably conservative when compared to actual tested capacities, refer Figure 58. AS3850 (SAI 2015) better matches the performance of headed anchors for concrete failure modes.

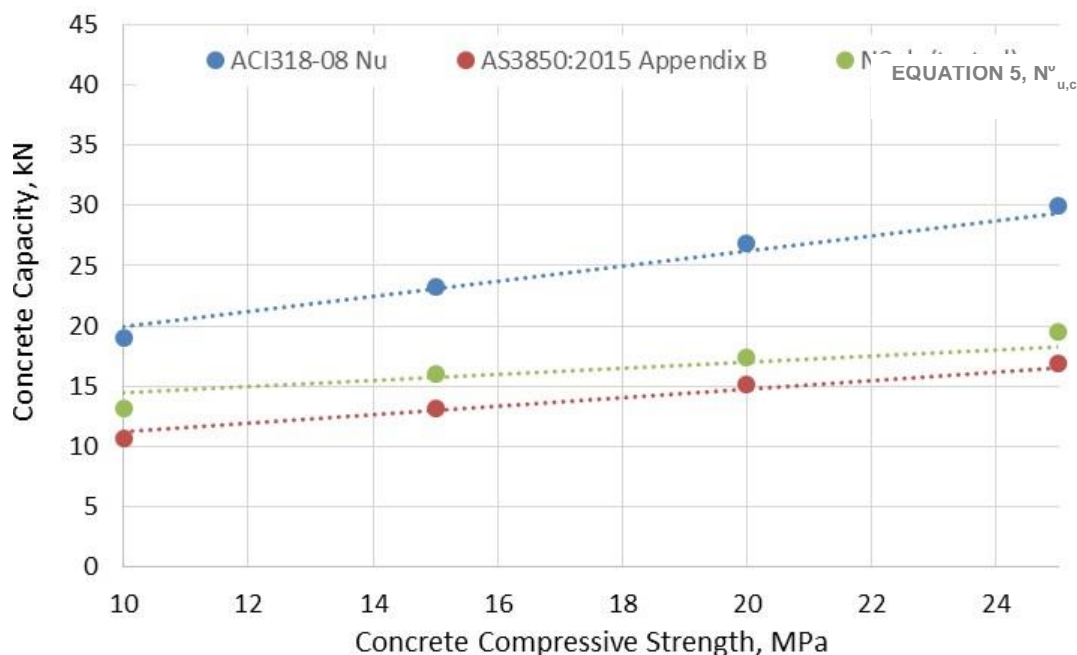


**Figure 58 - Predictive models for cast-in insert concrete cone capacity against tested characteristic values,  $N^0_{u,c}$**

For concrete compressive strengths greater than 25MPa, at 75mm embedment, the steel capacity, using 350MPa steel, is the failure mode of the insert. The model presented in AS3850 (SAI 2015) is suitably conservative for all concrete strengths where concrete cone is the mode of failure.



## 5 EXPERIMENTAL RESEARCH - Edgelift anchor capacities in early age concrete

This experimental section details the results of six hundred and sixty-four, 664, tests, conducted to establish the tensile capacity effect different steel reinforcing configurations around various cast-in anchors at various concrete compressive strengths and concrete mixtures.

These series of five different Edgelift anchor pull-out tests in concrete wall panel's covers the following:

- Edgelift test 1 – Anchor shape and configuration experimental program (section 5.1, test series TA1 – TA11)
- Edgelift test 2 - Panel reinforcement influence on failure loads (section 5.2, test series EP1 – EP8)
- Edgelift test 3 - Influence of anchor reinforcing on failure loads (section 5.3, test series EL1 – EL7)
- Edgelift test 4 – Anchor reinforcement influence on shear failure loads (section 5.4, test series ES1 – ES7)
- Edgelift test 5 - Stress distribution along an edgelift anchors length (section 5.5, test series A - G)

Section 5.1 includes a series of tests on an Edgelift insert to research the prediction of capacity in early age concrete. These tests include the results of one hundred and fifty, 150, tests conducted on three anchor types at various concrete compressive strengths and concrete maturity ages. Of the three types of anchor there is (a) three anchor embedment's depths,  $h_{ef}$ , with internally serrated teeth, (b) one anchor with wavy legs, (c) seven anchor embedment's depths,  $h_{ef}$ , as headed anchors. This series of test are referred to as TA1 – TA11.

Section 5.2 experimental program was conducted with one anchor type (internally serrated teeth) and one embedment depth, and with various steel reinforcement, both steel complimentary (attached to the anchor and part of the cast-in anchor configuration), and steel supplementary reinforcement (not attached to the anchor, but traversing across the anticipated concrete fracture surface) at various concrete compressive strengths and one concrete mixture. One hundred and ten, 110, tests are included in this section. This series of test are referred to as EP1-EP8.

Section 5.3 includes two hundred and sixty-nine, 269, tests where the test includes one hundred and fifty-four, 154, Edgelift anchor tests and one hundred and fifteen, 115, headed anchor tests. This is research assessed the effect of various panel steel reinforcement compared against a series of cast-in headed anchor tensile tests, to relate the cast-in Edgelift anchor performance against the published headed anchor CCD model in ACI318 (2008) and AS3850 (SAI 2015). This test series included various cast-in headed anchors effective embedment, and one type of cast-in Edgelift anchor, all at various embedment depths, concrete compressive strengths and reinforcement configurations. This series of test are referred to as EL1 – EL7,

Section 5.4 assesses one type of cast-in Edgelift anchors performance subject to a load applied in a shear direction, which is the first loading a thin concrete panel experiences as it is lifted from the casting bed. This experiment was conducted using variable panel thicknesses, various steel complimentary reinforcement and various concrete compressive strengths. One hundred and twenty-six, 126, tests are included in this section. This series of test are referred to as ES1 – ES7.

Section 5.5 is an experiment on a single cast-in Edgelift anchor using strain gauges along the legs of the anchor, while loading the cast-in anchor in tension. There are 9 test in this series. The assessment of the test shows the stress distribution along the length of the cast-in edgelift anchor that will be typically experienced and how this related to mechanical interlock, concrete crushing and stresses that may by induced on the surrounding concrete to the anchor. This series of test are referred to as A - G.

### 5.1. Edgelift test 1 – Anchor shape and configuration experimental program

Edgelift anchors (lifting inserts) are used to transfer lifting loads between the lifting equipment and concrete. These lifting inserts have embedded undercut feet to interlock with the concrete. They are unlike footed lifting anchors that have a single mechanical interlock, and Edgelift lifting inserts have multiple teeth along its lengths. The direction of the interlock changes from anchor to anchor, with two predominate technologies available on the market today. These 2 types of anchors rely either with internal teeth interlocking with the concrete, or both internal and external interlock with the concrete, as shown in Figure 59.



**Figure 59 - Anchor with internal interlock and the bottom anchor with internal and external interlock**

The interaction models available to engineers are derived from a single headed anchor interlock function. The anchor with both internal and external toothed legs, bottom anchor in Figure 59, can fail due to spalling to the surface in thin panels, or blow-out, Figure 4.

#### 5.1.1 *Experimental Program*

This experimental program included four cast-in Edgelift anchors, and eight cast-in headed anchor geometries. Of the four Edgelift anchor, three had internal serrations and one had wavy legs, and all have different effective embedment depths. The eight headed anchors have all different embedment depths. All tests were direct tensile load directions.

### 5.1 Edgelift test 1 – Anchor shape and configuration experimental program

A total of twenty (20) headed anchors for test series TA8 – TA11 with various effective embedment depths, 35mm, 45mm, 50mm and 65mm were cast in two reinforced concrete panels 2m x 2m x 150mm thick with 30 anchors in each panel. The reinforcing was SL82 mesh and an N16 perimeter bar located 50 mm from the edge of the panel. These anchors were tested in direct tension as the concrete matured; the average compressive strength of the concrete at time of testing was 21MPa. Concrete compressive data for all series is shown in Table 9. All anchors of Series TA8 – TA11 failed due to concrete cone failure. The headed anchors were arranged with sufficient edge distances such that concrete capacity was not reduced due to edge effects.

Thirty (30) headed anchors of Series TA5 – TA7 were cast in unreinforced concrete blocks of 2m x 2m x 0.6m deep with 2 anchors per block. The anchors of Series TA5 were tested in direct tension once the concrete had matured. The average compressive strength was 22 to 26MPa, with an average compressive strength at time of testing (which was at 28 days) of 23MPa (Table 8). This was to ensure the headed anchors failed not due to steel tensile failure but rather a concrete cone failure. The headed anchors of series TA5 – TA7 were of varying embedment depths; 120 mm, 170mm and 240 mm effective embedment depth. All anchors of Series TA6 and TA7 failed due to steel tensile failure of the anchor, and are not reported in the tested data.

Plate-type Edgelift anchor pull out tests (one hundred, 100) were conducted at concrete compressive strengths and embedment lengths that would ensure a concrete cone failure. The Edgelift anchors were series A  $h_{ef}=252\text{mm}$ , series B  $h_{ef}=272\text{mm}$  and series C  $h_{ef}=295\text{mm}$  effective embedment depth, 16 mm plate, with a profile as shown in Figure 59 shown as the top anchor with internal serrations. The Edgelift anchor for series D  $h_{ef}=370\text{mm}$  effective embedment depth, 16 mm plate, with a profile as shown in Figure 59 shown as the bottom anchor with wavy legs. They were all cast in thin (150 mm thick) panels with varying reinforcement arrangements in the panels and around the anchors.

Where reinforcement configuration A test panels had no reinforcement in the panels (as seen in Figure 61 (a)). Reinforcement configuration B test panels had an N12 shear bar, centrally placed SL82 mesh and a centrally placed N16 perimeter bar. Details are summarised in

## 5.1 Edgelift test 1 – Anchor shape and configuration experimental program

Table 9 and photos of the layout in Figure 61.

Normal strength concrete was used throughout all series of the tests; being 14 mm coarse aggregate, 0.44 water/cement ratio, and nominal grade 40MPa design strength supplied by a commercial ready-mix company. The range of concrete compressive strengths at time of test was 10.1MPa to 40MPa, with an average of 21MPa. Full concrete compressive data for all series is shown in Table 8.

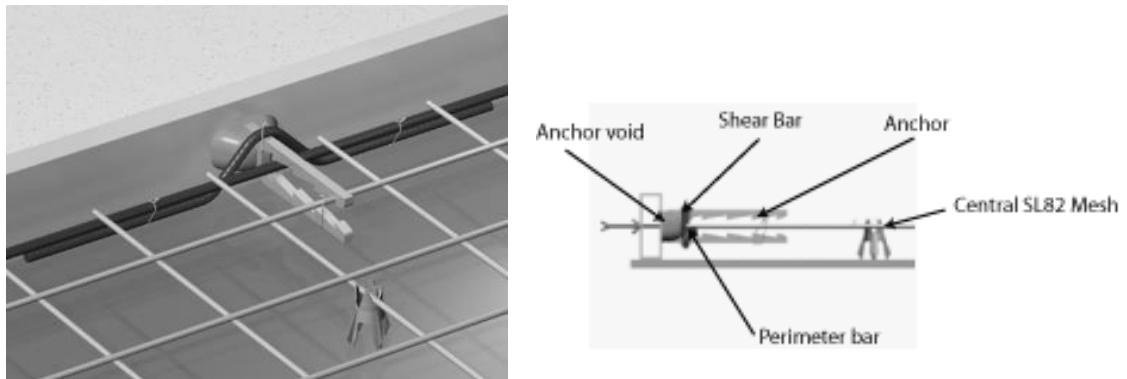


**Figure 60 - Reinforcement layout**

**Table 8 - Experiment test series**

Test Series	Type	$h_{ef}$ , mm	Reo types	Sample size, n	$f_{c,age}$ , MPa	Concrete age, days
TA1	Internal	252	B	25	22	2
TA2	Internal	272	B	25	22	2
TA3	Internal	295	B	25	22	2
TA4	Wavy	370	B	25	22	2
TA5	Headed	120	A	10	24	28
TA6	Headed	170	A	10	23	28
TA7	Headed	240	A	10	23	28
TA8	Headed	35	n/a	5	21	2
TA9	Headed	45	n/a	5	21	2
TA10	Headed	50	n/a	5	21	2
TA11	Headed	65	n/a	5	21	2

## 5.1 Edgelift test 1 – Anchor shape and configuration experimental program

**Table 9 - Reinforcement Configurations for Test Series TA1 – TA7**

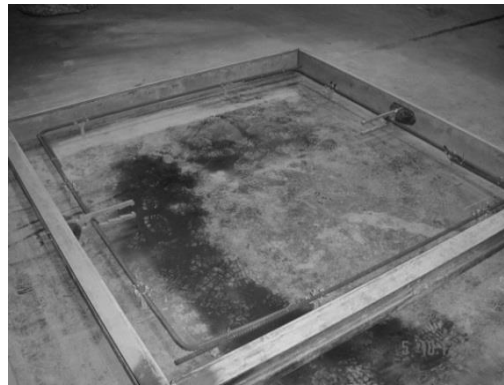
Reinforcement Configuration	N16 Shear bar	N12 Shear bar	Central SL82 mesh	N16 Perimeter bar
A	Nil	Nil	Nil	Nil
B	Nil	Yes	Yes	Yes

The preparation of the specimens for testing is shown in Figure 60.

Figure 61 (b) shows a typical 2m x 2m x 150mm thick panel formwork with N16 perimeter bar and 16mm x 295mm effective embedment depth plate Edgelift anchors in the form. As can be seen, this panel had two test anchors which was the typical arrangement. If, after testing one of the anchors, it was observed that cracking had propagated then the second anchor, whilst still tested, was excluded from the results presented in this analysis and experiment.



(a) Series 1 anchor with no reinforcement



(b) Series 2 prior to installation of shear bar



(c) Series 3 Test Panel prior to installation of perimeter bar with SL82 mesh



(d) Series 4 or 5

**Figure 61 - Typical Test Panels Prior to Casting**

The anchors were loaded under load-control at a rate of 20 kN/min via a hydraulic jack with a load cell. The test data recorded for each specimen included load-

### 5.1 Edgelift test 1 – Anchor shape and configuration experimental program

displacement (of the anchor relative to a fixed point on the test panel or block) and load-time. The panels with Edgelift plate anchors were tested horizontally and supported off the floor on timber gluts whilst the panel reacted against a steel frame with an open span of 1.8 m as the load was applied to the anchor. The spacing of the reaction frame for the anchors was outside the predicted failure zone for the concrete by at least 450mm as shown in Figure 62. The foot anchors embedded in the face of the panels and blocks were tested at the same loading rate in direct tension. The load was applied to the headed anchors via a tripod reaction frame with the legs of the reaction frame placed at a distance from the anchor of least three times the effective embedment depth of the anchor.

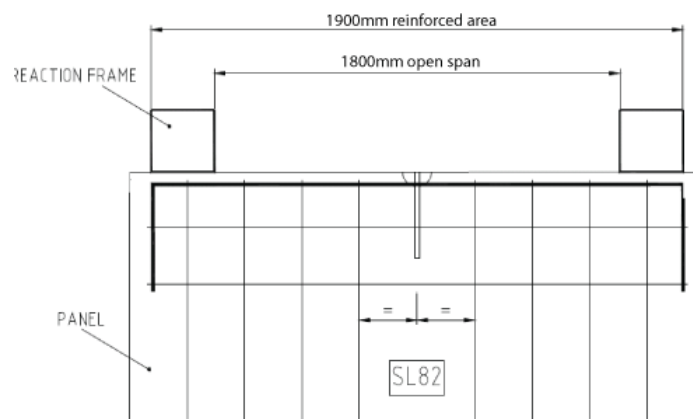


Figure 62 - Panel plan indicating open span of the reaction frame (Edgelift plate anchor tests)

## 5.1 Edgelift test 1 – Anchor shape and configuration experimental program

### 5.1.2 Test Results and Analysis

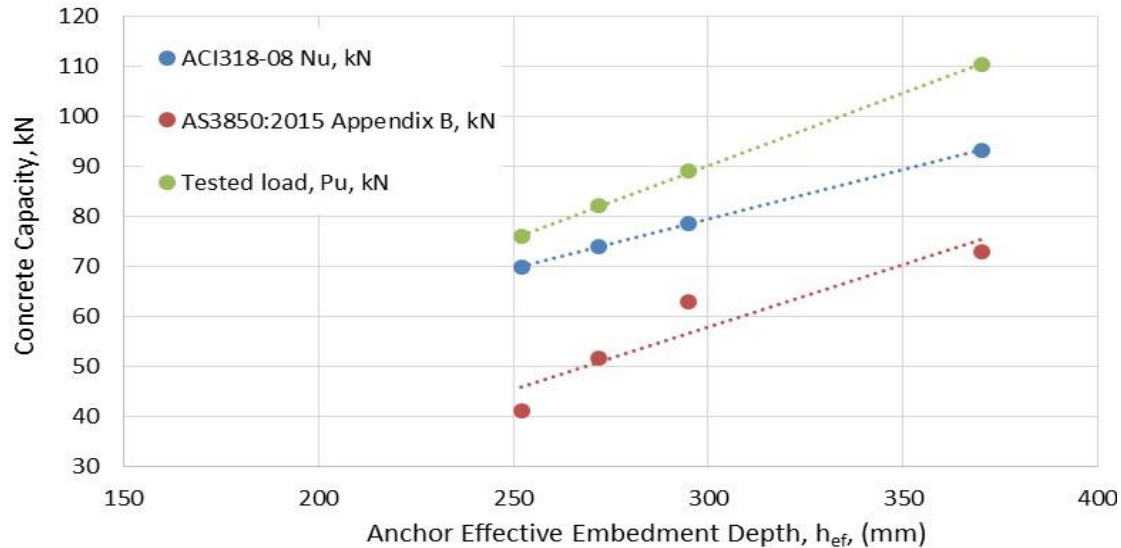


Figure 63 – Various  $h_{ef}$  tested loads vs ACI318 (2008) and AS3850 (SAI 2015) (test series TA1 – TA4)

When comparing the tested capacities,  $P_u$ , for various anchor embedment depths detailed in TA1 – TA4, against the models presented in AS3850 (SAI 2015) and ACI318 (2008), it is found that both the published models provide an adequately conservative prediction of the anchor capacity.

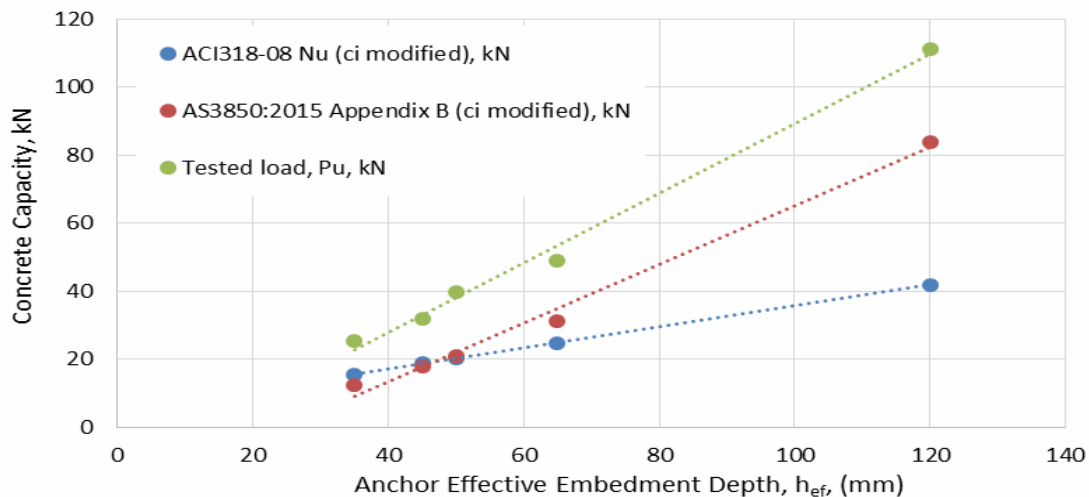
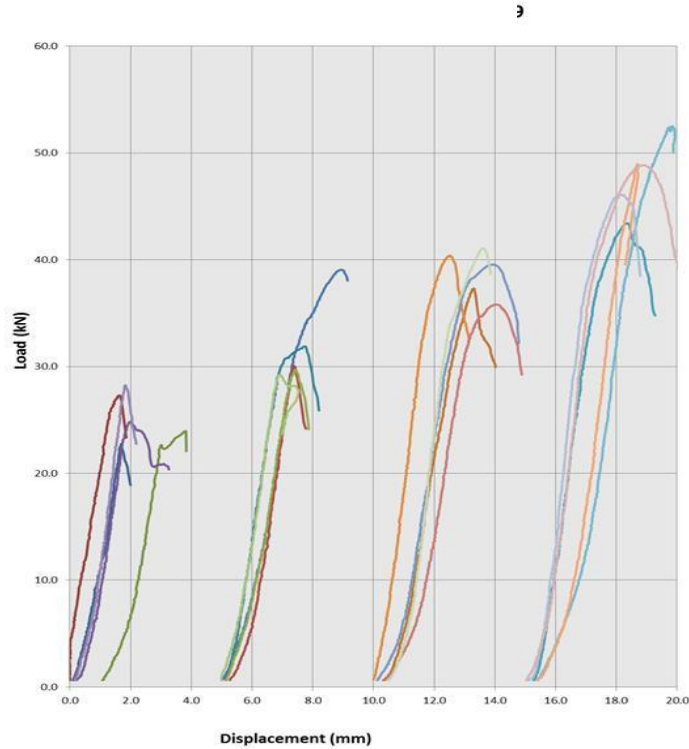


Figure 64 – Various  $h_{ef}$  tested loads vs edge modified cone capacity in ACI318 (2008) and AS3850 (SAI 2015) (test series TA5-TA8)



### 5.1 Edgelift test 1 – Anchor shape and configuration experimental program

The model presented in AS3850 (SAI 2015), modified for edge distance, correlates to the tested characteristic loads found in testing detailed in TA5 – TA8. As shown in Figure 64 the model presented in ACI318 (2008), with edge distance modifications applied, predict a more conservative model than AS3850 (SAI 2015).



**Figure 65 - Load vs displacement curves for test series TA1 - TA4**

The analysis of the test results concludes that both ACI318 (2008) and AS3850 (SAI 2015) are suitably conservative to predict the concrete capacity of these anchors, for both non edge reduced and edge reduced models.

### 5.1 Edgelift test 1 – Anchor shape and configuration experimental program

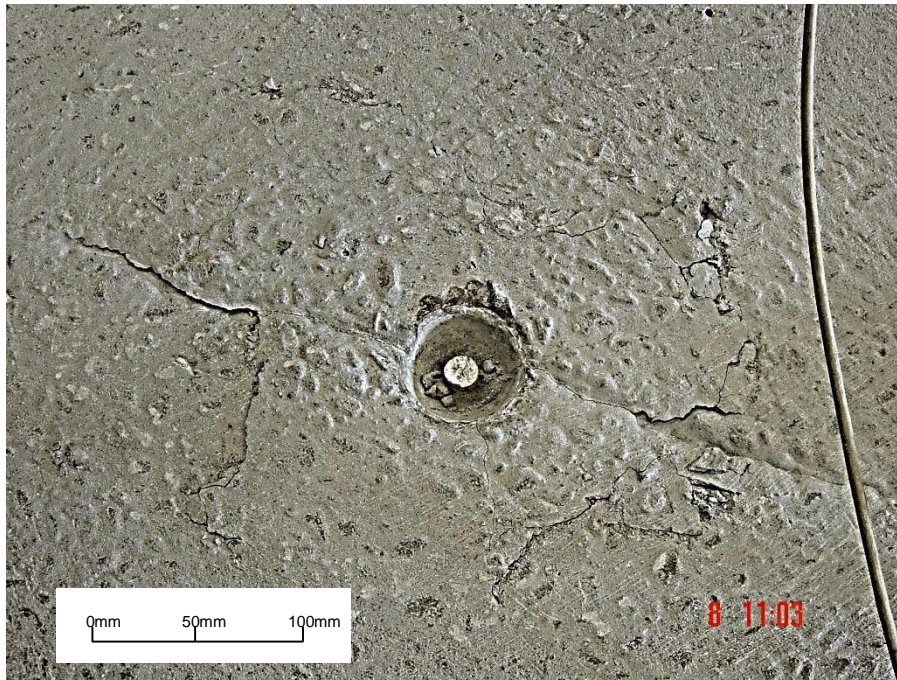


**Figure 66 - Panel of Series TA11 with failed headed anchor**

The Edgelift anchor test data was compared with the predicted capacity as determined using the ACI318 (2008) characteristic  $N_u$  formula as a mechanism of comparison to the well-established relationship for foot anchors presented in literature and verified in the tests shown in Section 5.2.

For the tests with Edgelift anchors and no central mesh reinforcement in the panels; Series TA1 and Series TA2, the following observations were made: The addition of shear and perimeter bars (Series TA2) resulted in a slightly increased absolute failure load for comparable tests and is indicated by a slightly higher average ratio of test/predicted compared to Series TA1. Since the manufacture of panels without central mesh is impractical, the number of tests conducted was small; however, the test results are valuable as an indicator that the provision of the perimeter bars is likely to be beneficial to the capacity of the anchor. Thus this detail (N16 perimeter bar) along with central panel mesh of SL82 was subsequently used in Series TA3, TA4 and TA5.

For the three series of panels with central mesh reinforcement and N16 perimeter bar in the panels; Series TA3, Series TA4 and Series TA5, the following observations were made: Series 3, the Edgelift anchors with no additional N12 or N16 shear bar reinforcement, has a significantly higher capacity than the unreinforced panels as

## 5.1 Edgelift test 1 – Anchor shape and configuration experimental program

indicated by the value of test/predicted ratio average of almost 2.5. The two series with additional shear bar of either N12 or N16 had similar average and range of test/predicted apparently less than the panels without shear bars.

### 5.1.3 Concluding remarks

This experiment is an evaluation of pull out test data for Edgelift anchors in thin walled elements. Using the formula in the ACI 318 (2008), developed predominantly for headed anchors, comparisons of the predicted capacity and the test pull out capacity of the Edgelift anchors is made. Three series of panels were reinforced with centrally placed SL82 mesh, and the ratios of test to predicted failure load indicate that the capacity of these anchors was well in excess of the predicted failure load as per ACI 318 (2008), approximately 1.43 to 1.92 times.

Overall, 140 tests were conducted using Edgelift anchors in direct tension; the variables tested include concrete compressive strength at time of testing which ranged from 21MPa to 44MPa with an average of 32MPa, and arrangement of reinforcement which included the provision or exclusion of perimeter bars, and shear bars (N16, N12 or nil) and central mesh reinforcement in the panel.

The tested tensile capacity of cast-in Edgelift anchors with various reinforcement configurations analysis are shown below.

Using Equation 5 to calculate the characteristic predicted capacity of the headed

anchors,  $\phi_t = \phi_c \sqrt{f_c} (h_{ef})^{3/2}$ , with no modification factor as these tested are

tested with a reaction frame greater than  $2 \times h_{ef}$ , and there are no spacing or edge reductions to account for and the anchor is a headed anchor.

Smaller coefficient of variation for all concrete strengths. The tested ultimate is smaller than the shallower embedded Edgelift anchors, and displays a different failure mode, being side blow-out.

## 5.1 Edgelift test 1 – Anchor shape and configuration experimental program

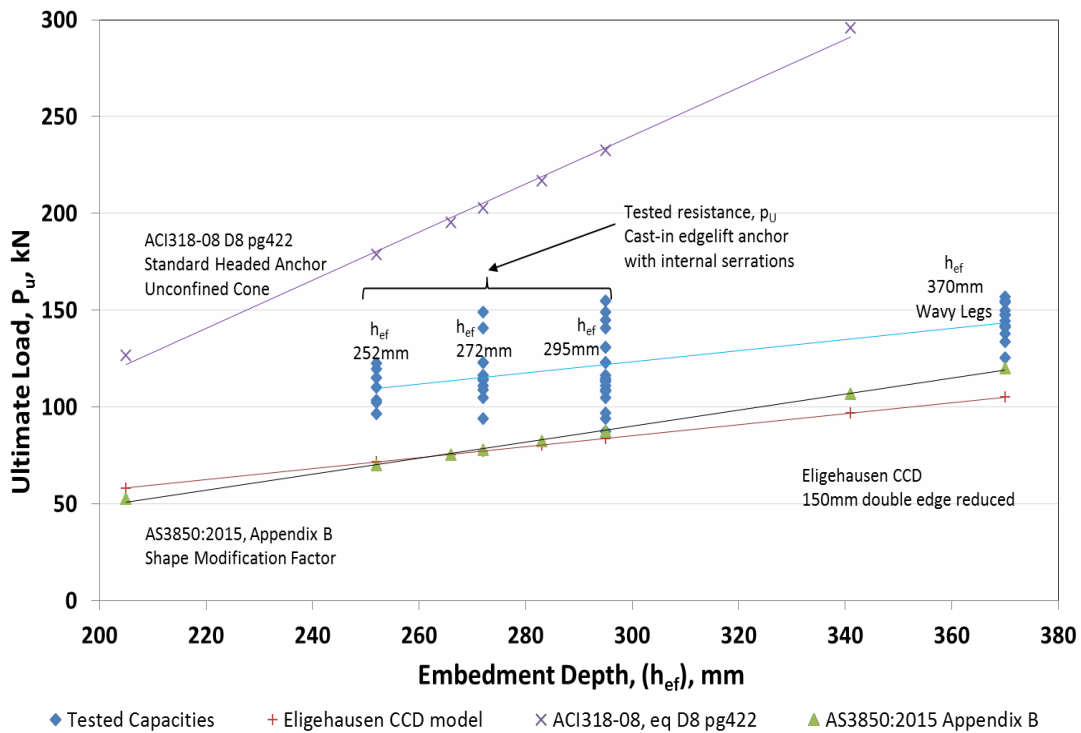


**Figure 67 - Tested tensile resistance versus predicted characteristic resistance of cast-in Edgelift anchors**

The values presented in Figure 67 for AS3850 (SAI 2015) values are calculated using Equation 3, for ACI318 (2008) Equation 2 was used, and Elgehausen CCD Equation 1 was used, where:

$$f_{cd} = 20\text{MPa}$$

$$h_{ef} = 210\text{mm}, 252\text{mm}, 265\text{mm}, 272\text{mm}, 285\text{mm}, 295\text{mm}, 340\text{mm} \text{ and } 370\text{mm}.$$

$$\phi_{cd} = 1.25 \text{ for non-cracked concrete}$$

$$\beta_{cd} = 0.876$$

## 5.1 Edgelift test 1 – Anchor shape and configuration experimental program

The modification factor for double edge reduction applied to the Elgehausen (2004) model is the power formula, as follows:

Edge reduced modification =

$$\sqrt{(\sin 30^\circ)^{c_{i,1}} (\sin 30^\circ)^{c_{i,2}} (\sin 30^\circ)^{c_{i,3}} (\sin 30^\circ)^{c_{i,4}}}$$

**Equation 18**

Where  $c_{i,1}$ ,  $c_{i,2}$ ,  $c_{i,3}$  and  $c_{i,4}$  are measured as follows:

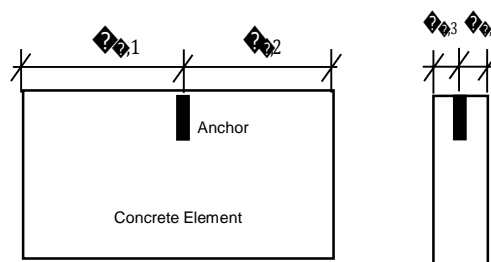


**Figure 68 - Distance to four edges for edge reduction modification, for  $c_{i,1}$ ,  $c_{i,2}$ ,  $c_{i,3}$  and  $c_{i,4}$**

## 5.2. Edgelift test 2 - Panel reinforcement influence on failure loads

This experiment summarises the pull out failure data (placed under both direct tensile and shear loads applied in a load controlled manner) of one hundred and ten, 110, Edgelift anchors embedded in concrete panels with various supplementary reinforcement (perimeter bar, shear bar, panel mesh) configurations around a plate style Edgelift anchor, shown in Figure 69.

Various configurations of supplementary reinforcement were load tested in tension using one anchor type (shown in Figure 69); including with and without panel mesh, with and without perimeter bar, with and without shear bar, and no tension bar. Whereas, shear tests were load tested with types of anchors, including a tension bar, and two variations of supplementary reinforcement; including a centrally placed perimeter bar or double perimeter bar, a shear bar and panel mesh, and both with a tension bar. The sizes, shapes and lengths were chosen based on common precast standard manufacturing practice. N Class<sup>3</sup> reinforcement steel, 16 mm thick plate Edgelift anchors were tested by pull out tests in a direct tensile and shear direction on anchors placed in 150mm thick panels measuring 2m x 2m perimeter. The tests were conducted using normal weight Portland cement concrete with a compressive strength at the time of testing of between 15MPa to 25MPa. The minimum strength recommended for lifting in a precast manufacturing application is 15MPa.

---

<sup>3</sup> Class N (normal ductility) reinforcing deformed bar complies with AS/NZS 4671 (SAI 2001) Steel reinforcing materials

## 5.2 Edgelifft test 2 - Panel reinforcement influence on failure loads

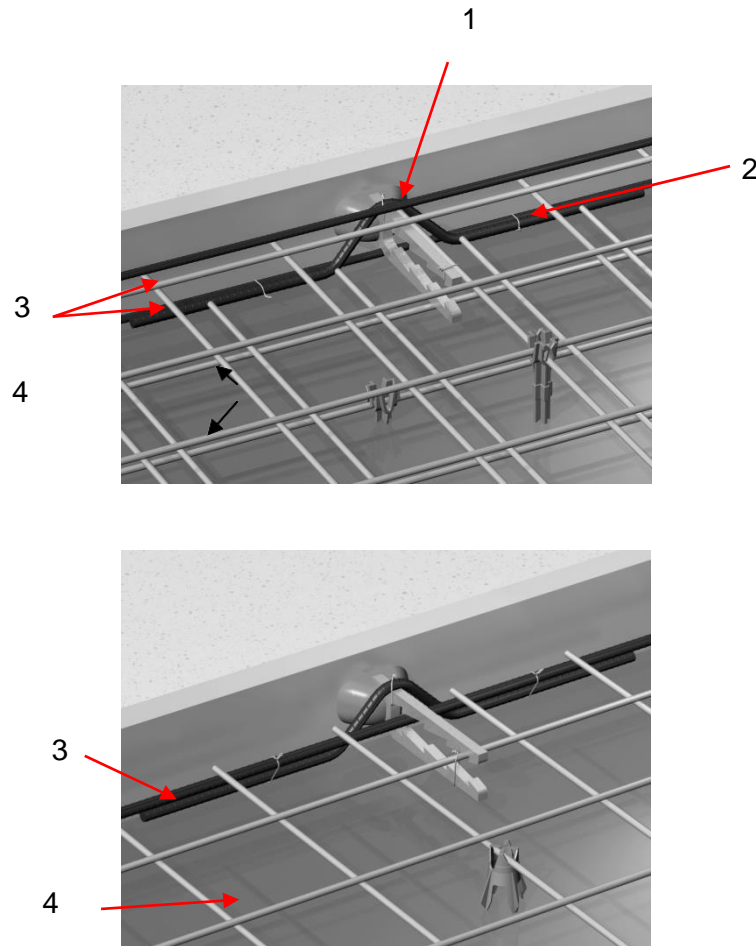


Figure 69 - Panel Reinforcement layout in relation to the lifting insert

(1), shear bar, (2), perimeter bar (3), double layered in the top picture and centrally placed in the bottom picture, both with SL82 panel mesh (4).

The pull-out failure loads are compared against each other to note the ultimate load, capacity increase with various reinforcing configurations, and spread of test data.

Both working stress and strength design methods are currently used in the design of lifting inserts. As cast-in anchors of the plate type used for Edgelifting vary considerably in the way they interlock mechanically with the concrete, it is unwise to assume the application of calculated capacities derived from published performance models if the particular anchor design is untested.

Working stress methods account for anchor placement and reduction factors that may have to be applied for variables such as edge distance from the anchor to the concrete surface and spacing to other anchors. The strength design methods are analytical approaches employing predictive equations as noted in ACI318 (2008), ACI 349 (2006), ACI355 (2003) and PCI Design Handbook (2004).

## 5.2 Edgelift test 2 - Panel reinforcement influence on failure loads

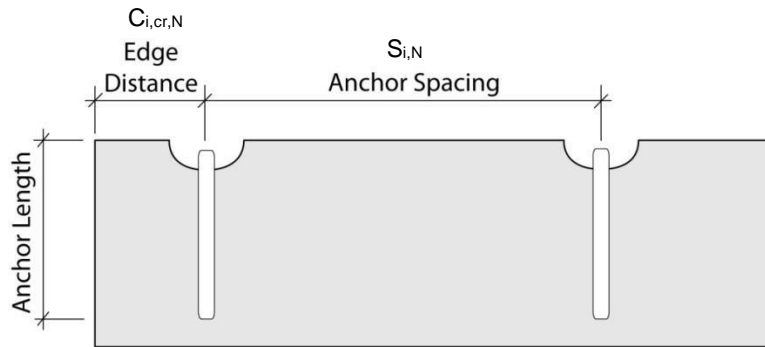


**Figure 70 - Anchor spacing,  $S_{i,N}$  and edge distances,  $C_{i,cr,N}$**

Anchor spacing and edge distances can be a unique characteristic to an anchors mechanical interlock features, where wavy legged plate anchor performance, Figure 71 (b), is adversely affected by edge distance to a greater degree than internally toothed plate anchors, see below photo.

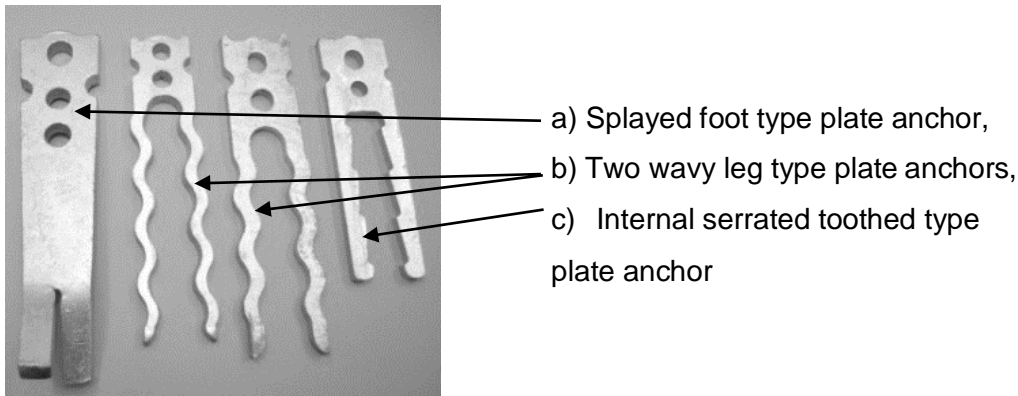


**Figure 71 - Anchor Types**

The above types of cast-in plate style anchor have unique mechanical interlock characteristics by the way the launcher legs are shaped, and which consequently influences load distribution embedded in concrete.

For the purposes of these tests the anchor (c) in Figure 71, was selected.

### 5.2.1 Experimental Program

The test method employed to establish failure loads of lifting inserts should be in compression zones, as would normally be experienced in lifting process. Different Edgelift plate anchor shapes will affect the ultimate capacity disproportionately with other variables such as: concrete type, aggregate specification, initial lifting concrete strengths, placement sensitivity to side splitting, moment couple to the shear bar in a



## 5.2 Edgelift test 2 - Panel reinforcement influence on failure loads

shear load direction, stress distribution along the anchors length, based on their individual mechanical interlock characteristics. When the capacity of an anchor is determined by brittle concrete failure, there may be limited distribution of the forces between the highly stressed and less stressed mechanical interlock sections of an anchor, and may be related to the geometry and shape of the anchor.

Plate-type Edgelift anchor pull out in a tensile (ninety, 90) and shear direction (twenty, 20) were conducted at concrete compressive strengths that would initiate a concrete cone failure. The perimeter bar used was either a centrally placed N16, or 2 x N12 perimeter bars placed either side of the anchor head. A shear bar was used in test series EP3, where a N16 x 90mm (height) x 250mm (leg length) was used. SL82 shrinkage mesh was used in test series EP4 and test series EP6. The same type of plate anchor was used throughout all the tests, which was 16 mm plate, with a profile as shown in Figure 72.

The test panel were all 150mm thick, with perimeter dimensions of 2m x 2m, the layouts and positions of the steel reinforcement, if used, is shown in Figure 72, Figure 73 and Figure 74.

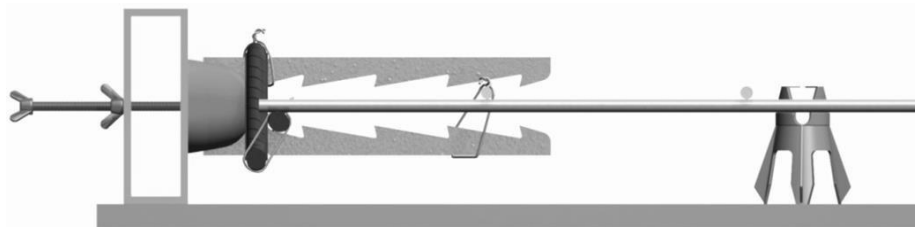


Figure 72 - Side view of mesh and perimeter bar placed central

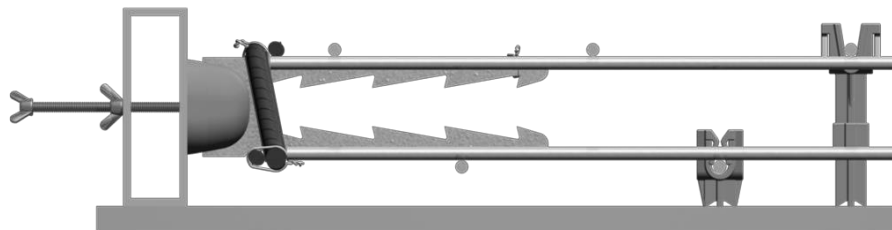
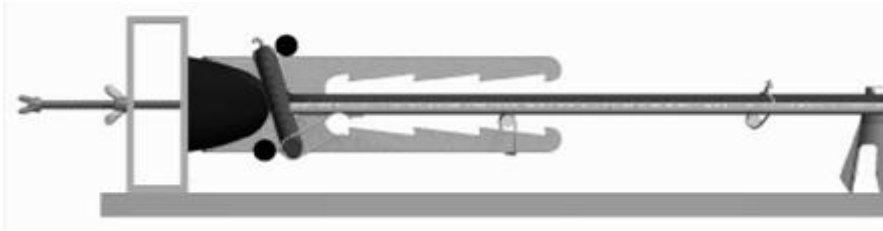


Figure 73 - Side view of double layer mesh and perimeter bars

## 5.2 Edgelift test 2 - Panel reinforcement influence on failure loads



**Figure 74 - Side view of tension bar, mesh and perimeter bar placed central**

Figure 72 side view layout shows a plate Edgelift anchor, N16 centrally placed perimeter bar and SL82 mesh, and a N16 x 90mm shear bar. Figure 73 side view layout shows a plate Edgelift anchor double N12 perimeter bars and double layer SL82 mesh, and a N16 x 90mm shear bar. Figure 74 side view layout shows a plate Edgelift anchor, double N12 perimeter bars, centrally placed SL82 mesh, and a N16 x 90mm shear bar.

Test Series EP1 to EP6 were tensile tests and Test Series EP7 and EP8 were shear tests. Test Series EP1 test panels were a 150mm thick panel, a plate Edgelift anchor of 80mm width x 16mm thick, with no additional reinforcement in the panel. Test Series EP2 test panels were a 150mm thick panel, a plate Edgelift anchor of 80mm width x 16mm thick, with a centrally placed N16 perimeter bar. Series EP3 test panels were a 150mm thick panel, a plate Edgelift anchor of 80mm width x 16mm thick, with a shear bar of N16 x 90mm height, and a centrally placed N16 perimeter bar. Series EP4 test panels were a 150mm thick panel, a plate Edgelift anchor of 80mm width x 16mm thick, with a centrally placed N16 perimeter bar and centrally placed SL82 shrinkage mesh. Series EP5 test panels were a 150mm thick panel, a plate Edgelift anchor of 80mm width x 16mm thick, with a top and bottom placed N12 perimeter bar. Test Series EP6 test panels were a 150mm thick panel, a plate Edgelift anchor of 80mm width x 16mm thick, with a top and bottom N12 perimeter bar, and top and bottom SL82 shrinkage mesh.

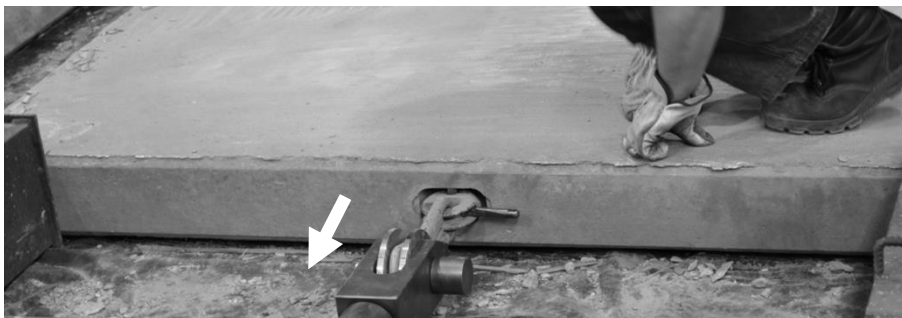


**Figure 75 - Tensile applied load rate 20kN/min, 150mm thick panel, and open span 1.8m**

## 5.2 Edgelif test 2 - Panel reinforcement influence on failure loads

Test Series EP7 test panels were a 150mm thick panel, a plate Edgelif anchor of 80mm width x 16mm thick, N16 x 500mm tension bar, with a centrally placed N16 perimeter bar and centrally placed SL82 shrinkage mesh. Test Series EP8 test panels were a 150mm thick panel, a plate Edgelif anchor of 80mm width x 16mm thick, N16 x 500mm tension bar, with a top and bottom N12 perimeter bar, and centrally placed SL82 shrinkage mesh.

Normal strength concrete was used throughout all series of the tests; being 14 mm coarse aggregate, 0.44 water/cement ratio, and nominal grade 40MPa design strength supplied by a commercial ready-mix company, with the mix detailed in Table 6. The test was scheduled to be conducted in 3 progressive concrete compressive strength intervals, being a target mean compressive strength at 15 +/-2.5 MPa, 20 +/-2.5 MPa and 25 +/-2.5 MPa, where the mean actual compressive strengths,  $f_{c,age}$ , 15.3MPa, 20.8MPa and 26.5MPa were achieved. Full concrete compressive data for all series is shown in Table 11. Concrete compressive strength,  $f_{c,age}$ , was recorded by means of cylinder compression tests. Where 4 anchors were setup in a panel for testing, 9 cylinder compressive strengths were recorded for each panel test, 3 at the beginning and end, and 1 after testing anchor 1, 2 and 3. The mean of these cylinder compressive strengths was calculated,  $f_{c,age}$ , for each panel test, and noted in Table 11.

**Table 10 - Reinforcement Configurations for Test Series**

Test Series	Applied Load Direction	Panel Reinforcement, N Class				Anchor Reinforcement	Sample Size, n
		Perimeter Bar, N16 Central	Perimeter Bar, N12 x2	Shear Bar, N16x90mm	SL82 Mesh	Tension bar, N16 x 500mm	
EP1	Tensile	Nil	Nil	Nil	Nil	Nil	15
EP2	Tensile	Yes	Nil	Nil	Nil	Nil	15
EP3	Tensile	Yes	Nil	Yes	Nil	Nil	15
EP4	Tensile	Yes	Nil	Nil	Yes	Nil	15
EP5	Tensile	Nil	Yes	Nil	Nil	Nil	15
EP6	Tensile	Nil	Yes	Nil	Yes	Nil	15
EP7	Shear	Yes	Nil	Yes	Yes	Yes	10
EP8	Shear	Nil	Yes	Yes	Yes	Yes	10

## 5.2 Edgelift test 2 - Panel reinforcement influence on failure loads

**Table 11 - Concrete Compressive Data, tested at 3 progressive strengths for each test panel**

Test Series	Lower Compressive Strength $f_{c,age}$ (MPa)	Mid Compressive Strength $f_{c,age}$ (MPa)	Higher Compressive Strength $f_{c,age}$ (MPa)
EP1	18	22	26
EP2	15	23	29
EP3	16	20	24
EP4	16	21	25
EP5	15	20	28
EP6	12	19	27
Average	15.3	20.8	26.5
EP7	16	Not applicable	
EP8	16		
Average	16		



**Figure 76 - View of EP2 panel setup – tensile test**

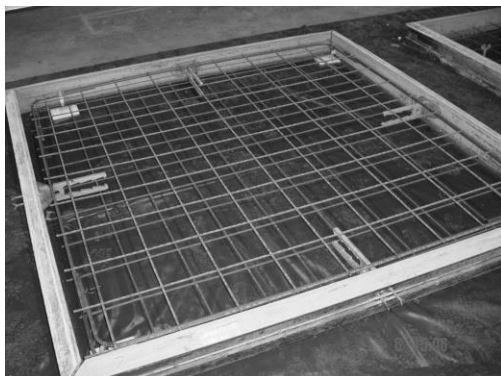


**Figure 77 - View of EP6 panel setup – tensile test**

## 5.2 Edgelift test 2 - Panel reinforcement influence on failure loads



**Figure 78 - View of EP8 panel setup – shear test**

Figure 76 shows the tensile test panel setup of an 80mm x 16mm plate Edgelift anchor, centrally placed N16 perimeter bar. Figure 77 shows the tensile test panel setup of an 80mm x 16mm plate Edgelift anchor, double N12 perimeter bars and SL82 shrinkage mesh. Figure 78 shows the shear test panel setup of an 80mm x 16mm plate Edgelift anchor, N16 x 500mm tension bar, double N12 perimeter bars, centrally placed SL82 shrinkage mesh. All anchors were tested in 150mm thick panels.

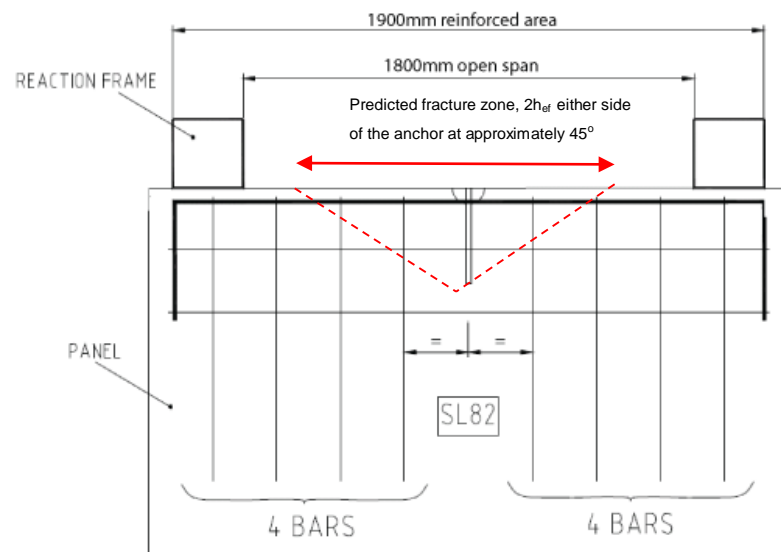


**Figure 79 - Tension panel reinforcement placement, where applicable**

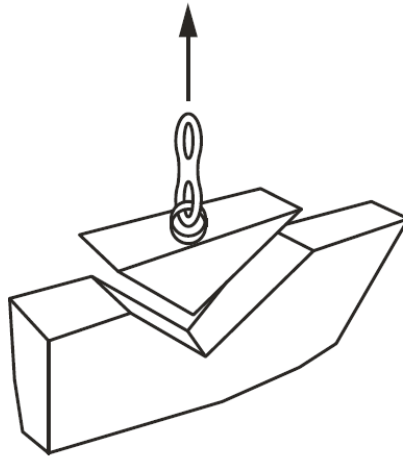


**Figure 80 - Predicted concrete fracture cone from a cast-in anchor in a thin panel, tensile load direction**

The anchors were loaded under load-control at a rate of 20kN/min via a hydraulic jack with a load cell. The anticipated failure mode is shown in figure 80. The test data recorded for each specimen included load-displacement (of the anchor relative to a fixed point on the test panel or block) and load-time. The full test data is detailed in Appendix B - Test Data. The panels were tested horizontally and supported off the floor on timber gluts whilst the panel reacted against a steel frame with an open span of 1.8 m as the load was applied to the anchor. The spacing of the reaction frame for the anchors was outside the predicted failure zone for the concrete by at least 900mm as shown in Figure 79.

### **5.2.2 Test Results and Analysis**

Plate-type Edgelift anchor tensile pull out tests (one hundred and ten, 110 off) were conducted at concrete compressive strengths that would initiate a concrete cone failure. The reinforcement used in these tests were N12 and N16 perimeter bar, SL82 shrinkage mesh and 80mm (width) x 16mm (thick) plate Edgelift anchors. They were cast in thin (150mm thick) panels with the various configurations of reinforcement in and around the anchor, detailed in Table 10. The range of concrete compressive strengths at time of test was 12MPa to 29MPa, with an average at each targeted compressive strength of 15.3MPa, 20.8MPa and 26.5MPa, which is detailed in Table 11.

## 5.2 Edgelifft test 2 - Panel reinforcement influence on failure loads

TENSILE TESTS			
EP1 - 150mm Panel, 80x16mm Anchor, No Reo			
Concrete Compressive Strength, $f_{c,age}$ , MPa	18	22	26
Mean	59	64	72
Count	5	5	5
Co-efficient of Variation	18.8%	21.4%	21.1%
EP2 - 150mm Panel, 80x10mm Anchor, N16 Perimeter bar			
Concrete Compressive Strength, $f_{c,age}$ , MPa	15	23	29
Mean	79	90	112
Count	5	5	5
Co-efficient of Variation	3.8%	3.9%	3.5%
EP3 - 150mm Panel, 80x16mm Anchor, Centrally placed N16 perimeter bar, N16x90mm Shear bar			
Concrete Compressive Strength, $f_{c,age}$ , MPa	16	20	24
Mean	63	71	79
Count	5	5	5
Co-efficient of Variation	14.8%	15.1%	15.2%
EP4 - 150mm Panel, 80x16mm Anchor, Centrally placed N16 Perimeter bar and SL82 mesh			
Concrete Compressive Strength, $f_{c,age}$ , MPa	16	21	25
Mean	122	131	141
Count	5	5	5
Co-efficient of Variation	6.5%	6.1%	6.3%
EP5 - 150mm Panel, 80x16mm Anchor, Double N12 Perimeter bar			
Concrete Compressive Strength, $f_{c,age}$ , MPa	15	20	28
Mean	86	100	112
Count	5	5	5
Co-efficient of Variation	3.7%	3.6%	4.0%
EP6 - 150mm Panel, 80x16mm Anchor, Double N12 Perimeter bar and SL82 mesh			
Concrete Compressive Strength, $f_{c,age}$ , MPa	12	19	27
Mean	148	173	192
Count	5	5	5
Co-efficient of Variation	5.2%	5.1%	4.8%

Table 12 - Tensile capacity results for test series EP1 - EP6



Figure 81 - Series EP1 typical failure, no panel reinforcement

## 5.2 Edgelift test 2 - Panel reinforcement influence on failure loads

Series EP1 displays brittle failure, with no steel reinforcement to provide ductility. The failure mode experienced was concrete truncated cone on one side, with root of the crack starting from within 5mm of the first anchor tooth. Flexure cracks (Figure 82 A and Figure 83 C) were observed very close to the ultimate load, within 5kN.



**Figure 82 - Series EP2 typical failure, N16 central perimeter bar**

Series EP2 displays brittle failure, a change in crack direction above the perimeter bar was noted. The failure mode experienced was concrete truncated cone, with root of the predominant crack within 5mm rearward of the position of the perimeter bar. The crack angle changes direction approximately 25mm from the panel edge.





Figure 83 - Series EP3 typical failure, N16 central perimeter bar, N16 x 90mm shear bar

Flexure cracks (Figure 83 C) were observed to within 10% of the ultimate applied load. Series EP3 displays brittle failure, with a change in crack direction when normal to the perimeter bar. The failure mode experienced was concrete truncated cone, with root of the predominate crack within 5mm rearward of the position of the perimeter bar. This predominant crack comes to the panel edge surface within 100mm of the anchor (Figure 83 A), and other horizontal cracks (Figure 83 A) are visible on the panel edge surface. The crack surface area is noticeably smaller than that observed in series EP2. Flexure cracks (Figure 84 A) were observed at approximately 50% of the ultimate applied load.

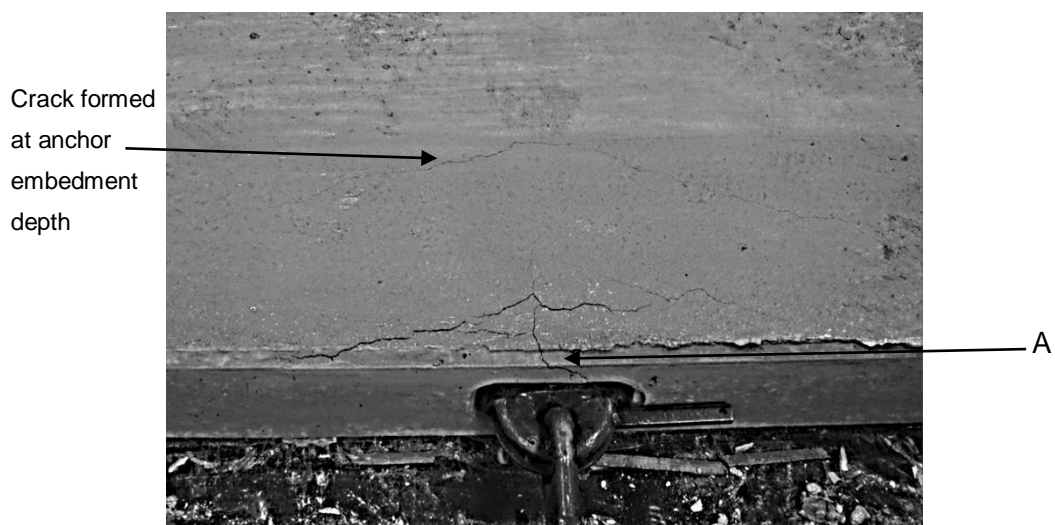
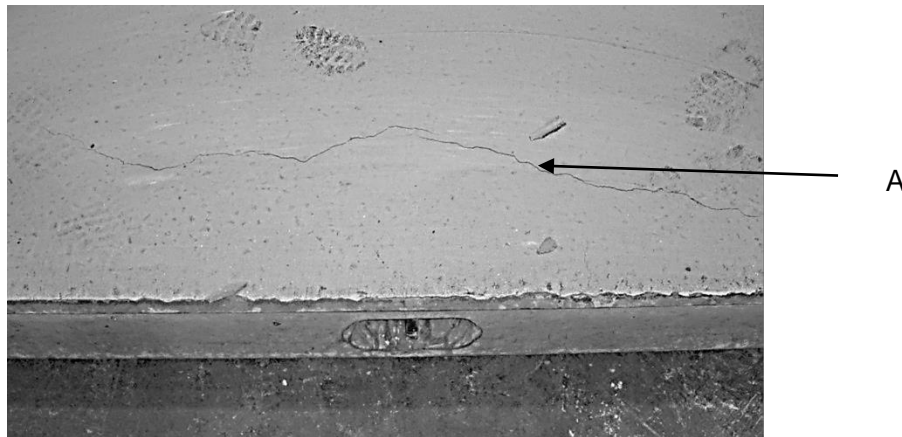


Figure 84 - Series EP4 typical failure, SL82 central mesh, N16 central perimeter bar

## 5.2 Edgelift test 2 - Panel reinforcement influence on failure loads

Series EP4, Figure 84, displays permanently displaced crack widths  $<1.5\text{mm}$  maximum, with the predominant crack normal to the perimeter bar and anchor intersection, and a secondary crack formation normal to the anchor embedment depth position. Crack distribution is less concentrated in series EP4 than those noted in series EP1-EP3. Flexure cracks as per Figure 84 were observed. A horizontal crack was observed on the surface, which opened up at approximately 50% of the ultimate applied load.



**Figure 85 - Series EP5 typical failure, N12 double perimeter bars**

Series EP5 displays permanently displaced crack widths  $<1.0\text{mm}$  maximum, with the secondary crack above the perimeter bar and anchor intersection, and the primary crack formation normal to the anchor embedment depth position, figure 85 A. Crack positions are similar to series EP4, where the secondary and primary cracks are swapped over.



**Figure 86 - Series EP6 typical failure, N12 double perimeter bars, SL82 double layer mesh**

Series EP6 displays a predominant crack on the panel broad face above the perimeter bar and anchor intersection, with no noticeable secondary crack. Other cracks were

## 5.2 Edgelift test 2 - Panel reinforcement influence on failure loads

observed on the panel edge face (Figure 86 A) originating from the anchor head in two directions on both sides.

Plate-type Edgelift anchor shear pull out tests (20 off) were conducted at a concrete compressive strength that would initiate a concrete cone failure. The reinforcement used in these tests were centrally placed N16 reinforcing bar, SL82 shrinkage mesh and 80mm (width) x 16mm (thick) plate Edgelift anchors, and a N16 x 500mm tension bar. They were cast in thin (2m x 2m x 0.15m thick) top panels, with a reaction base cast underneath (2.4m x 2.4m x 0.1m) with the various configurations of reinforcement in and around the anchor, detailed in table 2. Normal strength concrete was used throughout the series of the tests; being 14 mm coarse aggregate, 0.44 water/cement ratio, and nominal grade 40MPa design strength supplied by a commercial ready-mix company. The concrete compressive strength at time of test was 16MPa, which is detailed in Table 11.

SHEAR TESTS	
<b>EP7 - 150mm Panel, 80x16mm Anchor, Centrally placed N16 Perimeter bar and SL82 mesh</b>	
Concrete Compressive Strength, $f_{c,age}$ , MPa	16
Mean	51
Count	10
Co-efficient of Variation	6.0%
<b>EP8 - 150mm Panel, 80x16mm Anchor, Double N12 Perimeter bar and SL82 mesh</b>	
Concrete Compressive Strength, $f_{c,age}$ , MPa	15
Mean	62
Count	10
Co-efficient of Variation	7.0%

**Table 13 - Shear capacity results for test series EP7 and EP8**

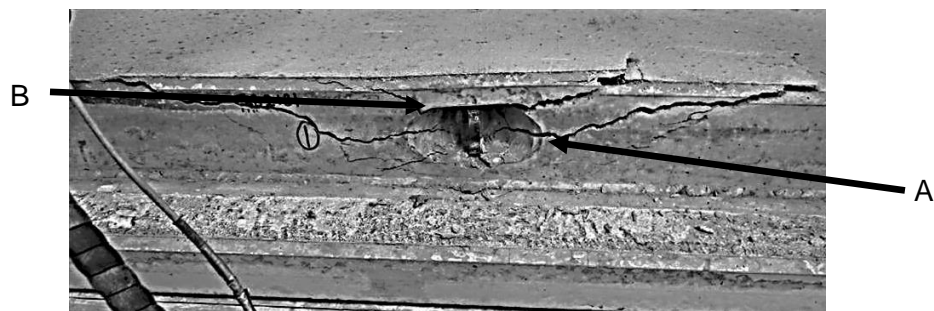


**Figure 87 - Series EP7 typical surface cracks**

Series EP7 displays the predominant crack origin normal to the perimeter bar and anchor intersection, on the panel edge face (Figure 87 A) with the secondary crack

## 5.2 Edgelift test 2 - Panel reinforcement influence on failure loads

originating from the head of the anchor, Figure 87 B. Cracks observed on the panel edge face (Figure 87 A) originated from the centre line of the anchor head in two directions on both sides.



**Figure 88 - panel near face failure surface observed for series EP7 and EP8**

Figure 88 depicts typical dual conical failure surfaces, with one originating from the anchor head and the other originating from either the perimeter bar position or shear bar effective embedment depth. Both cracks propagate to the surface of the panel broad face as a  $\frac{1}{2}$  cone.



**Figure 89 - Series EP8 typical surface cracks**

Series EP8 displays the start of predominant crack at the head of the anchor (Figure 89 A), and the secondary crack (Figure 89 B) normal to the centre of the anchor head, and on both sides of the anchor head. Smaller cracks, <1mm width, were observed on the panel edge face (Figure 89 C) originated from the base of the anchor in two directions on both sides.

The Edgelift anchor ultimate loads were used to establish the standard deviation, mean, and co-efficient of variation for each target concrete compressive strength and are represented in Table 12 and Table 13.

## 5.2 Edgelifth test 2 - Panel reinforcement influence on failure loads

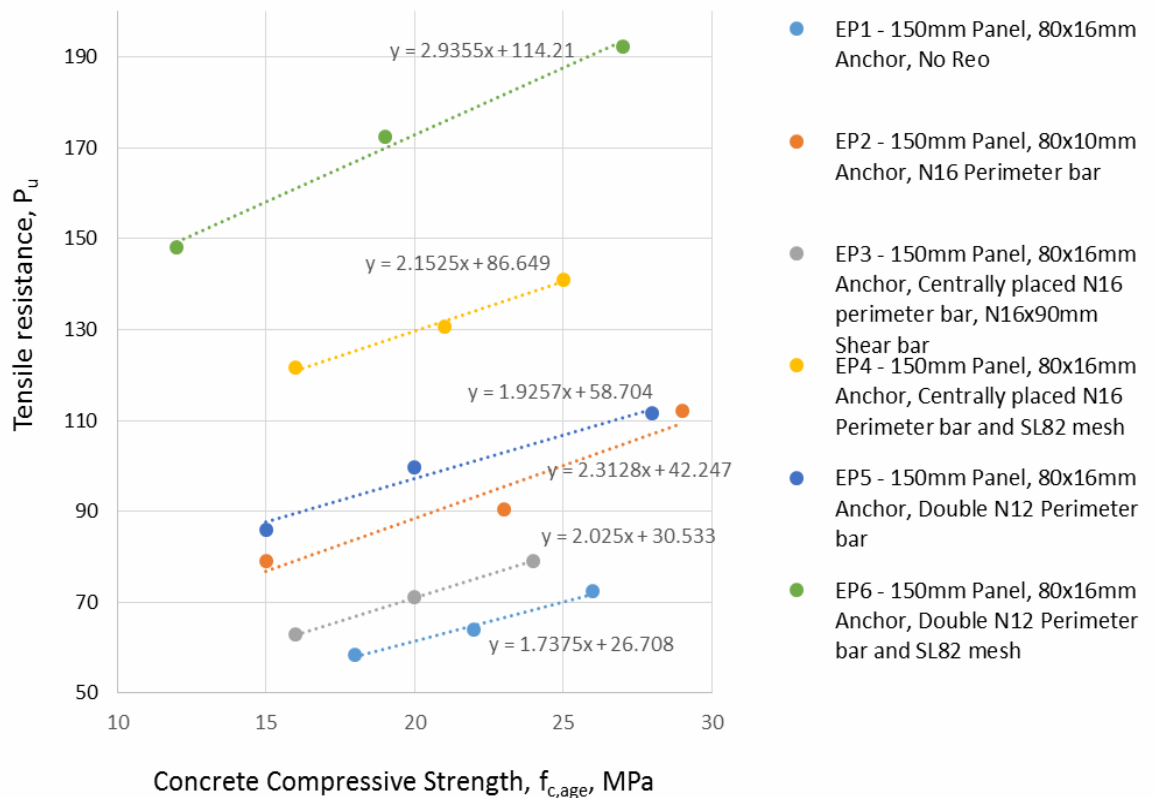


**Figure 90- Characteristic tensile failure loads at various concrete strengths,  $f_{c,age}$ , MPa**

There was a capacity increase observed in the test results from Series EP1 to Series EP2, this shows that an N16 perimeter bar adds slight tensile capacity compared against an unreinforced panel. The coefficient of variation for the unreinforced test panels, Series EP1, was on average above 20%, whereas the test panels with just the N16 perimeter bar, Series 2, tested at 4% coefficient of variation. The Pearson product moment correlation coefficient for Series 1 and 2 is calculated at 0.983 and 0.932 respectively. Series EP4, EP5 and EP6 test results calculated an average coefficient of variation of 6%, 4% and 5% respectively, whereas Series 3 test results calculated an average coefficient of variation of 15%. Series 3 was tested with a shear bar attached, whereas test series EP4, EP5 and EP6 did not. It should also be noted that Series 3 did not have panel mesh installed. Both test series EP4 and EP6 included panel mesh, SL82, and displayed a combined minimum test result, at 16MPa, of 113kN, whereas the combined maximum test result, at 15MPa, from Series EP3 and EP5 was 89kN. Since SL82 panel mesh includes both horizontal and vertical 8mm bars, further research would be required to establish the capacity contribution to ultimate load based on orientation to the crack failure surface.

## *5.2 Edgelift test 2 - Panel reinforcement influence on failure loads*

Series EP2 with series EP3 shows a decrease in ultimate anchor tensile capacity, with the reinforcing configurations being N16 perimeter bar for series EP2, and N16 perimeter bar and N16 shear bar for Series EP3. Test series EP3, including the shear bar, experienced panel flexural cracks at approximately 50% of ultimate load. SL82 panel mesh was not installed in either series EP2 or EP3.

Both Series EP4 and Series EP6 included SL82 panel mesh, perimeter bars (Series EP4 central N16, and Series EP6 double N12), where Series EP6 has a steeper ultimate load capacity gradient of 1:2.94, with increasing concrete compressive strength, than Series 4 with a gradient of 1:2.15. Series EP6 test results, which was tested with double N12 perimeter bars and SL82 panel mesh, show an increased ultimate load capacity of approximately 25% at 20MPa +/-1, compared against series EP4, which was tested with a centrally placed N16 perimeter bar and SL82 panel mesh. The calculated Pearson product moment correlation coefficient for Series EP4 and EP6 is 0.98 and 0.99 respectively.

It should also be noted that Series EP2 and Series EP5 ultimate load capacities tested at an average coefficient of variation of 4%, display similar gradients of increasing ultimate load capacity with concrete compressive strength increase.

## 5.2 Edgelift test 2 - Panel reinforcement influence on failure loads

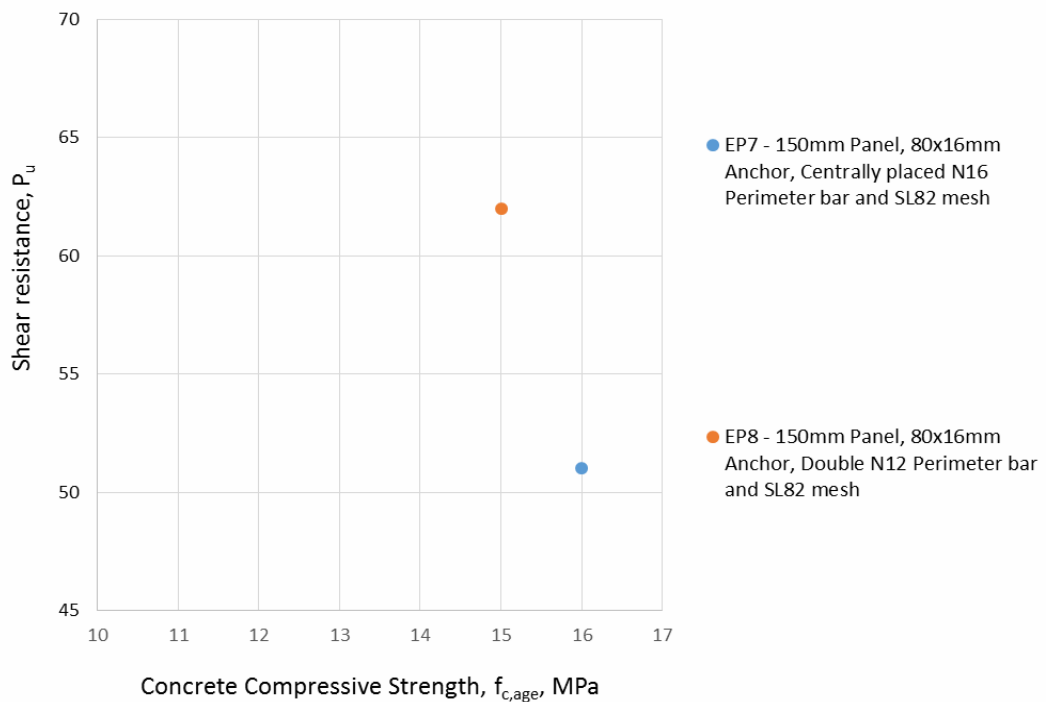


**Figure 91 - Characteristic shear failure loads at concrete compressive strengths,  $f_{c,age}$ , MPa**

The shear tests conducted show that double N12 perimeter bars contribute 20% additional anchor shear load capacity, at 16MPa, when compared to a centrally placed N16 perimeter bar. Both series EP7 and EP8 calculated a coefficient of 6% and 7% respectively, and include SL82 panel mesh.

### 5.2.3 Concluding remarks

This experiment is an evaluation of pull out test data for various configurations of panel reinforcement of Edgelift anchors in thin walled elements. Using the ultimate tested loads, an estimation of load contribution can be made for each variation of panel reinforcement.

Overall, one hundred and ten, 110, tests were conducted using Edgelift anchors in direct tension and 20 tests were conducted using Edgelift anchors in shear; the variables tested include concrete compressive strength at time of testing which had a target range of 15MPa, 20MPa and 25MPa. With a tested average of 15.3MPa, 20.8MPa and 26.5MPa respectively for the tensile tests, and 16MPa average concrete compressive strength for the shear tests.

## 5.2 Edgelift test 2 - Panel reinforcement influence on failure loads

The test results show that by using double N12 perimeter bars with a double layer SL82 mesh, compared against centrally placed SL82 shrinkage mesh and centrally placed N16 perimeter bar, the anchor capacity is increased, by a tensile ultimate anchor capacity of 25% at 20MPa,  $f_{c,age}$ , and a shear anchor ultimate load capacity increase of 20%. These tests show that a N16 perimeter bar and a N16 shear bar installed with a plate Edgelift anchor, the tensile ultimate load is reduced on average by 20%, at 16MPa, when compared to the same reinforcement configuration without a shear bar.

Adding a steel shear bar placed over the head of the anchor increases the reliability or coefficient of variation to the tested results. The capacity is increased when assessing the relative concrete failure modes.

Conducting an ANOVA analysis to this the entire data set shows that  $F > F_{crit}$ , therefore the null hypothesis is rejected. This means that of the 6 populations, EP1 – EP6 are not all equal. At least one of the means is different. Therefore, a t-Test was calculated to test each pair of means. First an F-Test was calculated to determine if the variances of the two populations are equal.

As the standard deviation between EP3, EP4 and EP6 is between 8 and 9, similar normal distribution of data, ANOVA analysis to separate increase in capacity over test error or normal data spread, the following ANOVA analysis was calculated.

The null hypothesis<sup>4</sup> for an ANOVA assumes the population means are equal. Hence the null hypothesis is:

$$H_0: \mu_1 = \mu_2 = \mu_3$$

NOTE: The concrete compressive strength capacities are normalised to 20MPa

The test statistics in ANOVA is the ratio of the between and within variation in the tested data, and follows the F distribution.

---

<sup>4</sup> Null hypothesis - No significant difference between specified populations, any observed difference is due to sampling or experimental error.



## 5.2 Edgelif test 2 - Panel reinforcement influence on failure loads

Total sum of squares,  $SS = \sum_{j=1}^c \sum_{i=1}^r (X_{ij} - \bar{X})^2$ , where  $r$  is 4 (samples size) and  $c$  is 3 (EP3, EP4 and EP6),  $\bar{X}$  is the grand mean, and  $X_{ij}$  is the  $i^{\text{th}}$  observation in the  $j^{\text{th}}$  column. Therefore, calculated as follows:

**Table 14 - ANOVA analysis for EP3, EP4 and EP6**

Groups	Count	Sum	Average	Variance
EP3	6	621.9	103.6	1745.9
EP4	4	659.1	164.8	104.7
EP6	4	560.5	140.1	11.8

### ANOVA

Source of Variation	SS	df	MS	F	P-value	F crit
Between Groups	9383.378	2	4691.7	5.7	0.0	4.0
Within Groups	9079.067	11	825.4			
Total	18462.44	13				

As  $F > F_{\text{crit}}$  we reject the null hypothesis and accept that adding SI82 over a N16 Shear bar and replacing a N16 perimeter bar with 2 x N12 perimeter bars adds capacity to the anchor.

The following calculations were made, t-tests and F-tests, for a series of combinations to establish whether there is a statistical difference between the tests or the difference is from the test method, materials or normal variation of the data distribution. The calculations are shown in Table 15, and summarised in Table 16.

### F-Test Two-Sample for Variances

	EP3	EP6
Mean	103.65	140.14
Variance	1745.95	11.78
Observations	6.00	4.00
df	5.00	3.00
F	148.25	
P(F<=f) one-tail	0.00	
F Critical one-tail	9.01	

## 5.2 Edgelif test 2 - Panel reinforcement influence on failure loads

<u>t-Test: Two-Sample Assuming Unequal Variances</u>		
	<i>EP3</i>	<i>EP6</i>
Mean	103.65	140.14
Variance	1745.95	11.78
Observations	6.00	4.00
Hypothesized Mean Difference	0.00	
df	5.00	
t Stat	-2.13	
P(T<=t) one-tail	0.04	
t Critical one-tail	2.02	
P(T<=t) two-tail	0.09	
t Critical two-tail	2.57	

**Table 15 - EP3 to EP6 F-Test and t-Test statistical differences is data**

Hence from the above there is no statistical difference in the spread of data to conclude that changing from using an N16 Perimeter bar and a N16 Shear bar to using a double N12 perimeter bar and SL82 mesh on the same anchor loaded in tension.

<b>Groups</b>	<b>F-Test</b>	<b>t-test</b>	<b>Benefit</b>	<b>Reinforcing configuration change (from and to)</b>
EP3 EP6	reject	accept	No	N16 PB + N16 SB to DBL N12 PB + SL82
EP1 EP2	reject	reject	Yes	No reo to N16 PB
EP5 EP2	accept		No	DBL N12 PB + SL82 to N16 PB
EP3 EP4	reject	reject	Yes	N16 PB + N16 SB to N16 PB + SL82
EP4 EP5	reject	reject	Yes	N16 PB + SL82 to DBL N12 PB
EP5 EP6	accept		No	DBL N12 PB to DBL N12 + SL82
EP2 EP3	accept		No	N16 PB to N16 PB + N16 SB
EP4 EP6	accept		No	N16 PB + SL82 to DBL N12 PB + SL82

### KEY

PB – Perimeter bar

SB – Shear bar

DBL - Double

**Table 16 - Combinations of ANOVA data distribution, accepted or rejected null hypothesis**

From the analysis in Table 16 there is statistical difference in the data distribution by adding a 2<sup>nd</sup> perimeter bar or adding mesh, when testing Edgelif anchors in tension.

### **5.3. Edgelift test 3 - Influence of anchor reinforcing on failure loads**

This research was conducted to establish the pull-out capacity (under direct tension loads applied in a load controlled manner) of 154 Edgelift anchors embedded in thin concrete panels with and without reinforcement provided near the anchor. Various configurations of reinforcement were tested in conjunction with the Edgelift anchors; including with or without a shear bar (reinforcement of the anchor in the shear direction, reference Appendix A – Lifting Design), with or without panel mesh and with or without a perimeter bar. The configurations were chosen based on common standard practice and recommendation. Grade 350MPa, 16mm thick Edgelift plate anchors,  $h_{ef} = 257\text{mm}$ , were tested in direct tension by pull out tests of the anchors in 150mm thick, 2m x 2m panels. The tests were conducted using normal weight Portland cement concrete with a compressive strength at the time of testing of at least 10MPa and up to 40MPa, using a nominal 40MPa mixture, as detailed in Table 6. In practice the minimum strength recommended for lifting is typically 15MPa but lower compressive strengths were included as a lower bound as they may occur in application.

The pull out failure loads were compared to the predicted capacities as determined by design provisions provided in ACI318 (2008) Appendix D which have been developed from the basis of extensive Headed anchor tests.

### 5.3 Edgelift test 3 - Influence of anchor reinforcing on failure loads

#### 5.3.1 Experimental Program

Table 17 - Edgelift anchor experimental program - various reinforcement

Test Series - Edgelift anchor reinforcement configurations	Sample Size, n	Concrete Age, days	$f_{c,age}$ , MPa	Anchor $h_{ef}$ , mm	Edge distance, $c_i$ , mm	Load rate kN/min
EL1 - No reinforcement	5	10	21	295	1,000	20
EL2 - N16 shear bar, N16 perimeter bar	6	12	23	295	1,000	20
EL3 - SL82 mesh, N16 perimeter bar	77	7	18	295	1,000	20
EL4 - N16 shear bar, SL82 mesh, N16 perimeter bar	29	10	22	295	1,000	20
EL5 - N12 shear bar, SL82 mesh, N16 perimeter bar	37	12	23	295	1,000	20
EL6 - Headed anchors various $h_{ef}$	5	7	10,	39, 50, 55, 90	>500	20
	5	7	10	50	1,000	20
	10	7	10	55	400	20
	6	6	10	90	400	20
	10	7	12		400	20
	10	8	17		400	20
	6	12	20		400	20
	3	20	25		400	20
EL7 - Headed anchors 50mm $h_{ef}$	60	10	21	50	>200	20

Plate-type Edgelift anchor pull out tests (154 off), tests EL1-5, were conducted at concrete compressive strengths and embedment lengths that would initiate a concrete cone failure. The inserts were cast with varying reinforcement arrangements

### 5.3 Edgelift test 3 - Influence of anchor reinforcing on failure loads

in the panels, 2,000mm x 2,000mm x 150mm, and reinforcement around the anchors, detailed in more detail below, refer Figure 92. The Edgelift anchors were made from 16 mm plate, with a profile as shown in Figure 93.

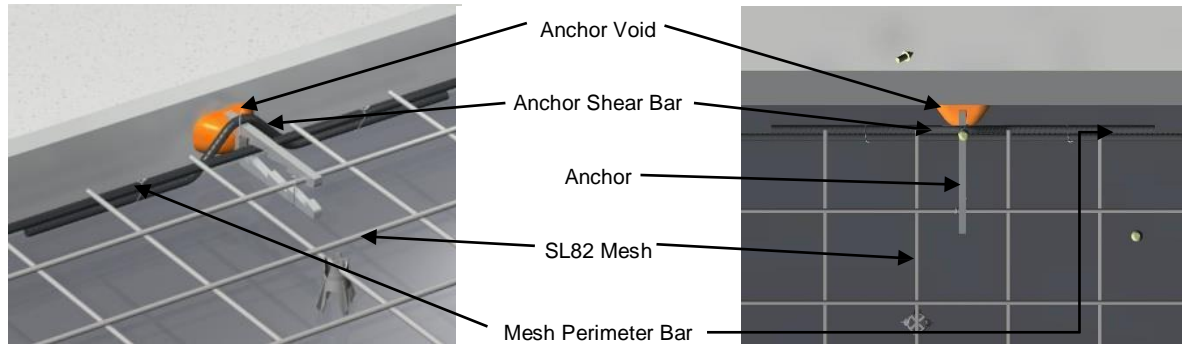


**Figure 92 - Edgelift anchor reinforcement layout**

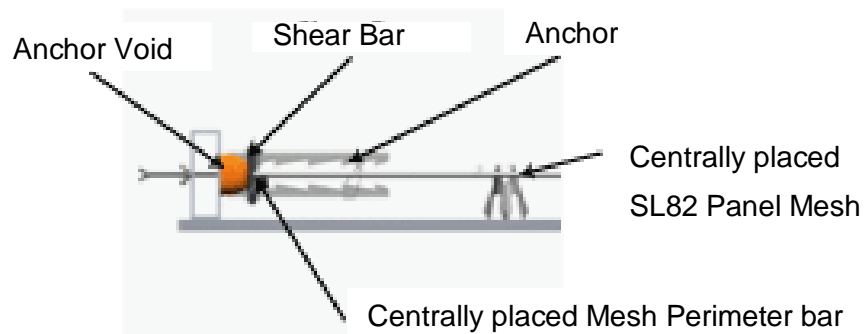


**Figure 93 - Placement of Edgelift anchor and anchor reinforcement in a thin walled concrete panel**

Thirty (35) headed anchors for EL6 were cast in unreinforced concrete blocks of 2m x 2m x 0.6m deep with 2 anchors per block. The anchors of EL6 were tested in direct tension once the concrete had matured. The concrete compressive strength was 42 to 46MPa, with an average compressive strength at time of testing (which was at 28 days) of 43MPa ( Table 18). This was to ensure the headed anchors failed due to steel tensile failure rather than a concrete cone failure. The headed anchors of test EL6 were of varying embedment depth; 39mm, 50mm, 55mm and 90mm effective embedment depth. Anchors in test EL6 that failed due to steel tensile failure of the anchor, is not reported in this experiment. All 4 anchor embedment depths had a concrete cone failure up to 20MPa, and the analysis of this experiment focussed on the concrete capacity of these anchor embedment depths between 10 and 20MPa concrete compressive strength.

### 5.3 Edgelift test 3 - Influence of anchor reinforcing on failure loads

Sixty (60) headed anchors of EL7 with a 50 mm effective embedment depth were cast in two reinforced concrete panels 2m x 2m x 150mm thick with 30 anchors in each panel. The reinforcing was SL82 mesh and an N16 perimeter bar located 50mm from the edge of the panel. These anchors were tested in direct tension as the concrete matured in order to initiate concrete cone failures; tests were conducted at compressive strengths ranging from 18MPa to 26MPa, with an average of 21MPa. Concrete compressive data for all series is shown in Table 18. All anchors of EL7 failed due to concrete cone failure. The headed anchors were arranged with sufficient edge distances such that concrete capacity was not reduced due to edge effects, i.e. no less than  $2 \times h_{ef}$ .

EL1 test panels had no reinforcement in the panels (as seen in Figure 94). EL2 had N16 shear bars placed over the notch of the Edgelift anchor and a centrally placed N16 perimeter bar which extended the length of the panel and was lapped at the corners of the panels (summarised in Figure 95). EL3 had no shear bar and had centrally placed SL82 mesh with centrally placed N16 perimeter bar. EL4 had an N16 shear bar, centrally placed SL82 mesh and a centrally placed N16 perimeter bar. EL5 had an N12 shear bar, centrally placed SL82 mesh and a centrally placed N16 perimeter bar. The reinforcement configurations are summarised in Table 17.

Normal strength concrete was used throughout all series of the tests; being 14mm coarse aggregate, 0.44 water/cement ratio, and nominal grade 40MPa design strength supplied by a commercial ready-mix company, mix design detailed in Table 6.

**Table 18 – Different concrete compressive data for the batches used during this experiment**

Test Series	Concrete Batches	$f_{c,age \text{ min}}$ (MPa)	$f'_c$ @ 28 days (MPa)
EL1	1	21	26
EL2	2	23	28
EL3	3a & 3b	18	36
EL4	4	22	40
EL5	5	23	35
EL6	6	10-25	28
EL7	7	21	26

The preparation of the specimens for testing is shown in the below photos. Figure 94, Figure 95, Figure 96 and Figure 97 show a typical 2m x 2m x 150mm thick panel

### 5.3 Edgelift test 3 - Influence of anchor reinforcing on failure loads

formwork with N16 perimeter bar and a 16mm x 295mm effective embedment depth,  $h_{ef}$ , plate Edgelift anchors in the formwork. In Figure 94 4 anchors were placed in each panel in each 2,000mm edge.



**Figure 94 - EL1 - Anchor with no reinforcement**

As can be seen in Figure 95 this panel had two test anchors which was the typical arrangement. If, after testing one of the anchors, and it was observed that cracking had propagated in the panel then the second anchor, whilst still tested, was excluded from the results presented in this experiment.

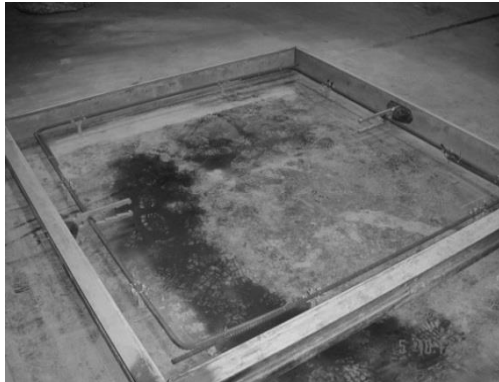


**Figure 95 – EL2 prior to installation of shear bar**

Figure 96 shows how the panel mesh, SL82, was placed centrally in the 150mm thick formwork. The reinforcing mesh reinforcing bar was also placed between the Edgelift anchors legs.

### 5.3 Edgelift test 3 - Influence of anchor reinforcing on failure loads

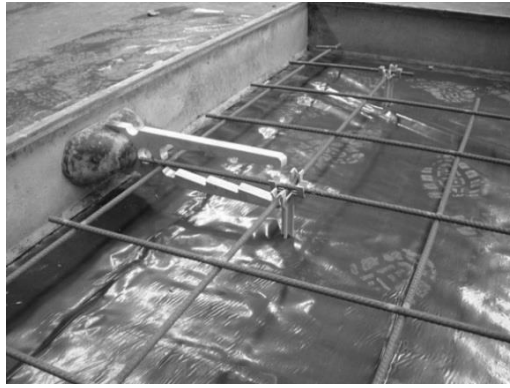


**Figure 96 – EL3 Panel prior to installation of perimeter bar with SL82 mesh**

Figure 97 shows the placement of the panel mesh and the N16 reinforcing bar placed at the perimeter of the mesh, and both placed centrally in the 150mm thick formwork. The reinforcing mesh and perimeter reinforcing bar was also placed between the Edgelift anchors legs. Figure 97 also shows the shear bar placed over the head of the Edgelift anchor.



**Figure 97 – EL4 & EL5 Panel installed with Edgelift anchor, shear bar, panel mesh and perimeter bar**

A test load, applied at a rate of 20kN/min, as per Table 17, was applied via a hydraulic jack and the load measured with an in-line load cell. The test data was recorded for each specimen, including load and displacement. The displacement was measured of the anchor relative to a fixed point on the test panel away from the anticipated fracture zone.

The thin walled concrete panels with Edgelift plate anchors were tested horizontally and supported off the floor on timber gluts whilst the panel reacted against a steel frame with an open span of 1.8m as the load was applied to the anchor. The spacing of the reaction frame for the anchors was outside the predicted failure zone, as shown



### 5.3 Edgelift test 3 - Influence of anchor reinforcing on failure loads

in for the concrete by at least 450mm as shown in Figure 98. For EL6 and EL7 the headed anchors embedded in the face of the panels and blocks were tested at the same loading rate in direct uniaxial tension. The load was applied to the headed anchors via a tripod reaction frame with the legs of the reaction frame placed at a distance from the anchor of least three times the effective embedment depth of the anchor.

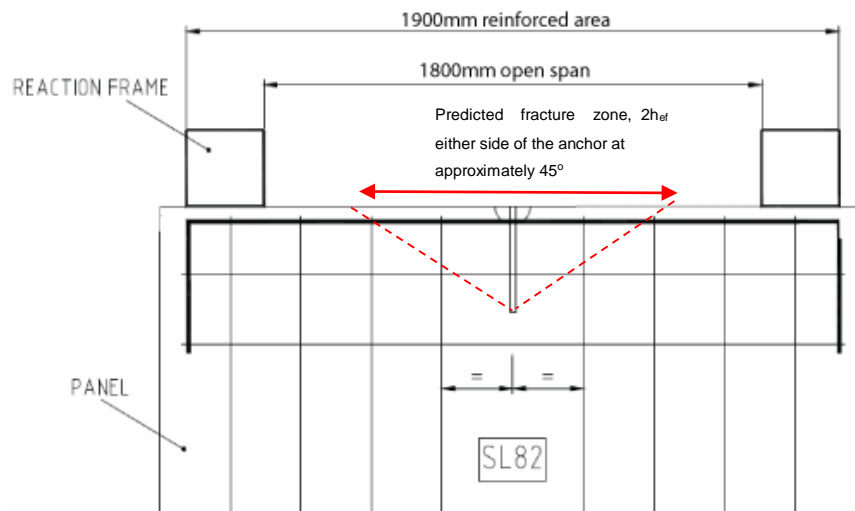


Figure 98 - Panel plan indicating open span to the reaction frame (for Edgelift plate anchor tests)

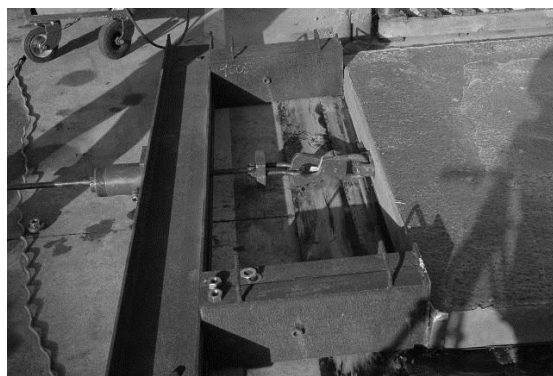


Figure 99 - Edgelift anchor test reaction frame setup

#### 5.3.2 Test Results and Analysis

From the analysis presented in Table 19 of the headed anchor tests which failed due to cone failure of the concrete (EL7 test specimens), it can be said that the ETAG 001 (EOTA 2013) and ACI318 (2008) average concrete capacity approach (four sided pyramid), refer EQUATION 6, better predicts the behaviour of the concrete failure load due to the similar average value to the PCI 5th equation, but with a smaller standard

### 5.3 Edgelift test 3 - Influence of anchor reinforcing on failure loads

deviation. This is since the model of the four-sided pyramid that forms a slope of 35° with the horizontal surface better simulates the failure surface and therefore failure load when compared with the PCI (5th edition) 45° model.

**Table 19 - Assessment of tensile strength due to concrete formula of ACI318 (2008) for panel tests conducted with edge-lift anchors**

<b>Test Series</b>	<b>n, number of Tests</b>	<b>Test / Predicted, (<math>N_{u,c}^0 / P_u</math>) @ 10MPa</b>	<b><math>h_{ef}</math>, mm</b>
EL1 - No reinforcement	5	1.03	257
EL2 - N16 shear bar, N16 perimeter bar	6	1.95	257
EL3 - SL82 mesh, N16 perimeter bar	77	1.57	257
EL4 - N16 shear bar, SL82 mesh, N16 perimeter bar	29	1.08	257
EL5 - N12 shear bar, SL82 mesh, N16 perimeter bar	37	1.25	257
EL6 – Headed anchor hef 39mm	5	2.00	39
EL6 – Headed anchor hef 50mm	5	1.58	50
EL6 – Headed anchor hef 55mm	10	1.56	55
EL6 – Headed anchor hef 90mm	35	1.22	90
EL7 – Headed anchor hef 90mm	60	1.93	90

It should be noted that in all of these pull out tests, edge effects were not a factor in the failure.

### 5.3 Edgelift test 3 - Influence of anchor reinforcing on failure loads

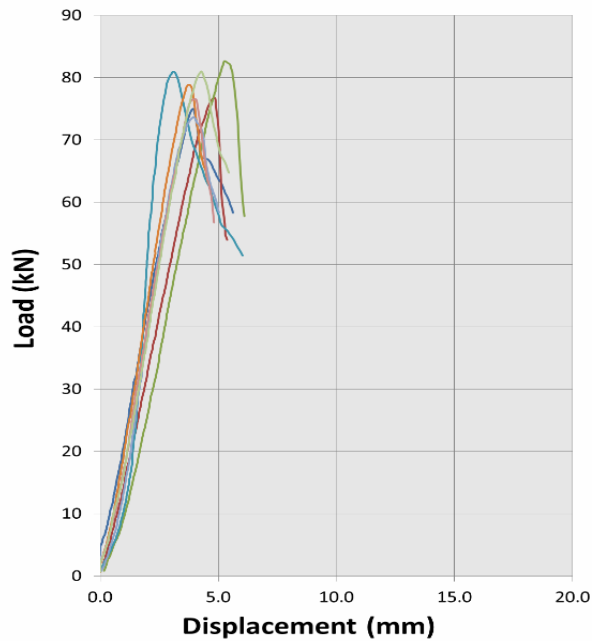


**Figure 100 - Typical Load vs Displacement curves for EL1**

Figure 100 shows the smallest displacement prior to the Edgelift anchor forming a concrete cone. EL1 has a similar displacement to EL2 at ultimate load. EL1 and EL2 are the only 2 tests in this experiment that do not have panel mesh.

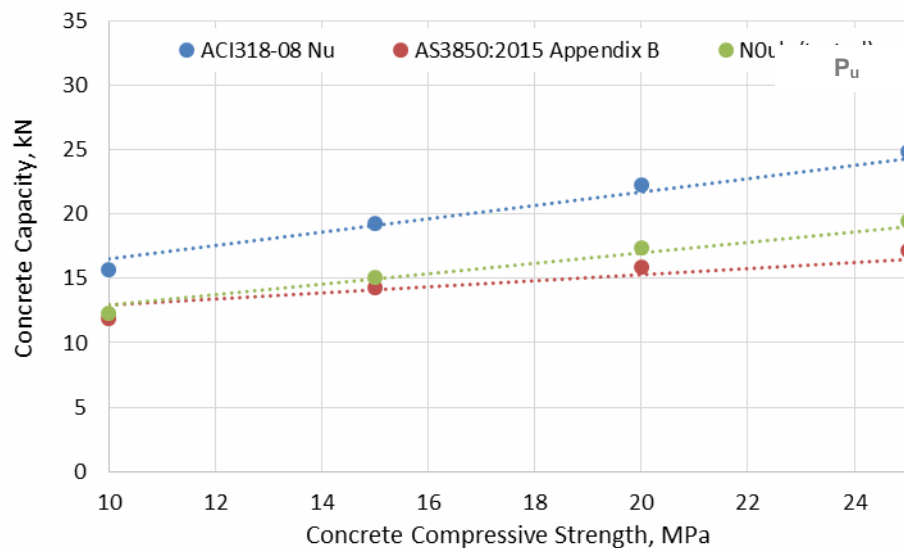
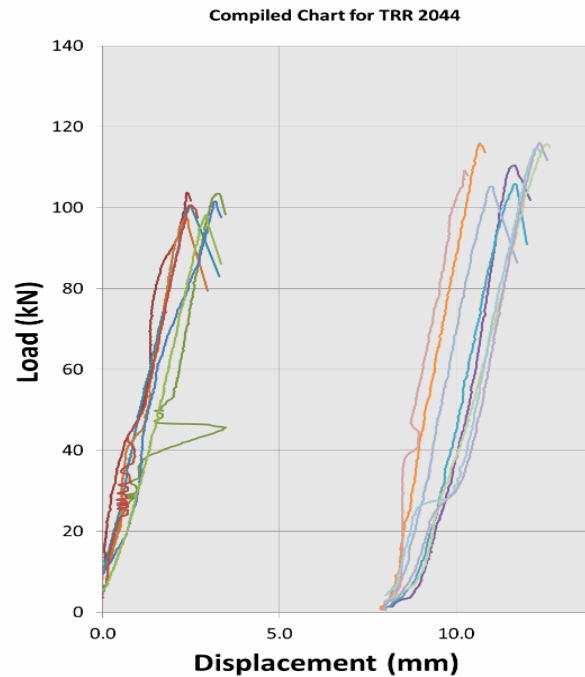


**Figure 101 - EL1 No reinforcement anchor capacity vs ACI318 (2008) and AS3850 (SAI 2015) models**

Edgelift anchor capacity with no associated steel reinforcement, when assessed using AS3850 (SAI 2015) appendix B Shape Modification Factor, the performance of the

### 5.3 Edgelift test 3 - Influence of anchor reinforcing on failure loads

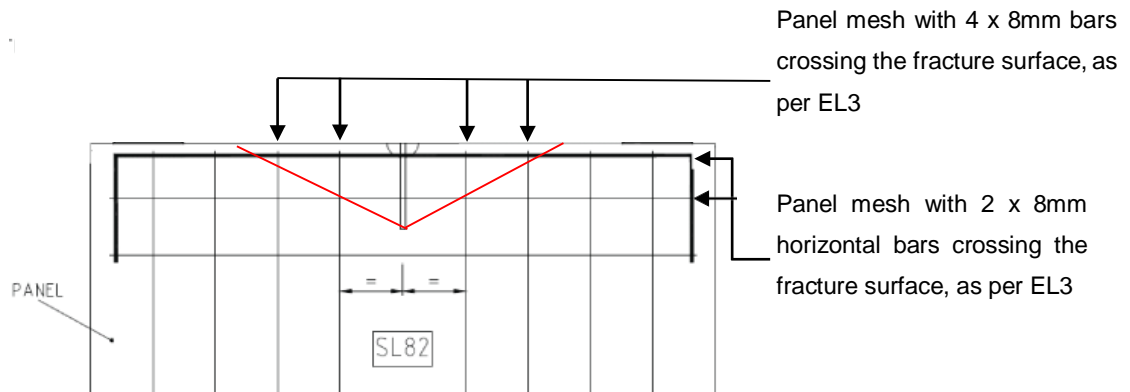
tested anchor is higher than that predicted in AS3850 (SAI 2015). However, the capacity of the Edgelift anchor when compared to the capacity of a headed insert placed in a thin panel, double edge reduced, results in a tested capacity less than that predicted in ACI318 (2008), when calculating the characteristic capacity with a concrete cone failure mode.



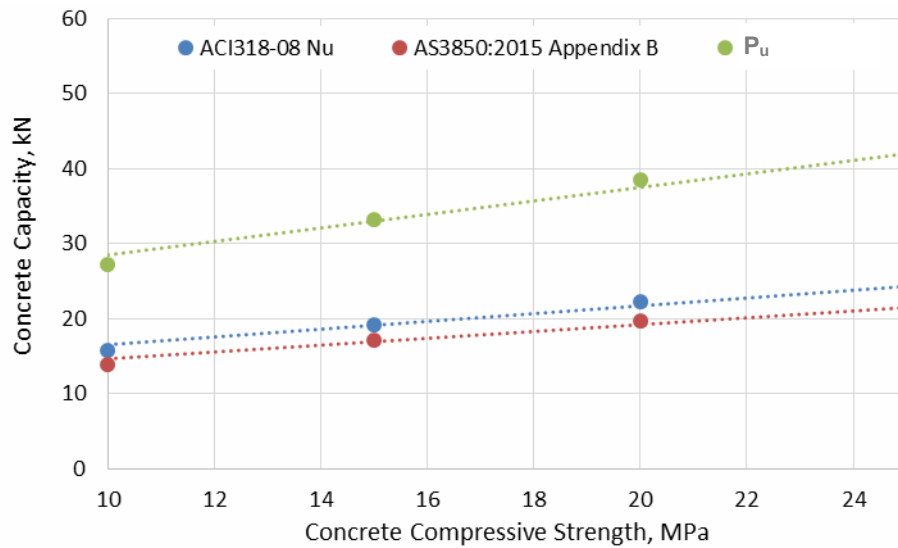
**Figure 102 - Typical Load vs Displacement curves for EL2 and EL3**

Figure 102 is showing the load versus displacement curves for EL2 and EL3 where EL2 has a shear bar and EL3 has panel mesh, and both have a perimeter bar. EL3 is shown on the right in Figure 102, displaying a 20% increase in load capacity of the anchor system when compared to EL2 which has a shear bar. The load carrying capacity of Edgelift anchors tested in EL3 includes the panel mesh, where the panel mesh crossing through the fracture surface is no less than 4 x 8mm bar parallel to the Edgelift anchor and 2 x 8mm perpendicular to the Edgelift anchor. Whereas the difference between EL3 and those in EL2, is where the EL2 Edgelift anchors have a shear bar perpendicular to the anchor and crosses the fracture surface 25mm from the thin edge of the panel, where it provides little load carrying capacity to the Edgelift anchor system.

### 5.3 Edgelifft test 3 - Influence of anchor reinforcing on failure loads



**Figure 103 - Typical fracture surface of EL2 and EL3 post ultimate load**



**Figure 104 - EL2 anchor capacity vs ACI318 (2008) and AS3850 (SAI 2015) models**

EL2 test results are suitably conservative when compared against AS3850 (SAI 2015) Appendix B, and ACI318 (2008).

### 5.3 Edgelift test 3 - Influence of anchor reinforcing on failure loads

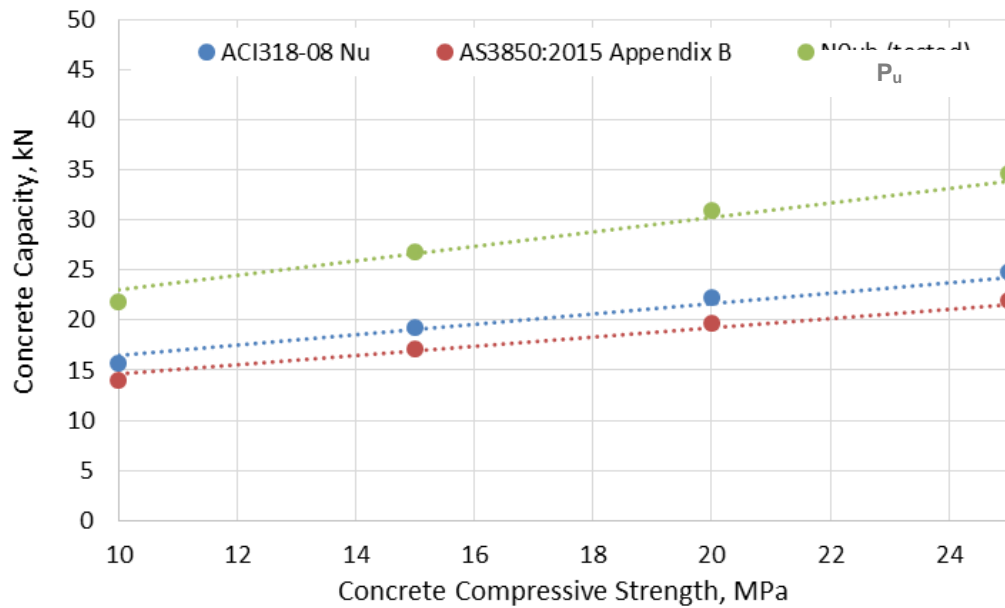


**Figure 105 - EL3 anchor capacity vs ACI318 (2008) and AS3850 (SAI 2015) models**

EL3 test results are suitably conservative when compared against AS3850 (SAI 2015) Appendix B, and ACI318 (2008).

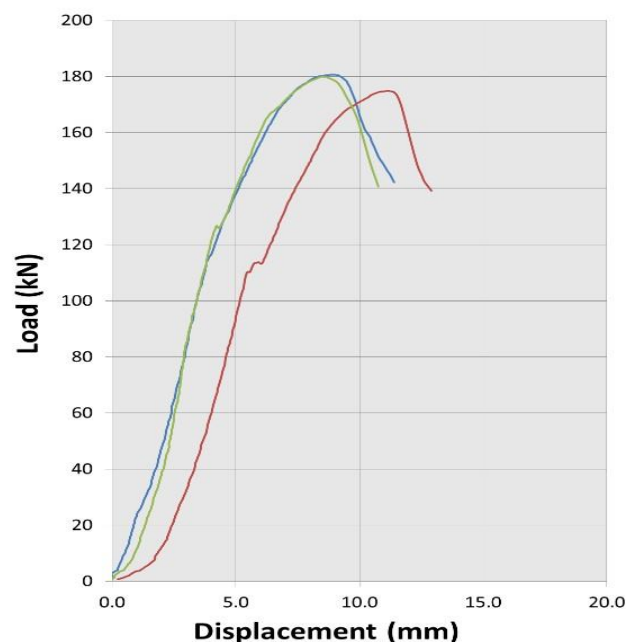


**Figure 106 - Typical Load vs Displacement curves for EL4 and EL5**

Figure 106 shows the largest displacement prior to the Edgelift anchor forming a concrete cone. Both EL4 and EL5 have a shear bar, SL82 mesh and a perimeter bar which is contributing to the ductility and extra displacement compared with EL1 – EL4.

### 5.3 Edgelift test 3 - Influence of anchor reinforcing on failure loads

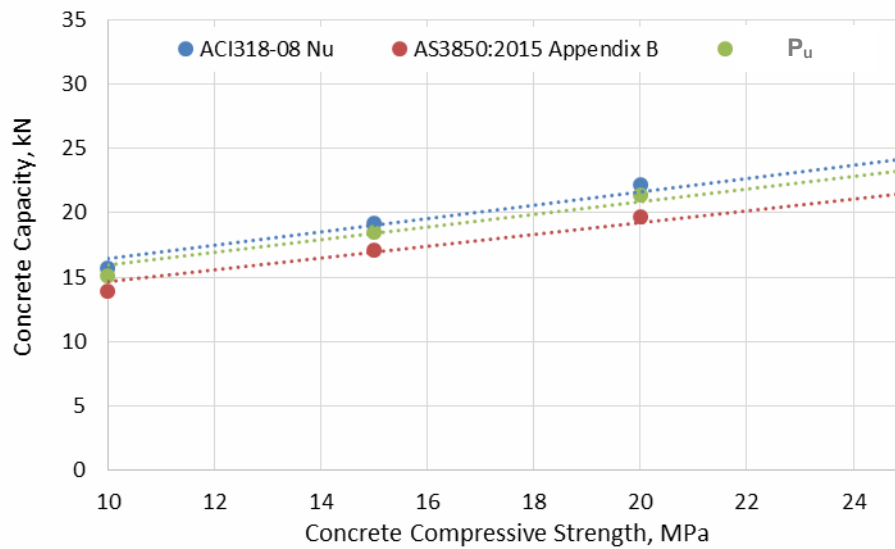


**Figure 107 - EL4 anchor capacity vs ACI318 (2008) and AS3850 (SAI 2015) models**

EL4 test results are similar when compared against AS3850 (2015) Appendix B. However, the capacity of the Edgelift anchor when compared to the capacity of a headed insert placed in a thin panel, double edge reduced, results in a tested capacity less than that predicted in ACI318 (2008), when calculating the characteristic capacity with a concrete cone failure mode.

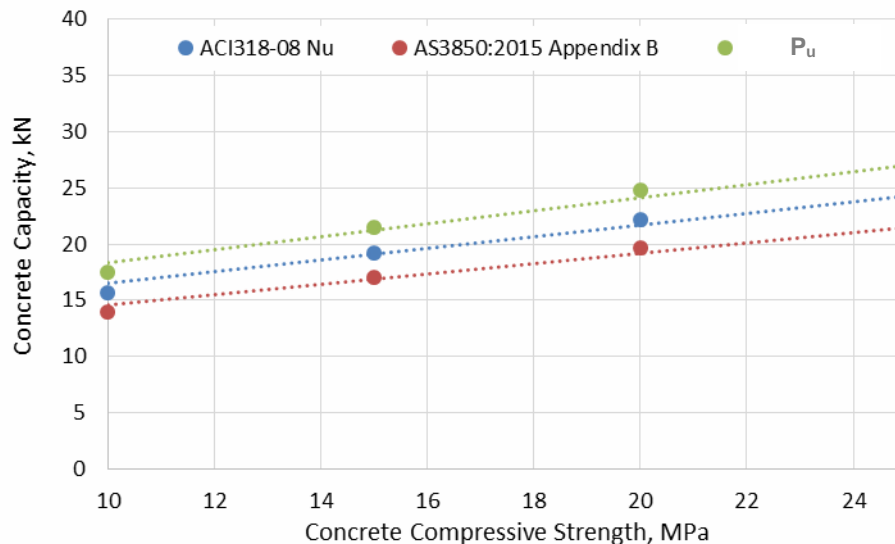


**Figure 108 - EL5 anchor capacity vs ACI318 (2008) and AS3850 (SAI 2015) models**

EL5 test results are suitably conservative when compared against AS3850 (SAI 2015) Appendix B, and ACI318 (2008).

### 5.3 Edgelift test 3 - Influence of anchor reinforcing on failure loads

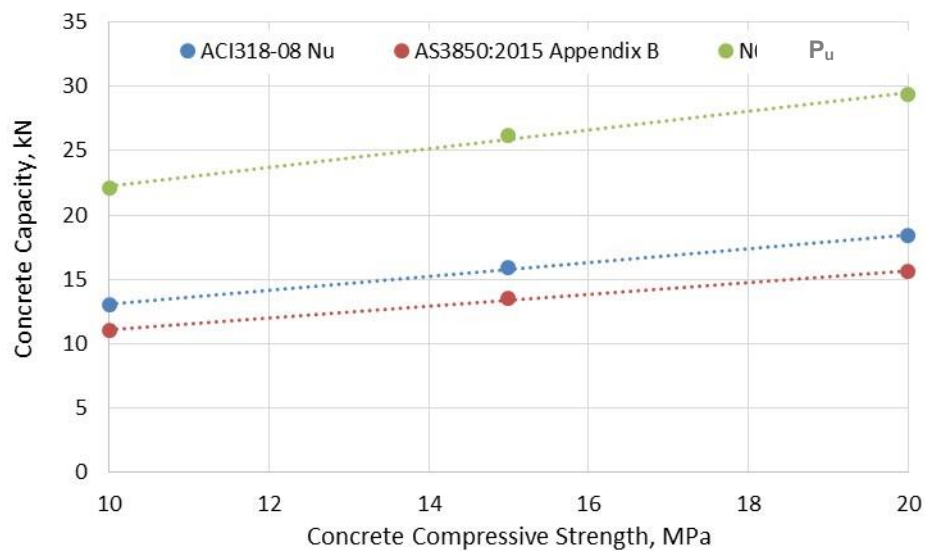


**Figure 109 - EL6  $h_{ef}$  39mm headed anchor capacity vs ACI318 (2008) and AS3850 (SAI 2015) models**

EL6 test results for a headed anchor,  $h_{ef}$  39mm, are suitably conservative when compared against AS3850 (SAI 2015) Appendix B, and ACI318 (2008).

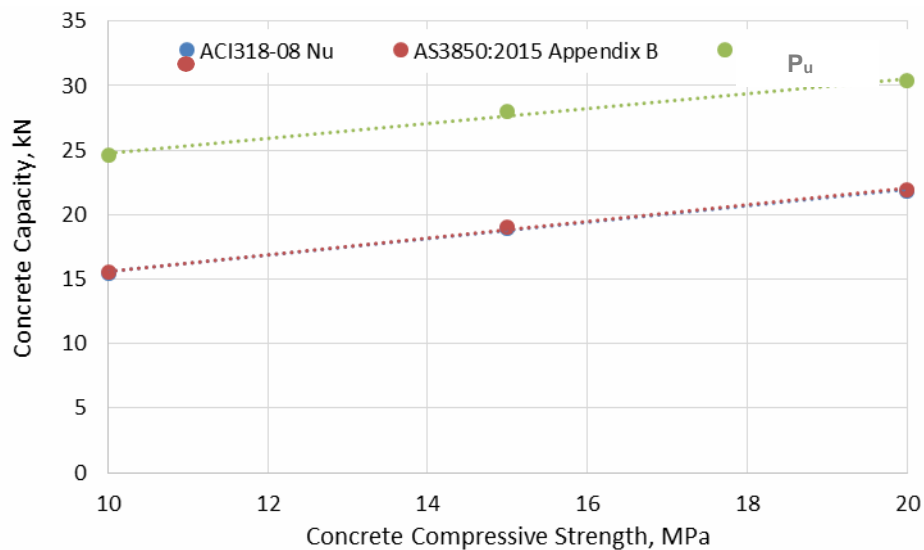


**Figure 110 - EL6  $h_{ef}$  50mm headed anchor capacity vs ACI318 (2008) and AS3850 (SAI 2015) models, (ACI318 and AS3850 data are similar)**

EL6 test results for a headed anchor,  $h_{ef}$  50mm, are suitably conservative when compared against AS3850 (SAI 2015) Appendix B, and ACI318 (2008).



### 5.3 Edgeliftest 3 - Influence of anchor reinforcing on failure loads

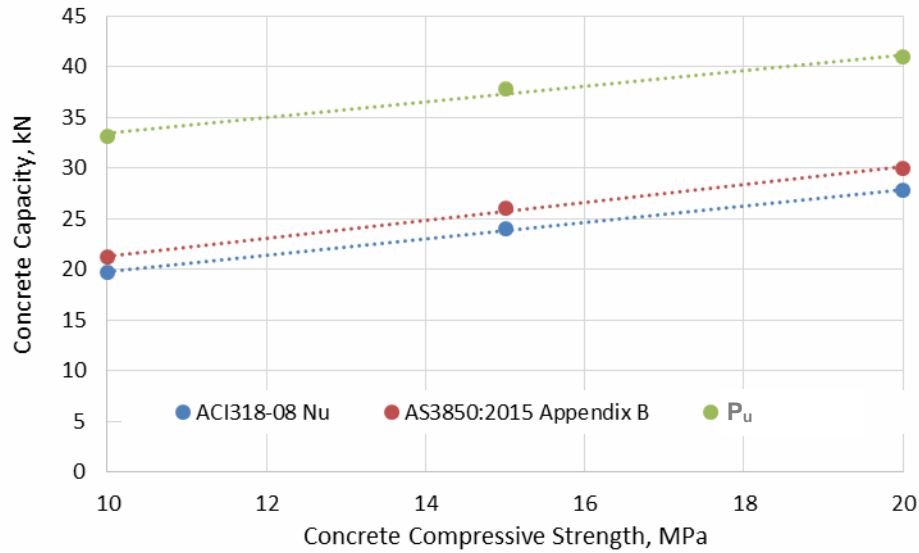


**Figure 111 - EL6 hef 55mm headed anchor capacity vs ACI318 (2008) and AS3850 (SAI 2015) models**

EL6 test results for a headed anchor,  $h_{ef}$  55mm, are suitably conservative when compared against AS3850 (SAI 2015) Appendix B, and ACI318 (2008).

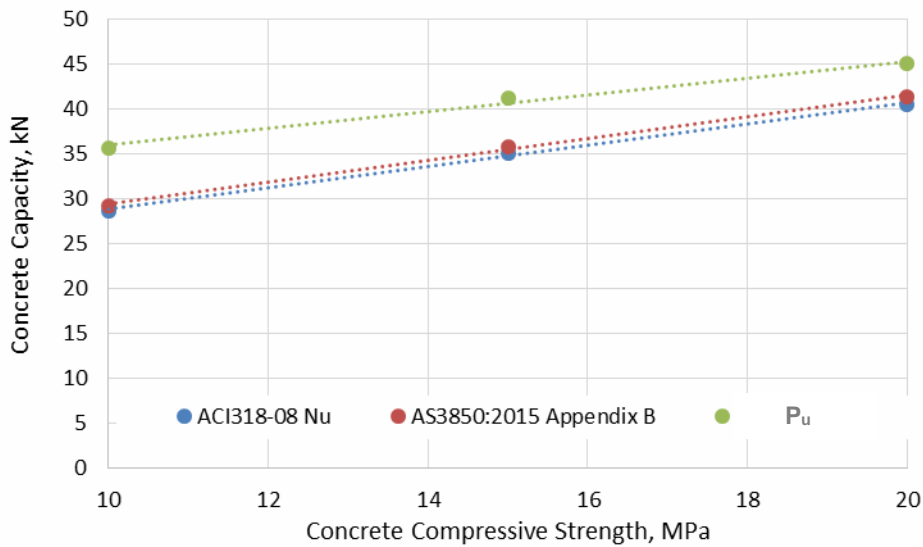


**Figure 112 - EL6 hef 90mm headed anchor capacity vs ACI318 (2008) and AS3850 (SAI 2015) models (ACI318 and AS3850 data are similar)**

EL6 test results for a headed anchor,  $h_{ef}$  90mm, are suitably conservative when compared against AS3850 (SAI 2015) Appendix B, and ACI318 (2008).

### 5.3 Edgelift test 3 - Influence of anchor reinforcing on failure loads

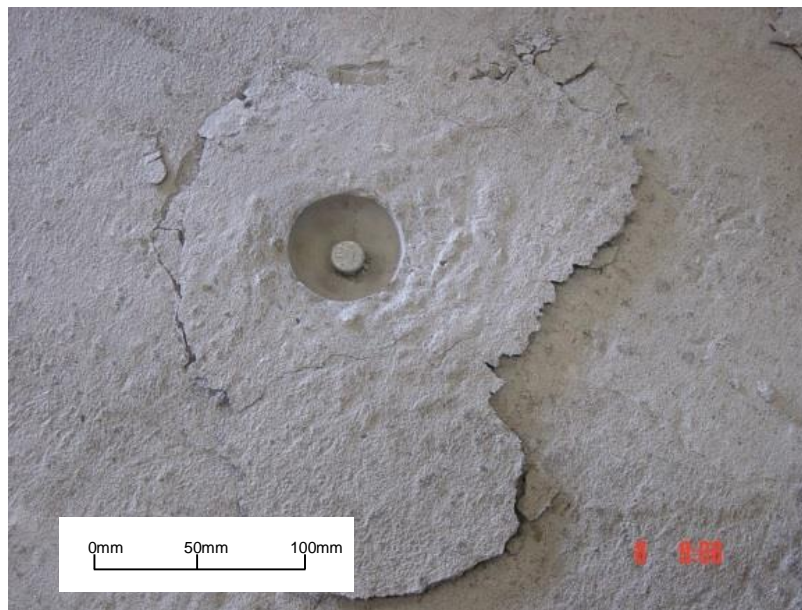


**Figure 113 - Photo of EL7 headed anchor,  $h_{ef}$  70mm, failure surface**

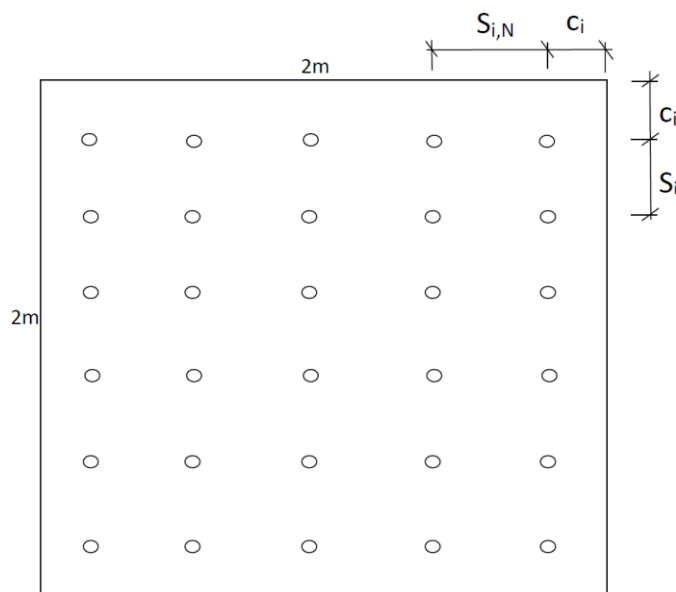


**Figure 114 - Concrete block layout for headed inserts (2m x 2m x 150mm) for EL7**

The placement of the head inserts, in EL7, ensured that the distance to the panel edge,  $c_i$ , from the centre of the headed anchor was no less than  $2 \times h_{ef}$ . The spacing,  $s_{i,N}$ , between the headed anchors was no less than  $4 \times h_{ef}$ .

### 5.3 Edgelift test 3 - Influence of anchor reinforcing on failure loads

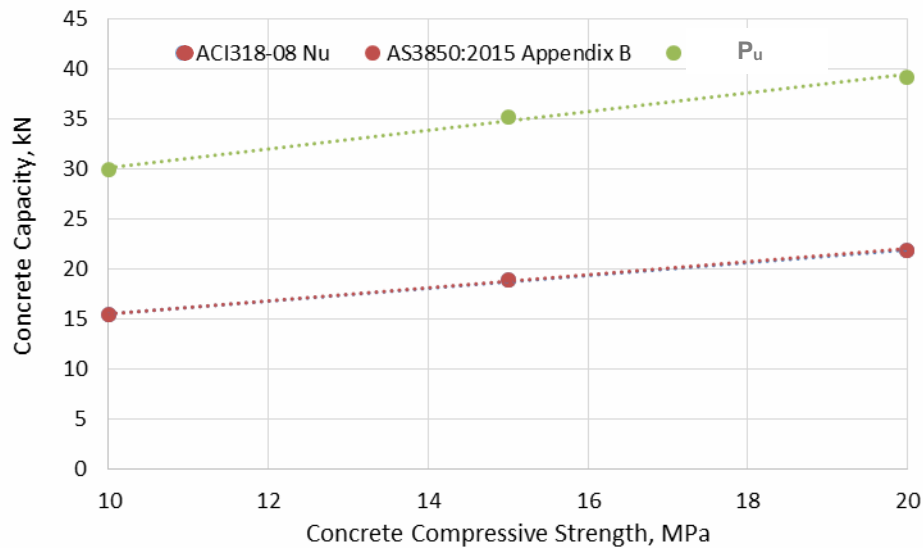


**Figure 115 - EL7 90mm headed anchor capacity vs ACI318 (2008) and AS3850 (SAI 2015) models (ACI318 and AS3850 data are similar)**

EL7 test results for a headed anchor,  $h_{ef}$  90mm, are suitably conservative when compared against AS3850 (SAI 2015) Appendix B, and ACI318 (2008).

The test data for all the tests in this experiment are tabulated in Appendix B - Test Data, and the analysis of the data is detailed below.

The Edgelift anchor test data was compared with the predicted capacity as determined using the ACI318 (2008) average capacity formula as a mechanism of comparison to the well-established relationship for foot anchors presented in literature and verified in the tests of EL7. The ratio of the test failure load and the predicted load as per ACI318 (2008) is shown in Figure 117 for each series of panel tests with Edgelift anchors. The ratio of test failure load to predicted failure load is plotted against the square root of the concrete compressive strength since the predicted strength is a function of and directly proportional to the square root of compressive strength.

For the two series of panels with Edgelift anchors and no central mesh reinforcement in the panels; tests A & B, the following observations were made: The addition of shear and perimeter bars (EL2) resulted in a slightly increased failure load and is indicated by a slightly higher average ratio of test/predicted compared to EL1. Since the manufacture of panels without central mesh is impractical, the number of tests

### 5.3 Edgelift test 3 - Influence of anchor reinforcing on failure loads

conducted was small; however, the test results are valuable as an indicator that the provision of the perimeter bars is likely to be beneficial to the capacity of the anchor. Thus this detail (N16 perimeter bar) along with central panel mesh of SL82 was subsequently used in tests EL3, EL4 and EL5.

For the three series of panels with central mesh reinforcement and N16 perimeter bar in the panels; EL3, EL4 and EL5, the following observations were made: EL3, the Edgelift anchors with no additional N12 or N16 shear bar reinforcement, has a significantly higher capacity than the unreinforced panels as indicated by the value of test/predicted ratio average of almost 2.5. The two series with additional shear bar of either N12 or N16 had similar average and range of test/predicted apparently less than the panels without shear bars; however, EL3 had more tests conducted at lower concrete strengths and it is these test results which appear to magnify the average ratio and the standard deviation of the data for EL3.

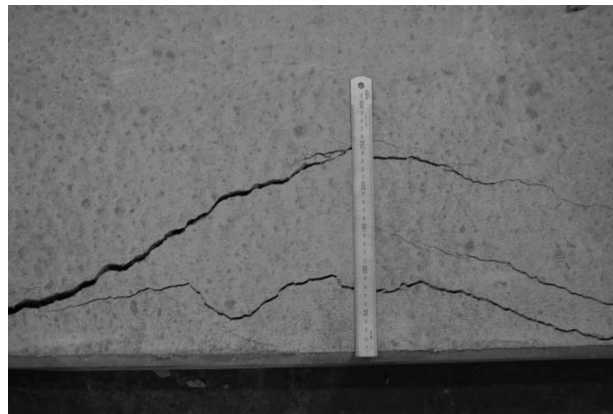


Figure 116 - Typical concrete failure surface

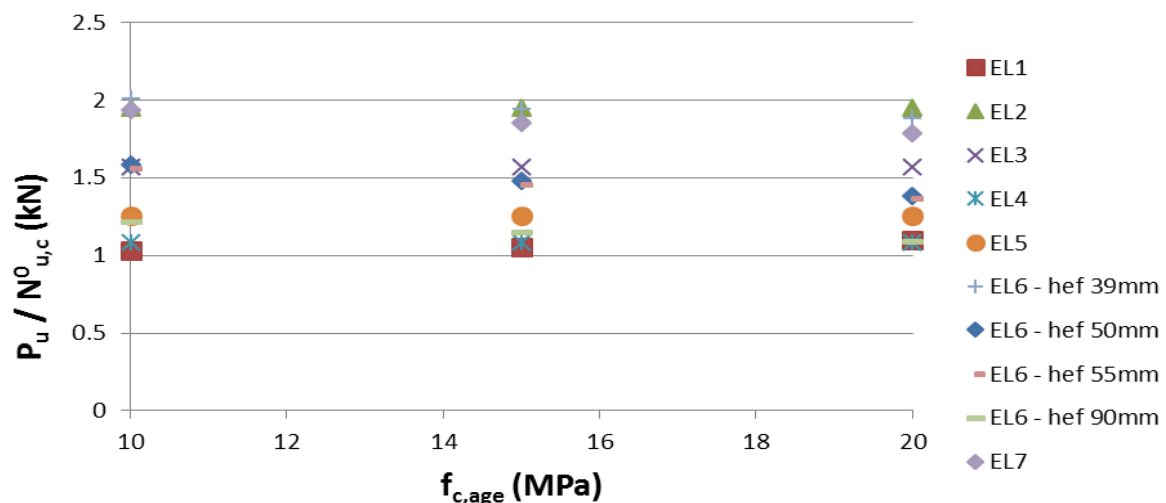


Figure 117 - Ratio of Test Failure Load to Predicted characteristic resistance for each test series

### 5.3 Edgelift test 3 - Influence of anchor reinforcing on failure loads

#### 5.3.3 Concluding remarks

This research is an evaluation of pull out test data for Edgelift anchors in thin walled elements. Using the formula in the ACI318 (2008), developed predominantly for headed anchors with the development of a full concrete cone failure, comparisons of the predicted capacity and the test pull out capacity of the Edgelift anchors is made. Three series of panels were reinforced with centrally placed SL82 mesh, and the ratios of test to predicted failure load indicate that the capacity of these anchors was well in excess of the predicted failure load as per ACI318 (2008), of the order of approximately 1.25 to 2.0 times.

Overall, 269 tests were conducted using Edgelift anchors in direct tension; the variables tested include concrete compressive strength at time of testing which ranged from 10MPa to 40MPa, and arrangement of reinforcement which included the provision or exclusion of perimeter bars, and shear bars (N16, N12 or nil) and central mesh reinforcement in the panel.

ANOVA analysis was calculated to assess the statistical significance of the spread of test data and to establish if the change in reinforcement configuration adds to the capacity of the anchor or the variation in data is a consequence of test method, material or normal variation.

**Table 20 - ANOVA statistical analysis for test and reinforcement significance**

Groups		F-Test	t-Test	Benefit	Change of reinforcement configuration
EL1	EL2	Accept		No	No Reinforcement to N16 SB + N16 PB
EL2	EL3	Accept		No	N16 SB, N16 PB to SL82, N16 PB
EL3	EL4	Accept		No	SL82, N16 PB to N16 SB, SL82, N16 PB
EL4	EL5	Reject	Accept	No	N16 SB, SL82, N16 PB to N12 SB, SL82, N16 PB
EL2	EL4	Accept		No	N16 SB, N16 PB to N16 SB, SL82, N16 PB

### 5.3 Edgelift test 3 - Influence of anchor reinforcing on failure loads

From Table 20 it can be deduced that the statistical variation in the test results do not clearly show that the addition or change of reinforcing configurations contribute more or less to the capacity of the anchor. Therefore, the conservative design criteria would be to assess the various reinforcing configuration as non-contributing to anchor load capacity.

#### 5.4. Edgelift test 4 – Anchor reinforcement influence on shear failure loads

Plate Edgelift anchors (lifting inserts) are used to transfer lifting loads between steel and concrete. Unlike headed anchors that have been investigated by numerous researchers worldwide, Edgelift plate anchors are relatively un-examined in published research. Advanced knowledge regarding insert to concrete is included in ACI318 (2008) Appendix D, CEB Design of Fastening in Concrete and PCI Design Handbook. Recommended design solutions are also included in ACI318 (2005) Appendix B that were meant to ensure the ductile behaviour of cast-in-place anchors. The ACI standard requires the actual tensile capacity of an anchor be greater than or equal to the calculated tensile strength of an idealized concrete cone surface, which is then used in precast lifting design. ACI-349 (2008) incorporates the approaches presented in ACI318 (2005) Appendix D.

This experiment summarizes the concrete breakout strength data (placed under shear loads applied with a load controlled rate) of 126 Edgelift anchors embedded in concrete panels with various reinforcement (shear anchoring) configurations on top of the anchor, shown in Figure 118 and Figure 119.

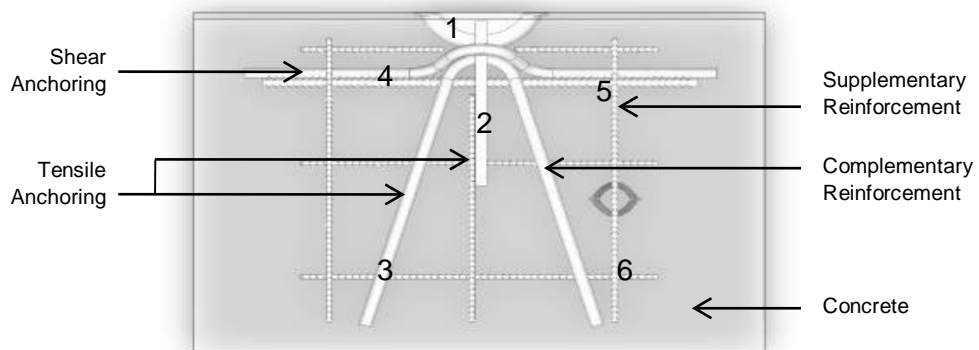


**Figure 118 - Plan view of a typical panel setup for Edgelifting**

Figure 118 shows the plate Edgelift anchor and the strength contributing steel reinforcement layout, with the anchor void (1), the plate Edgelift anchor (2), tension bar (3), shear bar (4), perimeter bar (5), and panel mesh (6).

#### 5.4 Edgelift test 4 – Anchor reinforcement influence on shear failure loads

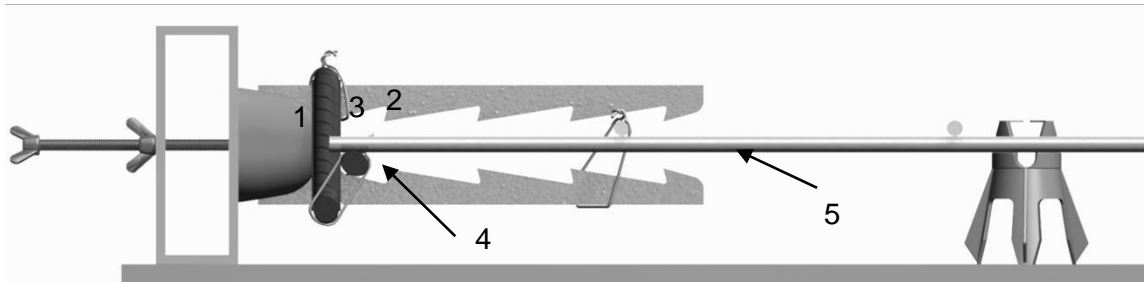


**Figure 119 - Side view of a typical panel setup for Edgelifting**

Figure 119 shows a side view of a typical test setup of the plate Edgelift anchor (2) placed centrally in a 150mm panel showing the anchor void (1), shear Bar x 90mm height (3), perimeter Bar (4), and panel mesh (5). The Edgelift plate anchor, if fitted with no shear bar, will have very little capacity in shear. The concrete breakout strength, in the case of no shear bar fitted, is gained from the embedment of the anchor from the panel near face to the long edge of the anchor, which with an 80mm centrally placed anchor in a 150mm panel is only 35mm cover.

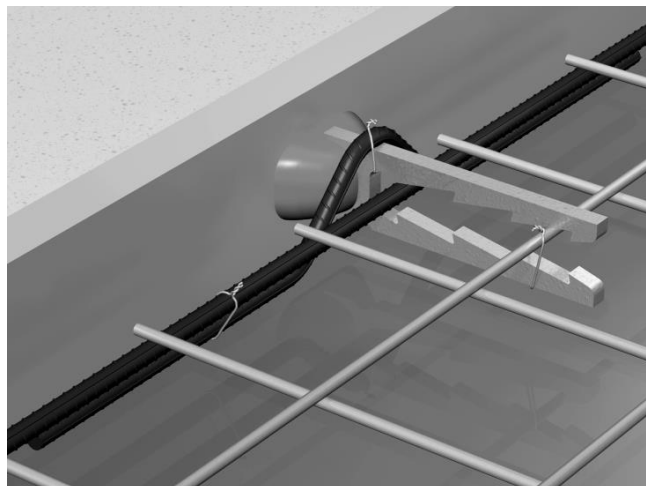


**Figure 120 - View of a typical anchor setup for thin panel Edgelifting**

The above figure 120 highlights the orientation of the shear bar and the positions where it is tied to the panel reinforcement.



#### 5.4 Edgelift test 4 – Anchor reinforcement influence on shear failure loads

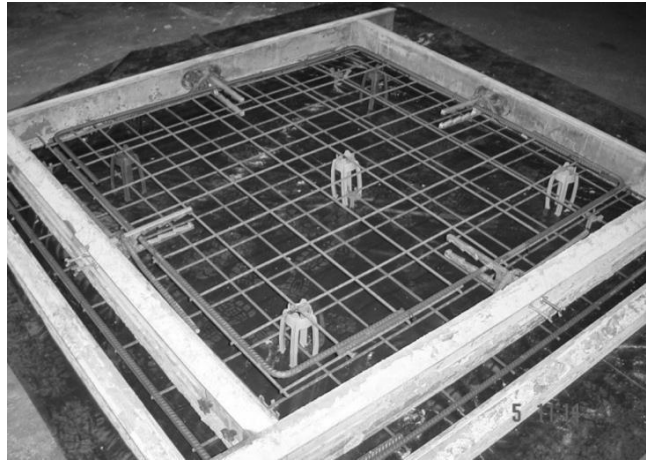


**Figure 121 - Typical shear panel setup prior to concrete pour**

The above figure 121 shows a panel setup with 4 x plate Edgelift anchors, shear bars placed over the anchors, perimeter bars and SL82 panel mesh. Various configurations of shear bar reinforcement were tested in conjunction with the Edgelift anchors; which included panel mesh and perimeter bar. The configurations were chosen on the basis of common standard industry practice. N Class reinforcement steel, 16 mm and 10mm thick Edgelift plate anchors were tested by pull out tests in a lateral tensile direction on anchors placed in 100mm, 125mm, 150mm and 175mm thick panels measuring 2m x 2m perimeter. The tests were conducted using normal weight Portland cement concrete with a compressive strength at the time of testing of between 8MPa and up to 45MPa, detailed in table 1. The minimum strength recommended for lifting is 15MPa but lower compressive strengths were included as a lower bound may occur in practice.

The tested breakout strengths were compared to the calculated capacities as determined by design provisions provided in ACI318 (2008) Appendix D 5.2. The predicted failure surface is shown in Figure 121.

##### **5.4.1 Predictive Strength Equations**

The predictive model used to estimate nominal concrete shear breakout strength,  $N_{cb}$ , of a single anchor is required to have edge modification factors applied. In the case of shear bars,  $h_{ef}$  is a function of panel thickness, anchor width and shear bar height.

#### 5.4 Edgelift test 4 – Anchor reinforcement influence on shear failure loads

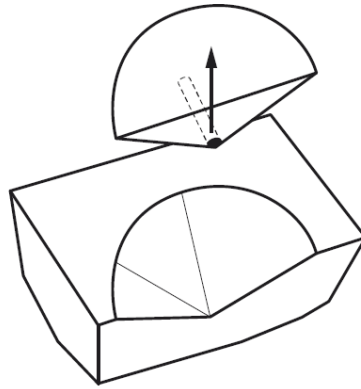


**Figure 122 - Predicted concrete fracture cone from a cast-in anchor to panel edge, shear load direction**

The nominal reduced concrete breakout strength,  $N_{cb}$ , of a single anchor loaded in tension is presented in ACI318 (2008) D5.2.1, as:

$$N_{cb} = \frac{A_{cC}}{A_{cC0}} \cdot \Psi_{ed,N} \cdot \Psi_{C,N} \cdot \Psi_{\epsilon,N} \cdot N_b$$

**Equation 19**

As distance to the edge,  $c_a$ , is less than  $1.5 h_{ef}$ , then the edge distance reduced projected concrete failure area,  $A_{NC}$ :

$$A_{cC} = (c_a + 1.5 h_{ef}) \cdot (2c_a + 1.5 h_{ef})$$

**Equation 20**

And the unrestricted project concrete failure area,  $A_{NC0}$ , ACI318 (2008) D5.2.1

$$A_{cC0} = 9 \cdot h_{ef}^2$$

**Equation 21**

Then the tensile edge modification factor,  $\Psi_{ed,N}$ , to apply is: ACI318 (2008) D5.2.5

$$\Psi_{ed,N} = 0.7 + 0.3 \frac{c_a}{1.5 h_{ef}}$$

**Equation 22**

Hence the basic concrete breakout shear capacity of a single anchor,  $N_b$ , can be calculated as: ACI318 (2008) sec D5.2.2

#### 5.4 Edgelift test 4 – Anchor reinforcement influence on shear failure loads

$$\phi_s = \phi_c \lambda \sqrt{\phi_c} h_c^{1.5}$$

Equation 23

Where:  $\lambda$  is the modification factor for lightweight concrete and not applicable for these tests,  $\Psi_{c,N}$  ACI318 (2008) D5.2.6 is taken as 1.25 for un-cracked concrete, and  $\Psi_{ep,N}$  ACI318 (2008) D5.2.7 is taken as a 1, as it is a modification factor for post-installed anchor edge reduction and not applicable to these tests.

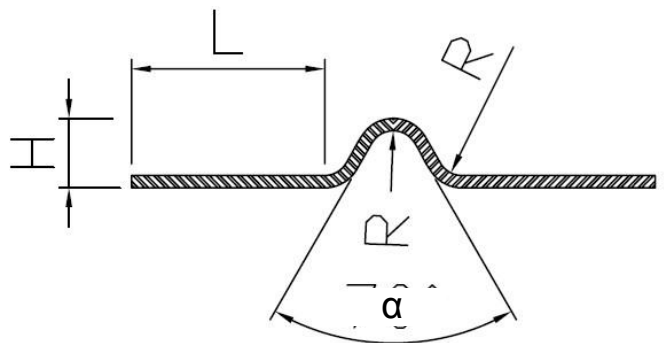
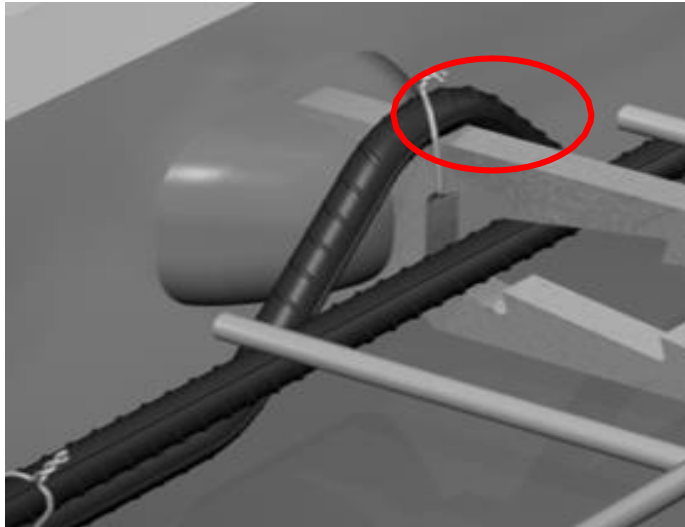


Figure 123 - Typical shear bar design

A typical shear bar is defined with variables such as height, H, (which is a function of embedment depth and related to the plate anchor) leg length, L, (which is related to the stress development length) and the bend angle,  $\alpha$ , (which is required to clear the void and allow the shear bar to sit in a position that has been designed and tested). The mandrel diameter used to bend the shear bar, if cold bent, is limited to at least 4 x the diameter of the bar, in accordance with AS4671 (SAI 2001).

When a load is applied to the anchor, the shear bar is subject to bending, especially at the centre of the bridge which is in contact with the anchor, as shown in Figure 124.

#### 5.4 Edgelift test 4 – Anchor reinforcement influence on shear failure loads



**Figure 124 - The shear bar bridge is subjected to bending when a shear load is applied**

When the shear bar is being installed into the panel formwork it is important for the installer to ensure that the bend radius sits in contact with the anchor, and is adequately tied in. In the case where there is a gap between the anchor and shear bar at this point, and a shear load is applied, the concrete will crack around the head of the anchor, allowing the anchor to move. Special care was taken during the test setup to ensure the shear bar was suitably tied in. This was done by first tying in the shear bar bridge prior to tying in the shear bar legs.

##### **5.4.2 Experimental Program**

Plate-type Edgelift anchor pull-out lateral tensile tests (one hundred and twenty-six, 126) were conducted at concrete compressive strengths and shear bar embedment heights that would initiate a concrete cone failure. The shear bar anchors were a combination of N16 and N12 reinforcement bars, with either a 90mm or 60mm bend height, refer H in Figure 123. Plate anchors used were manufactured from 10mm and 16mm plate, with a profile as shown in Figure 126 and Figure 127. They were cast in thin (100mm, 125mm, 150mm and 175mm thick) panels all with panel reinforcement using SL82 and a N16 Perimeter bar, described in more detail below.

#### 5.4 Edgelift test 4 – Anchor reinforcement influence on shear failure loads

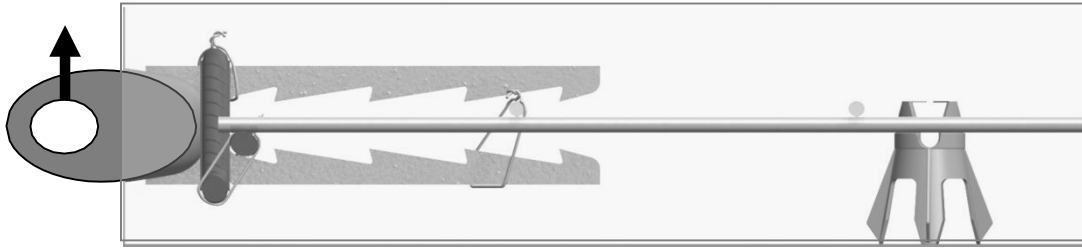


**Figure 125 - Shear loads applied in a lateral tensile direction**

Table 22 details Series ES1 test panels were 100mm thick, a plate Edgelift anchor of 60mm width x 10mm thick, with a shear bar of N12 x 60mm height. Series ES2 test panels were 125mm thick, a plate Edgelift anchor of 60mm width x 10mm thick, with a shear bar of N12 x 60mm height. Series ES3 test panels were 150mm thick, a plate Edgelift anchor of 60mm width x 10mm thick, with a shear bar of N12 x 60mm height. Series ES4 test panels were 150mm thick, a plate Edgelift anchor of 60mm width x 16mm thick, with a shear bar of N12 x 60mm height. Series ES5 test panels were 150mm thick, a plate Edgelift anchor of 75mm width x 16mm thick, with a shear bar of N12 x 90mm height. Series ES6 test panels were 150mm thick, a plate Edgelift anchor of 80mm width x 16mm thick, with a shear bar of N16 x 90mm height. Series ES7 test panels were 175mm thick, a plate Edgelift anchor of 60mm width x 16mm thick, with a shear bar of N12 x 60mm height. Details are summarised in Table 21 and shown in Figure 126 and Figure 127.

Normal strength concrete was used throughout all series of the tests; being 14 mm coarse aggregate, 0.44 water/cement ratio, and nominal grade 40MPa design strength supplied by a commercial ready-mix company. The range of concrete compressive strengths at time of test was 8MPa to 45MPa, with an average of 22MPa, detailed in Table 21.

#### 5.4 Edgelift test 4 – Anchor reinforcement influence on shear failure loads

**Table 21 - Concrete Compressive Strength Data for Test Series**

Test Series	Minimum (MPa)	Maximum (MPa)	$f_{c,age}$ Average (MPa)
ES1	19	22	20
ES2	22	37	29
ES3	10	32	16
ES4	15	37	21
ES5	8	35	22
ES6	8	45	26
ES7	30	45	42

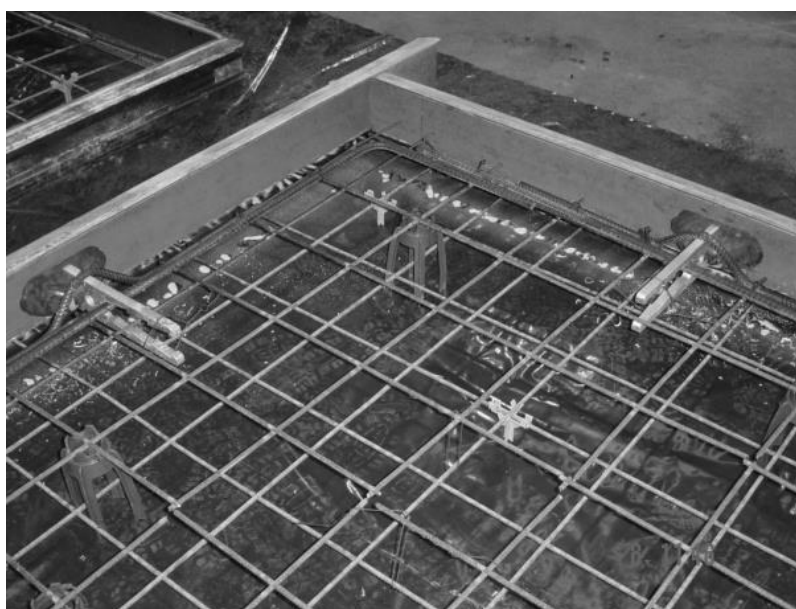


**Figure 126 - Series ES3 typical panel setups**

#### 5.4 Edgelift test 4 – Anchor reinforcement influence on shear failure loads



**Figure 127 - Series ES7 typical panel setups**

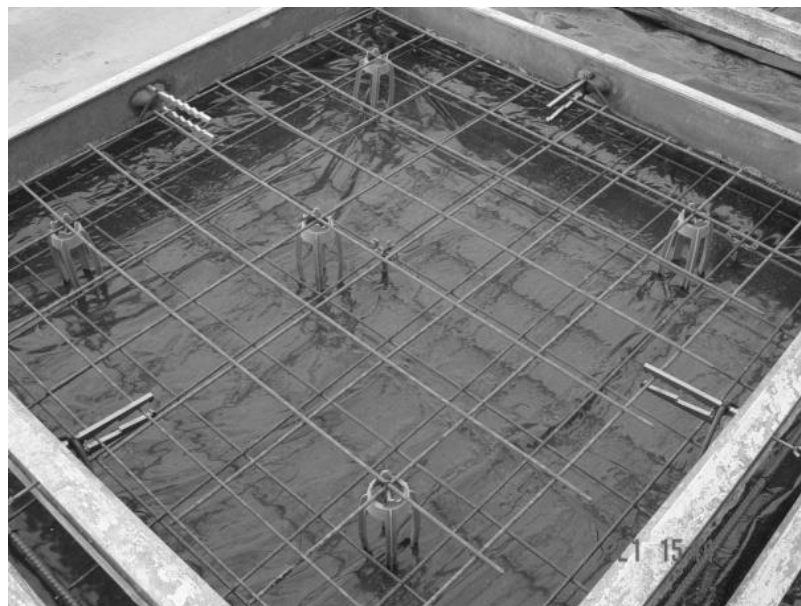


**Figure 128 - Series ES6 typical panel setups**

#### 5.4 Edgelift test 4 – Anchor reinforcement influence on shear failure loads

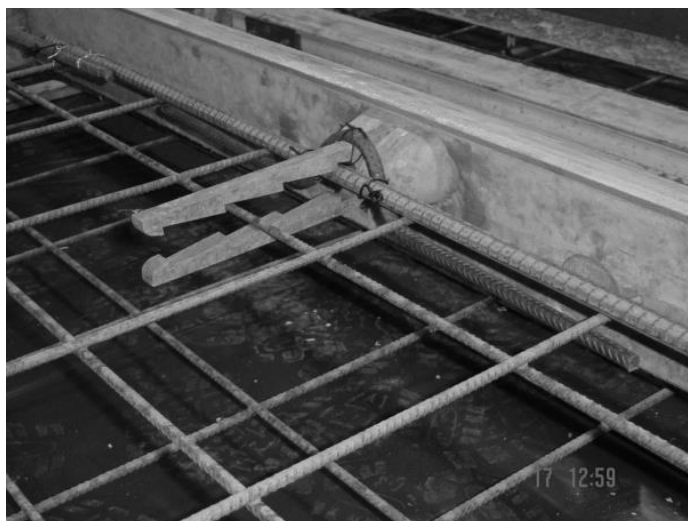


**Figure 129 - Series ES2 typical panel setups**

Figure 128 shows a typical panel setup with an 80mm plate anchor, N16 x 90mm shear bar in a 175mm panel. Figure 129 shows a typical panel setup with a 60mm plate anchor, N12 x 60mm shear bar in a 125mm panel.

Each test panel included four anchors. Concrete compressive strength,  $f_{c,age}$ , was recorded by means of cylinder compression tests. Where 4 anchors were setup in a panel for testing, 9 cylinder compressive strengths were recorded for each panel test, 3 at the beginning and end, and 1 after testing anchor 1, 2 and 3. The mean of these cylinder compressive strengths was calculated,  $f_{c,age}$ , for each panel test, and noted in Table 22.

**Table 22 - Reinforcement Configurations for Test Series**

Test Series	Panel Thickness, mm	Plate Edgelift Anchor		Shear Bar sizes, N Class		
		Width, mm	Thickness, mm	N16 x 90mm	N12 x 90mm	N12 x 60mm
ES1	100	60	10	Nil	Nil	Yes
ES2	125	60	10	Nil	Nil	Yes
ES3	150	60	10	Nil	Nil	Yes
ES4	150	60	16	Nil	Nil	Yes
ES5	150	75	16	Nil	Yes	Nil
ES6	150	80	16	Yes	Nil	Nil
ES7	175	60	16	Nil	Nil	Yes

Note: Each test panel included SL82 panel mesh and N16 perimeter bars.



#### 5.4 Edgelift test 4 – Anchor reinforcement influence on shear failure loads

The anchors were loaded under a load-controlled rate of 20 kN/min via a hydraulic jack with a load cell. The test data recorded for each specimen included load-displacement (of the anchor relative to a fixed point on the test panel) and load-time. The panels were tested horizontally and supported off the floor on timber gluts whilst the panel reacted against a steel frame with an open span of 2.0m as the load was applied to the anchor. The spacing of the reaction frame for the anchors was outside the predicted failure zone for the concrete by at least 1.0m, shown in Figure 130.

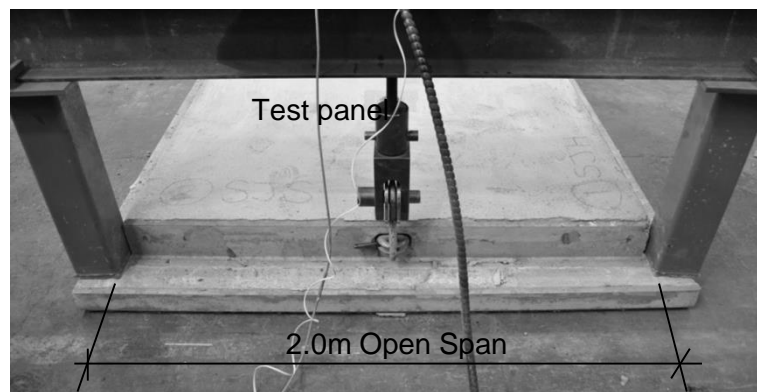


Figure 130 - Shear loads applied with 2.0m open span reaction frame

##### 5.4.3 Test Results and Analysis

Shear reinforced plate-type Edgelift anchor pull-out tests (126 off) were conducted at concrete compressive strengths and shear bar embedment heights that would initiate a concrete cone failure. The shear bar used on these Edgelift anchors were N Class, 60mm and 90mm height, 16mm and 12mm diameter reinforcement installed with 60mm, 75mm and 80mm wide plate anchors, (10mm and 16mm plate thicknesses). They were cast in thin (100mm, 125mm, 150mm and 175mm thickness) panels with the reinforcement configurations described in more detail below. Details of the combination are summarised in Table 23. Normal strength concrete was used throughout all series of the tests; being 14mm coarse aggregate, 0.44 water/cement ratio, and nominal grade 40MPa design strength supplied by a commercial ready-mix company, and mix design detailed in Table 6. The range of concrete compressive strengths at time of test was 8MPa to 45MPa, with an average of 22MPa.

#### 5.4 Edgelift test 4 – Anchor reinforcement influence on shear failure loads



Figure 131 - Typical failure surface propagating to the panel thin edge

The Edgelift anchor test data was compared with the predicted capacity as determined using the ACI318 (2008) concrete breakout strength calculations detailed in section D 5.2.1 including reduction factors. The ratio of the recorded breakout loads and the calculated strengths, as per ACI318 (2008) D 5.2, is shown in Table 23.

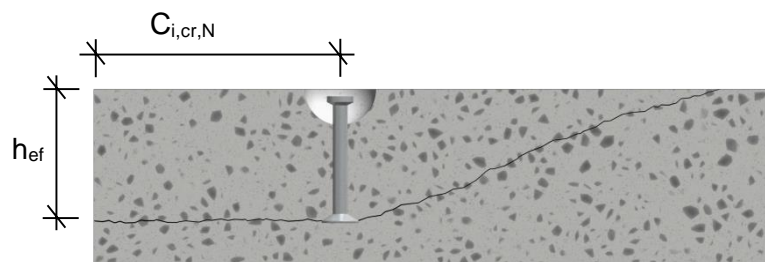


Figure 132 - Idealised fracture path as stated in ACI318 (2008) for a single cast-in anchor

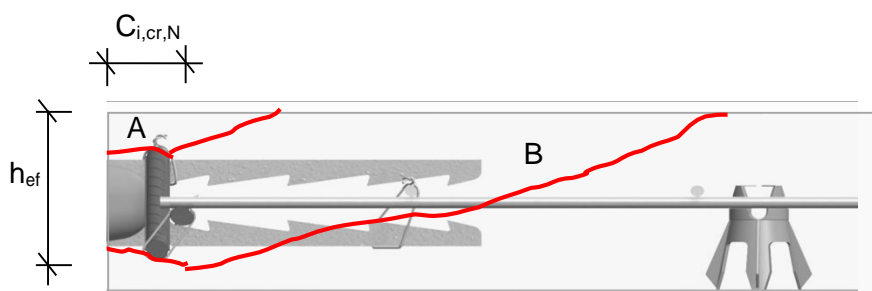


Figure 133 - Estimate fracture path from test results

If crack in position A starts to propagate and reach the panel surface prior to crack B being visible on the surface, this can be an indication that the bridge of the shear bar

#### 5.4 Edgelift test 4 – Anchor reinforcement influence on shear failure loads

is not seated adequately to the anchor. A panel flexure crack will also be present if crack A erupts to the surface prior to crack B.

Once crack B continues to open, the load on the shear bar bridge will increase, and bending of the shear bar may occur.



**Figure 134 - Actual fracture surface**

Figure 134 shows typical fracture cones propagated to the panel surface. Using equations 1-5, with the variables in Figure 133, the predicated values were calculated and compared with the test results and presented in Table 23.

## 5.4 Edgelift test 4 – Anchor reinforcement influence on shear failure loads

**Table 23 - Tensile breakout strength,  $P_u$ , compared with the reduced concrete breakout capacities,  $N_{cb}^0$ , presented by ACI318 (2008) D5.2**

Series	Number of Tests, n	Test / Predicted Range, $P_u / N_{cb}^0$	Mean	Variation Coefficient, %
<b>Series ES1:</b> 100mm Panel, 60x10mm Anchor, N12x60mm Shear bar	8	1.29 – 1.80	1.59	8
<b>Series ES2:</b> 125mm Panel, 60x10mm Anchor, N12x60mm Shear bar	10	1.15 – 2.82	1.60	14
<b>Series ES3:</b> 150mm Panel, 60x10mm Anchor, N12x60mm Shear bar	5	1.08 – 3.40	2.02	16
<b>Series ES4:</b> 150mm Panel, 60x16mm Anchor, N12x60mm Shear bar	32	1.04 – 2.64	1.75	20
<b>Series ES5:</b> 150mm Panel, 75x16mm Anchor, N12x90mm Shear bar	25	1.47 – 3.41	2.53	17
<b>Series ES6:</b> 150mm Panel, 60x16mm Anchor, N16x90mm Shear bar	42	1.08 – 2.70	1.67	23
<b>Series ES7:</b> 175mm Panel, 60x16mm Anchor, N12x60mm Shear bar	4	1.01 – 1.42	1.14	7

The failure loads all exceeded the predicted concrete breakout strengths calculated, demonstrating that the ACI model is adequate for shear capacity concrete strength predictions. The coefficient of variation for series ES2, ES3, ES4, ES5 and ES6 is statistically widespread, and since these tests were conducted under controlled conditions, a typical precast manufacturing environment should ensure suitable quality control procedures to monitor the adherence to installation recommendations from anchor manufacturers. Care should be taken to ensure the design intent of the shear bar is maintained.

### 5.4.4 Concluding remarks

This series of tests is an evaluation of concrete breakout capacities for shear reinforcement of Edgelift anchors in thin walled elements. Using the formula in the ACI318 (2008) D5.2, comparisons of the tested breakout strength and the shear test pull out capacity of the Edgelift anchors is made. All panels were reinforced with a

#### 5.4 Edgelift test 4 – Anchor reinforcement influence on shear failure loads

shear bar, centrally placed SL82 mesh and centrally placed N16 perimeter bar, and the ratios of test to predicted failure load indicate that the ultimate capacity of all the shear reinforced anchors was within the predicted breakout strengths noted by ACI318 (2008).

As the ratio of test to predicted approaches 1, showing that under less controlled conditions environments the designed performance may be greater than actual performance if suitable quality procedures are not used to monitor shear bar design and installation.

Overall, one hundred and twenty-six, 126, tests were conducted using shear reinforced Edgelift anchors in lateral tension; the variables tested include concrete compressive strength at time of testing which ranged from 8MPa to 45MPa with an average of 22MPa, and arrangement of shear reinforcement which included the provision of perimeter bars and central mesh reinforcement in the panel.

The load bearing capacity of an Edgelift anchor loaded in a shear direction and reinforced with a N12 60mm x 250mm shear bar, is shown below.

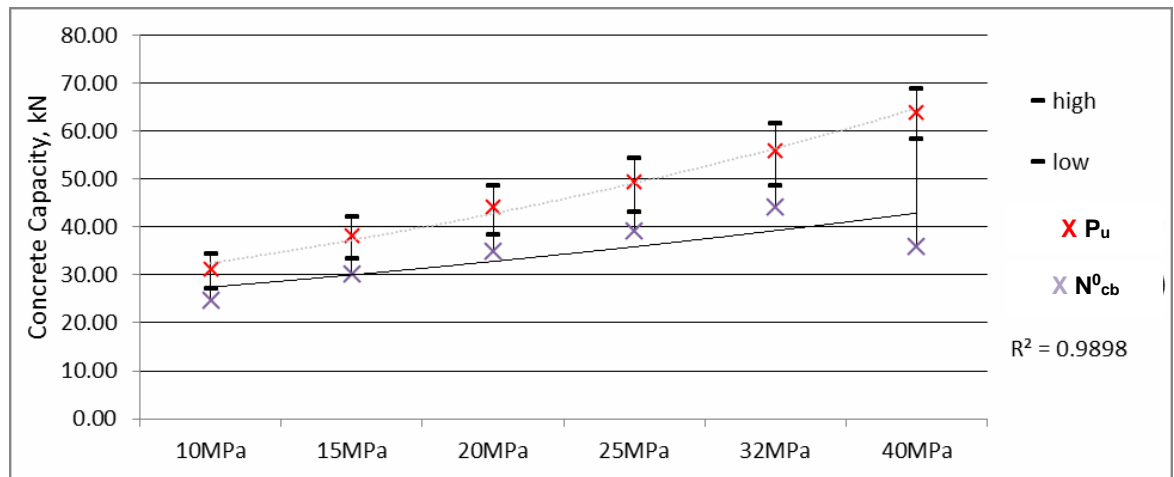


**Figure 135 – Average capacity vs Characteristic resistance of tested reinforced cast-in Edgelift 75x16mm anchors, 150mm panel**

$N_{cb}^0$  is the calculated lower 5% statistical value of a normal distribution referred to as the 5% fractal probability and derived as follows:

$$\text{Mean Tested Value, } P_u \times (1 - k_s) \times \text{Coefficient of Variation}$$

**Equation 24**

## 5.4 Edgelift test 4 – Anchor reinforcement influence on shear failure loads

Where:

$k_s$  – sampling factor from the  $k_s$  factors as per AS3850 (SAI 2015)

Coefficient of variation is calculated as:

Standard deviation of the distribution of tested results  $\div$  mean,  $P_u$

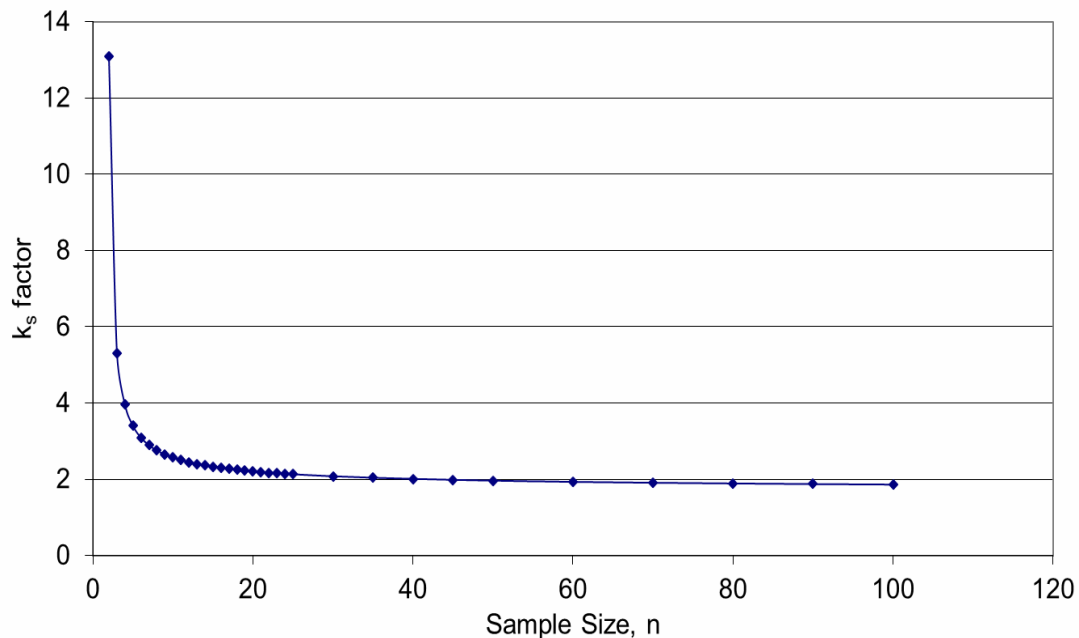


Figure 136 - Sampling factor,  $k_s$ , used for sample size of the test

The load bearing capacity of an Edgelift anchor loaded in a shear direction and no reinforced with a N16 90mm x 250mm shear bar, is shown below.

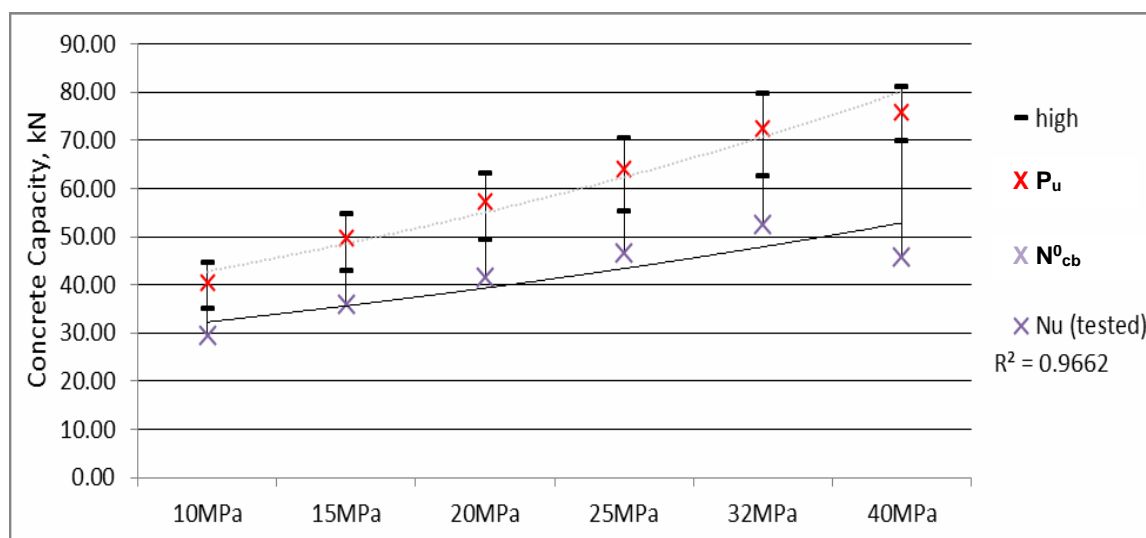


Figure 137 - Average capacity vs Characteristic resistance of tested unreinforced cast-in Edgelift 75x16mm anchor, 150mm panel

#### 5.4 Edgelift test 4 – Anchor reinforcement influence on shear failure loads

There is a 10-20% increase in shear capacity when the shear bar is increased in diameter from N12 to N16 and increased embedment of 30mm. The coefficient of variation is 8.1% to 8.8% respectively, and both produce a reliable capacity. The calculated capacity using equation 1 for cone capacity and equation 5 for edge reduce capacity, showing both are conservative.

### **5.5. Edgelift test 5 - Stress distribution along an edgelift anchors length**

Seven internal toothed lifting inserts were tested to record the ultimate concrete capacities in tension. Four of the lifting inserts had strain gauges attached at each internal tooth.

Five concrete test slabs were cast using 32MPa Panel Mix, refer to Table 6 for mix design. Two anchors were positioned at opposite sides in slabs A & B and one anchor per slab in C, D & E. A & B slab dimensions being 2.0m x 2.0m x 0.15m thick. C, D & E slab dimensions being 2.0m x 1.0m x 0.28m thick. No perimeter bars and no lifting insert tension bars. Steel reinforcing mesh being 500MPa SL82 centrally placed in slabs A & B only.

The scope of the test was to determine the performance capacities of the lifting inserts to concrete failure at a characteristic design concrete compressive strength of 32MPa, whilst monitoring the stress levels along the legs of the cast-in Edgelift anchor.

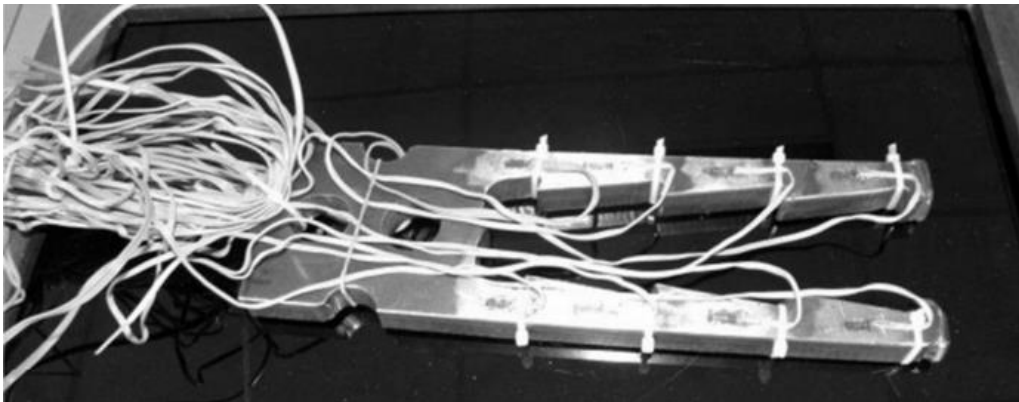


**Figure 138 - Lifting Insert with Strain gauge positions**

#### **5.5.1 Experimental Program**

The reinforcing was SL82 mesh and an N16 perimeter bar located 50 mm from the edge of the panel. These anchors were tested in direct tension as the concrete matured in order to initiate concrete cone failures; tests were conducted at a concrete compressive strength of 32MPa. All anchors failed due to concrete cone failure. The anchors were arranged with sufficient edge distances such that concrete capacity was not reduced due to edge effects.



## 5.5 Edgelift test 5 - Stress distribution along an edgelift anchors length

**Table 24 - Test series for Edgelift anchor stress distribution**

Test #	Sample size, n	Block size, L x W x D, m	Compressive Strength, $f_{c,age}$ , MPa	Panel Reinforcing	Effective Embedment, $h_{ef}$ , mm	Strain gauged
A	2	2x2x0.15	53.75	SL82	267	No
B	2	2x2x0.15	53.75	SL82	267	Yes
C	1	2x1x0.28	53.75	None	267	Yes
D	1	2x1x0.28	28.75	None	267	Yes
E	1	2x1x0.28	28.75	None	267	No
F	1	2x1x0.28	28.75	None	267	Yes
G	1	2x1x0.28	28.75	none	267	n/a

The strain gauges were assembled as per the below, Figure 139.

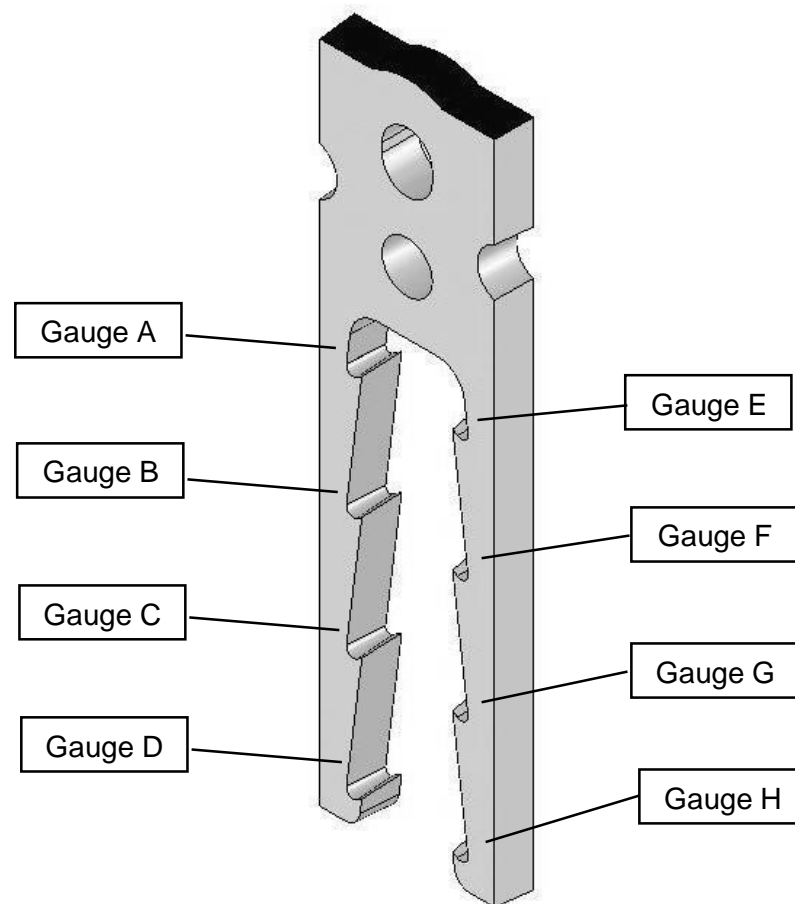


**Figure 139 - Strain Gauge Locations**

### 5.5 Edgelift test 5 - Stress distribution along an edgelift anchors length

The installation of the anchors in panels A & B are noted in the below Figure 140.

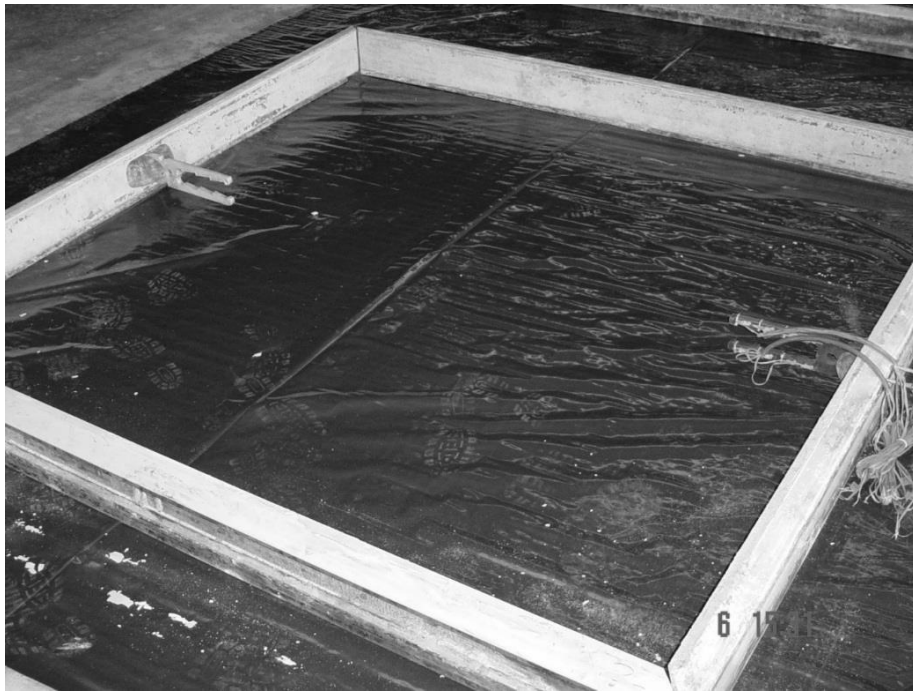


**Figure 140 - Typical panel layout for test panels A & B**

The installation of the anchors in panels C, D & E are noted in the below Figure 141.



**Figure 141 - Typical panel setup for test panels C, D and E**

The anchors were loaded under load-control at a rate of 20 kN/min via a hydraulic jack with a load cell. The test data recorded for each specimen included load-

### 5.5 Edgelift test 5 - Stress distribution along an edgelift anchors length

displacement (of the anchor relative to a fixed point on the test panel or block) and load-time. The panels with Edgelift plate anchors were tested horizontally and supported off the floor on timber gluts whilst the panel reacted against a steel frame with an open span of 1.8 m as the load was applied to the anchor. The spacing of the reaction frame for the anchors was outside the predicted failure zone for the concrete by at least 450mm as shown in Figure 62.

Testing commenced at approximately 27 hours with the average recorded  $f_{c,age}$  from 5 concrete compression cylinders recorded as 19.8MPa compressive strength at time of test. 2 tests were conducted at this time.

The remaining tests were conducted at approximately 46 hours. Concrete compression cylinders recorded was 30.5MPa.

The open span of the reaction frame was greater than  $4 \times h_{ef}$  of the Edgelift anchor, refer Figure 142.



**Figure 142 - Reaction frame being greater than  $4 \times h_{ef}$  open span**

Withdrawal testing was conducted by applying a tensile load to the Edgelift anchors. The load was applied at a constant rate until rupture of the concrete and complete

## 5.5 Edgelift test 5 - Stress distribution along an edgelift anchors length

withdrawal of the Edgelift anchor had occurred. Load vs time was recorded throughout the tests.

### 5.5.2 Test Results and Analysis

The load increased in a linear manner until the cone failure was observed, refer Figure 143. The failure mechanism observed was complete extraction of the Edgelift anchor from the concrete test panel, refer Figure 144. Post failure visual inspection did not reveal any evidence of plastic deformation or anchor failure, Figure 145.

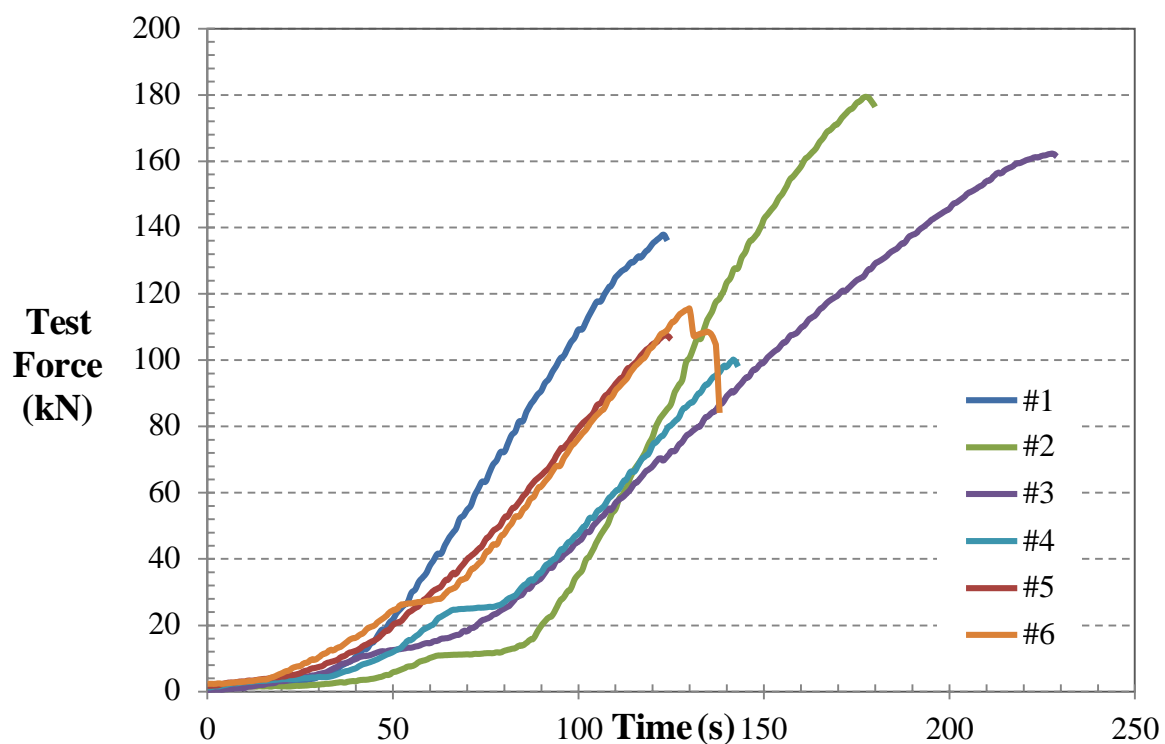


Figure 143 - Load vs Time for tested Edgelift anchors 1 to 6 (7<sup>th</sup> anchor was rejected), refer Table 25

### 5.5 Edgelift test 5 - Stress distribution along an edgelift anchors length



**Figure 144 - Post Test Concrete Failure**



**Figure 145 - Post-test Edgelift anchor exhibiting no plastic deformation, Anchor 2 Test panel D**

Test data for the 6 Edgelift insert tests is shown in the below table, refer Table 25 - Tension Test Data.

## 5.5 Edgelift test 5 - Stress distribution along an edgelift anchors length

**Table 25 - Tension Test Data**

Test Panel	Edgelift anchor	Strain gauged	Concrete Age @ test, hrs	Concrete Average Compressive Strength, $f_{c,age}$ , (MPa)	Ultimate test load, kN
E	1	No	28.5 – 29	19.8	138
D	2	Yes			179
C	3	Yes	53 – 54.5	30.5	162
A	4	Yes			100
A	5	No			107
B	6	Yes			115
B	7	n/a			n/a

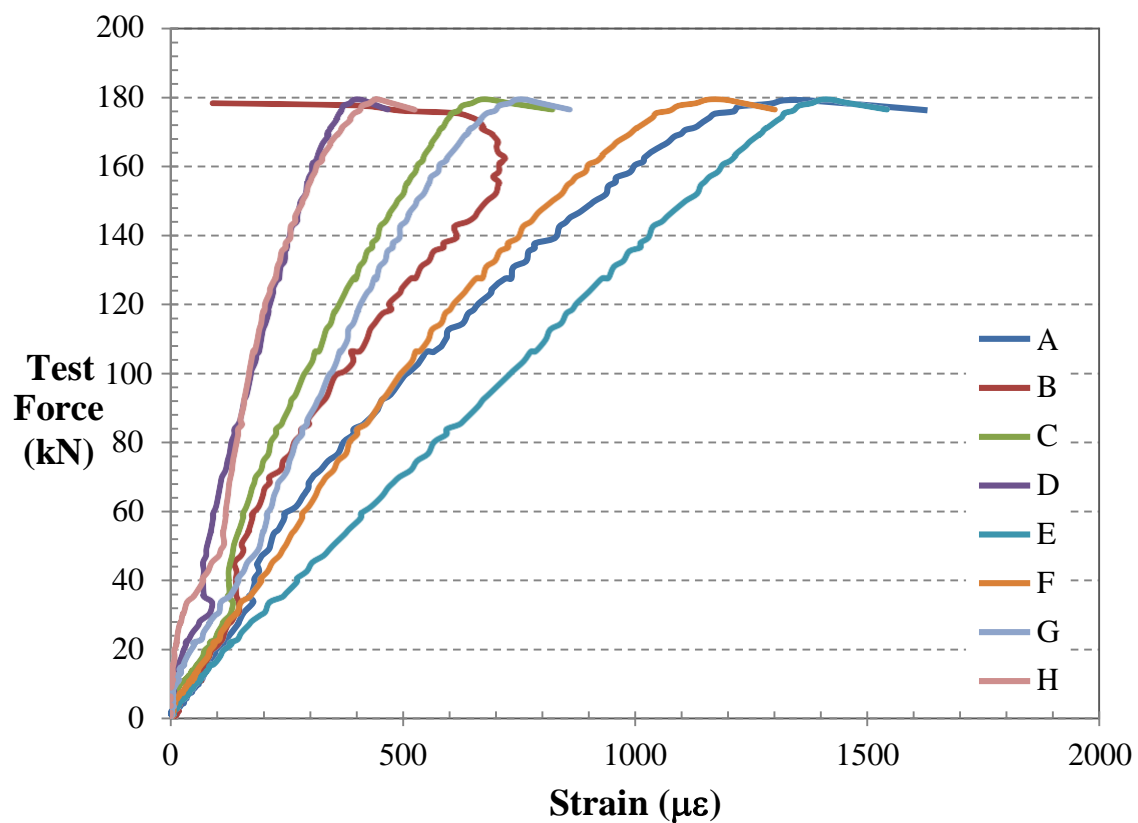


**Figure 146 - Strain v Load relationship for anchor 2 Test panel D**

### 5.5 Edgelift test 5 - Stress distribution along an edgelift anchors length

The paired teeth are closely matched, where the pair (B & F) are showing less matched correlation than the other paired teethed, but still lie between A/E & C/G, refer Figure 146.

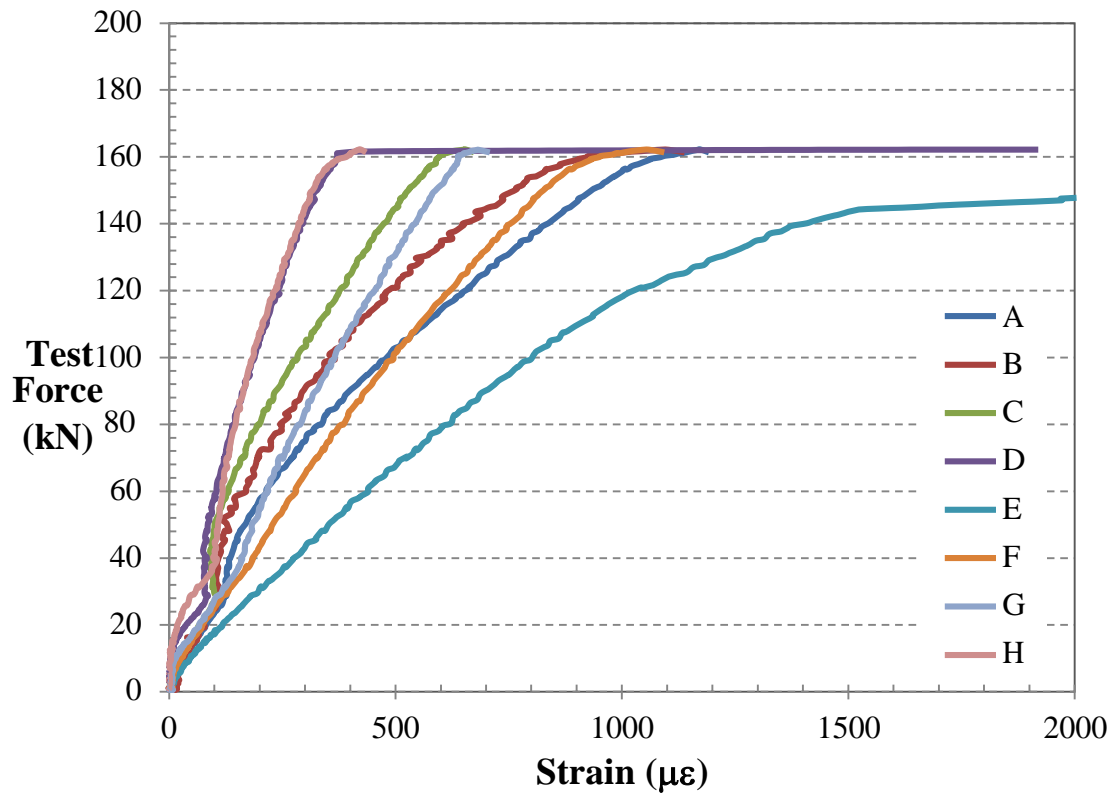


Figure 147 - Strain v Load relationship for anchor 3 test panel C

All the paired teeth are closely matched, where the pair (A & E) are showing less matched correlation than the other paired teethed, but still more than their next pair of teeth, B & F, refer Figure 147.

## 5.5 Edgelift test 5 - Stress distribution along an edgelift anchors length

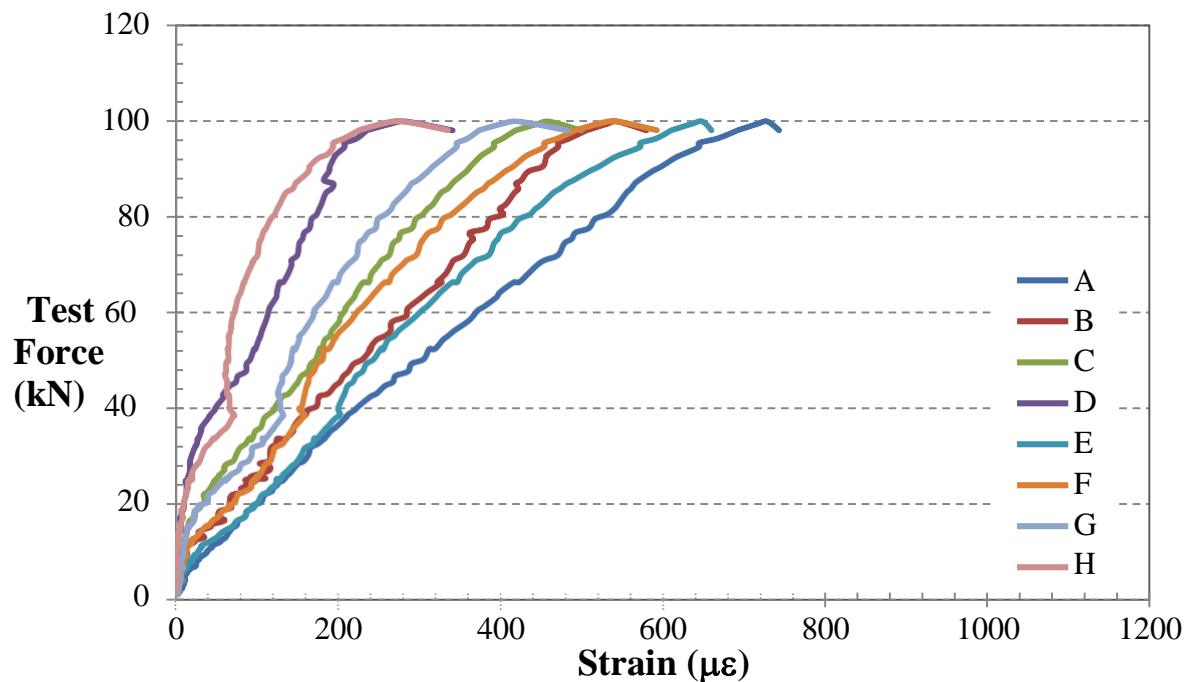


Figure 148 - Strain v Load relationship for anchor 4 test panel A

The paired teeth are closely matched, where the pair (B & F) are showing less matched correlation than the other paired teeth, but still lie between A/E & C/G refer Figure 148.

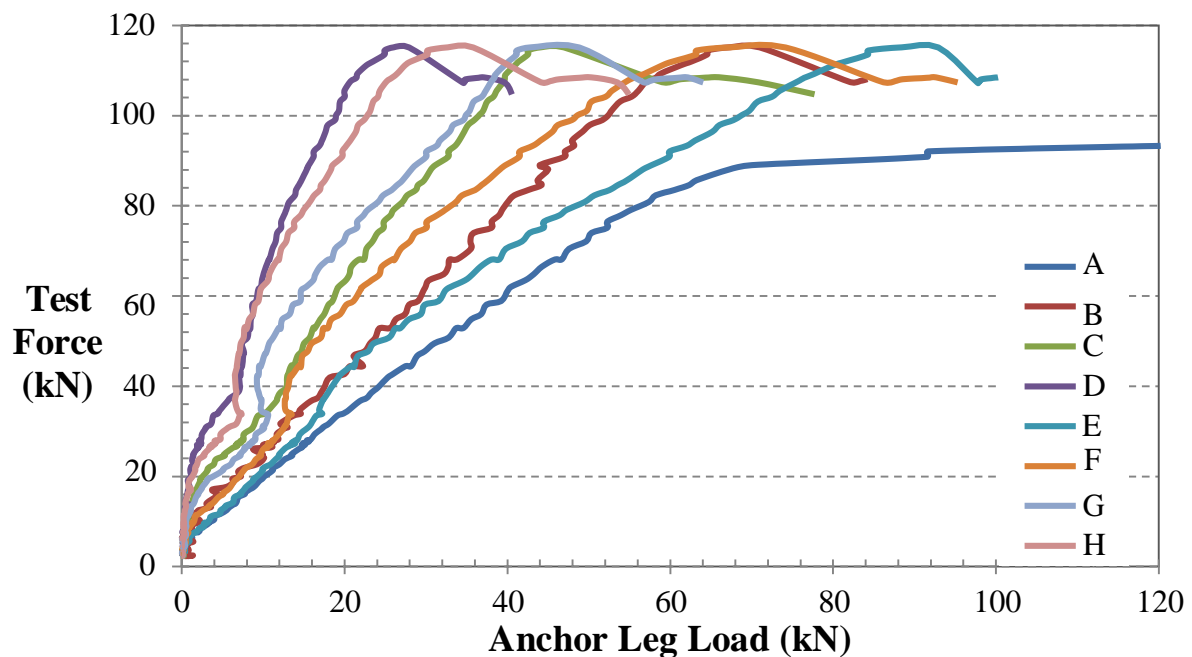


Figure 149 - Strain v Load relationship for anchor 6 Test panel B



### 5.5 Edgelift test 5 - Stress distribution along an edgelift anchors length

All the paired teeth carry similar loads, refer Figure 149.

#### 5.5.3 Concluding remarks

A summary of the data is as follows:

Anchor	Ultimate Anchor Load, kN	A-E Strain Gauge Load, kN	B-F Strain Gauge Load, kN	C-G Strain Gauge Load, kN	D-H Strain Gauge Load, kN	Load Sharing % (Refer fig below)
2 (280 panel)	179	72.5	60.3	37.8	22.5	41-34-21-13
3 (280 panel)	162	54.5	47.0	31.0	19.0	34-29-19-12
4 (150 panel)	100	35	29.3	24.5	17.0	35-29-25-17
6 (150 panel)	115	47.8	22.3	15.8	9.0	42-19-14-8

Anchors 2 and 3 were installed in blocks with no reo, whereas anchors 4 and 5 were installed in blocks with SL82 mesh installed.

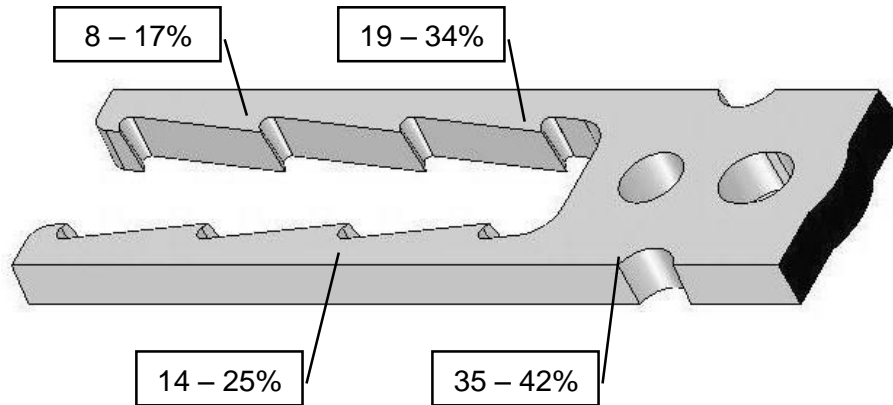


Figure 150 - Edgelift anchor load sharing %

Eighty percent of the load is carried by the 1st 3 pairs of teeth (A/E, B/F and C/G). The distribution of stress is equally shared between each pair of teeth. Centrally placed SL82 panel mesh does not influence the load sharing capability of the internal anchor teeth.

## 6 Discussion and analysis

This research shows that the capacity of cast-in inserts at early age develop their capacity not only relates to the concrete tensile capacity, but also to the mechanical interlock performance of an Edgelift anchor (its effective bearing area), in concrete less than 3 days of age.

Concrete at very early ages, less than 3 days, also showed higher than average pull-out results compared to what was predicted using the Concrete Capacity Design (CCD) methods. The tests in this experiment demonstrate that the model presented in AS3850 (SAI 2015) for the calculation of tensile pull-out in early concrete age is conservative and appropriate for prefabricated element Edgelift lifting design.

From this research, it is concluded that the tensile strength increases faster than compressive strength at early age when compared with the corresponding strength gains of mature concrete. This is determined from the higher slope of the tensile-to-compressive strength graph at early ages.

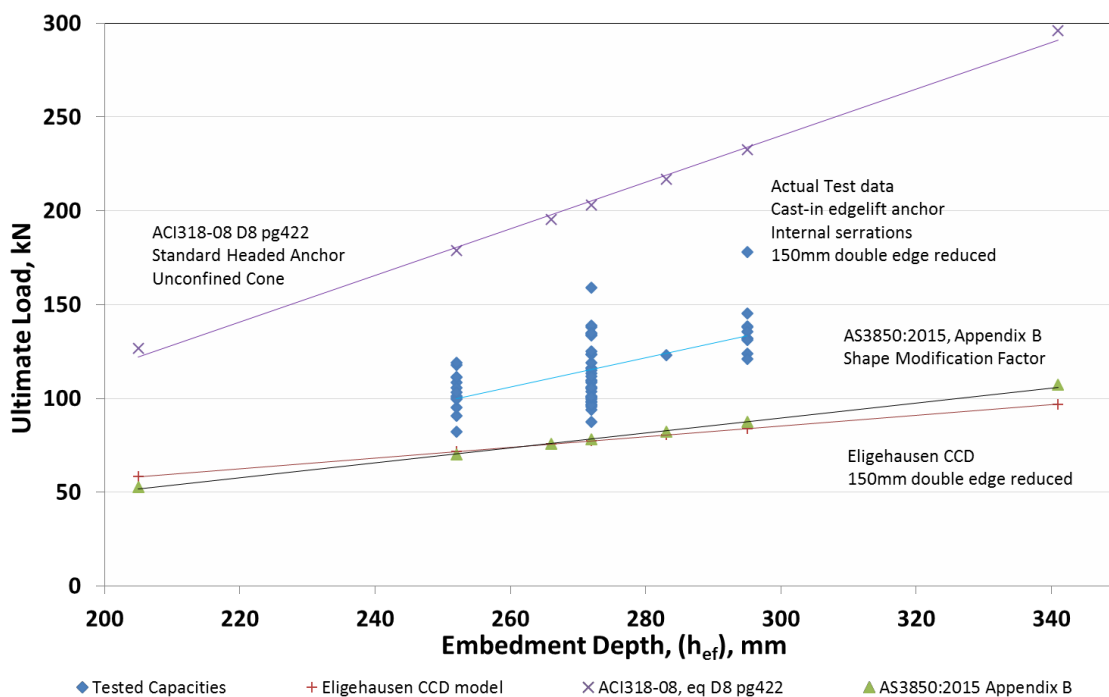


Figure 151 – 20MPa tensile capacity models for various embedment depths

## 6 Discussion and Analysis

The data above, Figure 151, is calculated in accordance with appropriate modification factors for 150mm panels, compared to tested Edgelift anchors

For  $h_{ef} = 50\text{mm}$ , and assuming a headed anchor tested with an unrestrained cone the AS3850 (SAI 2015) adopted model is shown to be suitably conservative when compared to actual tested capacities.

The tested tensile capacities of a cast-in Edgelift anchor,  $h_{ef} 257\text{mm}$ , in a 150mm panel, the following capacities were measured and compared against the calculated capacities and comparisons are relevant for each adopted failure mode. AS3850 (SAI 2015) and ACI 318 (2008) are closely matched in their predictions. These predicted capacities are also suitably conservative when compared to the actual tested anchor capacities, shown Figure 151.

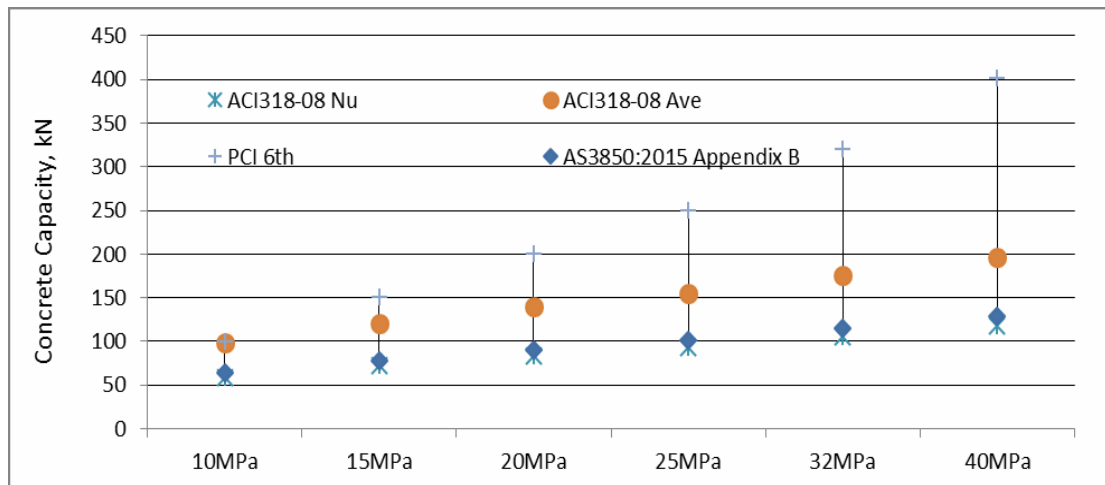


**Figure 152 - Calculated by various models versus  $N_{uc}$  tested in accordance with AS3850 (SAI 2015) Appendix B,  $h_{ef} 257\text{mm}$  in a 150mm panel (double edge reduced)**

Tested results of a cast-in reinforced with a N16 tension bar Edgelift anchor,  $h_{ef} 257\text{mm}$ , in a 150mm thick panel is as the below Figure 153. Noting the small coefficient of variation as all the tested ultimate loads are a steel rupture failure mode.

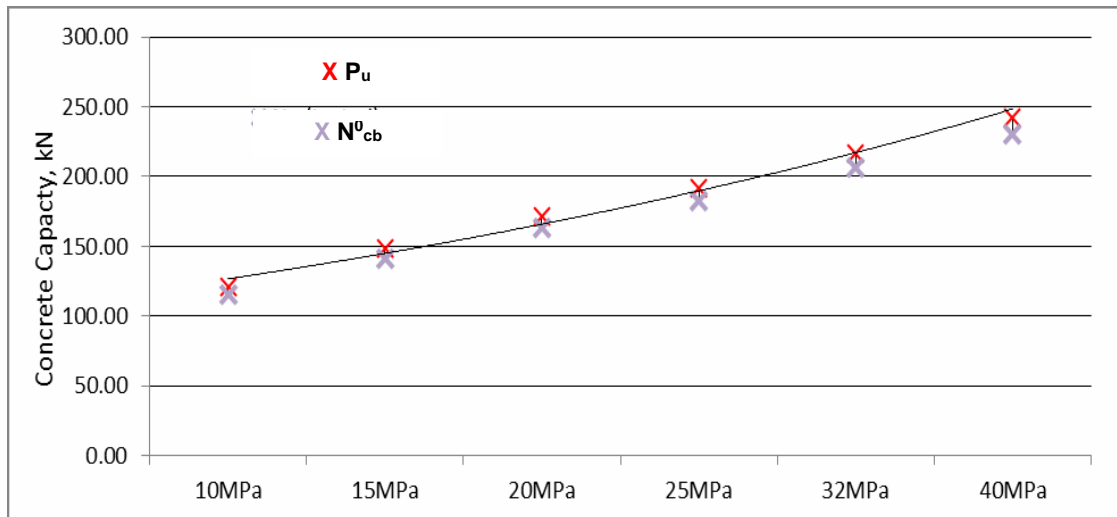


**Figure 153 - Average capacity vs Characteristic resistance of tested,  $h_{ef}$  257mm cast-in Edgelift anchor, N16x500mm tension bar, 150mm panel**

Pull-out capacity predictions when a load is applied to cast-in Edgelift insert with either internal teeth or both internal and external teeth on the legs of the anchor, refer the 2 types of anchor below, Figure 154.



**Figure 154 - Internal serrations and wavy legged Edgelift anchors**

Figure 155 shows the ultimate tensile results of a cast-in Edgelift anchor (serrations cut only on the inside of the anchor legs),  $h_{ef}$  257mm, in a 150mm panel, no shear bar, no tension bar, N16 panel mesh and N16 perimeter bar.

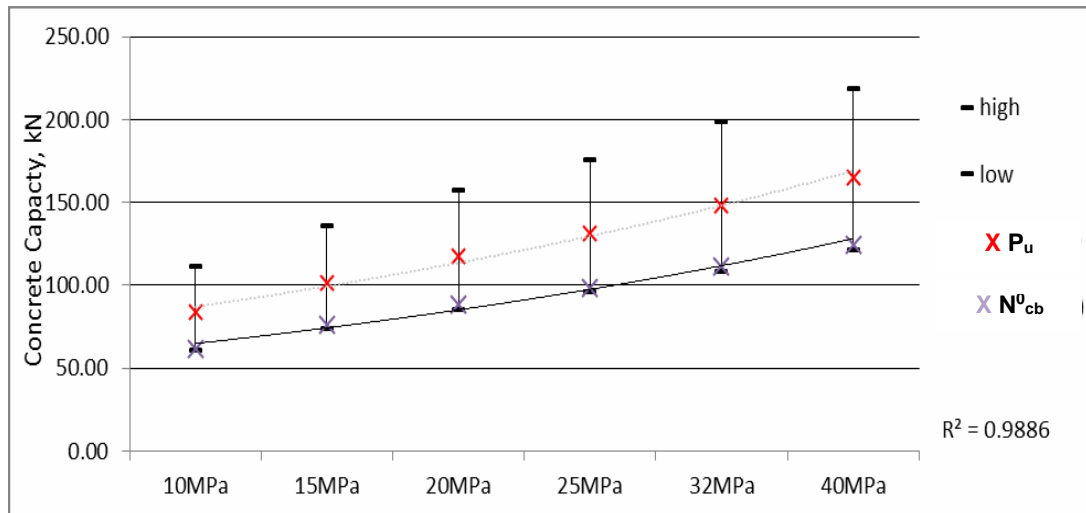


**Figure 155 - Average capacity vs Characteristic resistance of tested,  $h_{ef}$  257mm, 150mm panel, No Shear bar, SL82 and N16 Panel mesh**

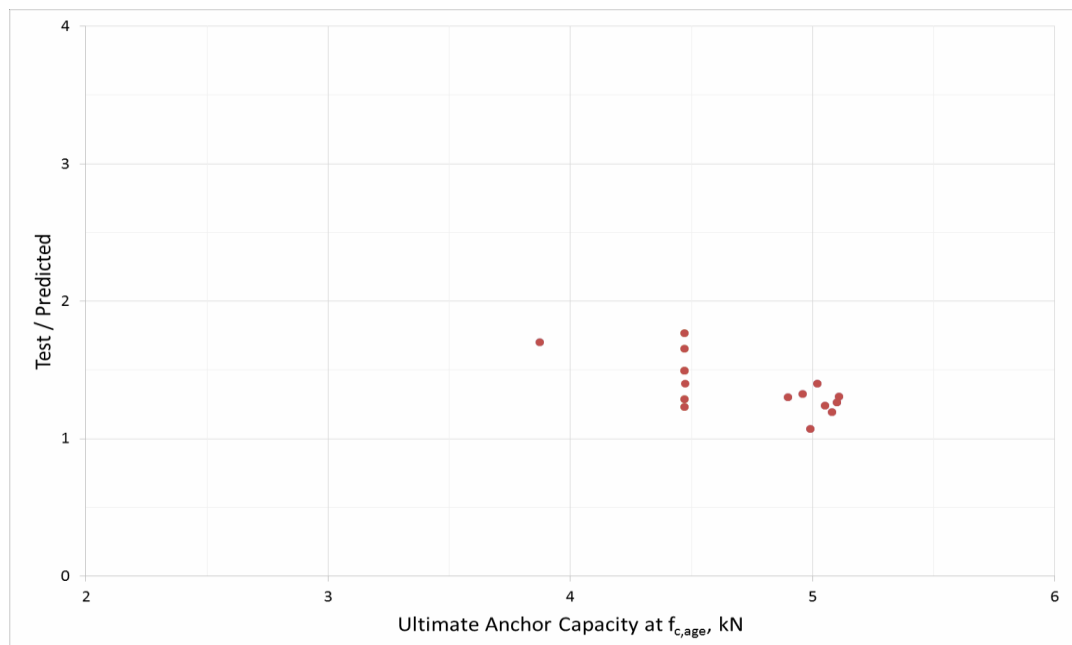


**Figure 156 - Tested vs Predicted in accordance with AS3850 (SAI 2015) Appendix B, Serrations to inside of anchor teeth,  $h_{ef}$  257mm, 150mm panel, No Shear bar, SL82 and N16 Panel mesh**

Figure 157, shows the ultimate tensile results of a cast-in Edgelift anchor (serrations cut on both sides of the anchor legs),  $h_{ef}$  370mm, in a 150mm panel, no shear bar, no tension bar, N16 panel mesh and N16 perimeter bar. Note for serviceability design this anchors capacity could be (depending on panel thickness and concrete compressive strength) limited to initial surface cracks that reach the surface of the panel before the Working load limit is reached.

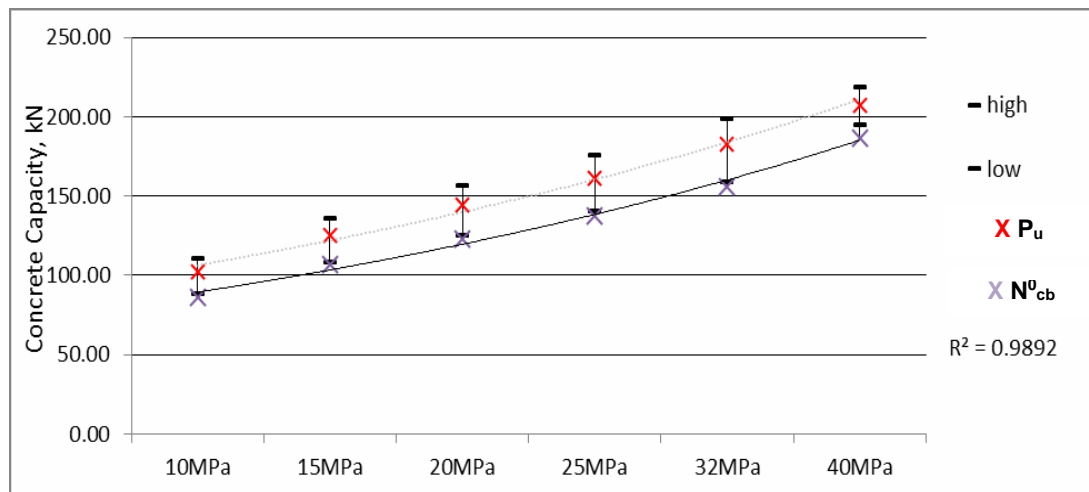


**Figure 157 - Average capacity vs Characteristic resistance of tested,  $h_{ef}$  370mm, 150mm panel, No Shear bar, SL82 and N16 Panel mesh**

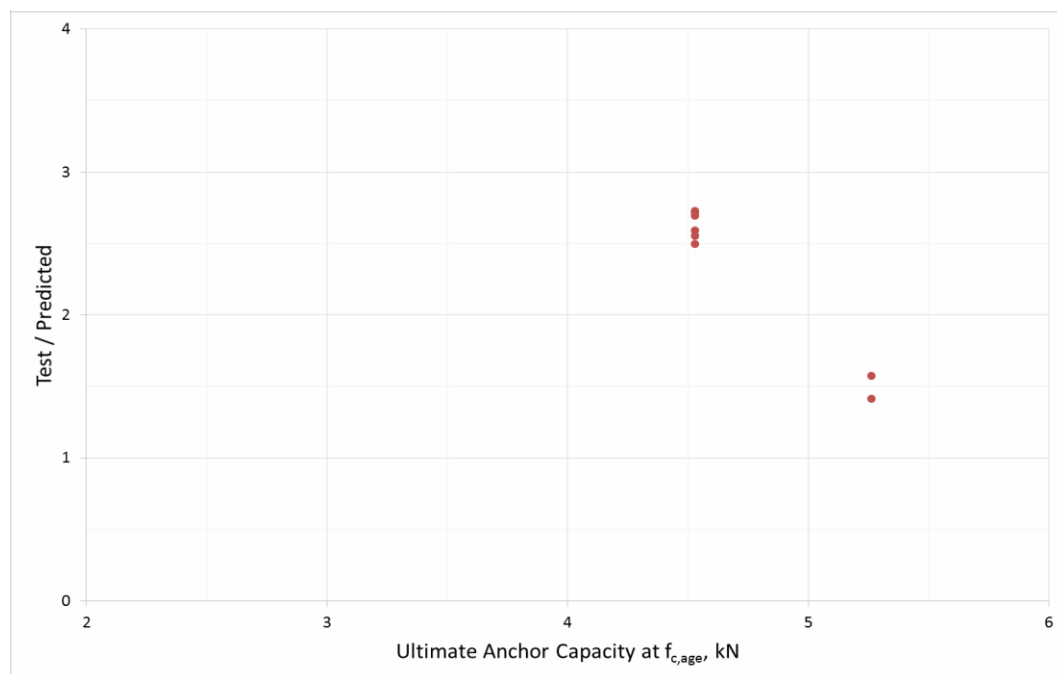


**Figure 158 - Tested vs Predicted in accordance with AS3850 (SAI 2015) Appendix B, Serrations to both sides of anchor legs,  $h_{ef}$  370mm, 150mm panel, No Shear bar, SL82 and N16 Panel mesh**

As can be seen from Figure 158, having steel reinforcement complimentary to the anchor provides for a more reliable capacity. If steel reinforcement is not complimentary to the anchor then having a deeper embedded anchor results in a smaller coefficient of variation, even though a concrete failure is the predominant failure mode.

## 7 Conclusions

The unrestrained concrete capacity model proposed in AS3850 (SAI 2015) is found to be suitably conservative for embedment depths less than 75mm, (section 5.1.). This model, applying the shape modification factor, was also found to be suitably conservative when applied to Edgelift anchors with double edge reduced concrete fracture cones. Headed anchors are suitably modelled in ACI318 (2008) and AS3850 (SAI 2015) for all concrete failure modes. The tensile strength gain was larger than the compressive strength gains for concrete ages less than 3 days old, no strength gain correction is proposed by this research for both standards as it is not significant.

For lifting design at early age, the anchor shape modification factors should be assessed for capacity at all ages and maturing concrete strengths, as it was found that the deeper the embedment, the less conservative the  $\beta$  model in AS3850 (SAI 2015) predicts anchor capacity. Even though the  $\beta$  model in AS3850 (SAI 2015) was found to be suitably conservative in all cases, care should be taken to assess an anchor's performance using characteristic values, as cast-in anchors are more sensitive to capacity variation than headed anchors.

For Edgelift anchors with double edge reduced concrete cones, as in thin wall panels 150 mm thick, additional reinforcement used to embed the anchor using the design recommendations for stress development length reduces the variation in tested anchor capacity. The design recommendations included in AS3850 (SAI 2015) specific to the use of tension bars confirms the recommendations of this research.

Adding additional steel that crossing the predicted concrete fracture surface increases an anchor's capacity, but variation in the load carrying capacity increases. Edgelift anchors should not rely on the extra capacity provided by additional panel reinforcement, as the extra capacity increases the variability of the capacity of the anchor, but does not increase the characteristic capacity of the anchor. The higher load carrying capacity is only provided by this reinforcement on the higher side of the normal distribution spread of tested results. Section 5.2. It was found that panel mesh intersecting the fracture surface increases the capacity of the anchor more so than other supplementary reinforcement.

## 7 Conclusions

The Coefficient of Variation of tested Edgelift anchors' tensile performance in a double edge reduced thin panel 150 mm thick, increases to over 10% when a shear bar is used. When no shear bar is used Coefficient of Variation of tested Edgelift anchors tensile performance in a double edge reduced thin panel 150 mm thick, is less than 10%. Refer Section 5.3. Shear bars are necessary to maintain a reliable capacity of the anchor when subject to shear loads, but if the stiffness of the anchor is sufficient to transfer the applied loads to the legs of the anchor, shear bars are not necessary to provide the sole source of capacity in a shear lift. Refer Section 5.3.

Steel cross sections along the anchor legs can be designed to accommodate the stress distributions as shown in section 5.5. When designing an Edgelift anchor, consideration should be made to the bearing area of the anchor legs, and can be optimising the stress along the legs of the anchor. Load bearing area of an anchor should account for the applied loads to be distributed along the lengths of the anchor. The overall capacity of an anchor is related the how the applied load sharing along the length of the anchor interacts with the concrete, and an associated effective embedment should be established if non-typical than headed anchors are being tested.



## 8 Recommendations

For anchors with a  $h_{ef}$  less than 75 mm, and an unrestrained and unmodified concrete cone, the model proposed for concrete cone capacity in AS3850 (SAI 2015) is suitably conservative, being;

$$F_{t,k} = \sqrt{f_{ctd}} \cdot (h_{ef})^{3/2}$$

An Edgelift anchor is recommended to have a coefficient of variation less than 15% to suitably satisfy design reliability for lifting anchors.

It is recommended for lifting design in lower concrete compressive strengths, due to variable anchor capacities, steel intersecting the predicted fracture surface should not be included in the assessment of an anchors performance, unless the steel is complimentary to the anchor.

A cast-in anchors performance should not include anchor capacity increases relating to supplementary anchor reinforcement or reinforcement used in the concrete element. A cast-in anchor used for lifting a precast concrete element, i.e. a reliable safety critical product, is recommended to perform independent of any contributing supplementary reinforcement.

For a lifting anchor to maintain its capacity reliably, the anchor must be assessed using characteristic performance analysis.

It is recommended to use a shear bar to reliably establish an anchors capacity when loaded in shear, unless the anchors steel cross sections are adequate enough to transfer the applied loads to the legs of the embedded anchor, prior to deformation from bending in that axis. The bearing area of the edgelift anchors legs are recommended to be designed to account for the unevenly distributed applied loads experienced during lifting.

Further work to compare mix proportions, effects of curing age against tensile strength gain. Size effect is another consideration not assessed during this research.

## 8 Recommendations

Crack formation and fracture energy depend on the mechanical interaction between inclusions (mainly large aggregate) and the cement based matrix, is an area for further research to expand the current knowledge for tensile concrete capacity.

## 9 References

- ACI318-08 Appendix C. 2008. *Building code requirements for structural concrete*. Farmington Hills, MI: American Concrete Institute.
- ACI 318-08. 2008. *Building code requirements for structural concrete*. Farmington Hills, MI: American Concrete Institute.
- ACI 355. 2007. *Anchorage to concrete*. Farmington Hills, MI: American Concrete Institute.
- ACI Committee 446. 2004. *Fracture Mechanics of Concrete*. Chicago, IL: ACI Foundation.
- ACI224.2R. 2001. *Cracking of concrete members in direct tension*. Farmington Hills MI: American Concrete Institute.
- ACI228.1R-03. 2003. *In-place methods to estimate concrete strength*. Farmington Hills, MI: American Concrete Institute.
- Anderson, N S, A Koray-Tureyen, and D F Meinheit. 2007. *Design criteria for headed studs: Phase 2, Tension and combined tension and shear*. IL, Wiss-Janney: Northbrook, Elstner Associates Inc.
- AS1012.10. 2000. *Methods of testing concrete: Method 10, Determination of in-direct tensile strength of concrete cylinders (Brazil of Splitting)*. Sydney, Australia: Standards Australia.
- AS1012.8.1. 2000. *Methods of testing concrete: Method 8.1: Method for making and curing concrete - Compression and indirect tensile test specimens*. Sydney, Australia: Standards Australia.
- AS2758.0. 2009. *Aggregates & rock for engineering purposes*. Sydney, Australia: Standards Australia.
- AS3600. 2009. *Concrete Structures*. Sydney, Australia: Standards Australia; SIA Global.
- AS3850. 2015. "Prefabricated Concrete Elements." Sydney Australia: Standards Australia, SAI Global.
- . 2003. "Tilt-up concrete construction." Sydney, Australia: SAI Global, Standards Australia.
- AS3972. 2010. *General purpose & blended cements*. Sydney, Australia: Standards Australia.
- AS4671. 2001. *Steel reinforcing materials*. Sydney, Australia: Standards Australia.

- ASTM C469-02. 2002. *Standard test method for static modulus of elasticity and poisson's ratio of concrete in compression*. West Conshohocken, PA, USA: [www.astm.org](http://www.astm.org).
- ATENA - Cervenka Consulting. 2015. *ATENA - Advanced Tool for Engineering Nonlinear Analysis*. Prague, Czech Republic.
- Barracough, A S. 2012. "Tensile and compressive behaviour of early age concrete." *Conference proceedings*. Nashville, USA: Precast Concrete Institute.
- Bischoff, P H. 2001. "Effects of shrinkage on tension stiffening and cracking in reinforced concrete." *Canadian Journal of Civil Engineering* 28 (3): 363-374.
- Browning, JoAnn, David Darwin, Diane Reynolds, and Benjamin Pendergrass. 2011. "Lightweight aggregate as Internal Curing Agent to Limit Concrete Shrinkage." *ACI Materials Journal - Technical papers* 638-644.
- BS8110. 2010. *Structural use of concrete*. London, UK: British Concrete Institute.
- CEB . 1994. *Fastenings to concrete and masonry structures, State of the art*. Lausanne, Switzerland: Thomas Telford Ltd.
- CEB. 1997. *Design of fastenings in concrete: Design guide* . Lausanne, Switzerland: Thomas-Telford.
- CEN/TR 14862. 2004. *Precast concrete products - Full scale testing requirements in standards on precast concrete products*. Europe: European Committee for Standardisation.
- CEN/TR 15728. 2008. "CEN/TR 15728:2008 - Design and use of inserts for lifting and handling of precast concrete elements." UK: BSI - British Standards Institute. 54.
- Dao, Vinh T, Peter F Dux, and Peter H Morris. 2009. "Tensile properties of early age concrete." *ACI Materials Journal* 483-492.
- Dela, B F. 2000. *Eigenstresses in hardening concrete*. Brovel Kgs, Lyngby: Department of structural engineering & materials science.
- Eligehausen, R. 2014. *fastening to concrete*. Presentation to CIA, Australia, Stuttgart, Germany: University of Stuttgart, Institute of Construction Materials.
- Eligehausen, Rolf, Malle, and Silva. 1990. *Advances In Concrete Fastening*. Hamburg: Elisivier.
- ETAG 001. 2013. "European Organisation for Technical Approvals." *Guideline for European Technical Approvals*. Avenue des Arts 40 Kunstlaan, B - 1040 Brussels: EOTA. 3-5.
- Fuchs, W, R Eligehausen, and J E Breen. 1995. "Concrete capacity design approach for fastening to concrete." *ACI Structural Journal* 73-94.

## 9 References

- Gambhir, M L. 2004. *Concrete Technology*. London, UK: McGraw-Hill Publishing Company Limited.
- Hauggaard-Nielsen, A B. 1997. *Mathematical modelling and experimental analysis of early age concrete: PhD Thesis*. Kgs Lyngby, Denmark: Department of Structural Engineering and Material Technical, University of Denmark, .
- Hawkins, Neil. 1984. "Fracture Process Zone of Concrete Cracks." *Journal of Engineering Mechanics* 110(8) 1174-1184.
- Hengjing, B A, S U Anshuang, GAO Xiaojian, and TAO Qi. Aug 2008. "Cracking tendency of restrained concrete at early ages." *Journal of Wuhan University of Technology* (CBI Research, Swedish council for building research) Mater Sci Ed.
- Holt, E E, and M T Leivo. 2000. "Methods for reducing early age shrinkage." *Proceedings of the international RILEM workshop, Shrinkage of concrete, Shrinkage 2000*. RILEM publications SARL draft print.
- Hoyer, O, E E Holt, and MT Leivo. 2000. "Methods of reducing early age shrinkage." *Proceedings of the international RILEM workshop* Publication SARL Draft print.
- Institute of Civil Engineers. 2014. *Early-age thermal crack control in concrete*. London: McGraw-Hill.
- Iso-Ahola, Vik, Bashar Sudah, and Vincent Zipparro. 2012. "Concrete thermal strain, shrinkage and cracking analysis." *Magazine of concrete research* 345-377.
- Jensen, O M, and P F Hansen. 2001. "Autogenous shrinkage and RH-change in perspective." *Cement & Concrete research*, 12 31: 1859-1865.
- Khan, M I, and C J Lynsdale. 2002. "Strength, Permeability and carbonation of high performance concrete." *Cement & concrete research*, 32 123-131.
- Mindess, S, F J Young, and D Darwin. August 30, 2002. *Concrete (2nd Edition)*. Prentice Hall.
- Nielsen, M P. 1999. *Limit analysis and concrete plasticity, 2nd Ed*. London, UK: CRC Press.
- Oluokun, F A. May-June 1991. "Prediction of concrete tensile strength from its compressive strength evaluation relations for normal weight concrete." *ACI Materials Journal*, Vol. 88, No. 3 302-309.
- PCI. 2004. *PCI - Design handbook, 6th ed.* . Chicago, IL, USA: Precast/Prestressed Concrete Institute.

## 9 References

- Prasad, B K, Rabindra Kumar Saha, and A R Gopalafrishnan. 2010. "Fracture behaviour of plain concrete beams - experimental verification of one parameter model." *ICCES* 65-83.
- Prasanna, W G, and A P Subhasashini. 2010. "Cracking due to temperature gradient in concrete." *International conference on sustainable built environment (ICSBE-2010)*. Kandy, Sri Lanka: Civil Engineering.
- RILEM Report 25. 2002. *Early age cracking in cementitious systems*. Bagneux, france: RILEM Publications.
- RILEM. 2001. *Test and design methods for steel fiber reinforced concrete. Recommendations for uniaxial tension test*. Chairlady L. Wandewalle: RILEM Committee TDF-162.
- SafeWork Australia. 2016. *National Code of Practice for Precast Tilt-Up and Concrete Elements in Building Construction*. National Code of Practice, Australia: SafeWork .
- Scanlon, A, and Bruce A Suprenant. 2011. "Estimating two-way slab deflections." *Concrete International*, July 29-34.
- Seigneur, V, O Bonneau, and P C Aitcin. 2000. "Influence of the curing regime and of shrinkage reducing admixture on shrinkage." *Proceedings of the international RILEM workshop: Shrinkage of Concrete; Shrinkage 2000*. RILEM Publications SARL Draft Print.
- Sule, M, and K van Breugel. 2001. "Cracking behaviour of reinforced concrete subjected to early age chrinkage." *Materials and Structures* 34 284-292.
- van Breugel, K. 2000. *Numerical modelling of volume changes ar early ages - potential pitfalls and challenges*. RILEM Publication SARL, Draft print.
- Vesely, V, and P Frantik. 2010. "Reconstruction of a fracture process zone during tensile failure of quasi-brittle materials." *Applied and computational mechanics* 237-250.
- Winters, James, and C W Dolan. 2013. "Concrete breakout capacity of cast-in place anchors in early age concrete." *PCI & R&D Research Report*.
- Wollmershauser, R E. 2004. *Anchor performance and the 5% fractile*. Tulsa, Oklahoma: Hilti Technical Services Bulletin, Hilti Inc. .
- (Hawkins 1984)

## Appendix A – Lifting Design

### Wall panel lifting

Load resistance factors of safety, FOS, set out in the Australian Code would typically denote a FOS of 5.0 for re-useable lifting equipment and an FOS of 2.5 for lifting anchors. The

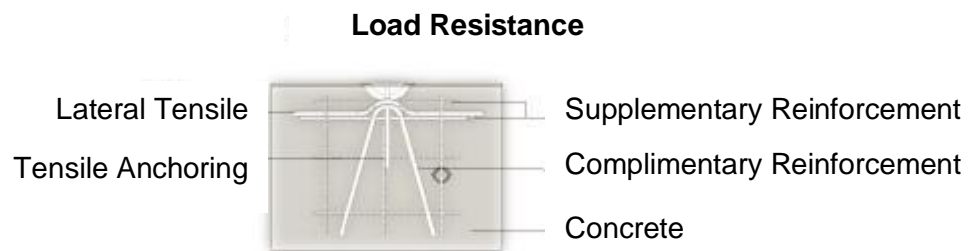


Figure 159 - Load resistance elements of an anchor system in a wall panel,

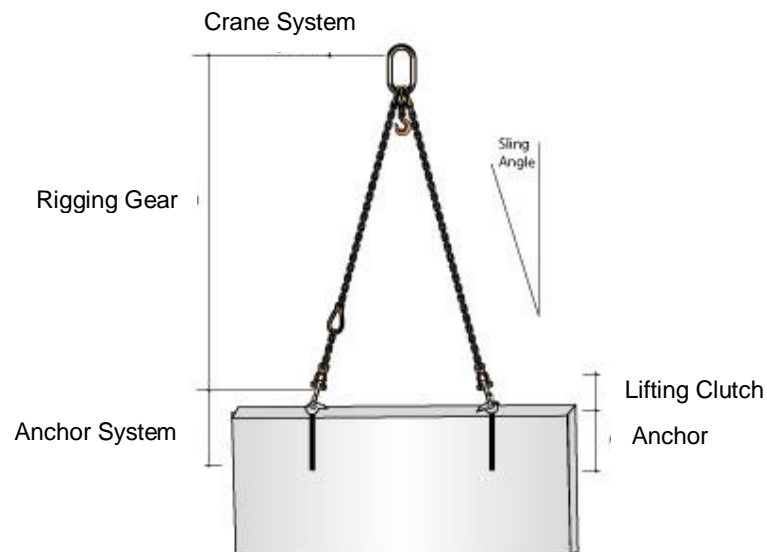


Figure 160 - Lifting system model for a thin section wall panel

The rigging arrangements can influence the applied anchor load, where statically indeterminate systems are not necessarily a design consideration, but can be used in practice.

### Basic Principles of wall panel lifting using cast-in inserts

The design engineer should specifically account for the applied loads expected during the lifting, transport and placement (or re-usability requirements) of the element and hence select the appropriate lifting anchor system. Flexure, casting bed suction, load direction (axial 'tensile', angular 'sling', transverse 'shear') are also load considerations to be accounted for in the lifting design of the element.

The anchor selection, together with additional reinforcement, and rigging arrangements is influenced by:

- The weight of the element
- The number of anchors in the element and the configuration of the anchor
- Capacity of the anchor at the specific concrete compressive strengths at time of lift
- The dynamic loads applied during lifting (suction to the casting bed, or crane dynamics)
- The rigging configuration

All of the above factors must be taken into consideration during the lifting design phase of the element.

Establishing the lifting anchor positions will influence the rigging arrangements used and therefore the static analysis of the rigging should be determined. Particular rigging configurations may be more suitable for particular job sites or lifting in place considerations, and the lifting design should denote the assumptions accordingly. For example, the statically determined systems, shown in Figure 161, where the determination of the loads is not always possible.

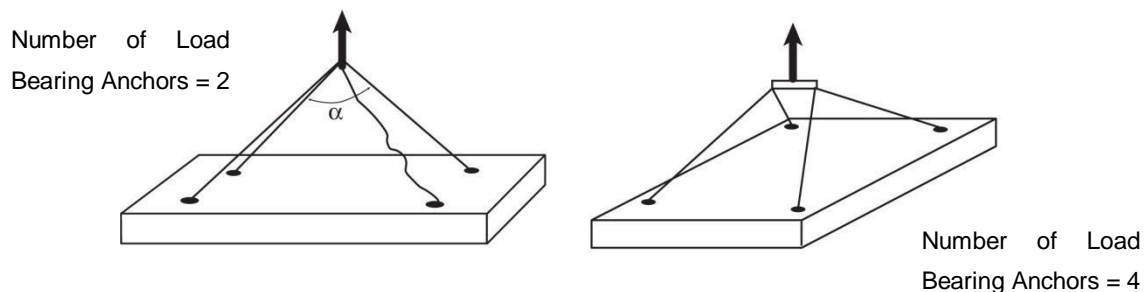


Figure 161 - Rigging configurations determining load sharing per anchor



## Appendix A – Lifting Design

Dynamic loads considered in lifting design are accounted for in two stages; suction to the casting bed on the initial lift and then the dynamic loads induced from crane vibration. These crane impact loads must be accounted for during transportation in the yard and on-site, and the coefficient increases from an overhead gantry crane through to a crane moving over rough terrain. Consideration for the entire transportation loads must be taken into account during the lifting design.

Consideration of different load combinations may result in wide variations required from the lifting insert. The load directions during production, transport and placement should be considered carefully. Depending on the planned load direction, either a different anchor may be included in the lifting design; alternatively, reinforcement may be included to reduce the possibility of element flexure crack damage. The configuration (size, position and quantity) of this reinforcement should be supplemented to the element reinforcement design to ensure for adequate capacity of the lifting design.

Lifting design is influenced by the steel / concrete interaction of the specific anchor selected. Different load cases are considered by the lifting design engineer, such as anchor susceptibility to edge distance, placement sensitivity, and anchor capacity at the specific concrete strength at time of lift. For example, a footed pin head style anchor maybe more susceptible to edge distance than a hairpin style anchor. Or a splayed anchor does not have the same tensile/axial capacity with the equivalent anchor length (effective embedment is greater on a Headed anchor than a splayed anchor of equivalent overall length).

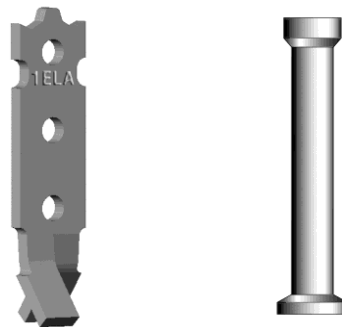


**Figure 162 - 2 anchors having the same overall length, but different Effective Embedment Depths,  $h_{ef}$**

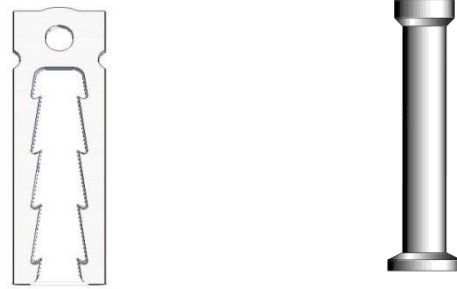


**Figure 163 - - 2 anchors having different concrete load interactions, where the footed anchor is more susceptible to side blow-out in thin wall sections**

**Table 26 - Casting bed suction coefficients, AS3850 (SAI 2003)**

$K_s$	Form Type
1.2	For a smooth oiled steel surface
1.3	For a timber surface varnished, oiled or rough steel
1.5	For a concrete to concrete separation (bondbreaker)

**Table 27 - Lifting equipment dynamic coefficients, AS3850 (SAI 2003)**

$K_D$	Handling Detail
1.2	Overhead Gantry Crane
1.2	Tower Crane
1.7	Mobile Crawler Crane
2.0	Mobile Tyre Crane
2.5 to 3.0	Over very rough ground

**Table 28 - Rigging equipment sling angle coefficients, AS3850 (SAI 2003)**

$K_{SL}$	Angle
1.00	0
1.04	30
1.16	60
1.42	90
2.00	120



**Figure 164 - Typical Tilt-up facelift systems – thin wall panels or thin section elements required to be face lifted**



**Figure 165 - Typical general element systems – facelift anchors normally placed in general precast elements**



**Figure 166 - Typical Edgelift systems – used for the majority of wall panel Edgelifting**

Figure 166 shows the anchors used in this research for concrete wall panel cast-in place Edgelift anchors.

## Appendix B - Test Data

Test ref #	Test Type	Anchor Type	Concrete Strength, MPa, $f_{c,age}$	Ultimate failure load, Pu, kN	Mode of Failure	Effective Embedment Depth, $h_{ef}$ , mm	Ultimate Test Loads normalised to $f_{c,age}$ , kN					
							10.00	15.00	20.00	25.00	32.00	40.00
1	shear	Internal Tooth	11.00	50.70	APO	128	48.34	59.20	68.36	76.43	86.47	96.68
2	shear	Internal Tooth	11.00	59.20	APO	128	56.44	69.13	79.83	89.25	100.97	112.89
3	shear	Internal Tooth	11.00	60.80	APO	128	57.97	71.00	81.98	91.66	103.70	115.94
4	shear	Internal Tooth	11.00	49.90	APO	128	47.58	58.27	67.29	75.23	85.11	95.16
5	shear	Internal Tooth	11.00	53.20	APO	128	50.72	62.12	71.73	80.20	90.74	101.45
6	shear	Internal Tooth	11.00	55.90	APO	128	53.30	65.28	75.38	84.27	95.34	106.60
7	tensile	Internal Tooth	9.30	226.00	CF	267	234.35	287.02	331.42	370.54	419.22	468.70
8	tensile	Internal Tooth	11.20	231.00	CF	267	218.27	267.33	308.69	345.12	390.46	436.55
9	tensile	Internal Tooth	10.40	234.00	CF	267	229.46	281.02	324.50	362.80	410.46	458.91
10	tensile	Internal Tooth	12.60	215.00	CF	267	191.54	234.58	270.87	302.85	342.63	383.07
11	tensile	Internal Tooth	13.10	234.00	CF	267	204.45	250.40	289.13	323.26	365.73	408.89
12	tensile	Internal Tooth	12.90	225.00	CF	267	198.10	242.62	280.16	313.23	354.37	396.20
13	tensile	Internal Tooth	13.10	228.00	CF	267	199.20	243.97	281.72	314.97	356.35	398.41
14	tensile	Internal Tooth	14.00	224.00	CF	267	189.31	231.86	267.73	299.33	338.66	378.63
15	tensile	Internal Tooth	17.50	233.00	CF	267	176.13	215.72	249.09	278.49	315.07	352.26
16	tensile	Internal Tooth	17.90	242.00	CF	267	180.88	221.53	255.80	286.00	323.57	361.76
17	tensile	Internal Tooth	18.30	243.00	CF	267	179.63	220.00	254.04	284.02	321.33	359.26
18	tensile	Internal Tooth	18.70	246.00	CF	267	179.89	220.32	254.41	284.44	321.80	359.79
19	tensile	Internal Tooth	19.10	251.00	CF	267	181.62	222.43	256.85	287.16	324.89	363.23
20	tensile	Internal Tooth	19.50	243.00	CF	267	174.02	213.13	246.10	275.14	311.29	348.03
21	tensile	Internal Tooth	19.90	245.00	CF	267	173.68	212.71	245.61	274.61	310.68	347.35
22	tensile	Internal Tooth	20.30	251.00	CF	267	176.17	215.76	249.14	278.55	315.14	352.33
23	tensile	Internal Tooth	20.2	151.0	APO	267	106.24	130.12	150.25	167.99	190.05	212.49
24	tensile	Internal Tooth	20.2	156.0	APO	267	109.76	134.43	155.23	173.55	196.35	219.52
25	tensile	Internal Tooth	12.1	99.6	CF	257	90.55	110.90	128.05	143.16	161.97	181.09
26	tensile	Internal Tooth	12.4	101.6	APO	257	91.24	111.75	129.03	144.26	163.21	182.48
27	tensile	Internal Tooth	12.4	105.0	APO	257	94.29	115.48	133.35	149.09	168.68	188.59
28	tensile	Internal Tooth	12.4	123.8	APO	257	111.18	136.16	157.23	175.78	198.88	222.35
29	tensile	Internal Tooth	12.4	103.2	APO	257	92.68	113.50	131.06	146.53	165.78	185.35
30	tensile	Internal Tooth	15.9	123.2	APO	267	97.70	119.66	138.17	154.48	174.78	195.41
31	tensile	Internal Tooth	15.9	124.0	APO	267	98.34	120.44	139.07	155.49	175.91	196.68
32	tensile	Internal Tooth	16.3	131.0	APO	267	102.61	125.67	145.11	162.24	183.55	205.21
33	tensile	Internal Tooth	16.3	112.0	APO	267	87.73	107.44	124.06	138.71	156.93	175.45
34	tensile	Internal Tooth	15.9	212.6	APO	267	168.60	206.50	238.44	266.58	301.61	337.21
35	tensile	Internal Tooth	15.9	222.2	APO	267	176.22	215.82	249.21	278.62	315.22	352.43
36	tensile	Internal Tooth	16.3	191.8	APO	267	150.23	183.99	212.46	237.53	268.74	300.46
37	tensile	Internal Tooth	16.3	181.4	APO	267	142.08	174.02	200.94	224.65	254.17	284.17
38	tensile	Internal Tooth	36.4	174.2	APO	257	91.31	111.83	129.13	144.37	163.33	182.61
39	tensile	Internal Tooth	36.4	174.2	APO	257	91.31	111.83	129.13	144.37	163.33	182.61
40	tensile	Internal Tooth	36.4	168.4	APO	257	88.27	108.10	124.83	139.56	157.89	176.53
41	tensile	Internal Tooth	36.4	175.4	SF ANCHOR	257	91.93	112.60	130.02	145.36	164.46	183.87
42	tensile	Internal Tooth	35.5	183.8	APO	267	97.55	119.47	137.96	154.24	174.50	195.10
43	tensile	Internal Tooth	35.5	174.8	APO	267	92.77	113.62	131.20	146.69	165.96	185.55
44	tensile	Internal Tooth	35.5	248.6	APO	267	131.94	161.60	186.60	208.62	236.03	263.89
45	tensile	Internal Tooth	35.5	249.4	APO	267	132.37	162.12	187.20	209.29	236.79	264.74
46	tensile	Internal Tooth	40.2	166.0	APO	267	82.79	101.40	117.09	130.91	148.11	165.59
47	tensile	Internal Tooth	40.2	155.4	APO	267	77.51	94.93	109.61	122.55	138.65	155.01
48	tensile	Internal Tooth	40.2	231.6	APO	267	115.51	141.47	163.36	182.64	206.63	231.02
49	tensile	Internal Tooth	40.2	257.4	APO	267	128.38	157.23	181.56	202.99	229.65	256.76
50	tensile	Wavy Legged	22.0	144.6	CF	370	97.49	119.40	137.87	154.14	174.39	194.98
51	tensile	Wavy Legged	25.0	161.8	CF	370	102.33	125.33	144.72	161.80	183.06	204.66
52	tensile	Wavy Legged	21.0	137.2	CF	370	94.68	115.96	133.89	149.70	169.36	189.35
53	tensile	Wavy Legged	21.0	128.6	CF	370	88.74	108.69	125.50	140.31	158.75	177.48
54	tensile	Internal Tooth	15.6	97.4	APO	257	77.98	95.51	110.28	123.30	139.50	155.96
55	tensile	Internal Tooth	15.6	105.6	APO	257	84.55	103.55	119.57	133.68	151.24	169.10
56	tensile	Wavy Legged	28.0	168.2	CF	370	100.52	123.11	142.15	158.93	179.81	201.04
57	tensile	Wavy Legged	32.0	179.6	CF	370	100.40	122.96	141.99	158.75	179.60	200.80
58	tensile	Wavy Legged	25.0	164.8	CF	370	104.23	127.65	147.40	164.80	186.45	208.46
59	tensile	Wavy Legged	19.0	153.0	CF	370	111.00	135.94	156.97	175.50	198.56	222.00
60	tensile	Internal Tooth	33.6	158.8	APO	257	86.63	106.10	122.52	136.98	154.97	173.27
61	tensile	Internal Tooth	33.6	149.2	APO	257	81.40	99.69	115.11	128.70	145.60	162.79
62	tensile	Internal Tooth	25.6	137.2	CF	267	85.75	105.02	121.27	135.58	153.39	171.50
63	tensile	Internal Tooth	25.6	188.4	CF	267	117.75	144.21	166.52	186.18	210.64	235.50
64	tensile	Internal Tooth	25.6	199.6	CF	267	124.75	152.79	176.42	197.25	223.16	249.50
65	tensile	Internal Tooth	25.6	142.2	CF	267	88.88	108.85	125.69	140.52	158.98	177.75
66	tensile	Internal Tooth	34.6	148.2	CF	267	79.67	97.58	112.67	125.97	142.52	159.35
67	tensile	Internal Tooth	34.6	144.0	CF	267	77.41	94.81	109.48	122.40	138.48	154.83
68	tensile	Internal Tooth	34.6	218.0	CF	267	117.20	143.54	165.74	185.31	209.65	234.40
69	tensile	Internal Tooth	34.6	186.6	CF	267	100.32	122.86	141.87	158.61	179.45	200.63
70	tensile	Internal Tooth	14.3	124.8	CF	267	104.36	127.82	147.59	165.01	186.69	208.73
71	tensile	Internal Tooth	14.3	121.4	CF	267	101.52	124.34	143.57	160.52	181.60	203.04
72	tensile	Internal Tooth	14.3	209.6	CF	267	175.28	214.67	247.88	277.14	313.54	350.55
73	tensile	Internal Tooth	14.3	218.2	CF	267	182.47	223.48	258.05	288.51	326.41	364.94
74	tensile	Internal Tooth	34.2	171.0	CF	267	92.47	113.25	130.77	146.20	165.41	184.93
75	tensile	Internal Tooth	34.2	173.4	SF ANCHOR	267	93.76	114.84	132.60	148.25	167.73	187.53
76	tensile	Internal Tooth	34.2	235.2	SF ANCHOR	267	127.18	155.77	179.86	201.09	227.51	254.36
77	tensile	Internal Tooth	34.2	238.0	SF ANCHOR	267	128.70	157.62	182.00	203.49	230.22	257.39
78	tensile	Wavy Legged	16.0	126.2	CF	370	99.77	122.19	141.10	157.75	178.47	199.54
79	tensile	Internal Tooth	17.8	97.8	APO	257	73.30	89.78	103.67	115.90	131.13	146.61
80	tensile	Internal Tooth	17.8	91.2	APO	257	68.36	83.72	96.67	108.08	122.28	136.71
81	tensile	Wavy Legged	24.0	169.6	SF ANCHOR	370	109.48	134.08	154.82	173.10	195.84	218.95
82	tensile	Internal Tooth	35.5	136.2	SF ANCHOR	257	72.29	88.53	102.23	114.30	129.31	144.57
83	tensile	Internal Tooth	35.5	130.8	APO	257	69.42	85.02	98.18	109.76	124.18	138.84
84	tensile	Internal Tooth	17.1	81.2	CF	257	62.10	76.05	87.82	98.18	111.08	124.19

## Appendix B - Test Data

Test ref #	Test Type	Anchor Type	Concrete Strength, MPa, $f_{c,age}$	Ultimate failure load, Pu, kN	Mode of Failure	Effective Embedment Depth, $h_{ef}$ , mm	Ultimate Test Loads normalised to $f_{c,age}$ , kN					
							10.00	15.00	20.00	25.00	32.00	40.00
85	tensile	Internal Tooth	17.1	99.4	CF	257	76.01	93.10	107.50	120.19	135.98	152.03
86	tensile	Internal Tooth	34.2	114.2	CF	257	61.75	75.63	87.33	97.64	110.47	123.50
87	tensile	Internal Tooth	34.2	125.0	CF	257	67.59	82.78	95.59	106.87	120.91	135.18
88	tensile	Internal Tooth	15.00	51.40	APO	125	41.97	51.40	59.35	66.36	75.07	83.94
89	tensile	Internal Tooth	15.00	64.80	APO	125	52.91	64.80	74.82	83.66	94.65	105.82
90	tensile	Internal Tooth	15.00	52.80	APO	125	43.11	52.80	60.97	68.16	77.12	86.22
91	tensile	Internal Tooth	15.00	59.00	APO	125	48.17	59.00	68.13	76.17	86.18	96.35
92	tensile	Internal Tooth	18.10	74.00	CF	125	55.00	67.37	77.79	86.97	98.39	110.01
93	tensile	Internal Tooth	18.10	78.60	SF ANCHOR	125	58.42	71.55	82.62	92.37	104.51	116.85
94	tensile	Internal Tooth	18.10	76.60	CF	125	56.94	69.73	80.52	90.02	101.85	113.87
95	tensile	Internal Tooth	18.10	81.40	SF ANCHOR	125	60.50	74.10	85.57	95.67	108.23	121.01
96	tensile	Internal Tooth	34.70	79.60	SF ANCHOR	125	42.73	52.34	60.43	67.56	76.44	85.46
97	tensile	Internal Tooth	34.70	76.80	SF ANCHOR	125	41.23	50.49	58.31	65.19	73.75	82.46
98	tensile	Internal Tooth	34.70	81.20	SF ANCHOR	125	43.59	53.39	61.65	68.92	77.98	87.18
99	tensile	Internal Tooth	34.70	80.40	SF ANCHOR	125	43.16	52.86	61.04	68.24	77.21	86.32
100	shear	Internal Tooth	30	45.6	SF ANCHOR	25	26.33	32.24	37.23	41.63	47.10	52.65
101	shear	Internal Tooth	30	44.6	CF	25	25.75	31.54	36.42	40.71	46.06	51.50
102	shear	Internal Tooth	37.3	51.6	SF ANCHOR	25	26.72	32.72	37.78	42.24	47.79	53.43
103	shear	Internal Tooth	37.3	50	SF ANCHOR	25	25.89	31.71	36.61	40.93	46.31	51.78
104	shear	Internal Tooth	30	48.6	SF ANCHOR	38	28.06	34.37	39.68	44.37	50.19	56.12
105	shear	Internal Tooth	30	39.8	SF ANCHOR	38	22.98	28.14	32.50	36.33	41.11	45.96
106	shear	Internal Tooth	37.3	48.2	SF ANCHOR	38	24.96	30.57	35.29	39.46	44.64	49.91
107	shear	Internal Tooth	37.3	37.2	SF ANCHOR	38	19.26	23.59	27.24	30.45	34.46	38.52
108	shear	Internal Tooth	34	57.2	CF	25	31.02	37.99	43.87	49.05	55.49	62.04
109	shear	Internal Tooth	34	61	CF	25	33.08	40.52	46.78	52.31	59.18	66.16
110	shear	Internal Tooth	35	60.8	SF ANCHOR	25	32.50	39.80	45.96	51.39	58.14	65.00
111	shear	Internal Tooth	35	63.6	CF	25	34.00	41.64	48.08	53.75	60.81	67.99
112	shear	Internal Tooth	34	62.2	SF ANCHOR	38	33.73	41.31	47.71	53.34	60.34	67.47
113	shear	Internal Tooth	34	64.4	SF ANCHOR	38	34.93	42.78	49.39	55.22	62.48	69.85
114	shear	Internal Tooth	35	62.8	SF ANCHOR	38	33.57	41.11	47.47	53.08	60.05	67.14
115	shear	Internal Tooth	35	59.8	SF ANCHOR	38	31.96	39.15	45.20	50.54	57.18	63.93
116	tensile	Internal Tooth	20.9	134.8	CF	267	93.24	114.20	131.87	147.43	166.80	186.49
117	tensile	Internal Tooth	20.9	244.4	SF ANCHOR	267	169.06	207.05	239.08	267.30	302.41	338.11
118	tensile	Internal Tooth	20.9	235.0	SF ANCHOR	267	162.55	199.09	229.88	257.02	290.78	325.11
119	tensile	Internal Tooth	20.9	222.0	SF LEG	267	153.56	188.07	217.17	242.80	274.70	307.12
120	shear	Internal Tooth	21	76.8	CF	36	53.00	64.91	74.95	83.80	94.80	105.99
121	shear	Internal Tooth	21	108.6	CF	36	74.94	91.78	105.98	118.49	134.06	149.88
122	shear	Internal Tooth	21	43.2	SF LEG	36	29.81	36.51	42.16	47.14	53.33	59.62
123	shear	Internal Tooth	21	89.8	SF LEG	36	61.97	75.89	87.64	97.98	110.85	123.94
124	shear	Internal Tooth	31	65.8	CF	36	37.37	45.77	52.85	59.09	66.85	74.74
125	shear	Internal Tooth	31	95.6	SF ANCHOR	36	54.30	66.50	76.79	85.85	97.13	108.59
126	shear	Internal Tooth	31	47.2	SF LEG	36	26.81	32.83	37.91	42.39	47.96	53.62
127	shear	Internal Tooth	31	59.8	SF LEG	36	33.96	41.60	48.03	53.70	60.76	67.93
128	shear	Internal Tooth	18.3	50.2	CF	36	37.11	45.45	52.48	58.67	66.38	74.22
129	shear	Internal Tooth	18.3	76.8	CF	36	56.77	69.53	80.29	89.76	101.56	113.54
130	shear	Internal Tooth	18.3	71.2	SF LEG	36	52.63	64.46	74.43	83.22	94.15	105.27
131	shear	Internal Tooth	18.3	76	CF	36	56.18	68.81	79.45	88.83	100.50	112.36
132	shear	Internal Tooth	29.7	79.8	CF	36	46.30	56.71	65.48	73.21	82.83	92.61
133	shear	Internal Tooth	29.7	112	SF ANCHOR	36	64.99	79.59	91.91	102.76	116.26	129.98
134	shear	Internal Tooth	29.7	95.6	SF ANCHOR	36	55.47	67.94	78.45	87.71	99.23	110.95
135	shear	Internal Tooth	29.7	74	SF LEG	36	42.94	52.59	60.73	67.89	76.81	85.88
136	shear	Internal Tooth	15.01	51.8	CF	36	42.28	51.78	59.79	66.85	75.63	84.56
137	shear	Internal Tooth	15.01	63.6	CF	36	51.91	63.58	73.41	82.08	92.86	103.82
138	shear	Internal Tooth	15.01	55.2	CF	36	45.06	55.18	63.72	71.24	80.60	90.11
139	shear	Internal Tooth	15.01	50.6	CF	36	41.30	50.58	58.41	65.30	73.88	82.60
140	shear	Internal Tooth	26	81.4	CF	36	50.48	61.83	71.39	79.82	90.31	100.96
141	shear	Internal Tooth	26	83.2	CF	36	51.60	63.19	72.97	81.58	92.30	103.20
142	shear	Internal Tooth	26	68.6	CF	36	42.54	52.11	60.17	67.27	76.10	85.09
143	shear	Internal Tooth	26	57.8	CF	36	35.85	43.90	50.69	56.68	64.12	71.69
144	shear	Internal Tooth	16.4	57.2	CF	38	44.67	54.70	63.17	70.62	79.90	89.33
145	shear	Internal Tooth	16.4	49.4	CF	38	38.57	47.24	54.55	60.99	69.00	77.15
146	shear	Internal Tooth	16.4	48.2	SF ANCHOR	38	37.64	46.10	53.23	59.51	67.33	75.28
147	shear	Internal Tooth	16.4	48.2	SF ANCHOR	38	37.64	46.10	53.23	59.51	67.33	75.28
148	Shear	Internal Tooth	16.40	59.2	CF	43	46.23	56.62	65.38	73.09	82.69	92.45
149	Shear	Internal Tooth	16.40	63	CF	43	49.19	60.25	69.57	77.78	88.00	98.39
150	Shear	Internal Tooth	16.40	45	SF ANCHOR	38	35.14	43.04	49.69	55.56	62.86	70.28
151	Shear	Internal Tooth	16.40	49	SF ANCHOR	38	38.26	46.86	54.11	60.50	68.45	76.53
152	tensile	Internal Tooth	27.2	144.6	CF	242	87.68	107.38	123.99	138.63	156.84	175.35
153	tensile	Internal Tooth	27.2	147.4	CF	242	89.37	109.46	126.39	141.31	159.88	178.75
154	tensile	Internal Tooth	27.2	133.6	SF ANCHOR	257	81.01	99.21	114.56	128.08	144.91	162.01
155	tensile	Internal Tooth	27.2	144.8	SF ANCHOR	257	87.80	107.53	124.16	138.82	157.06	175.60
156	Shear	Headed Anchor	26.00	46.60	CF	43	28.90	35.40	40.87	45.70	51.70	57.80
157	shear	Headed Anchor	26.00	49.20	CF	43	30.51	37.37	43.15	48.24	54.58	61.03
158	tensile	Internal Tooth	22.3	95.6	CF	242	64.02	78.41	90.54	101.22	114.52	128.04
159	tensile	Internal Tooth	22.3	86.8	CF	242	58.13	71.19	82.20	91.90	103.98	116.25
160	tensile	Internal Tooth	22.3	101.0	SF ANCHOR	257	67.63	82.84	95.65	106.94	120.99	135.27
161	tensile	Internal Tooth	22.3	103.8	SF ANCHOR	257	69.51	85.13	98.30	109.90	124.34	139.02
162	tensile	Internal Tooth	28.6	114.4	CF	242	67.65	82.85	95.67	106.96	121.01	135.29
163	tensile	Internal Tooth	28.6	110.4	CF	242	65.28	79.95	92.32	103.22	116.78	130.56
164	tensile	Internal Tooth	28.6	107.2	CF	242	63.39	77.63	89.65	100.23	113.39	126.78
165	tensile	Internal Tooth	28.6	117.4	CF	242	69.42	85.02	98.17	109.76	124.18	138.84
166	tensile	Internal Tooth	28.6	126.8	SF ANCHOR	257	74.98	91.83	106.04	118.55	134.13	149.96
167	tensile	Internal Tooth	28.6	132.8	SF ANCHOR	257	78.53	96.17	111.05	124.16	140.47	157.05
168	tensile	Internal Tooth	28.6	136.4	SF ANCHOR	257	80.66	98.78	114.06	127.53	144.28	161.31

## Appendix B - Test Data

Test ref #	Test Type	Anchor Type	Concrete Strength, MPa, $f_{c,age}$	Ultimate failure load, Pu, kN	Mode of Failure	Effective Embedment Depth, $h_{ef}$ , mm	Ultimate Test Loads normalised to $f'_{c,age}$ , kN					
							10.00	15.00	20.00	25.00	32.00	40.00
169	tensile	Internal Tooth	28.6	131.4	SF ANCHOR	257	77.70	95.16	109.88	122.85	138.99	155.40
170	tensile	Internal Tooth	22.0	105.5	APO	242	71.13	87.11	100.59	112.46	127.24	142.26
171	tensile	Internal Tooth	22.0	99.8	APO	242	67.29	82.41	95.16	106.39	120.36	134.57
172	tensile	Internal Tooth	22.0	104.4	APO	242	70.39	86.21	99.54	111.29	125.91	140.77
173	tensile	Internal Tooth	22.0	108.4	APO	242	73.08	89.51	103.36	115.55	130.74	146.17
174	tensile	Internal Tooth	23.0	212.0	APO	267	139.79	171.21	197.69	221.03	250.06	279.58
175	tensile	Internal Tooth	22.0	216.6	SF TBAR	267	146.03	178.85	206.52	230.90	261.23	292.06
176	tensile	Internal Tooth	23.0	230.0	APO	267	151.66	185.74	214.48	239.79	271.29	303.32
177	tensile	Internal Tooth	23.5	209.0	SF TBAR	267	136.34	166.98	192.81	215.57	243.89	272.67
178	tensile	Internal Tooth	24.0	218.0	SF TBAR	267	140.72	172.34	199.01	222.50	251.72	281.44
179	tensile	Internal Tooth	23.0	208.0	SF TBAR	267	137.15	167.98	193.96	216.85	245.34	274.30
180	tensile	Internal Tooth	23.0	191.0	SF TBAR	267	125.94	154.25	178.11	199.13	225.29	251.88
181	tensile	Internal Tooth	23.5	218.0	SF TBAR	267	142.21	174.17	201.11	224.85	254.39	284.42
182	shear	Internal Tooth	20.4	61	APO	128	42.71	52.31	60.40	67.53	76.40	85.42
183	shear	Internal Tooth	20.4	50.1	APO	128	35.08	42.96	49.61	55.46	62.75	70.15
184	shear	Internal Tooth	20.4	42.6	APO	126	29.83	36.53	42.18	47.16	53.35	59.65
185	shear	Internal Tooth	20.4	53.2	APO	126	37.25	45.62	52.68	58.89	66.63	74.49
186	tensile	Internal Tooth	21.5	240.8	APO	267	164.22	201.13	232.25	259.66	293.77	328.45
187	tensile	Internal Tooth	21.5	239.8	APO	267	163.54	200.30	231.28	258.58	292.55	327.08
188	tensile	Internal Tooth	21.5	228.2	SF TBAR	267	155.63	190.61	220.10	246.07	278.40	311.26
189	tensile	Internal Tooth	21.5	246.8	APO	267	168.32	206.14	238.04	266.13	301.09	336.63
190	tensile	Internal Tooth	45.5	250.0	SF TBAR	267	117.20	143.54	165.75	185.31	209.66	234.40
191	tensile	Internal Tooth	45.5	257.0	SF TBAR	267	120.48	147.56	170.39	190.50	215.53	240.97
192	tensile	Internal Tooth	45.5	234.0	SF TBAR	267	109.70	134.36	155.14	173.45	196.24	219.40
193	tensile	Internal Tooth	45.5	244.0	SF TBAR	267	114.39	140.10	161.77	180.86	204.63	228.78
194	tensile	Internal Tooth	27.6	238.8	APO	267	143.74	176.05	203.28	227.27	257.13	287.48
195	tensile	Internal Tooth	27.6	231.0	APO	267	139.05	170.30	196.64	219.85	248.73	278.09
196	tensile	Internal Tooth	27.6	223.8	APO	267	134.71	164.99	190.51	213.00	240.98	269.42
197	tensile	Internal Tooth	27.6	224.6	SF ANCHOR	267	135.19	165.58	191.19	213.76	241.84	270.39
198	tensile	Internal Tooth	40.2	257.0	APO	267	128.18	156.99	181.27	202.67	229.30	256.36
199	tensile	Internal Tooth	40.2	240.2	APO	267	119.80	146.73	169.42	189.42	214.31	239.60
200	tensile	Internal Tooth	40.2	255.0	SF ANCHOR	267	127.18	155.77	179.86	201.09	227.51	254.36
201	tensile	Internal Tooth	40.2	232.4	APO	267	115.91	141.96	163.92	183.27	207.35	231.82
202	tensile	Wavy Legged	20.5	223.6	SF TBAR	272	156.17	191.27	220.86	246.92	279.36	312.34
203	tensile	Wavy Legged	20.5	215.6	SF TBAR	272	150.58	184.42	212.95	238.09	269.37	301.16
204	tensile	Wavy Legged	20.5	220.6	SF TBAR	272	154.07	188.70	217.89	243.61	275.62	308.15
205	tensile	Wavy Legged	20.5	235.6	SF TBAR	272	164.55	201.53	232.71	260.18	294.36	329.10
206	tensile	Wavy Legged	20.5	232.6	SF TBAR	272	162.45	198.97	229.75	256.86	290.61	324.91
207	tensile	Wavy Legged	20.5	234.8	SF ANCHOR	272	163.99	200.85	231.92	259.29	293.36	327.98
208	tensile	Internal Tooth	21.8	243.2	SF TBAR	267	164.72	201.73	232.94	260.44	294.65	329.43
209	tensile	Internal Tooth	21.8	221.4	SF TBAR	267	149.95	183.65	212.06	237.09	268.24	299.90
210	tensile	Internal Tooth	21.8	215.2	SF TBAR	267	145.75	178.51	206.12	230.45	260.73	291.50
211	tensile	Internal Tooth	21.8	229.8	SF TBAR	267	155.64	190.62	220.11	246.09	278.42	311.28
212	shear	Internal Tooth	21.8	83.9	APO	126	56.82	69.60	80.36	89.85	101.65	113.65
213	shear	Internal Tooth	21.8	75.9	APO	126	51.41	62.96	72.70	81.28	91.96	102.81
214	shear	Internal Tooth	21.8	80.9	APO	126	54.79	67.11	77.49	86.63	98.02	109.58
215	tensile	Internal Tooth	21.8	250.8	APO	267	169.86	208.04	240.22	268.58	303.86	339.73
216	tensile	Internal Tooth	21.8	243.6	APO	267	164.99	202.07	233.33	260.87	295.14	329.97
217	tensile	Internal Tooth	21.8	227.4	APO	267	154.01	188.63	217.81	243.52	275.51	308.03
218	tensile	Internal Tooth	21.8	244.2	APO	267	165.39	202.56	233.90	261.51	295.86	330.79
219	tensile	Internal Tooth	20.0	113.4	APO	257	80.19	98.21	113.40	126.79	143.44	160.37
220	tensile	Internal Tooth	20.0	110.0	APO	257	77.78	95.26	110.00	122.98	139.14	155.56
221	tensile	Internal Tooth	20.0	152.4	APO	257	107.76	131.98	152.40	170.39	192.77	215.53
222	tensile	Internal Tooth	20.0	154.6	APO	257	109.32	133.89	154.60	172.85	195.56	218.64
223	tensile	Internal Tooth	19.8	50.2	APO	125	35.71	43.73	50.50	56.46	63.87	71.41
224	tensile	Internal Tooth	19.8	54.2	APO	125	38.55	47.21	54.52	60.95	68.96	77.10
225	tensile	Internal Tooth	19.8	54.0	APO	125	38.41	47.04	54.32	60.73	68.71	76.82
226	tensile	Wavy Legged	21.0	86.4	SF ANCHOR	125	59.62	73.02	84.32	94.27	106.65	119.24
227	tensile	Wavy Legged	26.0	93.0	SF ANCHOR	125	57.68	70.64	81.57	91.19	103.17	115.35
228	tensile	Internal Tooth	26.0	76.8	APO	125	47.63	58.33	67.36	75.31	85.20	95.26
229	tensile	Internal Tooth	26.0	74.1	APO	125	45.95	56.28	64.99	72.66	82.21	91.91
230	tensile	Internal Tooth	36.0	84.0	APO	125	44.27	54.22	62.61	70.00	79.20	88.54
231	tensile	Internal Tooth	36.0	85.6	APO	125	45.12	55.25	63.80	71.33	80.70	90.23
232	shear	Internal Tooth	23	35.5	SF ANCHOR	95	23.41	28.67	33.10	37.01	41.87	46.82
233	shear	Internal Tooth	32.01	45.4	SF ANCHOR	107	25.38	31.08	35.89	40.12	45.39	50.75
234	shear	Internal Tooth	32.01	49.6	CF	91	27.72	33.95	39.21	43.83	49.59	55.45
235	shear	Internal Tooth	25.01	56.9	CF	126	35.98	44.07	50.88	56.89	64.36	71.96
236	shear	Internal Tooth	15.00	82.9	CF	128	67.69	82.90	95.72	107.02	121.08	135.38
237	shear	Internal Tooth	10.01	50.6	SF ANCHOR	107	50.57	61.94	71.52	79.97	90.47	101.15
238	shear	Internal Tooth	10.01	41.4	SF ANCHOR	107	41.38	50.68	58.52	65.43	74.02	82.76
239	shear	Wavy Legged	15.01	35.6	SF ANCHOR	107	29.06	35.59	41.09	45.94	51.98	58.12
240	shear	Internal Tooth	15.01	40.4	SF ANCHOR	107	32.98	40.39	46.63	52.14	58.99	65.95
241	tensile	Internal Tooth	10.0	69.0	APO	125	68.97	84.47	97.53	109.04	123.37	137.93
242	tensile	Internal Tooth	10.0	69.2	APO	125	69.17	84.71	97.81	109.36	123.73	138.33
243	tensile	Wavy Legged	15.0	98.8	SF ANCHOR	125	80.64	98.77	114.05	127.51	144.26	161.29
244	tensile	Internal Tooth	15.0	68.8	APO	125	56.16	68.78	79.42	88.79	100.46	112.31
245	tensile	Internal Tooth	11.0	259.0	267	267	246.95	302.45	349.24	390.46	441.75	493.89
246	tensile	Internal Tooth	11.0	266.8	267	267	254.38	311.56	359.75	402.22	455.06	508.77
247	tensile	Internal Tooth	11.0	264.2	267	267	251.90	308.52	356.25	398.30	450.62	503.81
248	tensile	Internal Tooth	11.0	213.8	267	267	203.85	249.66	288.29	322.32	364.66	407.70
249	tensile	Internal Tooth	14.0	248.0	267	267	209.60	256.70	296.42	331.40	374.94	419.20
250	tensile	Internal Tooth	14.0	250.6	267	267	211.80	259.40	299.52	334.88	378.87	423.59
251	tensile	Internal Tooth	18.0	265.0	267	267	197.52	241.91	279.33	312.31	353.33	395.04
252	tensile	Internal Tooth	14.0	238.0	267	267	201.15	246.35	284.46	318.04	359.82	402.29

## Appendix B - Test Data

Test ref #	Test Type	Anchor Type	Concrete Strength, MPa, $f_{c,age}$	Ultimate failure load, Pu, kN	Mode of Failure	Effective Embedment Depth, $h_{ef}$ , mm	Ultimate Test Loads normalised to $f'_{c,age}$ , kN					
							10.00	15.00	20.00	25.00	32.00	40.00
253	tensile	Internal Tooth	20.0	103.6	CF	257	73.26	89.72	103.60	115.83	131.04	146.51
254	tensile	Internal Tooth	15.0	129.2	CF	268	105.46	129.16	149.14	166.74	188.65	210.91
255	shear	Internal Tooth	15.00	53.60	APO	128	43.76	53.60	61.89	69.20	78.29	87.53
256	shear	Internal Tooth	15.00	70.60	APO	128	57.64	70.60	81.52	91.14	103.12	115.29
257	shear	Internal Tooth	15.00	62.40	APO	128	50.95	62.40	72.05	80.56	91.14	101.90
258	shear	Internal Tooth	15.00	54.80	APO	128	44.74	54.80	63.28	70.75	80.04	89.49
259	shear	Internal Tooth	15.00	64.90	APO	128	52.99	64.90	74.94	83.79	94.79	105.98
260	shear	Internal Tooth	15.00	56.30	APO	128	45.97	56.30	65.01	72.68	82.23	91.94
261	shear	Internal Tooth	15.00	57.00	APO	128	46.54	57.00	65.82	73.59	83.25	93.08
262	tensile	Internal Tooth	15	213.20	CF	267	174.08	213.20	246.18	275.24	311.40	348.15
263	tensile	Internal Tooth	16	77.80	CF	267	61.51	75.33	86.98	97.25	110.03	123.01
264	tensile	Internal Tooth	17	90.90	CF	267	69.72	85.39	98.59	110.23	124.71	139.43
265	tensile	Internal Tooth	18	61.20	CF	267	45.62	55.87	64.51	72.12	81.60	91.23
266	tensile	Internal Tooth	19	199.90	CF	267	145.02	177.62	205.09	229.30	259.42	290.05
267	tensile	Internal Tooth	20	66.20	CF	267	46.81	57.33	66.20	74.01	83.74	93.62
268	tensile	Internal Tooth	21	100.00	CF	267	69.01	84.52	97.59	109.11	123.44	138.01
269	tensile	Internal Tooth	22	57.20	CF	267	38.56	47.23	54.54	60.98	68.99	77.13
270	tensile	Internal Tooth	23	201.10	CF	267	132.60	162.40	187.53	209.66	237.20	265.20
271	tensile	Internal Tooth	24	77.90	CF	267	50.28	61.59	71.11	79.51	89.95	100.57
272	tensile	Internal Tooth	25	93.60	CF	267	59.20	72.50	83.72	93.60	105.90	118.40
273	tensile	Internal Tooth	26	75.70	CF	267	46.95	57.50	66.39	74.23	83.98	93.89
274	tensile	Internal Tooth	27	186.43	CF	267	113.46	138.96	160.45	179.39	202.96	226.92
275	tensile	Internal Tooth	28	74.00	CF	267	44.22	54.16	62.54	69.92	79.11	88.45
276	tensile	Internal Tooth	32	95.00	CF	267	53.11	65.04	75.10	83.97	95.00	106.21
277	tensile	Internal Tooth	33	63.40	CF	267	34.90	42.74	49.36	55.18	62.43	69.80
278	tensile	Internal Tooth	32	261.40	CF	267	146.13	178.97	206.65	231.05	261.40	292.25
279	tensile	Internal Tooth	32	248.60	CF	267	138.97	170.20	196.54	219.73	248.60	277.94
280	tensile	Internal Tooth	32	253.40	CF	267	141.65	173.49	200.33	223.98	253.40	283.31
281	tensile	Internal Tooth	32	242.60	CF	267	135.62	166.10	191.79	214.43	242.60	271.24
282	tensile	Internal Tooth	14.7	200.80	CF	267	165.62	202.84	234.22	261.86	296.26	331.23
283	tensile	Internal Tooth	15	230.60	CF	267	188.28	230.60	266.27	297.70	336.81	376.57
284	tensile	Internal Tooth	15.5	161.20	CF	267	129.48	158.58	183.11	204.72	231.62	258.96
285	tensile	Internal Tooth	15.5	59.40	CF	267	47.71	58.43	67.47	75.44	85.35	95.42
286	tensile	Internal Tooth	16	76.00	CF	267	60.08	73.59	84.97	95.00	107.48	120.17
287	tensile	Internal Tooth	17	130.60	CF	267	100.17	122.68	141.66	158.38	179.18	200.33
288	tensile	Internal Tooth	24	226.80	CF	267	146.40	179.30	207.04	231.48	261.89	292.80
289	tensile	Internal Tooth	24	207.20	CF	267	133.75	163.81	189.15	211.47	239.25	267.49
290	tensile	Internal Tooth	24	157.80	CF	267	101.86	124.75	144.05	161.05	182.21	203.72
291	tensile	Internal Tooth	24	85.40	CF	267	55.13	67.51	77.96	87.16	98.61	110.25
292	tensile	Internal Tooth	26	104.00	CF	267	64.50	78.99	91.21	101.98	115.38	129.00
293	tensile	Internal Tooth	26	245.20	CF	267	152.07	186.24	215.05	240.44	272.02	304.13
294	tensile	Internal Tooth	26	170.40	CF	267	105.68	129.43	149.45	167.09	189.04	211.36
295	tensile	Internal Tooth	32.0	238.6	SF TBAR	267	133.36	163.33	188.60	210.86	238.56	266.72
296	tensile	Internal Tooth	32.0	265.2	SF TBAR	267	148.23	181.54	209.63	234.37	265.16	296.46
297	tensile	Internal Tooth	32.0	250.0	SF TBAR	267	139.73	171.14	197.61	220.94	249.96	279.46
298	tensile	Internal Tooth	32.0	238.6	SF TBAR	267	133.36	163.33	188.60	210.86	238.56	266.72
299	tensile	Internal Tooth	32.0	244.2	SF TBAR	267	136.49	167.17	193.03	215.81	244.16	272.98
300	tensile	Internal Tooth	32.0	253.2	SF TBAR	267	141.52	173.33	200.14	223.76	253.16	283.04
301	tensile	Internal Tooth	18.5	101.00	CF	242	74.26	90.95	105.01	117.41	132.83	148.51
302	tensile	Internal Tooth	18.5	106.00	CF	242	77.93	95.45	110.21	123.22	139.41	155.87
303	tensile	Internal Tooth	18.5	100.00	CF	242	73.52	90.05	103.98	116.25	131.52	147.04
304	tensile	Internal Tooth	18.5	109.00	CF	242	80.14	98.15	113.33	126.71	143.36	160.28
305	tensile	Internal Tooth	18.5	131.00	CF	267	96.31	117.96	136.21	152.28	172.29	192.63
306	tensile	Internal Tooth	18.5	129.00	CF	267	94.84	116.16	134.13	149.96	169.66	189.69
307	tensile	Internal Tooth	18.5	128.00	CF	267	94.11	115.26	133.09	148.80	168.34	188.21
308	tensile	Internal Tooth	18.5	119.00	CF	267	87.49	107.15	123.73	138.33	156.51	174.98
309	tensile	Internal Tooth	24	141.00	CF	267	91.02	111.47	128.71	143.91	162.81	182.03
310	tensile	Internal Tooth	24	139.00	CF	267	89.72	109.89	126.89	141.87	160.50	179.45
311	tensile	Internal Tooth	24	144.00	CF	267	92.95	113.84	131.45	146.97	166.28	185.90
312	tensile	Internal Tooth	24	144.00	CF	267	92.95	113.84	131.45	146.97	166.28	185.90
313	tensile	Internal Tooth	24	132.00	CF	242	85.21	104.36	120.50	134.72	152.42	170.41
314	tensile	Internal Tooth	24	126.00	CF	242	81.33	99.61	115.02	128.60	145.49	162.67
315	tensile	Internal Tooth	24	120.00	CF	242	77.46	94.87	109.54	122.47	138.56	154.92
316	tensile	Internal Tooth	24	123.00	CF	242	79.40	97.24	112.28	125.54	142.03	158.79
317	tensile	Internal Tooth	19.5	132.9	CF	257	95.16	116.55	134.58	150.47	170.24	190.33
318	tensile	Internal Tooth	19.5	132.0	CF	257	94.53	115.77	133.68	149.46	169.10	189.05
319	tensile	Internal Tooth	19.5	137.0	CF	257	98.11	120.16	138.75	155.12	175.50	196.22
320	tensile	Internal Tooth	19.5	122.0	CF	257	87.37	107.00	123.55	138.14	156.29	174.73
321	tensile	Internal Tooth	20.6	125.4	CF	257	87.37	107.01	123.56	138.14	156.29	174.74
322	tensile	Internal Tooth	20.8	137.5	CF	257	95.33	116.76	134.82	150.73	170.54	190.66
323	tensile	Internal Tooth	20.8	127.4	CF	257	88.34	108.19	124.93	139.67	158.02	176.67
324	tensile	Internal Tooth	18.0	100.4	CF	242	74.85	91.67	105.85	118.35	133.89	149.70
325	tensile	Internal Tooth	18.0	105.6	CF	242	78.71	96.40	111.31	124.45	140.80	157.42
326	tensile	Internal Tooth	19.0	98.8	CF	242	71.67	87.78	101.36	113.32	128.21	143.34
327	tensile	Internal Tooth	19.0	108.6	CF	242	78.77	96.48	111.40	124.55	140.91	157.54
328	tensile	Internal Tooth	18.0	130.8	CF	267	97.51	119.42	137.90	154.17	174.43	195.01
329	tensile	Internal Tooth	18.0	128.8	CF	267	95.99	117.57	135.76	151.78	171.72	191.99
330	tensile	Internal Tooth	19.0	127.9	CF	267	92.78	113.63	131.21	146.70	165.97	185.56
331	tensile	Internal Tooth	19.0	118.1	CF	267	85.69	104.95	121.19	135.49	153.29	171.39
332	tensile	Internal Tooth	16.0	94.8	CF	257	74.95	91.79	105.99	118.50	134.07	149.89
333	tensile	Internal Tooth	16.0	102.3	CF	257	80.88	99.05	114.37	127.88	144.67	161.75
334	tensile	Internal Tooth	16.0	100.1	CF	257	79.14	96.92	111.92	125.13	141.56	158.27
335	tensile	Internal Tooth	16.0	90.6	CF	257	71.63	87.72	101.29	113.25	128.13	143.25
336	tensile	Internal Tooth	16.0	104.10	CF	242	82.30	100.79	116.39	130.13	147.22	164.60



## Appendix B - Test Data

Test ref #	Test Type	Anchor Type	Concrete Strength, MPa, f <sub>c,age</sub>	Ultimate failure load, Pu, kN	Mode of Failure	Effective Embedment Depth, h <sub>ef</sub> , mm	Ultimate Test Loads normalised to f <sub>c,age</sub> , kN					
							10.00	15.00	20.00	25.00	32.00	40.00
337	tensile	Internal Tooth	16.0	96.10		242	75.97	93.05	107.44	120.13	135.91	151.95
338	tensile	Internal Tooth	16.0	99.50		242	78.66	96.34	111.24	124.38	140.71	157.32
339	tensile	Internal Tooth	16.0	92.10		242	72.81	89.18	102.97	115.13	130.25	145.62
340	tensile	Internal Tooth	16.0	106.70		267	84.35	103.31	119.29	133.38	150.90	168.71
341	tensile	Internal Tooth	16.0	101.20		267	80.01	97.99	113.15	126.50	143.12	160.01
342	tensile	Internal Tooth	16.0	121.40		267	95.98	117.55	135.73	151.75	171.69	191.95
343	tensile	Internal Tooth	16.0	105.80		267	83.64	102.44	118.29	132.25	149.62	167.28
344	tensile	Internal Tooth	33.0	130.4		257	71.78	87.92	101.52	113.50	128.41	143.57
345	tensile	Internal Tooth	33.0	145.7		257	80.21	98.23	113.43	126.82	143.48	160.41
346	tensile	Internal Tooth	33.0	135.7		257	74.70	91.49	105.64	118.11	133.63	149.40
347	tensile	Internal Tooth	33.0	135.0		257	74.32	91.02	105.10	117.50	132.94	148.40
348	tensile	Internal Tooth	33.0	163.00		267	89.73	109.89	126.90	141.87	160.51	179.46
349	tensile	Internal Tooth	33.0	148.00		267	81.47	99.78	115.22	128.82	145.74	162.94
350	tensile	Internal Tooth	33.0	170.10		267	93.64	114.68	132.42	148.05	167.50	187.27
351	tensile	Internal Tooth	33.0	172.30		267	94.85	116.16	134.14	149.97	169.67	189.70
352	tensile	Internal Tooth	20	131.00		268	92.63	113.45	131.00	146.46	165.70	185.26
353	tensile	Internal Tooth	20	131.00		268	92.63	113.45	131.00	146.46	165.70	185.26
354	tensile	Internal Tooth	20	145.00		268	102.53	125.57	145.00	162.11	183.41	205.06
355	tensile	Internal Tooth	20	108.00		268	76.37	93.53	108.00	120.75	136.61	152.74
356	tensile	Internal Tooth	20	113.00		268	79.90	97.86	113.00	126.34	142.93	159.81
357	tensile	Internal Tooth	20	155.00		268	109.60	134.23	155.00	173.30	196.06	219.20
358	tensile	Internal Tooth	20.0	123.0	CF	268	86.95	106.49	122.97	137.48	155.55	173.90
359	tensile	Internal Tooth	12.5	110.00		242	98.39	120.50	139.14	155.56	176.00	196.77
360	tensile	Internal Tooth	12.5	106.00		242	94.81	116.12	134.08	149.91	169.60	189.62
361	tensile	Internal Tooth	32.5	146.00		242	80.99	99.19	114.53	128.05	144.87	161.97
362	tensile	Internal Tooth	32.5	150.00		242	83.21	101.90	117.67	131.56	148.84	166.41
363	tensile	Internal Tooth	37.5	151.00		242	77.98	95.50	110.27	123.29	139.49	155.95
364	tensile	Internal Tooth	37.5	156.00		242	80.56	98.66	113.93	127.37	144.11	161.12
365	tensile	Internal Tooth	22.5	139.00		242	92.67	113.49	131.05	146.52	165.77	185.33
366	tensile	Internal Tooth	22.5	124.00		242	82.67	101.25	116.91	130.71	147.88	165.33
367	tensile	Internal Tooth	22.5	120.00		242	80.00	97.98	113.14	126.49	143.11	160.00
368	tensile	Internal Tooth	22.5	125.30		242	83.53	102.31	118.13	132.08	149.43	167.07
369	tensile	Internal Tooth	22.5	107.00		242	71.33	87.37	100.88	112.79	127.60	142.67
370	tensile	Internal Tooth	22.5	98.00		242	65.33	80.02	92.40	103.30	116.87	130.67
371	tensile	Internal Tooth	33.0	131.00		257	72.11	88.32	101.98	114.02	129.00	144.23
372	tensile	Internal Tooth	33.0	146.00		257	80.37	98.43	113.66	127.08	143.77	160.74
373	tensile	Internal Tooth	33.0	136.00		257	74.87	91.69	105.88	118.37	133.92	149.73
374	tensile	Internal Tooth	33.0	136.00		257	74.87	91.69	105.88	118.37	133.92	149.73
375	tensile	Internal Tooth	33.0	163.00		267	89.73	109.89	126.90	141.87	160.51	179.46
376	tensile	Internal Tooth	33.0	150.00		267	82.57	101.13	116.77	130.56	147.71	165.14
377	tensile	Internal Tooth	33.0	170.00		267	93.58	114.61	132.34	147.97	167.40	187.16
378	tensile	Internal Tooth	33.0	173.00		267	95.23	116.64	134.68	150.58	170.36	190.47
379	shear	Internal Tooth	20.0	72.00		126	50.91	62.35	72.00	80.50	91.07	101.82
380	shear	Internal Tooth	20.0	59.90		126	42.36	51.87	59.90	66.97	75.77	84.71
381	shear	Internal Tooth	20.0	60.00		126	42.43	51.96	60.00	67.08	75.89	84.85
382	shear	Internal Tooth	20.0	44.00		126	31.11	38.11	44.00	49.19	55.66	62.23
383	tensile	Internal Tooth	11	135.00	CF	267	128.72	157.65	182.03	203.52	230.26	257.43
384	tensile	Internal Tooth	12	137.00	CF	267	125.06	153.17	176.87	197.74	223.72	250.13
385	tensile	Internal Tooth	13	143.00	CF	267	125.42	153.61	177.37	198.31	224.36	250.84
386	tensile	Internal Tooth	15	140.00	CF	267	114.31	140.00	161.66	180.74	204.48	228.62
387	tensile	Internal Tooth	22	112.00	CF	257	75.51	92.48	106.79	119.39	135.08	151.02
388	tensile	Internal Tooth	22	104.00	CF	257	70.12	85.88	99.16	110.86	125.43	140.23
389	tensile	Internal Tooth	22	108.00	CF	257	72.81	89.18	102.97	115.13	130.25	145.63
390	tensile	Internal Tooth	21	109.00	CF	257	75.22	92.12	106.37	118.93	134.55	150.43
391	tensile	Internal Tooth	21	104.00	CF	257	71.77	87.90	101.49	113.47	128.38	143.53
392	tensile	Internal Tooth	22	108.00	CF	257	72.81	89.18	102.97	115.13	130.25	145.63
393	tensile	Internal Tooth	19	98.00	CF	257	71.10	87.08	100.55	112.41	127.18	142.19
394	tensile	Internal Tooth	22	119.00	CF	257	80.23	98.26	113.46	126.85	143.52	160.46
395	tensile	Internal Tooth	20	102.00	CF	257	72.12	88.33	102.00	114.04	129.02	144.25
396	tensile	Internal Tooth	23	115.00	CF	257	75.83	92.87	107.24	119.90	135.65	151.66
397	tensile	Internal Tooth	23	103.00	CF	257	67.92	83.18	96.05	107.38	121.49	135.83
398	tensile	Internal Tooth	22	90.00	CF	257	60.68	74.32	85.81	95.94	108.54	121.36
399	tensile	Internal Tooth	22	122.00	CF	257	82.25	100.74	116.32	130.05	147.14	164.50
400	tensile	Internal Tooth	23	99.00	CF	257	65.28	79.95	92.32	103.21	116.77	130.56
401	tensile	Internal Tooth	15	104.00	CF	242	84.92	104.00	120.09	134.26	151.90	169.83
402	tensile	Internal Tooth	15	96.00	CF	242	78.38	96.00	110.85	123.94	140.22	156.77
403	tensile	Internal Tooth	15	100.00	CF	242	81.65	100.00	115.47	129.10	146.06	163.30
404	tensile	Internal Tooth	14	92.00	CF	242	77.75	95.23	109.96	122.94	139.09	155.51
405	tensile	Internal Tooth	14	107.00	CF	267	90.43	110.76	127.89	142.98	161.77	180.86
406	tensile	Internal Tooth	15	101.00	CF	267	82.47	101.00	116.62	130.39	147.52	164.93
407	tensile	Internal Tooth	17	121.00	CF	267	92.80	113.66	131.24	146.73	166.01	185.61
408	tensile	Internal Tooth	16	106.00	CF	267	83.80	102.63	118.51	132.50	149.91	167.60
409	tensile	Internal Tooth	19	95.00	CF	257	68.92	84.41	97.47	108.97	123.29	137.84
410	tensile	Internal Tooth	17	91.00	CF	257	69.79	85.48	98.70	110.35	124.85	139.59
411	tensile	Internal Tooth	17	102.00	CF	257	78.23	95.81	110.63	123.69	139.94	156.46
412	tensile	Internal Tooth	17	100.00	CF	257	76.70	93.93	108.47	121.27	137.20	153.39
413	tensile	Internal Tooth	32	131.00	CF	257	73.23	89.69	103.56	115.79	131.00	146.46
414	tensile	Internal Tooth	34	146.00	CF	257	79.18	96.97	111.98	125.19	141.64	158.36
415	tensile	Internal Tooth	35	136.00	CF	257	72.70	89.03	102.81	114.94	130.04	145.39
416	tensile	Internal Tooth	34	136.00	CF	257	73.76	90.33	104.31	116.62	131.94	147.51
417	tensile	Internal Tooth	35	163.00	CF	267	87.13	106.71	123.22	137.76	155.86	174.25
418	tensile	Internal Tooth	34	150.00	CF	267	81.35	99.63	115.04	128.62	145.52	162.70
419	tensile	Internal Tooth	33	170.00	CF	267	93.58	114.61	132.34	147.97	167.40	187.16
420	tensile	Internal Tooth	33	173.00	CF	267	95.23	116.64	134.68	150.58	170.36	190.47



## Appendix B - Test Data

Test ref #	Test Type	Anchor Type	Concrete Strength, MPa, $f_{c,age}$	Ultimate failure load, Pu, kN	Mode of Failure	Effective Embedment Depth, $h_{ef}$ , mm	Ultimate Test Loads normalised to $f_{c,age}$ , kN					
							10.00	15.00	20.00	25.00	32.00	40.00
421	tensile	Internal Tooth	20	123.00		257	86.97	106.52	123.00	137.52	155.58	173.95
422	tensile	Internal Tooth	20	128.00		257	90.51	110.85	128.00	143.11	161.91	181.02
423	tensile	Internal Tooth	20	124.00		257	87.68	107.39	124.00	138.64	156.85	175.36
424	tensile	Internal Tooth	20	125.00		257	88.39	108.25	125.00	139.75	158.11	176.78
425	tensile	Internal Tooth	20	123.00		257	86.97	106.52	123.00	137.52	155.58	173.95
426	tensile	Internal Tooth	20	121.00		257	85.56	104.79	121.00	135.28	153.05	171.12
427	tensile	Internal Tooth	20	142.00		257	100.41	122.98	142.00	158.76	179.62	200.82
428	tensile	Internal Tooth	20	132.00		257	93.34	114.32	132.00	147.58	166.97	186.68
429	tensile	Internal Tooth	19.40	123.00	CF	257	88.31	108.16	124.89	139.63	157.97	176.62
430	tensile	Internal Tooth	19.49	128.00	CF	257	91.69	112.29	129.66	144.97	164.01	183.37
431	tensile	Internal Tooth	19.58	124.00	CF	257	88.62	108.53	125.32	140.12	158.52	177.23
432	tensile	Internal Tooth	19.67	125.00	CF	257	89.13	109.16	126.04	140.92	159.43	178.25
433	tensile	Internal Tooth	19.76	123.00	CF	257	87.50	107.17	123.74	138.35	156.53	175.00
434	tensile	Internal Tooth	19.85	121.00	CF	257	85.88	105.18	121.46	135.79	153.63	171.77
435	tensile	Internal Tooth	19.94	142.00	CF	257	100.56	123.16	142.21	159.00	179.89	201.12
436	tensile	Internal Tooth	20.03	132.00	CF	257	93.27	114.23	131.90	147.47	166.84	186.54
437	tensile	Internal Tooth	24.0	125.00		268	80.69	98.82	114.11	127.58	144.34	161.37
438	tensile	Internal Tooth	24.6	129.00		268	82.25	100.73	116.32	130.04	147.13	164.49
439	tensile	Internal Tooth	24.9	105.00		268	66.54	81.50	94.10	105.21	119.03	133.08
440	tensile	Internal Tooth	25.2	138.00		268	86.93	106.47	122.94	137.45	155.51	173.86
441	tensile	Internal Tooth	25.5	123.00		268	77.03	94.34	108.93	121.79	137.79	154.05
442	tensile	Internal Tooth	25.8	119.00		268	74.09	90.74	104.77	117.14	132.53	148.17
443	tensile	Internal Tooth	26.0	126.40		268	78.39	96.01	110.86	123.95	140.23	156.78
444	tensile	Internal Tooth	26.1	131.00		268	81.09	99.31	114.67	128.21	145.05	162.17
445	tensile	Internal Tooth	14.00	253.40	SF ANCHOR	81	214.16	262.29	302.87	338.62	383.10	428.32
446	tensile	Internal Tooth	14.00	245.50	SF ANCHOR	81	207.49	254.12	293.43	328.06	371.16	414.97
447	tensile	Internal Tooth	14.00	257.00	SF ANCHOR	81	217.20	266.02	307.17	343.43	388.55	434.41
448	tensile	Internal Tooth	14.00	158.80	SF ANCHOR	81	134.21	164.37	189.80	212.21	240.08	268.42
449	tensile	Internal Tooth	15.00	246.00	SF ANCHOR	81	200.86	246.00	284.06	317.58	359.31	401.72
450	tensile	Internal Tooth	15.00	245.10	SF ANCHOR	81	200.12	245.10	283.02	316.42	357.99	400.25
451	tensile	Internal Tooth	15.00	245.00	SF ANCHOR	81	200.04	245.00	282.90	316.29	357.85	400.08
452	tensile	Internal Tooth	16.00	245.10	SF ANCHOR	81	193.77	237.32	274.03	306.38	346.62	387.54
453	tensile	Internal Tooth	16.00	246.00	SF ANCHOR	81	194.48	238.19	275.04	307.50	347.90	388.96
454	tensile	Internal Tooth	16.00	253.10	SF ANCHOR	81	200.09	245.06	282.97	316.38	357.94	400.19
455	tensile	Internal Tooth	11.00	186.00	SF TBAR	81	177.34	217.20	250.80	280.41	317.24	354.69
456	tensile	Internal Tooth	11.00	182.00	SF TBAR	81	173.53	212.53	245.41	274.38	310.42	347.06
457	tensile	Internal Tooth	11.00	191.00	SF TBAR	81	182.11	223.04	257.54	287.94	325.77	364.22
458	tensile	Internal Tooth	11.00	194.00	SF TBAR	81	184.97	226.54	261.59	292.47	330.89	369.94
459	tensile	Internal Tooth	12.00	192.00	SF TBAR	81	175.27	214.66	247.87	277.13	313.53	350.54
460	tensile	Internal Tooth	12.00	185.00	SF TBAR	81	168.88	206.84	238.83	267.02	302.10	337.76
461	tensile	Internal Tooth	12.00	206.00	SF TBAR	81	188.05	230.32	265.94	297.34	336.40	376.10
462	tensile	Internal Tooth	14.00	195.00	SF TBAR	81	164.81	201.84	233.07	260.58	294.81	329.61
463	tensile	Internal Tooth	14.00	193.00	SF TBAR	81	163.11	199.77	230.68	257.91	291.79	326.23
464	tensile	Internal Tooth	14.00	218.00	SF TBAR	81	184.24	225.65	260.56	291.31	329.59	368.49
465	shear	Internal Tooth	12.00	50.50	CF	125	46.10	56.46	65.20	72.89	82.47	92.20
466	shear	Internal Tooth	12.00	61.50	CF	125	56.14	68.76	79.40	88.77	100.43	112.28
467	shear	Internal Tooth	12.00	48.90	CF	125	44.64	54.67	63.13	70.58	79.85	89.28
468	shear	Internal Tooth	12.00	57.40	CF	125	52.40	64.18	74.10	82.85	93.73	104.80
469	shear	Internal Tooth	13.00	52.00	CF	125	45.61	55.86	64.50	72.11	81.58	91.21
470	shear	Internal Tooth	13.00	54.90	CF	125	48.15	58.97	68.10	76.13	86.13	96.30
471	shear	Internal Tooth	13.00	54.60	CF	125	47.89	58.65	67.72	75.72	85.66	95.77
472	shear	Internal Tooth	14.00	55.40	CF	125	46.82	57.34	66.22	74.03	83.76	93.64
473	shear	Internal Tooth	14.00	52.70	CF	125	44.54	54.55	62.99	70.42	79.67	89.08
474	shear	Internal Tooth	14.00	57.30	CF	125	48.43	59.31	68.49	76.57	86.63	96.85
475	shear	Internal Tooth	14.00	51.70	CF	125	43.69	53.51	61.79	69.09	78.16	87.39
476	tensile	Wavy Legged	10.30	212.00	CF	350	208.89	255.84	295.41	330.28	373.67	417.78
477	tensile	Wavy Legged	10.30	207.00	CF	350	203.96	249.80	288.45	322.49	364.86	407.93
478	tensile	Wavy Legged	10.30	239.00	CF	350	235.49	288.42	333.04	372.35	421.26	470.99
479	tensile	Wavy Legged	10.30	223.00	CF	350	219.73	269.11	310.74	347.42	393.06	439.46
480	tensile	Wavy Legged	10.30	232.00	SF ANCHOR	350	228.60	279.97	323.28	361.44	408.93	457.19
481	tensile	Wavy Legged	10.30	230.00	CF	350	226.63	277.56	320.50	358.33	405.40	453.25
482	tensile	Internal Tooth	12.50	226.36		267	202.46	247.96	286.33	320.12	362.18	404.93
483	tensile	Internal Tooth	12.50	230.52		267	206.18	252.52	291.59	326.00	368.83	412.37
484	tensile	Internal Tooth	12.50	234.31		267	209.57	256.67	296.38	331.36	374.90	419.15
485	tensile	Internal Tooth	12.50	215.00		267	192.30	235.52	271.96	304.06	344.00	384.60
486	tensile	Internal Tooth	12.50	234.17		267	209.45	256.52	296.20	331.17	374.67	418.90
487	tensile	Internal Tooth	12.50	224.76		267	201.03	246.21	284.30	317.86	359.62	402.06
488	tensile	Internal Tooth	12.50	227.52		267	203.50	249.24	287.79	321.76	364.03	407.00
489	tensile	Internal Tooth	12.50	224.18		267	200.51	245.58	283.57	317.04	358.69	401.03
490	tensile	Internal Tooth	18.00	233.10		267	173.74	212.79	245.71	274.71	310.80	347.48
491	tensile	Internal Tooth	18.00	242.40		267	180.67	221.28	255.51	285.67	323.20	361.35
492	tensile	Internal Tooth	18.00	243.00		267	181.12	221.83	256.14	286.38	324.00	362.24
493	tensile	Internal Tooth	18.00	245.60		267	183.06	224.20	258.89	289.44	327.47	366.12
494	tensile	Internal Tooth	18.00	250.80		267	186.94	228.95	264.37	295.57	334.40	373.87
495	tensile	Internal Tooth	18.00	243.00		267	181.12	221.83	256.14	286.38	324.00	362.24
496	tensile	Internal Tooth	18.00	244.60		267	182.31	223.29	257.83	288.26	326.13	364.63
497	tensile	Internal Tooth	18.00	251.00		267	187.08	229.13	264.58	295.81	334.67	374.17
498	tensile	Internal Tooth	15.00	87.40		242	71.36	87.40	100.92	112.83	127.66	142.72
499	tensile	Internal Tooth	15.00	93.20		242	76.10	93.20	107.62	120.32	136.13	152.19
500	tensile	Internal Tooth	15.00	82.70		242	67.52	82.70	95.49	106.77	120.79	135.05
501	tensile	Internal Tooth	15.00	80.10		242	65.40	80.10	92.49	103.41	116.99	130.80
502	tensile	Internal Tooth	15.00	97.90		242	79.94	97.90	113.05	126.39	142.99	159.87
503	tensile	Internal Tooth	15.00	97.90		242	79.94	97.90	113.05	126.39	142.99	159.87
504	tensile	Internal Tooth	15.00	79.10		242	64.58	79.10	91.34	102.12	115.53	129.17

## Appendix B - Test Data

Test ref #	Test Type	Anchor Type	Concrete Strength, MPa, $f_{c,age}$	Ultimate failure load, Pu, kN	Mode of Failure	Effective Embedment Depth, $h_{ef}$ , mm	Ultimate Test Loads normalised to $f'_{c,age}$ , kN					
							10.00	15.00	20.00	25.00	32.00	40.00
505	tensile	Internal Tooth	15.00	82.20		242	67.12	82.20	94.92	106.12	120.06	134.23
506	shear	Internal Tooth	15.00	33.50		78	27.35	33.50	38.68	43.25	48.93	54.71
507	shear	Internal Tooth	15.00	32.90		78	26.86	32.90	37.99	42.47	48.05	53.73
508	shear	Internal Tooth	15.00	33.80		78	27.60	33.80	39.03	43.64	49.37	55.20
509	shear	Internal Tooth	15.00	33.60		78	27.43	33.60	38.80	43.38	49.08	54.87
510	shear	Internal Tooth	15.00	37.20		78	30.37	37.20	42.95	48.02	54.33	60.75
511	shear	Internal Tooth	15.00	31.30		78	25.56	31.30	36.14	40.41	45.72	51.11
512	shear	Internal Tooth	15.00	33.80		78	27.60	33.80	39.03	43.64	49.37	55.20
513	shear	Internal Tooth	15.00	38.00		78	31.03	38.00	43.88	49.06	55.50	62.05
514	tensile	Internal Tooth	11.00	187.00		81	178.30	218.37	252.15	281.91	318.95	356.60
515	tensile	Internal Tooth	11.00	193.00		81	184.02	225.38	260.24	290.96	329.18	368.04
516	tensile	Internal Tooth	11.00	191.00		81	182.11	223.04	257.54	287.94	325.77	364.22
517	tensile	Internal Tooth	11.00	185.00		81	176.39	216.03	249.45	278.90	315.54	352.78
518	shear	Internal Tooth	11.00	45.60		125	43.48	53.25	61.49	68.74	77.78	86.96
519	shear	Internal Tooth	11.00	38.40		125	36.61	44.84	51.78	57.89	65.50	73.23
520	shear	Internal Tooth	11.00	46.50		125	44.34	54.30	62.70	70.10	79.31	88.67
521	shear	Internal Tooth	11.00	47.60		125	45.38	55.58	64.18	71.76	81.19	90.77
522	shear	Internal Tooth	10.00	21.90		82	21.90	26.82	30.97	34.63	39.18	43.80
523	shear	Internal Tooth	10.00	23.40		82	23.40	28.66	33.09	37.00	41.86	46.80
524	shear	Internal Tooth	15.00	23.80		82	19.43	23.80	27.48	30.73	34.76	38.87
525	shear	Internal Tooth	15.00	24.40		82	19.92	24.40	28.17	31.50	35.64	39.85
526	shear	Internal Tooth	10.00	46.50		115	46.50	56.95	65.76	73.52	83.18	93.00
527	shear	Internal Tooth	10.00	35.50		115	35.50	43.48	50.20	56.13	63.50	71.00
528	shear	Internal Tooth	15.00	39.70		115	32.41	39.70	45.84	51.25	57.99	64.83
529	shear	Internal Tooth	15.00	37.00		115	30.21	37.00	42.72	47.77	54.04	60.42
530	shear	Internal Tooth	10.00	37.60		114	37.60	46.05	53.17	59.45	67.26	75.20
531	shear	Internal Tooth	10.00	41.30		114	41.30	50.58	58.41	65.30	73.88	82.60
532	shear	Internal Tooth	15.00	39.50		114	32.25	39.50	45.61	50.99	57.69	64.50
533	shear	Internal Tooth	15.00	42.80		114	34.95	42.80	49.42	55.25	62.51	69.89
534	shear	Internal Tooth	15.00	43.40		98	35.44	43.40	50.11	56.03	63.39	70.87
535	shear	Internal Tooth	15.00	45.80		98	37.40	45.80	52.89	59.13	66.90	74.79
536	shear	Internal Tooth	15.00	39.20		126	32.01	39.20	45.26	50.61	57.26	64.01
537	shear	Internal Tooth	15.00	37.60		126	30.70	37.60	43.42	48.54	54.92	61.40
538	shear	Headed Anchor	21.00	37.60	CF	103	25.95	31.78	36.69	41.02	46.41	51.89
539	shear	Headed Anchor	21.00	40.10	CF	103	27.67	33.89	39.13	43.75	49.50	55.34
540	shear	Headed Anchor	21.00	38.60	CF	103	26.64	32.62	37.67	42.12	47.65	53.27
541	shear	Headed Anchor	21.00	51.90	CF	103	35.81	43.86	50.65	56.63	64.07	71.63
542	shear	Headed Anchor	21.00	51.70	CF	103	35.68	43.69	50.45	56.41	63.82	71.35
543	shear	Headed Anchor	21.00	61.90	CF	103	42.72	52.32	60.41	67.54	76.41	85.43
544	tensile	Headed Anchor	10.00	22.80	CF	39	22.80	27.92	32.24	36.05	40.79	45.60
545	tensile	Headed Anchor	10.00	27.30	CF	39	27.30	33.44	38.61	43.17	48.84	54.60
546	tensile	Headed Anchor	10.00	24.00	CF	39	24.00	29.39	33.94	37.95	42.93	48.00
547	tensile	Headed Anchor	10.00	31.90	CF	49	31.90	39.07	45.11	50.44	57.06	63.80
548	tensile	Headed Anchor	10.00	37.30	CF	54	37.30	45.68	52.75	58.98	66.72	74.60
549	tensile	Headed Anchor	10.00	39.10	CF	49	39.10	47.89	55.30	61.82	69.94	78.20
550	tensile	Headed Anchor	10.00	30.10	CF	49	30.10	36.86	42.57	47.59	53.84	60.20
551	tensile	Headed Anchor	10.00	29.70	CF	49	29.70	36.37	42.00	46.96	53.13	59.40
552	tensile	Headed Anchor	10.00	24.80	CF	39	24.80	30.37	35.07	39.21	44.36	49.60
553	tensile	Headed Anchor	10.00	43.40	CF	54	43.40	53.15	61.38	68.62	77.64	86.80
554	tensile	Headed Anchor	10.00	40.40	CF	54	40.40	49.48	57.13	63.88	72.27	80.80
555	tensile	Headed Anchor	10.00	39.60	CF	54	39.60	48.50	56.00	62.61	70.84	79.20
556	tensile	Headed Anchor	10.00	35.80	CF	54	35.80	43.85	50.63	56.60	64.04	71.60
557	tensile	Headed Anchor	10.00	29.20	CF	49	29.20	35.76	41.30	46.17	52.23	58.40
558	tensile	Headed Anchor	10.00	28.30	CF	39	28.30	34.66	40.02	44.75	50.62	56.60
559	tensile	Headed Anchor	10.00	52.30	CF	54	52.30	64.05	73.96	82.69	93.56	104.60
560	tensile	Headed Anchor	10.00	49.00	CF	54	49.00	60.01	69.30	77.48	87.65	98.00
561	tensile	Headed Anchor	10.00	46.10	CF	54	46.10	56.46	65.20	72.89	82.47	92.20
562	tensile	Headed Anchor	10.00	48.90	CF	54	48.90	59.89	69.16	77.32	87.47	97.80
563	tensile	Headed Anchor	10.00	41.10	CF	54	41.10	50.34	58.12	64.98	73.52	82.20
564	tensile	Internal Tooth	25.00	110.00		267	69.57	85.21	98.39	110.00	124.45	139.14
565	tensile	Internal Tooth	25.00	104.00		267	65.78	80.56	93.02	104.00	117.66	131.55
566	tensile	Internal Tooth	25.00	104.00		267	65.78	80.56	93.02	104.00	117.66	131.55
567	tensile	Internal Tooth	25.00	101.00		267	63.88	78.23	90.34	101.00	114.27	127.76
568	tensile	Internal Tooth	25.00	97.60		267	61.73	75.60	87.30	97.60	110.42	123.46
569	tensile	Internal Tooth	25.00	102.00		267	64.51	79.01	91.23	102.00	115.40	129.02
570	tensile	Internal Tooth	25.00	101.00		267	63.88	78.23	90.34	101.00	114.27	127.76
571	tensile	Internal Tooth	25.00	98.20		267	62.11	76.07	87.83	98.20	111.10	124.21
572	tensile	Internal Tooth	25.00	110.00		267	69.57	85.21	98.39	110.00	124.45	139.14
573	tensile	Internal Tooth	25.00	106.00		267	67.04	82.11	94.81	106.00	119.93	134.08
574	tensile	Internal Tooth	25.00	116.00		267	73.36	89.85	103.75	116.00	131.24	146.73
575	tensile	Internal Tooth	25.00	105.00		267	66.41	81.33	93.91	105.00	118.79	132.82
576	tensile	Internal Tooth	25.00	109.00		267	68.94	84.43	97.49	109.00	123.32	137.88
577	tensile	Internal Tooth	25.00	116.00		267	73.36	89.85	103.75	116.00	131.24	146.73
578	tensile	Internal Tooth	25.00	116.00		267	73.36	89.85	103.75	116.00	131.24	146.73
579	tensile	Internal Tooth	25.00	115.00		267	72.73	89.08	102.86	115.00	130.11	145.46
580	shear	Headed Anchor	15.00	50.50	CF	108	41.23	50.50	58.31	65.20	73.76	82.47
581	shear	Headed Anchor	15.00	53.80	CF	108	43.93	53.80	62.12	69.46	78.58	87.86
582	tensile	Headed Anchor	23.00	68.40	CF	177	45.10	55.24	63.78	71.31	80.68	90.20
583	tensile	Headed Anchor	23.00	70.40	CF	177	46.42	56.85	65.65	73.40	83.04	92.84
584	tensile	Headed Anchor	23.00	91.60	CF	247	60.40	73.97	85.42	95.50	108.05	120.80
585	tensile	Headed Anchor	23.00	86.60	CF	247	57.10	69.94	80.75	90.29	102.15	114.20
586	shear	Headed Anchor	23.00	59.70	CF	108	39.37	48.21	55.67	62.24	70.42	78.73
587	shear	Headed Anchor	23.00	55.00	CF	108	36.27	44.42	51.29	57.34	64.87	72.53
588	shear	Headed Anchor	23.00	52.15	CF	108	34.39	42.11	48.63	54.37	61.51	68.77

## Appendix B - Test Data

Test ref #	Test Type	Anchor Type	Concrete Strength, MPa, $f_{c,age}$	Ultimate failure load, Pu, kN	Mode of Failure	Effective Embedment Depth, $h_{ef}$ , mm	Ultimate Test Loads normalised to $f_{c,age}$ , kN					
							10.00	15.00	20.00	25.00	32.00	40.00
589	shear	Headed Anchor	23.00	59.30	CF	108	39.10	47.89	55.30	61.82	69.95	78.20
590	shear	Headed Anchor	23.00	60.64	CF	108	39.98	48.97	56.55	63.22	71.53	79.97
591	shear	Headed Anchor	23.00	48.00	CF	108	31.65	38.76	44.76	50.04	56.62	63.30
592	shear	Headed Anchor	23.00	50.00	CF	108	32.97	40.38	46.63	52.13	58.98	65.94
593	shear	Internal Tooth	10.00	43.70	cf	38	43.70	53.52	61.80	69.10	78.17	87.40
594	shear	Internal Tooth	10.00	43.00	cf	38	43.00	52.66	60.81	67.99	76.92	86.00
595	shear	Internal Tooth	10.00	45.70	cf	38	45.70	55.97	64.63	72.26	81.75	91.40
596	shear	Internal Tooth	10.00	47.40	cf	38	47.40	58.05	67.03	74.95	84.79	94.80
597	shear	Internal Tooth	15.00	53.30	cf	98	43.52	53.30	61.55	68.81	77.85	87.04
598	shear	Internal Tooth	15.00	58.70	cf	98	47.93	58.70	67.78	75.78	85.74	95.86
599	shear	Internal Tooth	15.00	51.00	cf	98	41.64	51.00	58.89	65.84	74.49	83.28
600	shear	Internal Tooth	15.00	53.30	cf	98	43.52	53.30	61.55	68.81	77.85	87.04
601	tensile	Headed Anchor	10.00	56.16	CF	89	56.16	68.78	79.42	88.80	100.46	112.32
602	tensile	Headed Anchor	10.00	56.16	CF	89	56.16	68.78	79.42	88.80	100.46	112.32
603	tensile	Headed Anchor	10.00	57.24	CF	89	57.24	70.10	80.95	90.50	102.39	114.48
604	tensile	Headed Anchor	10.00	58.32	CF	89	58.32	71.43	82.48	92.21	104.33	116.64
605	tensile	Headed Anchor	10.00	52.92	CF	89	52.92	64.81	74.84	83.67	94.67	105.84
606	tensile	Headed Anchor	10.00	52.92	CF	89	52.92	64.81	74.84	83.67	94.67	105.84
607	tensile	Headed Anchor	20.00	54.00	CF	89	38.18	46.77	54.00	60.37	68.31	76.37
608	tensile	Headed Anchor	20.00	59.40	CF	89	42.00	51.44	59.40	66.41	75.14	84.00
609	tensile	Headed Anchor	20.00	57.24	CF	89	40.47	49.57	57.24	64.00	72.40	80.95
610	tensile	Headed Anchor	20.00	55.08	CF	89	38.95	47.70	55.08	61.58	69.67	77.89
611	tensile	Headed Anchor	20.00	55.08	CF	89	38.95	47.70	55.08	61.58	69.67	77.89
612	tensile	Headed Anchor	20.00	57.24	CF	89	40.47	49.57	57.24	64.00	72.40	80.95
613	tensile	Headed Anchor	25.00	58.21	CF	89	36.82	45.09	52.07	58.21	65.86	73.63
614	tensile	Headed Anchor	25.00	58.21	CF	89	36.82	45.09	52.07	58.21	65.86	73.63
615	tensile	Headed Anchor	25.00	59.40	CF	89	37.57	46.01	53.13	59.40	67.20	75.14
616	shear	Internal Tooth	21.00	60.00	CF	126	41.40	50.71	58.55	65.47	74.07	82.81
617	tensile	Internal Tooth	25.00	234.00	SF	267	147.99	181.26	209.30	234.00	264.74	295.99
618	tensile	Internal Tooth	25.00	243.00	SF	267	153.69	188.23	217.35	243.00	274.92	307.37
619	tensile	Internal Tooth	25.00	246.00	SF	267	155.58	190.55	220.03	246.00	278.32	311.17
620	tensile	Internal Tooth	25.00	249.00	SF	267	157.48	192.87	222.71	249.00	281.71	314.96
621	tensile	Internal Tooth	25.00	242.00	SF	267	153.05	187.45	216.45	242.00	273.79	306.11
622	tensile	Internal Tooth	25.00	248.00	SF	267	156.85	192.10	221.82	248.00	280.58	313.70
623	tensile	Internal Tooth	25.00	248.00	SF	267	156.85	192.10	221.82	248.00	280.58	313.70
624	tensile	Internal Tooth	25.00	247.00	SF	267	156.22	191.33	220.92	247.00	279.45	312.43
625	tensile	Internal Tooth	25.00	248.00	SF	267	156.85	192.10	221.82	248.00	280.58	313.70
626	tensile	Internal Tooth	15.00	177.00	AF	257	144.52	177.00	204.38	228.51	258.53	289.04
627	tensile	Internal Tooth	15.00	170.00	AF	257	138.80	170.00	196.30	219.47	248.30	277.61
628	tensile	Internal Tooth	15.00	178.00	SF ANCHOR	257	145.34	178.00	205.54	229.80	259.99	290.67
629	tensile	Internal Tooth	15.00	178.00	SF ANCHOR	257	145.34	178.00	205.54	229.80	259.99	290.67
630	tensile	Internal Tooth	15.00	178.00	SF ANCHOR	257	145.34	178.00	205.54	229.80	259.99	290.67
631	tensile	Internal Tooth	15.00	176.00	SF ANCHOR	257	143.70	176.00	203.23	227.22	257.06	287.41
632	shear	Internal Tooth	15.00	48.30	SF ANCHOR	128	39.44	48.30	55.77	62.36	70.55	78.87
633	shear	Internal Tooth	15.00	41.20	SF ANCHOR	98	33.64	41.20	47.57	53.19	60.18	67.28
634	shear	Internal Tooth	15.00	39.80	SF ANCHOR	98	32.50	39.80	45.96	51.38	58.13	64.99
635	shear	Internal Tooth	15.00	40.40	SF ANCHOR	98	32.99	40.40	46.65	52.16	59.01	65.97
636	shear	Internal Tooth	20.00	51.10	SF ANCHOR	128	36.13	44.25	51.10	57.13	64.64	72.27
637	shear	Internal Tooth	20.00	41.30	SF ANCHOR	98	29.20	35.77	41.30	46.17	52.24	58.41
638	shear	Internal Tooth	20.00	45.75	SF ANCHOR	98	32.35	39.62	45.75	51.15	57.87	64.70
639	shear	Internal Tooth	20.00	48.70	SF ANCHOR	98	34.44	42.18	48.70	54.45	61.60	68.87
640	shear	Internal Tooth	15.00	26.90	CF	82	21.96	26.90	31.06	34.73	39.29	43.93
641	shear	Internal Tooth	15.00	27.50	CF	82	22.45	27.50	31.75	35.50	40.17	44.91
642	shear	Internal Tooth	15.00	28.80	CF	82	23.52	28.80	33.26	37.18	42.07	47.03
643	shear	Internal Tooth	15.00	27.10	CF	82	22.13	27.10	31.29	34.99	39.58	44.25
644	shear	Internal Tooth	20.00	33.70	CF	95	23.83	29.19	33.70	37.68	42.63	47.66
645	shear	Internal Tooth	20.00	37.00	CF	95	26.16	32.04	37.00	41.37	46.80	52.33
646	shear	Internal Tooth	20.00	32.90	CF	95	23.26	28.49	32.90	36.78	41.62	46.53
647	shear	Internal Tooth	20.00	33.80	CF	95	23.90	29.27	33.80	37.79	42.75	47.80
648	shear	Internal Tooth	15.00	49.80	CF	133	40.66	49.80	57.50	64.29	72.74	81.32
649	shear	Internal Tooth	15.00	50.20	CF	128	40.99	50.20	57.97	64.81	73.32	81.98
650	shear	Internal Tooth	15.00	53.50	CF	128	43.68	53.50	61.78	69.07	78.14	87.37
651	shear	Internal Tooth	15.00	54.70	CF	128	44.66	54.70	63.16	70.62	79.89	89.32
652	shear	Internal Tooth	20.00	48.60	CF	133	34.37	42.09	48.60	54.34	61.47	68.73
653	shear	Internal Tooth	20.00	49.50	CF	128	35.00	42.87	49.50	55.34	62.61	70.00
654	shear	Internal Tooth	20.00	57.50	CF	128	40.66	49.80	57.50	64.29	72.73	81.32
655	shear	Internal Tooth	20.00	53.80	CF	128	38.04	46.59	53.80	60.15	68.05	76.08
656	shear	Internal Tooth	15.00	45.80	CF	128	37.40	45.80	52.89	59.13	66.90	74.79
657	shear	Internal Tooth	15.00	50.70	CF	128	41.40	50.70	58.54	65.45	74.05	82.79
658	shear	Internal Tooth	15.00	59.20	CF	128	48.34	59.20	68.36	76.43	86.47	96.67
659	shear	Internal Tooth	15.00	60.80	CF	128	49.64	60.80	70.21	78.49	88.80	99.29
660	shear	Internal Tooth	20.00	46.30	CF	128	32.74	40.10	46.30	51.76	58.57	65.48
661	shear	Internal Tooth	20.00	49.90	CF	128	35.28	43.21	49.90	55.79	63.12	70.57
662	shear	Internal Tooth	20.00	53.20	CF	128	37.62	46.07	53.20	59.48	67.29	75.24
663	shear	Internal Tooth	20.00	55.90	CF	128	39.53	48.41	55.90	62.50	70.71	79.05
664	shear	Internal Tooth	15.00	39.70	CF	98	32.41	39.70	45.84	51.25	57.99	64.83
665	shear	Internal Tooth	15.00	44.20	CF	98	36.09	44.20	51.04	57.06	64.56	72.18
666	shear	Internal Tooth	15.00	42.50	CF	98	34.70	42.50	49.07	54.87	62.08	69.40
667	shear	Internal Tooth	15.00	50.50	CF	98	41.23	50.50	58.31	65.20	73.76	82.47
668	shear	Internal Tooth	15.00	34.90	CF	98	28.50	34.90	40.30	45.06	50.97	56.99
669	shear	Internal Tooth	15.00	33.40	CF	98	27.27	33.40	38.57	43.12	48.78	54.54
670	shear	Internal Tooth	15.00	40.10	CF	98	32.74	40.10	46.30	51.77	58.57	65.48
671	shear	Internal Tooth	15.00	35.20	CF	98	28.74	35.20	40.65	45.44	51.41	57.48
672	shear	Internal Tooth	32.00	53.10	AF	128	29.68	36.36	41.98	46.93	53.10	59.37

## Appendix B - Test Data

Test ref #	Test Type	Anchor Type	Concrete Strength, MPa, $f_{c,age}$	Ultimate failure load, Pu, kN	Mode of Failure	Effective Embedment Depth, $h_{ef}$ , mm	Ultimate Test Loads normalised to $f_{c,age}$ , kN					
							10.00	15.00	20.00	25.00	32.00	40.00
673	shear	Internal Tooth	32.00	42.90	CF	128	23.98	29.37	33.92	37.92	42.90	47.96
674	shear	Internal Tooth	32.00	46.40	CF	128	25.94	31.77	36.68	41.01	46.40	51.88
675	shear	Internal Tooth	32.00	41.20	CF	128	23.03	28.21	32.57	36.42	41.20	46.06
676	shear	Internal Tooth	32.00	51.80	AF	128	28.96	35.47	40.95	45.79	51.80	57.91
677	shear	Internal Tooth	32.00	48.70	CF	128	27.22	33.34	38.50	43.05	48.70	54.45
678	shear	Internal Tooth	32.00	48.40	AF	128	27.06	33.14	38.26	42.78	48.40	54.11
679	shear	Internal Tooth	32.00	40.60	CF	128	22.70	27.80	32.10	35.89	40.60	45.39
680	shear	Internal Tooth	40.00	54.70	AF	128	27.35	33.50	38.68	43.24	48.93	54.70
681	shear	Internal Tooth	40.00	56.80	CF	128	28.40	34.78	40.16	44.90	50.80	56.80
682	shear	Internal Tooth	40.00	59.20	CF	128	29.60	36.25	41.86	46.80	52.95	59.20
683	shear	Internal Tooth	40.00	53.60	CF	128	26.80	32.82	37.90	42.37	47.94	53.60
684	tensile	Internal Tooth	15.00	106.00	CF	242	86.55	106.00	122.40	136.85	154.82	173.10
685	tensile	Internal Tooth	15.00	102.00	CF	257	83.28	102.00	117.78	131.68	148.98	166.57
686	tensile	Internal Tooth	15.00	103.00	CF	242	84.10	103.00	118.93	132.97	150.44	168.20
687	tensile	Internal Tooth	15.00	108.00	CF	257	88.18	108.00	124.71	139.43	157.74	176.36
688	tensile	Internal Tooth	15.00	111.00	CF	242	90.63	111.00	128.17	143.30	162.13	181.26
689	tensile	Internal Tooth	15.00	110.00	CF	257	89.81	110.00	127.02	142.01	160.67	179.63
690	tensile	Internal Tooth	15.00	98.50	CF	242	80.42	98.50	113.74	127.16	143.87	160.85
691	tensile	Internal Tooth	15.00	106.00	CF	257	86.55	106.00	122.40	136.85	154.82	173.10
692	tensile	Internal Tooth	25.00	116.00	CF	242	73.36	89.85	103.75	116.00	131.24	146.73
693	tensile	Internal Tooth	25.00	119.00	CF	257	75.26	92.18	106.44	119.00	134.63	150.52
694	tensile	Internal Tooth	25.00	117.00	CF	242	74.00	90.63	104.65	117.00	132.37	147.99
695	tensile	Internal Tooth	25.00	124.00	CF	257	78.42	96.05	110.91	124.00	140.29	156.85
696	tensile	Internal Tooth	25.00	121.00	CF	242	76.53	93.73	108.23	121.00	136.90	153.05
697	tensile	Internal Tooth	25.00	114.00	CF	257	72.10	88.30	101.96	114.00	128.98	144.20
698	tensile	Internal Tooth	25.00	120.00	CF	242	75.89	92.95	107.33	120.00	135.76	151.79
699	tensile	Internal Tooth	25.00	113.00	CF	257	71.47	87.53	101.07	113.00	127.84	142.93
700	tensile	Internal Tooth	12.00	94.10	AF	125	85.90	105.21	121.48	135.82	153.66	171.80
701	tensile	Internal Tooth	12.00	94.20	SF ANCHOR	125	85.99	105.32	121.61	135.97	153.83	171.98
702	Tensile	Internal Tooth	12.00	95.00	SF ANCHOR	125	86.72	106.21	122.64	137.12	155.13	173.45
703	tensile	Internal Tooth	12.00	92.80	SF ANCHOR	125	84.71	103.75	119.80	133.95	151.54	169.43
704	Tensile	Internal Tooth	15.00	93.90	AF	125	76.67	93.90	108.43	121.22	137.15	153.34
705	tensile	Internal Tooth	15.00	87.80	No info	125	71.69	87.80	101.38	113.35	128.24	143.38
706	Tensile	Internal Tooth	15.00	88.20	SF ANCHOR	125	72.01	88.20	101.84	113.87	128.82	144.03
707	Tensile	Internal Tooth	15.00	95.20	SF ANCHOR	125	77.73	95.20	109.93	122.90	139.05	155.46
708	tensile	Internal Tooth	15.00	44.90	CF	125	36.66	44.90	51.85	57.97	65.58	73.32
709	tensile	Internal Tooth	15.00	56.40	CF	125	46.05	56.40	65.13	72.81	82.38	92.10
710	tensile	Internal Tooth	15.00	57.70	CF	125	47.11	57.70	66.63	74.49	84.28	94.22
711	tensile	Internal Tooth	15.00	61.20	CF	125	49.97	61.20	70.67	79.01	89.39	99.94
712	tensile	Internal Tooth	15.00	62.90	CF	125	51.36	62.90	72.63	81.20	91.87	102.72
713	tensile	Internal Tooth	15.00	59.40	CF	125	48.50	59.40	68.59	76.69	86.76	97.00
714	tensile	Internal Tooth	15.00	51.20	CF	125	41.80	51.20	59.12	66.10	74.78	83.61
715	tensile	Internal Tooth	15.00	59.30	CF	125	48.42	59.30	68.47	76.56	86.61	96.84
716	tensile	Internal Tooth	25.00	73.90	CF	125	46.74	57.24	66.10	73.90	83.61	93.48
717	tensile	Internal Tooth	25.00	70.40	CF	125	44.52	54.53	62.97	70.40	79.65	89.05
718	tensile	Internal Tooth	25.00	64.70	CF	125	40.92	50.12	57.87	64.70	73.20	81.84
719	tensile	Internal Tooth	25.00	78.40	CF	125	49.58	60.73	70.12	78.40	88.70	99.17
720	tensile	Internal Tooth	25.00	75.00	CF	125	47.43	58.09	67.08	75.00	84.85	94.87
721	tensile	Internal Tooth	25.00	78.10	CF	125	49.39	60.50	69.85	78.10	88.36	98.79
722	tensile	Internal Tooth	25.00	75.10	CF	125	47.50	58.17	67.17	75.10	84.97	94.99
723	tensile	Internal Tooth	25.00	71.70	CF	125	45.35	55.54	64.13	71.70	81.12	90.69
724	tensile	Internal Tooth	16.80	82.80	CF	125	63.88	78.24	90.34	101.01	114.27	127.76
725	tensile	Internal Tooth	16.80	80.30	CF	125	61.95	75.88	87.61	97.96	110.82	123.91
726	tensile	Internal Tooth	16.80	78.30	CF	125	60.41	73.99	85.43	95.52	108.06	120.82
727	tensile	Internal Tooth	16.80	85.80	CF	125	66.20	81.07	93.62	104.67	118.42	132.39
728	tensile	Internal Tooth	15.00	79.20	CF	125	64.67	79.20	91.45	102.25	115.68	129.33
729	tensile	Internal Tooth	15.00	76.40	CF	125	62.38	76.40	88.22	98.63	111.59	124.76
730	tensile	Internal Tooth	20.00	84.80	AF	125	59.96	73.44	84.80	94.81	107.26	119.93
731	tensile	Internal Tooth	20.00	87.00	CF	125	61.52	75.34	87.00	97.27	110.05	123.04
732	tensile	Internal Tooth	19.00	90.20	CF	125	65.44	80.14	92.54	103.47	117.06	130.88
733	tensile	Internal Tooth	20.00	93.30	AF	125	65.97	80.80	93.30	104.31	118.02	131.95
734	tensile	Internal Tooth	20.00	88.60	AF	125	62.65	76.73	88.60	99.06	112.07	125.30
735	tensile	Internal Tooth	20.60	80.40	CF	125	56.02	68.61	79.22	88.57	100.21	112.03
736	tensile	Internal Tooth	15.00	87.30	CF	125	71.28	87.30	100.81	112.70	127.51	142.56
737	tensile	Internal Tooth	15.00	86.80	AF	125	70.87	86.80	100.23	112.06	126.78	141.74
738	Tensile	Internal Tooth	15.00	78.90	CF	125	64.42	78.90	91.11	101.86	115.24	128.84
739	Tensile	Internal Tooth	15.00	83.50	CF	125	68.18	83.50	96.42	107.80	121.96	136.35
740	shear	Internal Tooth	15.00	54.40	CF	126	44.42	54.40	62.82	70.23	79.46	88.83
741	shear	Internal Tooth	15.00	62.00	CF	126	50.62	62.00	71.59	80.04	90.56	101.25
742	shear	Internal Tooth	15.00	58.10	CF	126	47.44	58.10	67.09	75.01	84.86	94.88
743	shear	Internal Tooth	15.00	65.30	CF	126	53.32	65.30	75.40	84.30	95.38	106.63
744	shear	Internal Tooth	15.00	49.10	CF	125	40.09	49.10	56.70	63.39	71.72	80.18
745	shear	Internal Tooth	15.00	62.30	CF	126	50.87	62.30	71.94	80.43	90.99	101.74
746	shear	Internal Tooth	15.00	66.60	CF	126	54.38	66.60	76.90	85.98	97.28	108.76
747	shear	Internal Tooth	15.00	59.30	CF	126	48.42	59.30	68.47	76.56	86.61	96.84
748	shear	Internal Tooth	15.00	47.90	CF	115	39.11	47.90	55.31	61.84	69.96	78.22
749	shear	Internal Tooth	15.00	52.90	CF	115	43.19	52.90	61.08	68.29	77.27	86.39
750	shear	Internal Tooth	15.00	57.60	CF	115	47.03	57.60	66.51	74.36	84.13	94.06
751	shear	Internal Tooth	15.00	56.30	CF	115	45.97	56.30	65.01	72.68	82.23	91.94
752	shear	Internal Tooth	15.00	36.50	CF	82	29.80	36.50	42.15	47.12	53.31	59.60
753	shear	Internal Tooth	15.00	44.00	CF	82	35.93	44.00	50.81	56.80	64.27	71.85
754	shear	Internal Tooth	15.00	46.30	CF	82	37.80	46.30	53.46	59.77	67.63	75.61
755	shear	Internal Tooth	15.00	41.90	CF	82	34.21	41.90	48.38	54.09	61.20	68.42
756	shear	Internal Tooth	15.00	54.40	CF	126	44.42	54.40	62.82	70.23	79.46	88.83

## Appendix B - Test Data

Test ref #	Test Type	Anchor Type	Concrete Strength, MPa, $f_{c,age}$	Ultimate failure load, Pu, kN	Mode of Failure	Effective Embedment Depth, $h_{ef}$ , mm	Ultimate Test Loads normalised to $f'_{c,age}$ , kN					
							10.00	15.00	20.00	25.00	32.00	40.00
757	shear	Internal Tooth	15.00	62.00	CF	126	50.62	62.00	71.59	80.04	90.56	101.25
758	shear	Internal Tooth	15.00	58.10	CF	126	47.44	58.10	67.09	75.01	84.86	94.88
759	shear	Internal Tooth	15.00	65.30	CF	126	53.32	65.30	75.40	84.30	95.38	106.63
760	shear	Internal Tooth	15.00	49.10	CF	125	40.09	49.10	56.70	63.39	71.72	80.18
761	shear	Internal Tooth	15.00	62.30	CF	125	50.87	62.30	71.94	80.43	90.99	101.74
762	shear	Internal Tooth	15.00	66.60	CF	125	54.38	66.60	76.90	85.98	97.28	108.76
763	shear	Internal Tooth	15.00	59.30	CF	125	48.42	59.30	68.47	76.56	86.61	96.84
764	shear	Headed Anchor	15.00	46.20	CF	43	37.72	46.20	53.35	59.64	67.48	75.44
765	shear	Headed Anchor	20.00	51.50	CF	43	36.42	44.60	51.50	57.58	65.14	72.83
766	shear	Headed Anchor	35.00	52.10	CF	43	27.85	34.11	39.38	44.03	49.82	55.70
767	tensile	Wavy Legged	25.00	162.00	CF	370	102.46	125.48	144.90	162.00	183.28	204.92
768	tensile	Wavy Legged	25.00	137.00	CF	272	86.65	106.12	122.54	137.00	155.00	173.29
769	tensile	Internal Tooth	25.00	138.00	CF	257	87.28	106.89	123.43	138.00	156.13	174.56
770	tensile	Wavy Legged	25.00	157.00	CF	370	99.30	121.61	140.43	157.00	177.63	198.59
771	tensile	Wavy Legged	25.00	157.00	CF	272	99.30	121.61	140.43	157.00	177.63	198.59
772	tensile	Wavy Legged	26.00	171.00	CF	370	106.05	129.88	149.98	167.68	189.71	212.10
773	tensile	Wavy Legged	27.70	125.00	CF	350	75.11	91.98	106.21	118.75	134.35	150.21
774	tensile	Wavy Legged	27.70	158.00	CF	272	94.93	116.27	134.26	150.10	169.82	189.87
775	tensile	Internal Tooth	27.70	124.00	CF	257	74.50	91.25	105.37	117.80	133.28	149.01
776	tensile	Wavy Legged	23.00	165.00	AF	370	108.80	133.25	153.86	172.02	194.62	217.60
777	tensile	Wavy Legged	27.70	129.00	CF	350	77.51	94.93	109.61	122.55	138.65	155.02
778	tensile	Wavy Legged	27.70	142.00	CF	272	85.32	104.49	120.66	134.90	152.62	170.64
779	tensile	Internal Tooth	27.70	137.00	CF	257	82.32	100.82	116.41	130.15	147.25	164.63
780	Tensile	Internal Tooth	15.00	116.00	CF	257	94.71	116.00	133.95	149.76	169.43	189.43
781	Tensile	Internal Tooth	15.00	177.00	AF	257	144.52	177.00	204.38	228.51	258.53	289.04
782	Tensile	Internal Tooth	15.00	110.00	CF	257	89.81	110.00	127.02	142.01	160.67	179.63
783	Tensile	Internal Tooth	15.00	204.00	CF	257	166.57	204.00	235.56	263.36	297.96	333.13
784	Shear	Internal Tooth	15.00	40.40	CF	38	32.99	40.40	46.65	52.16	59.01	65.97
785	Shear	Internal Tooth	15.00	38.10	CF	38	31.11	38.10	43.99	49.19	55.65	62.22
786	Tensile	Headed Anchor	12.00	50.00	CF	89	45.64	55.90	64.55	72.17	81.65	91.29
787	Tensile	Headed Anchor	12.00	52.00	CF	89	47.47	58.14	67.13	75.06	84.92	94.94
788	Tensile	Headed Anchor	12.00	52.00	CF	89	47.47	58.14	67.13	75.06	84.92	94.94
789	Tensile	Headed Anchor	12.00	53.00	CF	89	48.38	59.26	68.42	76.50	86.55	96.76
790	Tensile	Headed Anchor	12.00	54.00	CF	89	49.30	60.37	69.71	77.94	88.18	98.59
791	Tensile	Headed Anchor	12.00	49.00	CF	89	44.73	54.78	63.26	70.73	80.02	89.46
792	Tensile	Headed Anchor	12.00	49.00	CF	89	44.73	54.78	63.26	70.73	80.02	89.46
793	Tensile	Headed Anchor	12.00	50.00	CF	89	45.64	55.90	64.55	72.17	81.65	91.29
794	Tensile	Headed Anchor	12.00	55.00	CF	89	50.21	61.49	71.00	79.39	89.81	100.42
795	Tensile	Headed Anchor	12.00	53.00	CF	89	48.38	59.26	68.42	76.50	86.55	96.76
796	Tensile	Headed Anchor	17.00	51.00	CF	89	39.12	47.91	55.32	61.85	69.97	78.23
797	Tensile	Headed Anchor	17.00	51.00	CF	89	39.12	47.91	55.32	61.85	69.97	78.23
798	Tensile	Headed Anchor	17.00	53.00	CF	89	40.65	49.78	57.49	64.27	72.72	81.30
799	Tensile	Headed Anchor	17.00	53.90	CF	89	41.34	50.63	58.46	65.36	73.95	82.68
800	Tensile	Headed Anchor	17.00	53.90	CF	89	41.34	50.63	58.46	65.36	73.95	82.68
801	Tensile	Headed Anchor	17.00	55.00	CF	89	42.18	51.66	59.66	66.70	75.46	84.37
802	Tensile	Headed Anchor	17.00	60.50	CF	89	46.40	56.83	65.62	73.37	83.01	92.80
803	Tensile	Headed Anchor	17.00	58.30	CF	89	44.71	54.76	63.24	70.70	79.99	89.43
804	Tensile	Headed Anchor	17.00	56.10	CF	89	43.03	52.70	60.85	68.03	76.97	86.05
805	Tensile	Headed Anchor	17.00	56.10	CF	89	43.03	52.70	60.85	68.03	76.97	86.05
806	Tensile	Headed Anchor	43.00	36.60	CF	89	17.65	21.62	24.96	27.91	31.57	35.30
807	Tensile	Headed Anchor	43.00	31.40	CF	89	15.14	18.55	21.41	23.94	27.09	30.28
808	Tensile	Headed Anchor	43.00	34.70	CF	89	16.73	20.49	23.67	26.46	29.93	33.47
809	Tensile	Headed Anchor	43.00	27.70	CF	89	13.36	16.36	18.89	21.12	23.90	26.72
810	Tensile	Headed Anchor	43.00	28.40	CF	89	13.70	16.77	19.37	21.65	24.50	27.39
811	Tensile	Headed Anchor	43.00	28.80	CF	89	13.89	17.01	19.64	21.96	24.84	27.78
812	Tensile	Headed Anchor	43.00	33.90	CF	89	16.35	20.02	23.12	25.85	29.24	32.70
813	Tensile	Headed Anchor	43.00	33.30	CF	89	16.06	19.67	22.71	25.39	28.73	32.12
814	Tensile	Headed Anchor	43.00	31.50	CF	89	15.19	18.60	21.48	24.02	27.17	30.38
815	Tensile	Headed Anchor	43.00	36.00	CF	89	17.36	21.26	24.55	27.45	31.06	34.72
816	tensile	Headed Anchor	50.00	60.00	CF	50	26.83	32.86	37.95	42.43	48.00	53.67
817	tensile	Headed Anchor	50.00	45.80	CF	50	20.48	25.09	28.97	32.39	36.64	40.96
818	tensile	Headed Anchor	50.00	61.90	CF	50	27.68	33.90	39.15	43.77	49.52	55.37
819	tensile	Headed Anchor	50.00	52.40	CF	50	23.43	28.70	33.14	37.05	41.92	46.87
820	tensile	Headed Anchor	50.00	42.80	CF	50	19.14	23.44	27.07	30.26	34.24	38.28
821	tensile	Headed Anchor	50.00	39.00	CF	50	17.44	21.36	24.67	27.58	31.20	34.88
822	tensile	Headed Anchor	50.00	51.10	CF	50	22.85	27.99	32.32	36.13	40.88	45.71
823	tensile	Headed Anchor	50.00	43.10	CF	50	19.27	23.61	27.26	30.48	34.48	38.55
824	tensile	Headed Anchor	50.00	62.30	CF	50	27.86	34.12	39.40	44.05	49.84	55.72
825	tensile	Headed Anchor	50.00	47.00	CF	50	21.02	25.74	29.73	33.23	37.60	42.04
826	tensile	Headed Anchor	50.00	84.90	CF	50	37.97	46.50	53.70	60.03	67.92	75.94
827	tensile	Headed Anchor	50.00	61.20	CF	50	27.37	33.52	38.71	43.27	48.96	54.74
828	tensile	Headed Anchor	50.00	51.40	CF	50	22.99	28.15	32.51	36.35	41.12	45.97
829	tensile	Headed Anchor	50.00	42.60	CF	50	19.05	23.33	26.94	30.12	34.08	38.10
830	tensile	Headed Anchor	50.00	47.40	CF	50	21.20	25.96	29.98	33.52	37.92	42.40
831	tensile	Headed Anchor	50.00	51.60	CF	50	23.08	28.26	32.63	36.49	41.28	46.15
832	tensile	Headed Anchor	50.00	67.90	CF	50	30.37	37.19	42.94	48.01	54.32	60.73
833	tensile	Headed Anchor	50.00	47.50	CF	50	21.24	26.02	30.04	33.59	38.00	42.49
834	tensile	Headed Anchor	50.00	60.40	CF	50	27.01	33.08	38.20	42.71	48.32	54.02
835	tensile	Headed Anchor	50.00	53.00	CF	50	23.70	29.03	33.52	37.48	42.40	47.40
836	tensile	Headed Anchor	50.00	64.00	CF	50	28.62	35.05	40.48	45.25	51.20	57.24
837	tensile	Headed Anchor	50.00	58.10	CF	50	25.98	31.82	36.75	41.08	46.48	51.97
838	tensile	Headed Anchor	50.00	49.80	CF	50	22.27	27.28	31.50	35.21	39.84	44.54
839	tensile	Headed Anchor	50.00	48.50	CF	50	21.69	26.56	30.67	34.29	38.80	43.38
840	tensile	Headed Anchor	50.00	65.50	CF	50	29.29	35.88	41.43	46.32	52.40	58.58



## Appendix B - Test Data

Test ref #	Test Type	Anchor Type	Concrete Strength, MPa, $f_{c,age}$	Ultimate failure load, Pu, kN	Mode of Failure	Effective Embedment Depth, $h_{ef}$ , mm	Ultimate Test Loads normalised to $f_{c,age}$ , kN					
							10.00	15.00	20.00	25.00	32.00	40.00
841	tensile	Headed Anchor	50.00	52.90	CF	50	23.66	28.97	33.46	37.41	42.32	47.32
842	tensile	Headed Anchor	50.00	55.90	CF	50	25.00	30.62	35.35	39.53	44.72	50.00
843	tensile	Headed Anchor	50.00	69.60	CF	50	31.13	38.12	44.02	49.21	55.68	62.25
844	shear	Internal Tooth	15.00	47.90	CF	36	39.11	47.90	55.31	61.84	69.96	78.22
845	shear	Internal Tooth	10.00	26.46	CF	36	26.46	32.41	37.42	41.84	47.33	52.92
846	shear	Internal Tooth	10.00	36.00	CF	36	36.00	44.09	50.91	56.92	64.40	72.00
847	shear	Internal Tooth	30.00	25.00	CF	36	14.43	17.68	20.41	22.82	25.82	28.87
848	shear	Internal Tooth	30.00	43.20	CF	36	24.94	30.55	35.27	39.44	44.62	49.88
849	shear	Internal Tooth	13.40	54.50	CF	126	47.08	57.66	66.58	74.44	84.22	94.16
850	shear	Internal Tooth	13.40	47.20	CF	36	40.77	49.94	57.66	64.47	72.94	81.55
851	shear	Internal Tooth	13.40	47.10	CF	36	40.69	49.83	57.54	64.33	72.79	81.38
852	shear	Internal Tooth	13.40	40.90	CF	36	35.33	43.27	49.97	55.87	63.20	70.66
853	shear	Internal Tooth	13.40	52.00	CF	126	44.92	55.02	63.53	71.03	80.36	89.84
854	shear	Internal Tooth	13.40	44.20	CF	36	38.18	46.76	54.00	60.37	68.30	76.37
855	shear	Internal Tooth	13.40	41.70	CF	36	36.02	44.12	50.94	56.96	64.44	72.05
856	shear	Internal Tooth	13.40	42.00	CF	36	36.28	44.44	51.31	57.37	64.90	72.56
857	shear	Internal Tooth	13.40	54.00	CF	126	46.65	57.13	65.97	73.76	83.45	93.30
858	shear	Internal Tooth	13.40	40.10	CF	36	34.64	42.43	48.99	54.77	61.97	69.28
859	shear	Internal Tooth	13.40	45.20	CF	36	39.05	47.82	55.22	61.74	69.85	78.09
860	shear	Internal Tooth	13.40	45.50	CF	36	39.31	48.14	55.59	62.15	70.31	78.61
861	shear	Internal Tooth	13.40	52.20	CF	126	45.09	55.23	63.77	71.30	80.67	90.19
862	shear	Internal Tooth	13.40	43.70	CF	36	37.75	46.24	53.39	59.69	67.53	75.50
863	shear	Internal Tooth	13.40	43.90	CF	36	37.92	46.45	53.63	59.96	67.84	75.85
864	shear	Internal Tooth	13.40	41.60	CF	36	35.94	44.01	50.82	56.82	64.29	71.87
865	tensile	Internal Tooth	15.00	130.00	CF	267	106.14	130.00	150.11	167.83	189.88	212.29
866	tensile	Internal Tooth	15.00	110.00	CF	235	89.81	110.00	127.02	142.01	160.67	179.63
867	tensile	Internal Tooth	15.00	118.00	CF	267	96.35	118.00	136.25	152.34	172.35	192.69
868	tensile	Internal Tooth	15.00	122.00	CF	235	99.61	122.00	140.87	157.50	178.19	199.23
869	shear	Internal Tooth	10.00	50.40	CF	38	50.40	61.73	71.28	79.69	90.16	100.80
870	shear	Internal Tooth	15.00	31.00	CF	38	25.31	31.00	35.80	40.02	45.28	50.62
871	shear	Internal Tooth	10.00	50.40	CF	38	50.40	61.73	71.28	79.69	90.16	100.80
872	shear	Internal Tooth	15.00	41.70	CF	38	34.05	41.70	48.15	53.83	60.91	68.10
873	shear	Internal Tooth	15.00	44.60	CF	38	36.42	44.60	51.50	57.58	65.14	72.83
874	shear	Internal Tooth	15.00	39.20	CF	38	32.01	39.20	45.26	50.61	57.26	64.01
875	tensile	Internal Tooth	25.00	125.50	CF	221	79.37	97.21	112.25	125.50	141.99	158.75
876	shear	Internal Tooth	25.00	132.00	CF	38	83.48	102.25	118.06	132.00	149.34	166.97
877	tensile	Internal Tooth	14.60	204.60		221	169.33	207.38	239.47	267.73	302.90	338.66
878	tensile	Internal Tooth	14.60	210.40		221	174.13	213.26	246.25	275.32	311.49	348.26
879	tensile	Internal Tooth	12.50	161.00	CF	221	144.00	176.37	203.65	227.69	257.60	288.01
880	tensile	Internal Tooth	12.50	167.60	CF	221	149.91	183.60	212.00	237.02	268.16	299.81
881	tensile	Internal Tooth	12.50	104.00	CF	221	93.02	113.93	131.55	147.08	166.40	186.04
882	tensile	Internal Tooth	12.50	90.40	CF	221	80.86	99.03	114.35	127.84	144.64	161.71
883	tensile	Internal Tooth	12.50	187.60	CF	221	167.79	205.51	237.30	265.31	300.16	335.59
884	tensile	Internal Tooth	12.50	174.80	CF	221	156.35	191.48	221.11	247.20	279.68	312.69
885	tensile	Internal Tooth	17.00	100.60	CF	221	77.16	94.50	109.12	122.00	138.02	154.31
886	tensile	Internal Tooth	17.00	97.40	CF	221	74.70	91.49	105.65	118.11	133.63	149.40
887	shear	Internal Tooth	17.00	46.80	CF	25	35.89	43.96	50.76	56.75	64.21	71.79
888	shear	Internal Tooth	17.00	52.20	CF	25	40.04	49.03	56.62	63.30	71.62	80.07
889	shear	Internal Tooth	17.00	51.20	CF	25	39.27	48.09	55.53	62.09	70.25	78.54
890	shear	Internal Tooth	12.00	51.80	CF	38	47.29	57.91	66.87	74.77	84.59	94.57
891	shear	Internal Tooth	17.00	68.00	CF	50	52.15	63.87	73.76	82.46	93.30	104.31
892	tensile	Internal Tooth	15.00	184.50	CF	221	150.64	184.50	213.04	238.19	269.48	301.29
893	tensile	Internal Tooth	15.00	192.20	CF	221	156.93	192.20	221.93	248.13	280.73	313.86
894	tensile	Internal Tooth	13.00	207.50	CF	221	181.99	222.89	257.37	287.75	325.55	363.98
895	tensile	Internal Tooth	13.00	208.60	CF	221	182.95	224.07	258.74	289.28	327.28	365.91
896	tensile	Internal Tooth	20.00	105.00	CF	221	74.25	90.93	105.00	117.39	132.82	148.49
897	tensile	Internal Tooth	20.00	121.50	CF	221	85.91	105.22	121.50	135.84	153.69	171.83
898	tensile	Internal Tooth	14.00	215.60	SF Anchor	221	182.22	223.17	257.69	288.11	325.96	364.43
899	tensile	Internal Tooth	15.00	190.80	CF	221	155.79	190.80	220.32	246.32	278.68	311.58
900	tensile	Internal Tooth	25.00	222.00	CF	221	140.41	171.96	198.56	222.00	251.16	280.81
901	tensile	Internal Tooth	15.00	93.00	CF	221	75.93	93.00	107.39	120.06	135.84	151.87
902	tensile	Internal Tooth	15.00	96.80	CF	221	79.04	96.80	111.78	124.97	141.39	158.07
903	tensile	Internal Tooth	10.00	202.80	SF Anchor	221	202.80	248.38	286.80	320.65	362.78	405.60
904	tensile	Internal Tooth	10.00	202.80	SF Anchor	221	202.80	248.38	286.80	320.65	362.78	405.60
905	tensile	Internal Tooth	15.00	94.00	CF	221	76.75	94.00	108.54	121.35	137.30	153.50
906	shear	Internal Tooth	15.00	104.00	CF	25	84.92	104.00	120.09	134.26	151.90	169.83
907	shear	Internal Tooth	12.00	40.00	CF	25	36.51	44.72	51.64	57.74	65.32	73.03
908	shear	Internal Tooth	12.00	38.60	CF	25	35.24	43.16	49.83	55.71	63.03	70.47
909	shear	Internal Tooth	12.00	46.90	CF	25	42.81	52.44	60.55	67.69	76.59	85.63
910	shear	Internal Tooth	12.00	30.80	CF	38	28.12	34.44	39.76	44.46	50.30	56.23
911	shear	Internal Tooth	10.00	41.00	CF	38	41.00	50.21	57.98	64.83	73.34	82.00
912	shear	Internal Tooth	10.00	41.00	CF	38	41.00	50.21	57.98	64.83	73.34	82.00
913	shear	Internal Tooth	12.00	32.20	CF	50	29.39	36.00	41.57	46.48	52.58	58.79
914	shear	Internal Tooth	12.00	57.10	CF	50	52.12	63.84	73.72	82.42	93.24	104.25
915	shear	Internal Tooth	12.00	51.30	CF	50	46.83	57.36	66.23	74.05	83.77	93.66
916	shear	Internal Tooth	12.00	59.60	CF	50	54.41	66.63	76.94	86.03	97.33	108.81
917	shear	Internal Tooth	12.00	39.10	CF	50	35.69	43.72	50.48	56.44	63.85	71.39
918	tensile	Internal Tooth	19.00	179.00	SF Anchor	257	129.86	159.05	183.65	205.33	232.30	259.72
919	tensile	Internal Tooth	19.00	162.30	CF	221	117.74	144.21	166.52	186.17	210.63	235.49
920	tensile	Internal Tooth	19.00	201.40	CF	221	146.11	178.95	206.63	231.02	261.37	292.22
921	tensile	Internal Tooth	19.00	206.50	SF Anchor	221	149.81	183.48	211.86	236.87	267.99	299.62
922	tensile	Internal Tooth	19.00	97.80	CF	221	70.95	86.90	100.34	112.18	126.92	141.90
923	tensile	Internal Tooth	19.00	83.60	CF	221	60.65	74.28	85.77	95.90	108.49	121.30
924	tensile	Internal Tooth	19.00	199.40	CF	221	144.66	177.17	204.58	228.73	258.78	289.32

## Appendix B - Test Data

Test ref #	Test Type	Anchor Type	Concrete Strength, MPa, $f_{c,age}$	Ultimate failure load, Pu, kN	Mode of Failure	Effective Embedment Depth, $h_{ef}$ , mm	Ultimate Test Loads normalised to $f_{c,age}$ , kN					
							10.00	15.00	20.00	25.00	32.00	40.00
925	tensile	Internal Tooth	19.00	198.20	CF	221	143.79	176.11	203.35	227.35	257.22	287.58
926	tensile	Internal Tooth	19.00	199.40	SF TBar	221	144.66	177.17	204.58	228.73	258.78	289.32
927	tensile	Internal Tooth	19.00	195.50	CF	221	141.83	173.71	200.58	224.25	253.71	283.66
928	tensile	Internal Tooth	19.00	192.20	CF	221	139.44	170.77	197.19	220.47	249.43	278.87
929	tensile	Internal Tooth	19.00	193.20	CF	221	140.16	171.66	198.22	221.62	250.73	280.32
930	tensile	Internal Tooth	19.00	191.40	CF	221	138.86	170.06	196.37	219.55	248.39	277.71
931	tensile	Internal Tooth	17.00	191.40	SF TBar	221	146.80	179.79	207.60	232.11	262.60	293.59
932	tensile	Internal Tooth	19.00	202.80	SF Anchor	221	147.13	180.19	208.07	232.63	263.19	294.25
933	tensile	Internal Tooth	17.00	193.50	SF TBar	221	148.41	181.76	209.88	234.65	265.48	296.82
934	tensile	Internal Tooth	17.00	191.40	SF TBar	221	146.80	179.79	207.60	232.11	262.60	293.59
935	tensile	Internal Tooth	30.00	225.60	CF	221	130.25	159.52	184.20	205.94	233.00	260.50
936	tensile	Internal Tooth	30.00	230.60	CF	221	133.14	163.06	188.28	210.51	238.16	266.27
937	tensile	Internal Tooth	30.00	231.00	CF	221	133.37	163.34	188.61	210.87	238.58	266.74
938	tensile	Internal Tooth	30.00	215.50	CF	221	124.42	152.38	175.96	196.72	222.57	248.84
939	tensile	Internal Tooth	19.00	179.50	CF	257	130.22	159.49	184.16	205.90	232.95	260.45
940	tensile	Internal Tooth	19.00	234.50	CF	221	170.12	208.36	240.59	268.99	304.33	340.25
941	tensile	Internal Tooth	19.00	232.50	CF	221	168.67	206.58	238.54	266.70	301.73	337.35
942	tensile	Internal Tooth	19.00	234.40	SF TBar	221	170.05	208.27	240.49	268.88	304.20	340.10
943	tensile	Internal Tooth	19.00	232.60	SF TBar	221	168.75	206.67	238.64	266.81	301.86	337.49
944	tensile	Internal Tooth	19.00	84.60	CF	257	61.38	75.17	86.80	97.04	109.79	122.75
945	tensile	Internal Tooth	19.00	99.60	CF	221	72.26	88.50	102.19	114.25	129.26	144.51
946	tensile	Internal Tooth	19.00	102.80	CF	221	74.58	91.34	105.47	117.92	133.41	149.16
947	tensile	Internal Tooth	19.00	88.40	CF	221	64.13	78.55	90.70	101.40	114.72	128.26
948	tensile	Internal Tooth	19.00	102.40	CF	221	74.29	90.98	105.06	117.46	132.89	148.58
949	tensile	Internal Tooth	19.00	105.50	CF	221	76.54	93.74	108.24	121.02	136.91	153.08
950	tensile	Internal Tooth	19.00	206.50	CF	221	149.81	183.48	211.86	236.87	267.99	299.62
951	tensile	Internal Tooth	19.00	215.20	CF	221	156.12	191.21	220.79	246.85	279.28	312.24
952	tensile	Internal Tooth	19.00	196.00	SF Anchor	221	142.19	174.15	201.09	224.83	254.36	284.39
953	shear	Internal Tooth	12.00	29.00	CF	25	26.47	32.42	37.44	41.86	47.36	52.95
954	shear	Internal Tooth	12.00	38.20	CF	25	34.87	42.71	49.32	55.14	62.38	69.74
955	shear	Internal Tooth	12.00	37.80	CF	25	34.51	42.26	48.80	54.56	61.73	69.01
956	shear	Internal Tooth	12.00	38.20	CF	25	34.87	42.71	49.32	55.14	62.38	69.74
957	shear	Internal Tooth	12.00	39.40	CF	38	35.97	44.05	50.87	56.87	64.34	71.93
958	shear	Internal Tooth	12.00	52.40	CF	38	47.83	58.58	67.65	75.63	85.57	95.67
959	shear	Internal Tooth	12.00	49.00	CF	38	44.73	54.78	63.26	70.73	80.02	89.46
960	shear	Internal Tooth	12.00	47.00	CF	38	42.90	52.55	60.68	67.84	76.75	85.81
961	shear	Internal Tooth	12.00	38.20	CF	50	34.87	42.71	49.32	55.14	62.38	69.74
962	shear	Internal Tooth	12.00	50.40	CF	50	46.01	56.35	65.07	72.75	82.30	92.02
963	shear	Internal Tooth	12.00	54.30	CF	50	49.57	60.71	70.10	78.38	88.67	99.14
964	shear	Internal Tooth	12.00	53.60	CF	50	48.93	59.93	69.20	77.36	87.53	97.86
965	tensile	Internal Tooth	25.00	243.70	SF	221	154.13	188.77	217.97	243.70	275.72	308.26
966	tensile	Internal Tooth	25.00	248.80	SF	221	157.35	192.72	222.53	248.80	281.49	314.71
967	tensile	Internal Tooth	25.00	247.70	SF	221	156.66	191.87	221.55	247.70	280.24	313.32
968	tensile	Internal Tooth	25.00	236.30	SF	221	149.45	183.04	211.35	236.30	267.34	298.90
969	tensile	Internal Tooth	25.00	249.10	SF	221	157.54	192.95	222.80	249.10	281.82	315.09
970	tensile	Internal Tooth	25.00	249.11	SF	221	157.55	192.96	222.81	249.11	281.84	315.10
971	tensile	Internal Tooth	25.00	252.20	SF	221	159.51	195.35	225.57	252.20	285.33	319.01
972	tensile	Internal Tooth	25.00	257.90	SF	221	163.11	199.77	230.67	257.90	291.78	326.22
973	shear	Internal Tooth	9.90	40.40	cf	25	40.60	49.73	57.42	64.20	72.63	81.21
974	shear	Internal Tooth	9.90	36.40	cf	25	36.58	44.81	51.74	57.84	65.44	73.17
975	shear	Internal Tooth	9.90	36.30	cf	25	36.48	44.68	51.59	57.68	65.26	72.97
976	shear	Internal Tooth	9.90	38.30	cf	25	38.49	47.14	54.44	60.86	68.86	76.99
977	shear	Internal Tooth	9.90	37.50	cf	25	37.69	46.16	53.30	59.59	67.42	75.38
978	shear	Internal Tooth	9.90	34.70	cf	25	34.87	42.71	49.32	55.14	62.39	69.75
979	shear	Internal Tooth	9.90	34.00	cf	25	34.17	41.85	48.33	54.03	61.13	68.34
980	shear	Internal Tooth	9.90	34.30	cf	25	34.47	42.22	48.75	54.51	61.67	68.95
981	tensile	Internal Tooth	9.90	185.00	cf	221	185.93	227.72	262.95	293.98	332.61	371.86
982	tensile	Internal Tooth	9.90	92.90	cf	221	93.37	114.35	132.04	147.63	167.02	186.74
983	tensile	Internal Tooth	9.90	90.10	cf	221	90.55	110.91	128.06	143.18	161.99	181.11
984	tensile	Internal Tooth	9.90	154.30	SF TBar	221	155.08	189.93	219.31	245.20	277.41	310.15
985	tensile	Internal Tooth	9.90	183.50	SF TBar	221	184.42	225.87	260.82	291.60	329.91	368.85
986	tensile	Internal Tooth	9.90	181.20	SF TBar	221	182.11	223.04	257.55	287.95	325.77	364.23
987	tensile	Internal Tooth	9.90	95.70	cf	221	96.18	117.80	136.02	152.08	172.06	192.36
988	tensile	Internal Tooth	9.90	100.40	cf	221	100.91	123.58	142.70	159.55	180.51	201.81
989	tensile	Internal Tooth	18.80	100.00	cf	221	72.93	89.32	103.14	115.32	130.47	145.86
990	tensile	Internal Tooth	18.80	114.00	cf	221	83.14	101.83	117.58	131.46	148.73	166.29
991	tensile	Internal Tooth	18.80	209.50	sf	221	152.79	187.13	216.08	241.59	273.33	305.59
992	tensile	Internal Tooth	18.80	189.20	cf	221	137.99	169.00	195.14	218.18	246.84	275.98
993	tensile	Internal Tooth	18.80	94.00	cf	221	68.56	83.96	96.95	108.40	122.64	137.11
994	tensile	Internal Tooth	18.80	200.20	cf	221	146.01	178.83	206.49	230.86	261.19	292.02
995	tensile	Internal Tooth	18.80	230.30	cf	221	167.96	205.71	237.54	265.57	300.46	335.93
996	tensile	Internal Tooth	18.80	102.50	cf	221	74.76	91.56	105.72	118.20	133.73	149.51
997	shear	Internal Tooth	18.80	45.40	cf	38	33.11	40.55	46.83	52.35	59.23	66.22
998	shear	Internal Tooth	18.80	48.60	cf	38	35.45	43.41	50.13	56.04	63.41	70.89
999	shear	Internal Tooth	18.80	43.80	cf	38	31.94	39.12	45.18	50.51	57.14	63.89
1000	shear	Internal Tooth	18.80	45.50	cf	38	33.18	40.64	46.93	52.47	59.36	66.37
1001	shear	Internal Tooth	18.80	53.20	cf	38	38.80	47.52	54.87	61.35	69.41	77.60
1002	shear	Internal Tooth	18.80	48.40	cf	38	35.30	43.23	49.92	55.81	63.15	70.60
1003	shear	Internal Tooth	18.80	43.90	cf	38	32.02	39.21	45.28	50.62	57.27	64.03
1004	shear	Internal Tooth	15.70	49.60	cf	38	39.59	48.48	55.98	62.59	70.81	79.17
1005	shear	Internal Tooth	15.70	50.40	cf	38	40.22	49.26	56.88	63.60	71.95	80.45
1006	shear	Internal Tooth	15.70	51.70	cf	38	41.26	50.53	58.35	65.24	73.81	82.52
1007	shear	Internal Tooth	15.70	49.90	cf	38	39.82	48.77	56.32	62.97	71.24	79.65
1008	shear	Internal Tooth	15.70	46.10	cf	38	36.79	45.06	52.03	58.17	65.82	73.58

## Appendix B - Test Data

Test ref #	Test Type	Anchor Type	Concrete Strength, MPa, $f_{cage}$	Ultimate failure load, Pu, kN	Mode of Failure	Effective Embedment Depth, $h_{ef}$ , mm	Ultimate Test Loads normalised to $f_{c,age}$ , kN					
							10.00	15.00	20.00	25.00	32.00	40.00
1009	shear	Internal Tooth	15.70	44.50	cf	38	35.51	43.50	50.23	56.15	63.53	71.03
1010	shear	Internal Tooth	15.70	44.30	cf	38	35.36	43.30	50.00	55.90	63.25	70.71
1011	shear	Internal Tooth	15.70	214.00	cf	38	170.79	209.17	241.53	270.04	305.52	341.58
1012	shear	Internal Tooth	15.70	207.90	cf	38	165.92	203.21	234.65	262.35	296.81	331.84
1013	shear	Internal Tooth	15.70	115.40	cf	38	92.10	112.80	130.25	145.62	164.75	184.20
1014	shear	Internal Tooth	15.70	127.50	cf	38	101.76	124.63	143.90	160.89	182.03	203.51
1015	shear	Internal Tooth	15.70	117.90	cf	38	94.09	115.24	133.07	148.78	168.32	188.19
1016	shear	Internal Tooth	15.70	212.00	CF	38	169.19	207.22	239.28	267.52	302.66	338.39
1017	shear	Internal Tooth	15.70	218.30	CF	38	174.22	213.38	246.39	275.47	311.66	348.44
1018	shear	Internal Tooth	15.70	122.30	CF	38	97.61	119.54	138.04	154.33	174.60	195.21
1019	shear	Internal Tooth	22.90	59.10	CF	38	39.05	47.83	55.23	61.75	69.86	78.11
1020	shear	Internal Tooth	22.90	65.00	CF	38	42.95	52.61	60.75	67.91	76.84	85.91
1021	shear	Internal Tooth	22.90	48.40	CF	38	31.98	39.17	45.23	50.57	57.21	63.97
1022	shear	Internal Tooth	22.90	48.30	CF	38	31.92	39.09	45.14	50.47	57.10	63.84
1023	shear	Internal Tooth	22.90	58.70	CF	38	38.79	47.51	54.86	61.33	69.39	77.58
1024	shear	Internal Tooth	22.90	55.40	CF	38	36.61	44.84	51.77	57.88	65.49	73.22
1025	shear	Internal Tooth	22.90	52.00	CF	38	34.36	42.09	48.60	54.33	61.47	68.73
1026	shear	Internal Tooth	22.90	49.30	CF	38	32.58	39.90	46.07	51.51	58.28	65.16
1027	tensile	Internal Tooth	22.90	106.20	CF	221	70.18	85.95	99.25	110.96	125.54	140.36
1028	tensile	Internal Tooth	22.90	192.70	CF	221	127.34	155.96	180.09	201.34	227.79	254.68
1029	tensile	Internal Tooth	22.90	200.10	CF	221	132.23	161.95	187.00	209.07	236.54	264.46
1030	tensile	Internal Tooth	22.90	79.50	CF	221	52.54	64.34	74.30	83.07	93.98	105.07
1031	tensile	Internal Tooth	22.90	85.70	CF	221	56.63	69.36	80.09	89.54	101.31	113.26
1032	tensile	Internal Tooth	22.90	181.70	CF	221	120.07	147.06	169.81	189.85	214.79	240.14
1033	tensile	Internal Tooth	22.90	181.50	CF	221	119.94	146.89	169.62	189.64	214.55	239.88
1034	tensile	Internal Tooth	22.90	83.20	CF	221	54.98	67.34	77.75	86.93	98.35	109.96
1035	shear	Internal Tooth	16.00	69.20	CF	63	54.71	67.00	77.37	86.50	97.86	109.41
1036	shear	Internal Tooth	16.00	66.10	CF	63	52.26	64.00	73.90	82.63	93.48	104.51
1037	shear	Internal Tooth	16.00	66.80	CF	63	52.81	64.68	74.68	83.50	94.47	105.62
1038	shear	Internal Tooth	16.00	59.60	CF	63	47.12	57.71	66.63	74.50	84.29	94.24
1039	shear	Internal Tooth	16.00	64.80	CF	63	51.23	62.74	72.45	81.00	91.64	102.46
1040	shear	Internal Tooth	16.00	65.90	CF	63	52.10	63.81	73.68	82.38	93.20	104.20
1041	shear	Internal Tooth	16.00	71.10	CF	63	56.21	68.84	79.49	88.88	100.55	112.42
1042	shear	Internal Tooth	16.00	61.30	CF	63	48.46	59.35	68.54	76.63	86.69	96.92
1043	tensile	Internal Tooth	16.00	246.50	CF	221	194.88	238.67	275.60	308.13	348.60	389.75
1044	tensile	Internal Tooth	16.00	231.60	SF TBar	221	183.10	224.25	258.94	289.50	327.53	366.19
1045	tensile	Internal Tooth	16.00	98.50	CF	221	77.87	95.37	110.13	123.13	139.30	155.74
1046	tensile	Internal Tooth	16.00	102.90	CF	221	81.35	99.63	115.05	128.63	145.52	162.70
1047	tensile	Internal Tooth	16.00	218.70	CF	221	172.90	211.76	244.51	273.38	309.29	345.80
1048	tensile	Internal Tooth	16.00	237.60	CF	221	187.84	230.06	265.64	297.00	336.02	375.68
1049	tensile	Internal Tooth	16.00	107.60	CF	221	85.07	104.18	120.30	134.50	152.17	170.13
1050	tensile	Internal Tooth	16.00	104.70	CF	221	82.77	101.38	117.06	130.88	148.07	165.55
1051	shear	Internal Tooth	19.30	54.30	cf	38	39.09	47.87	55.28	61.80	69.92	78.17
1052	shear	Internal Tooth	19.30	54.30	cf	38	39.09	47.87	55.28	61.80	69.92	78.17
1053	shear	Internal Tooth	19.30	62.80	cf	38	45.20	55.36	63.93	71.47	80.86	90.41
1054	shear	Internal Tooth	19.30	62.70	cf	38	45.13	55.28	63.83	71.36	80.74	90.26
1055	shear	Internal Tooth	19.30	55.30	cf	38	39.81	48.75	56.29	62.94	71.21	79.61
1056	shear	Internal Tooth	19.30	54.50	cf	38	39.23	48.05	55.48	62.03	70.18	78.46
1057	shear	Internal Tooth	19.30	56.80	cf	38	40.89	50.07	57.82	64.65	73.14	81.77
1058	shear	Internal Tooth	19.30	52.60	cf	38	37.86	46.37	53.55	59.87	67.73	75.72
1059	tensile	Internal Tooth	19.30	96.40	cf	221	69.39	84.99	98.13	109.72	124.13	138.78
1060	tensile	Internal Tooth	19.30	227.00	cf	221	163.40	200.12	231.08	258.36	292.30	326.80
1061	tensile	Internal Tooth	19.30	98.10	cf	221	70.61	86.48	99.86	111.65	126.32	141.23
1062	tensile	Internal Tooth	19.30	89.40	cf	221	64.35	78.81	91.01	101.75	115.12	128.70
1063	tensile	Internal Tooth	19.30	214.20	cf	221	154.18	188.84	218.05	243.79	275.81	308.37
1064	tensile	Internal Tooth	19.30	208.20	SF Anchor	221	149.87	183.55	211.94	236.96	268.09	299.73
1065	tensile	Internal Tooth	19.30	97.20	cf	221	69.97	85.69	98.95	110.63	125.16	139.93
1066	tensile	Internal Tooth	11	97.8	cf	221	93.25	114.21	131.87	147.44	166.81	186.50
1067	tensile	Internal Tooth	11	83.6	cf	221	79.71	97.62	112.73	126.03	142.59	159.42
1068	tensile	Internal Tooth	11	199.4	sf tbar	221	190.12	232.85	268.87	300.61	340.10	380.24
1069	tensile	Internal Tooth	11	191.8	sf anchor	221	182.87	223.97	258.62	289.15	327.14	365.75
1070	tensile	Internal Tooth	11	191.6	sf tbar	221	182.68	223.74	258.35	288.85	326.79	365.37
1071	tensile	Internal Tooth	16	202.8	sf anchor	221	160.33	196.36	226.74	253.50	286.80	320.65
1072	tensile	Internal Tooth	11	193.2	sf tbar	221	184.21	225.61	260.51	291.26	329.52	368.42
1073	tensile	Internal Tooth	11	191.4	sf tbar	221	182.49	223.51	258.08	288.55	326.45	364.99
1074	tensile	Internal Tooth	21	225.6	sf tbar	221	155.68	190.67	220.16	246.15	278.49	311.36
1075	tensile	Internal Tooth	21	230.6	sf tbar	221	159.13	194.89	225.04	251.61	284.66	318.26
1076	tensile	Internal Tooth	26	231	sf anchor	221	143.26	175.46	202.60	226.51	256.27	286.52
1077	tensile	Internal Tooth	16	215.4	sf anchor	257	170.29	208.56	240.82	269.25	304.62	340.58
1078	tensile	Internal Tooth	16	234.4	sf tbar	221	185.31	226.96	262.07	293.00	331.49	370.62
1079	tensile	Internal Tooth	16	232.6	sf tbar	221	183.89	225.21	260.05	290.75	328.95	367.77
1080	tensile	Internal Tooth	16	84.6	cf	257	66.88	81.91	94.59	105.75	119.64	133.76
1081	tensile	Internal Tooth	16	99.6	cf	221	78.74	96.44	111.36	124.50	140.86	157.48
1082	tensile	Internal Tooth	16	102.8	cf	221	81.27	99.54	114.93	128.50	145.38	162.54
1083	tensile	Internal Tooth	16	88.4	cf	221	69.89	85.59	98.83	110.50	125.02	139.77
1084	tensile	Internal Tooth	16	102.4	cf	221	80.95	99.15	114.49	128.00	144.82	161.91
1085	tensile	Internal Tooth	16	105.4	cf	221	83.33	102.05	117.84	131.75	149.06	166.65
1086	tensile	Internal Tooth	16	206.4	sf anchor	221	163.17	199.85	230.76	258.00	291.89	326.35
1087	tensile	Internal Tooth	16	215.2	sf anchor	221	170.13	208.37	240.60	269.00	304.34	340.26
1088	shear	Internal Tooth	12	39.4	cf	38	35.97	44.05	50.87	56.87	64.34	71.93
1089	shear	Internal Tooth	12	52.4	cf	38	47.83	58.58	67.65	75.63	85.57	95.67
1090	shear	Internal Tooth	12	49	cf	38	44.73	54.78	63.26	70.73	80.02	89.46
1091	shear	Internal Tooth	12	47	cf	38	42.90	52.55	60.68	67.84	76.75	85.81
1092	shear	Internal Tooth	12	38.2	cf	50	34.87	42.71	49.32	55.14	62.38	69.74



## Appendix B - Test Data

Test ref #	Test Type	Anchor Type	Concrete Strength, MPa, $f_{c,age}$	Ultimate failure load, Pu, kN	Mode of Failure	Effective Embedment Depth, $h_{ef}$ , mm	Ultimate Test Loads normalised to $f'_{c,age}$ , kN					
							10.00	15.00	20.00	25.00	32.00	40.00
1093	shear	Internal Tooth	12	50.6	cf	50	46.19	56.57	65.32	73.03	82.63	92.38
1094	shear	Internal Tooth	12	54	cf	50	49.30	60.37	69.71	77.94	88.18	98.59
1095	shear	Internal Tooth	12	53.6	cf	50	48.93	59.93	69.20	77.36	87.53	97.86